

**Hydrothermal Treatment for Biofuels: Lignocellulosic Biomass to Bioethanol,  
Biocrude, and Biochar**

by

Sandeep Kumar

A dissertation submitted to the Graduate Faculty of  
Auburn University  
in partial fulfillment of the  
requirements for the Degree of  
Doctor of Philosophy

Auburn, Alabama  
May 14, 2010

Keywords: subcritical, supercritical, biocrude, liquefaction,  
pretreatment, carbonization

Copyright 2010 by Sandeep Kumar

Approved by

Ram B. Gupta, Chair, Professor of Chemical Engineering  
Christopher B. Roberts, Professor of Chemical Engineering  
Yoon Y. Lee, Professor of Chemical Engineering  
Sushil Adhikari, Assistant Professor of Biosystem Engineering

## Abstract

Biofuels are viewed as an alternative, renewable fuel and an important component of energy security for the future. The dissertation work is directly aimed at supporting the commercial production of biofuels from lignocellulosic biomass. The prime objective is to apply chemical engineering fundamentals for capitalizing on the extraordinary solvent properties of water at elevated temperature and support green and sustainable chemistry. Hydrothermal treatment refers to processing of biomass in sub- and super-critical water medium.

Microcrystalline cellulose (MCC) was pretreated (Chapter 2) using subcritical water in a continuous flow reactor for enhancing its enzymatic digestibility. The degree of polymerization of cellulose steadily decreased with an increase in the pretreatment temperature, with a rapid drop occurring above 300°C. The partial transformation of cellulose I to II polymorph was noticed in the MCC treated at  $\geq 300$  °C in subcritical water. A nearly three-fold increase in the initial enzymatic reactivity was observed for the sample treated at 315°C. The hydrothermal pretreatment of switchgrass (Chapter 3) was conducted in a flow through reactor to enhance and optimize the enzymatic digestibility of pretreated biomass. More than 80% of glucan digestibility could be achieved at 190°C in hydrothermal medium. Addition of K<sub>2</sub>CO<sub>3</sub> (0.45-0.9 wt%) in water helped in enhancing the enzymatic activity of biomass. An alternate pathway for the utilization of liquid hydrolyzate was developed and sugar loss in the liquid fraction during pretreatment was recovered as high heating value solids.

Liquefaction of cellulose in sub- and super-critical water was studied (Chapter 4) in a continuous flow reactor. The focus of this study was to maximize the yield of sugar products (oligomers and monomers) from cellulose hydrolysis. About 65% of cellulose converted to the oligomers and monomers at 335°C in 4.8 s and also at 354°C in 3.5 s. In the supercritical region, the produced oligomers and monomers partially degraded to degradation products.

Liquefaction of switchgrass (Chapter 5) in subcritical water was studied to produce biocrude. The effects of reaction temperature and catalysis by K<sub>2</sub>CO<sub>3</sub> were examined. Potassium carbonate significantly enhanced the hydrolysis of switchgrass components into water soluble products. More than 50 wt% of organic carbon available in switchgrass was converted to biocrude at 235°C in the presence of 0.15 wt% of K<sub>2</sub>CO<sub>3</sub>. Biocrude contained oxygenated hydrocarbons. The subcritical water treatment caused the complete breakdown of lignocellulosic structure of switchgrass.

Hydrothermal carbonization of switchgrass (Chapter 6) was studied to produce the high energy density (coal-like) biochar. The effects of temperature, residence time, and pressure on the yield and heating value of biochar were examined. Besides the solid fuel application, biochar was also studied for its sorption properties for removing heavy metal contaminants from ground water. The batch adsorption results (Chapter 7) with uranium [U(VI)] as a solute showed that biochar can be a potential low cost adsorbent for such application.

Future work (Chapter 8) involves the upgrade of biocrude to liquid / gaseous fuel. Also pyrolysis / gasification properties of biochar may be investigated. Biochar adsorption properties may be further tested for removing other metal contaminants.

## Acknowledgments

I would like to express my sincere gratitude to my advisor Dr. Ram B. Gupta, for his continued guidance, discussion, motivation, and support during my dissertation work. It would have been impossible for me to complete this work without his mentoring and moral support.

I would like to express my sincere thanks to the committee members, Dr. Christopher B. Roberts, Dr. Yoon Y. Lee, and Dr. Sushil Adhikari for their valuable comments and suggestions.

Dr. Y.Y. Lee's research group has been very supportive and accommodating. I have frequently used their analytical instruments. I would like to thank all his group members. Special thanks to Ms. Urvi Kothari for supporting me in sample analyses and also conducting collaborative studies.

Chemical engineering staff, Karen Cochran, Sue Allen, Georgetta Dennis, and Jennifer Harris deserves special thanks for helping me with logistic, academic and financial matters. Brian Schwieker (Engineering Technician) needs special thanks for his great help in building up the experimental setup and prompt maintenance support. I also enjoyed the constant support from Burak Aksoy and David J. Webster in doing the industrial projects for the Alabama Centre for Paper and Bioresource Engineering.

My group colleagues, Adam Byrd, Ganesh Sanganwar, Melinda Hemmigway, Dr. Lingzhao Kong, Hema Ramsrun, Courtney Ober, and Jin Yang need special appreciation for their assistance and creating a joyful environment in the laboratory.

I would like to extend my sincere thanks to my friend Rajesh Gupta and his family for being a great support during my transition period and thereafter. Rajesh has provided invaluable suggestions, technical inputs and moral supports. I also thank him for doing a collaborative study and co-authoring a research article. I would also like to thank my dear friends Chaudhary Devraj Nayak and Vijay A. Loganathan for their constant encouragements and emotional supports.

My parents deserve credit for all my achievements. They have supported me whole heartily in all my endeavors. My mother who passed away recently will remain the source of inspiration throughout my life. She inculcated the fighting spirit in me. Continued support of my wife, Sweta Kumari is the most important factor which helped me in carrying out the family responsibilities along with the research and academic work. Love and sweet smile of my son “Shashank” is always a source of rejuvenation after exhaustive work. I wish to thank my brother, sister and entire family members for their love and support.

I want to thank National Science Foundation (grant # DE-FC26-05424.56) and Alabama Centre for Paper and Bioresource Engineering for their continued financial support for my research study.

## Table of Contents

Abstract	ii
Acknowledgements	iv
List of Figures	xii
List of Tables	xviii
1 Introduction	1
1.1 Importance of Biofuels	1
1.2 Lignocellulosic Biomass	2
1.3 Conversion Routes for Lignocellulosic Biomass to Biofuels	4
1.3.1 Thermochemical Pathways	5
1.3.2 Biochemical Pathways	8
1.4 Pretreatment Methods for Bioethanol	8
1.4.1 Physical	9
1.4.2 Chemical Pretreatments	9
1.4.3 Hydrothermal Pretreatments	13
1.4.4 Physiochemical Pretreatments	14
1.5 Supercritical Fluid Technology	15
1.6 Sub-and Supercritical water	16

1.7	Sub- and Supercritical Water Technology for Biofuels	19
1.7.1	Biochar	21
1.7.2	Bioethanol	22
1.7.3	Biocrude	23
1.7.4	Hydrothermal Gasification	26
1.8	Challenges of Hydrothermal Processing	26
1.9	Research Plan	27
1.9.1	Pretreatment of Biomass for Bioethanol	28
1.9.2	Liquefaction of Biomass for Biocrude	28
1.9.3	Carbonization of Biomass for Biochar	30
1.10	References	31
2	Cellulose pretreatment in subcritical water: Effect of temperature on molecular structure and enzymatic reactivity	41
2.1	Abstract	41
2.2	Introduction	42
2.3	Experimental Section	46
2.4	Product Analyses	49
2.5	Results and Discussion	52
2.5.1	Solid Analysis	53
2.5.2	Liquid Analysis	64
2.6	Conclusion	66
2.7	Acknowledgment	67

2.8	Nomenclature	67
2.9	References	70
3	Hydrothermal Pretreatment of Switchgrass and Corn Stover for Production of Ethanol and Carbon Microspheres	73
3.1	Abstract	73
3.2	Introduction	74
3.3	Experimental Section	79
3.4	Product Characterization	84
	3.4.1 Pretreatment	84
	3.4.2 Carbonization	86
3.5	Results and Discussions	87
	3.5.1 Pretreatment	87
	3.5.2 Hydrothermal Carbonization	98
3.6	Conclusion	106
3.7	Acknowledgment	107
3.8	References	107
4	Hydrolysis of Microcrystalline Cellulose in Subcritical and Supercritical Water in a Continuous Flow Reactor	115
4.1	Abstract	115
4.2	Introduction	116
4.3	Experimental Section	119
4.4	Product Analyses	122

4.5	Results	123
4.6	Discussion	133
4.7	Conclusion	137
4.8	Acknowledgment	138
4.9	Product Nomenclature	138
4.10	References	138
5	Biocrude Production from Switchgrass using Subcritical Water	144
5.1	Abstract	144
5.2	Introduction	145
5.3	Experimental Section	149
5.4	Product Separation	152
5.5	Product Characterization	154
5.6	Results	155
5.7	Discussion	165
5.8	Conclusion	169
5.9	Acknowledgment	170
5.10	References	170
6	Production of Biochar from Switchgrass by Hydrothermal Carbonization	177
6.1	Abstract	177
6.2	Introduction	178
6.3	Experimental Section	181

6.4	Product Characterization	184
6.5	Results and Discussion	185
6.6	Conclusion	198
6.7	Acknowledgment	198
6.8	References	199
7	Application of Biochar for the Removal of Heavy Metal Contaminants from Ground Water	203
7.1	Introduction	203
7.2	Experimental Section	205
7.3	Results and Discussion	206
7.4	Conclusion	211
7.5	References	212
8	Summary and Future Works	214
	Appendix A: Structure and Composition of Lignocellulosic Biomass	217
A.1	Introduction	217
A.2	Composition and Structure	217
A.3	References	225
	Appendix B: Summary of Pretreatment Methods	227
	Appendix C: Reaction Pathway of Cellulose, Hemicelluloses, and Lignin in Hydrothermal Medium	229
C.1	Cellulose Reaction Pathways	229
C.2	Hemicelluloses Reaction Pathways	230

C.3 Lignin	231
C.4 References	232
Appendix D: Salt Solubility in Hydrothermal Medium	234
D.1 Salt-Water Binary System	234
D.2 References	236
Appendix E: Journal Publications and Conference Presentations	237

## List of Figures

Figure 1.1 Annual biomass resource potential from forest and agricultural resources.	2
Figure 1.2 Typical composition of lignocellulosic biomass.	3
Figure 1.3 Major pathways for the conversion of biomass to biofuels.	5
Figure 1.4 Physical properties of water with temperature, at 24 MPa.	18
Figure 1.5 Hydrothermal treatment applications referenced to pressure-temperature phase diagram of water.	20
Figure 1.6 Generation of in-situ alkali catalyst nanoparticles in hydrothermal reactor.	29
Figure 2.1 Ionization constant ( $K_w$ ) of water as a function of temperature	44
Figure 2.2 Apparatus for cellulose pretreatment in subcritical water.	46
Figure 2.3 Degree of polymerization ( $DP_v$ ) versus pretreatment temperature.	54
Figure 2.4 XRD results for MCC and group I samples.	56
Figure 2.5 XRD results for original MCC and group II samples.	57
Figure 2.6a Plot after regression analysis of enzymatic hydrolysis data at 3.5 FPU and after 1 h.	59

Figure 2.6b Plot after regression analysis of enzymatic hydrolysis data at 3.5 FPU and after 24 h.	59
Figure 2.6c Plot after regression analysis of enzymatic hydrolysis data at 60 FPU and after 1 h.	60
Figure 2.6d Plot after regression analysis of enzymatic hydrolysis data at 60 FPU and after 24 h.	60
Figure 2.7. SEM images of samples: (a) MCC, (b) run 5, (c) run 7, and (d) run 9.	62
Figure 2.8 DSC thermograms of MCC, group I (run 6) and group II (run 7 and 9) samples.	63
Figure 2.9 Simplified reaction scheme of cellulose in subcritical water.	69
Figure 3.1 Apparatus for the hydrothermal pretreatment of biomass.	80
Figure 3.2 Typical temperature cycle during pretreatment process	82
Figure 3.3 Batch reactor for hydrothermal carbonization process	82
Figure 3.4 Percentage removal of hemicelluloses and lignin with temperature for the switchgrass pretreated at 3.4 MPa and 20 min steady operation time	87
Figure 3.5 Glucan digestibility (72 h) of hydrothermally pretreated switchgrass	89
Figure 3.6 Glucan digestibility (72 h) of switchgrass pretreated at 150°C in the presence of K <sub>2</sub> CO <sub>3</sub>	90
Figure 3.7 SEM images of untreated and pretreated (run 3) switchgrass taken at 600X magnification	91

Figure 3.8 Glucan digestibility (72 h) of K <sub>2</sub> CO <sub>3</sub> (0.9 wt%) assisted hydrothermally pretreated switchgrass	91
Figure 3.9 Percentage removal of hemicelluloses and lignin with temperature for the switchgrass pretreated in the presence of 0.9 wt% of K <sub>2</sub> CO <sub>3</sub>	92
Figure 3.10 Material balance for hydrothermally pretreated switchgrass (run 6) at 190°C	93
Figure 3.11 Material balance for K <sub>2</sub> CO <sub>3</sub> assisted hydrothermally pretreated switchgrass (run 7) at 190°C	93
Figure 3.12 XRD pattern of untreated and pretreated (run 6 and 7) switchgrass	96
Figure 3.13 Glucan digestibility (72 h) of untreated and pretreated corn stover	97
Figure 3.14 SEM images of untreated and pretreated (run 8) corn stover taken at 600X magnification	98
Figure 3.15 Percentage conversion of liquid hydrolyzate (based on TOC of input) of run 6 and glucose solution	100
Figure 3.16 SEM images (at 20,000X magnifications) of carbon microspheres produced from (a) glucose solution and (b) liquid hydrolyzate of run 6	100
Figure 3.17 GC-MS spectra of liquid product from (a) run IV, (b) run V, and (c) run VI	102
Figure 3.18 Simplified reaction pathway of glucose during hydrothermal carbonization reactions	104

Figure 3.19 FTIR spectra of solids recovered in run II and V	104
Figure 4.1 Apparatus for cellulose hydrolysis in subcritical and supercritical water	121
Figure 4.2 Yield of hydrolysis products obtained from cellulose treatment in subcritical and supercritical water at 27.6 MPa	125
Figure 4.3 Yield of glucose obtained from cellulose treatment in subcritical and supercritical water at 27.6 MPa	125
Figure 4.4 HMF yield in liquids obtained from cellulose treatment in subcritical and supercritical water at 27.6 MPa	126
Figure 4.5 TOC in liquid products obtained from cellulose treatment in subcritical and supercritical water at 27.6 MPa	127
Figure 4.6 HPLC chromatograph of run 5 (335°C, and 4.7 s residence time)	139
Figure 4.7 HPLC chromatograph of run 7	130
Figure 4.8 HPLC chromatograph of run 14 (405 °C, and 2.5 s residence time)	131
Figure 4.9 Products obtained at 302°C, 5.2 s, 27.6 MPa in the presence of (a) 0% K <sub>2</sub> CO <sub>3</sub> , (b) 0.22% K <sub>2</sub> CO <sub>3</sub> , and (c) 0.44% K <sub>2</sub> CO <sub>3</sub> .	132
Figure 5.1 Ionization constant ( $K_w$ ) of water as a function of temperature at 25 MPa	146
Figure 5.2 Major pathways for the conversion of biomass to biofuels	147
Figure 5.3 Apparatus for biocrude production	150
Figure 5.4 Heating profile in a typical experiment	151
Figure 5.5 Products separation scheme	153

Figure 5.6 Total organic content (TOC) of aqueous phase versus steady operation time	156
Figure 5.7 Conversion of switchgrass (weight loss) for runs 6, 7, and 8	157
Figure 5.8 Composition of aqueous phase from run 8 by HPLC analysis	159
Figure 5.9 XRD patterns for untreated switchgrass and solid precipitate from run 8	161
Figure 5.10 XRD pattern of untreated switchgrass and biochars from runs 6 and 8	162
Figure 5.11 FTIR spectra of untreated switchgrass and biochar from run 8	163
Figure 5.12 SEM image of (a) switchgrass, and (b) biochar from run 8	164
Figure 6.1 Apparatus for HTC process	182
Figure 6.2 Products separation scheme in two stage HTC process	184
Figure 6.3 Yield (%) of obtained biochar at 200°C and 230°C	187
Figure 6.4 HHV of obtained biochar at 200°C and 230°C	187
Figure 6.5 Yield (%) of obtained biochar at 200-280°C	189
Figure 6.6 HHV of obtained biochar at 200-280°C	189
Figure 6.7 Yield (%) of obtained biochar at 280°C	190
Figure 6.8 HHV of obtained biochar at 280°C	191
Figure 6.9 FTIR spectra of switchgrass and biochar, reaction time 4.0 h A-switchgrass, B-200°C, C-230°C, D-260°C, E-280°C	192
Figure 6.10 SEM image of switchgrass (A) and biochar (B) obtained at 260°C, 4.0 h	194
Figure 6.11 XRD patterns of untreated switchgrass and biochar obtained at	

280°C, 4.0 h	195
Figure 6.12 Conversion efficiency of carbon from biocrude	196
Figure 6.13 SEM image of biotar particles (HTC of biocrude obtained at 200°C) obtained at 200°C, 2.0 h	197
Figure 7.1a TG and DTG pattern of switchgrass under inert atmosphere	208
Figure 7.1b TG and DTG pattern of biochar under inert atmosphere	208
Figure 7.2 Kinetics of U(VI) adsorption on to biochar at different solid loadings and initial U(VI) concentrations	209
Figure 7.3 Adsorption isotherm of U(VI) on to biochar. SSR: 5 g L <sup>-1</sup> pH: 3.9 ± 0.2; ionic strength: 0.1 M NaNO <sub>3</sub>	210
Figure 7.4 Adsorption of U(VI) on to biochar at different SSR. pH: 3.9 ± 0.2; ionic strength: 0.1 M NaNO <sub>3</sub>	211
Figure A.10 Inter-conversion of polymorphs of cellulose	219
Figure A.11 Lignin monomers (a) trans- <i>p</i> -coumaryl alcohol, (b) coniferyl alcohol, and (c) sinapyl alcohol	222
Figure C.12 Key reaction products from cellulose hydrolysis in catalyst free hydrothermal medium	230
Figure C.13 A segment of hardwood xylan, <i>O-acetyl-4-O-methylglucuronoxylan</i>	231
Figure C.14 Reaction pathway of lignin in supercritical water	232

## List of Tables

Table 1.1 Comparison of liquefaction and pyrolysis.	6
Table 1.2 Comparison of ambient and supercritical water.	18
Table 2.1 Summary of experimental conditions (at 27.6 MPa).	48
Table 2.2 Lattice planes of cellulose I and II and the diffraction angles in XRD spectra.	50
Table 2.3 Enzymatic digestibility of MCC, group I, and group II samples.	53
Table 2.4. Crystallinity of samples by XRD analysis.	55
Table 2.5 Yields of different compounds in the liquid product.	64
Table 3.2 Pretreatment details conducted at 3.4 MPa and 20 min steady operation time and the weight loss of switchgrass after pretreatment	81
Table 3.3 Details of hydrothermal carbonization experiments	84
Table 3.4 BET surface area of switchgrass and samples from run 6 and 7	95
Table 3.5 Sugar compounds analyzed by HPLC in liquid hydrolyzate collected at 190°C during run 6	99
Table 3.6 Key compounds identified in the product liquid from run IV, V, and VI and their trend with reaction time	102
Table 3.7 Functional groups in the FTIR spectra of carbon rich microspheres from run II and V	104

Table 4.1 HPLC standards used for analysis of liquid products	120
Table 4.2 Liquid products yield from cellulose treatment in subcritical and supercritical water at 27.6 MPa	124
Table 4.3 Carbon balance in the liquid products obtained from subcritical and supercritical treatment of cellulose at 27.6 MPa	128
Table 4.4 Experimental conditions of cellulose runs in presence of catalyst K <sub>2</sub> CO <sub>3</sub> in subcritical water	132
Table 5.1 Composition (wt%) of switchgrass	149
Table 5.2 Experiment details of various runs	152
Table 5.3 Biocrude yield from switchgrass conversion (wt%, carbon basis)	158
Table 5.4 Identified compounds in biocrude from run 8 by GC-MS analysis	160
Table 5.5 Position of infrared absorption bands of switchgrass	163
Table 6.1 Comparison of biomass and biochar as solid fuel	178
Table 6.2 Main physical and chemical properties of the switchgrass	182
Table 6.3 Experiment summary and results	186
Table 6.4 FTIR spectrum of the switchgrass and biochar	193
Table 6.5 Key compounds in biocrude identified during HPLC analysis	196
Table 7.5 Composition of switchgrass and biochar	207
Table A.6 Composition and degree of polymerization (DP) of hemicelluloses	221
Table B.7 Summary of the important pretreatment methods	227
Table D.8 Classification of salt-water binary system	235

## 1. Introduction

### 1.1 Importance of Biofuels

Energy security, sustainability, and climate change concerns has led the world to look for renewable and alternative energy resources. The large scale substitution of petroleum based fuels and products with renewable sources are needed to minimize the environmental issues.<sup>1</sup> Biomass is the world's fourth largest energy source worldwide, following coal, oil and natural gas. Biomass is an attractive feedstock for fuel and biomaterials due to the three main reasons. First, it is a carbon-neutral renewable resource that could be sustainably developed for the production of bioenergy and biomaterials. Second, it is environmentally benign, as it does not add to the green house gas emission, and possibly reduces NO<sub>x</sub> and SO<sub>x</sub> depending on the fossil-fuels displaced. Though, when combusted in traditional stoves, emission of polycyclic aromatic hydrocarbons, dioxins, furans, and heavy metals is a concern.<sup>2</sup> Third, it appears to have a significant economic potential given the fluctuating prices of the fossil fuels. Moreover, development of bio-based economy brings the opportunity for rural empowerment and also the energy security, since biomass resource is distributed all over the world.

United States is a net importer of petroleum products. As per the department of energy sources, in the year 2006, US had 2% of world oil reserve share and used 24% of the world supply.<sup>3</sup> Nearly 60% of the oil is imported to meet the energy demand.

In recent years, government has sponsored numerous research studies and projects, for developing abundantly available biomass resources of the country for biofuels applications. The billion ton vision report concludes that land resources of US are capable of producing sustainable supply of biomass sufficient to displace 30% or more of current petroleum consumption with biofuels by year 2030.<sup>4</sup> Figure 1.1 show that more than a billion ton annual biomass resource potential from forest and agricultural resources are available for sustainable biofuels production.

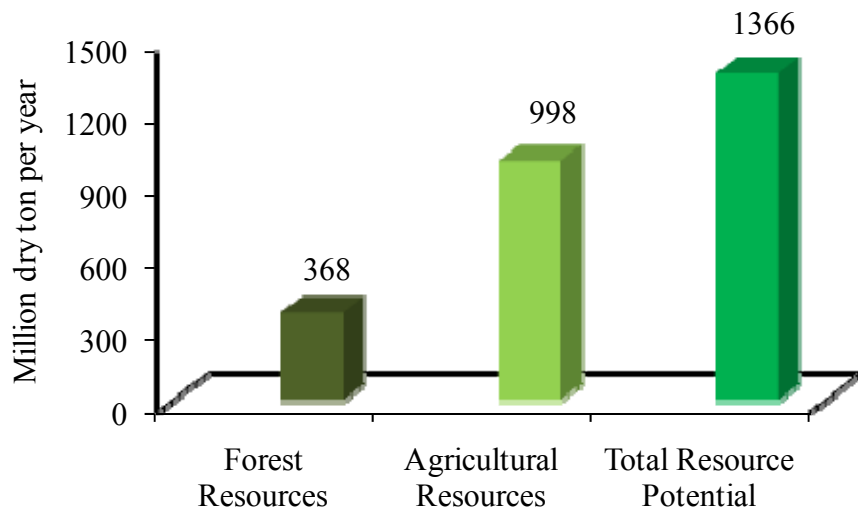


Figure 1.1 Annual biomass resource potential from forest and agricultural resources.<sup>4</sup>

Energy Independence and Security Act (EISA) 2007 requires replacing 20% of fossil by renewable fuel by 2017. The major focus is on non food resources or so called “second” generation biofuels from lignocellulosic biomass.

## 1.2 Lignocellulosic Biomass

Lignocellulose is a generic term for describing the main constituents in most plants, namely cellulose, hemicelluloses, and lignin (Figure 1.2). It is the non starch

based fibrous part of plant material. Lignocellulsoic biomass is renewable and abundantly available resource, and is considered as potential feedstock for second generation biofuels.

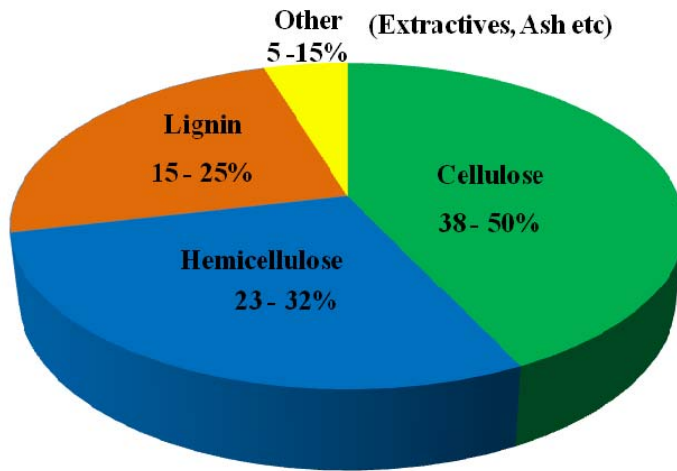


Figure 1.2 Typical composition of lignocellulosic biomass.<sup>5</sup>

The components of lignocelluloses form three-dimensional polymeric composites to provide structure and rigidity to the plant. Cellulose is an unbranched chain of anhydroglucoside ( $C_6H_{10}O_5$ ) linked head to tail by  $\beta$ -glycosidic linkages. The  $\beta$ -linkages in cellulose form linear chains that are highly stable and resistant to chemical attack because of the high degree of intra and intermolecular hydrogen bonding.<sup>6</sup> Hemicelluloses are a class of polymers of sugars including the six carbon sugars (mannose, galactose, glucose and 4-*O*-methyl-D-glucuronic acid) and five carbon sugars (xylose and arabinose). Unlike cellulose, hemicelluloses possess side chains.<sup>7</sup> Lignin is a complex network of different phenyl propane units (p-coumaryl alcohol, coniferyl alcohol, sinapyl alcohol). In general, cellulose provides rigidity. Hemicelluloses stick and glue to cellulose via hydrogen bonds, to create polysaccharide microfibrils. Lignin mainly acts as adhesive or

binder that provides strength and structure to the cellular composites of the plant and protects against microorganism or chemical attack. It controls the fluid flow, acts as antioxidant by absorbing UV lights and stores energy. When lignin binds, it crosslinks with the regular structure of the microfibrils made of cellulose and hemicelluloses. The composition of lignocellulosic materials varies with several factors such as type of plant, growth conditions, on the part of plant, and on the age of harvesting.<sup>8-10</sup> The structural and composition details of the lignocellulosic materials have been discussed further in Appendix-A.

### **1.3 Conversion Routes for Lignocellulosic Biomass to Biofuels**

Lignocellulosic biomass consists of a variety of materials with distinctive physical and chemical characteristics. Typically it is categorized into either woody, herbaceous, or crop residues. Most of these biomass are already used, without preliminary conversion, as a fuel for heating purpose and also to produce steam for generating electricity. Direct combustion is best suited to biomass having low contents of moisture and ash. In fact, until the start of 20<sup>th</sup> century, biomass and coal were the major sources of fuels and chemicals. The recent energy crisis, fluctuating oil prices and political factors associated with the import of fossil fuels has brought the focus again on the utilization of abundantly available biomass resources for producing easy to handle forms of energy such as gases, liquids, and charcoal.<sup>11, 12</sup> Biomass may be converted to energy by many different processes, depending on the raw characteristics of the material and the type of energy desired. Figure 1.3 shows some of the major competing conversion pathways for converting the biomass to liquid fuel, chemicals and hydrogen.

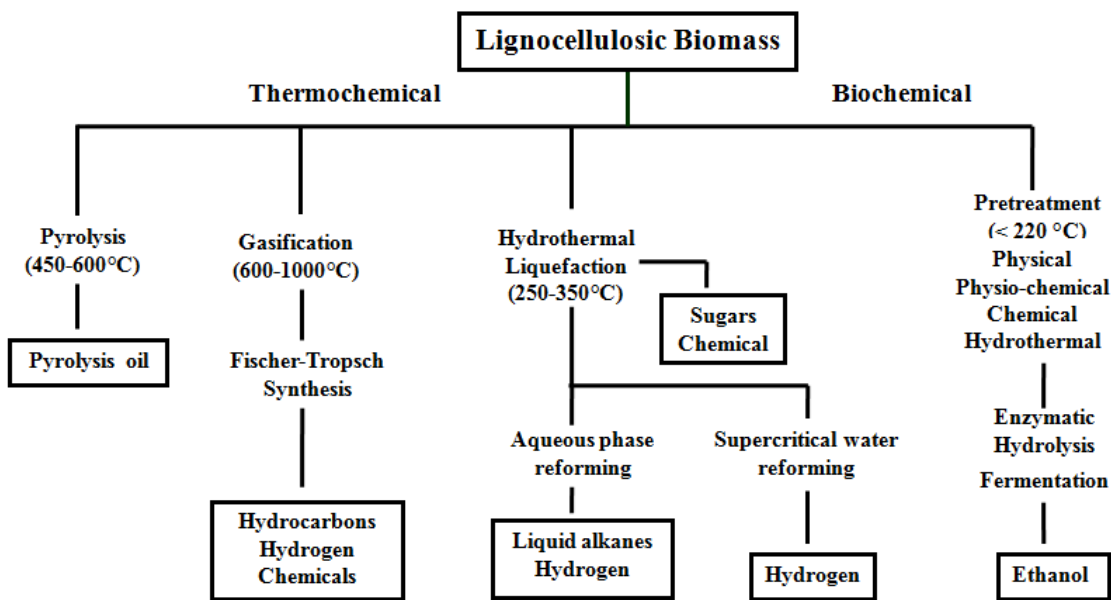


Figure 1.3 Major pathways for the conversion of biomass to biofuels.

### 1.3.1 Thermochemical Pathways

Thermochemical processes depend on the relationship between heat and chemical action as a means of extracting and creating products and energy. Pyrolysis, gasification, and liquefaction which are conducted at a temperature of several hundred degrees celsius are categorized in thermochemical processes.

**Pyrolysis:** Pyrolysis is defined as the thermal degradation of biomass in the absence of oxygen to produce condensable vapors, gases, and charcoal; in some instances a small amount of air may be admitted to promote this endothermic process. The products of pyrolysis can be gas, liquid, and/or solid. In flash pyrolysis, biomass is rapidly heated (e.g., at rates of 100-10,000°C/s) to 400-600°C, while limiting the vapor residence time to less than 2 seconds.<sup>13</sup> The oil production is maximized at the expense of char and gas. Pyrolysis processes typically use dry and finely ground biomass. Pyrolysis and direct liquefaction processes are sometimes confused with each other, and a simplified

comparison of the two follows. Both are thermochemical processes in which feedstock organic compounds are converted into liquid products. In the case of liquefaction, feedstock macro-molecules are decomposed into fragments of light molecules in the presence of a suitable catalyst. At the same time, these fragments, which are unstable and reactive, repolymerize into oily compounds having appropriate molecular weights.<sup>14</sup> With pyrolysis, on the other hand, a catalyst is usually unnecessary, and the light decomposed fragments are converted to oily compounds through homogeneous reactions in the gas phase. The differences in operating conditions for liquefaction and pyrolysis are shown in Table 1.1.

Table 1.1 Comparison of liquefaction and pyrolysis.

Process	Temperature (°C)	Pressure (MPa)	Biomass drying
Liquefaction	250-350	5-20	Not needed
Pyrolysis	450-600	0.1-0.5	Needed

*Gasification:* In gasification oxygen-deficient thermal decomposition of organic matter primarily produces synthesis gas. Gasification can be thought of as a combination of pyrolysis and combustion. Gasification has a good potential for near-term commercial application due to the benefits over combustion including more flexibility in terms of energy applications, higher economical and thermodynamic efficiency at smaller scales, and potentially lower environmental impact when combined with gas cleaning and refining technologies. An efficient gasifier decomposes high-molecular-weight organic compounds released during pyrolysis into low-molecular-weight, non condensable compounds in a process referred to as tar cracking. Undesirable char that is produced

during gasification participates in a series of endothermic reactions at temperatures above 800°C which converts carbon into a gaseous fuel. Typically gaseous products include: CO, H<sub>2</sub>, and CH<sub>4</sub>. Fisher-Tropsch synthesis can be used to convert the gaseous products into liquid fuels through the use of catalysts. Gasification requires feedstock that contains less than 10% moisture.<sup>15, 16</sup>

*Hydrothermal Liquefaction:* Hydrothermal liquefaction of biomass is conducted near (subcritical) or above (supercritical) the critical point of water (374°C, 22.1 MPa). Density and dielectric constant of the water medium play major role in solubilizing organic compounds in subcritical and supercritical water. Dielectric constant of water near the critical point decreases considerably, which enhances the solubility of organic compounds. Use of sub- and supercritical water (hydrothermal medium) for the liquefaction of biomass is one of the most promising technologies to produce aqueous carbohydrate solution (biocrude) derived from the direct liquefaction of biomass. Water acts both as a reactant and as a solvent. Water as reactant favors the hydrolysis reactions over thermal decomposition and rapidly degrades the polymeric structure of biomass components to water soluble products. The intermediates formed during the reactions show a high solubility in sub- and supercritical water; hence reaction steps are mainly homogeneous. Diffusion related problems such as mass transfer through the interface are not encountered in homogeneous reaction.<sup>17-19</sup> The process can utilize mixed biomass feedstock without any pretreatment at a comparatively low temperature. Moisture content of biomass is not an issue. Moreover, biomass residue generated from the any other processes can be utilized to produce biocrude.

### **1.3.2 Biochemical Pathways**

Biochemical processes takes place at ambient to slightly higher temperature levels using a biological catalyst to bring out the desired chemical transformation. Ethanol from lignocellulosic biomass is produced mainly via biochemical routes. The biomass is first pretreated by different pretreatment methods (discussed later) for the improving the accessibility of enzymes. After the pretreatment, biomass goes through the enzymatic hydrolysis for conversion of polysaccharides into monomer sugars such glucose, xylose etc. Subsequently sugars are fermented to ethanol by the use of different microorganisms. Pretreated biomass can directly be converted to ethanol by using the process called simultaneous saccharification and fermentation (SSF).<sup>20</sup> Therefore, pretreatment is a crucial step to overcome lignocellulose recalcitrance in the conversion of biomass to ethanol.<sup>21</sup> Pretreatment of biomass is necessary for enhancing the enzymatic hydrolysis of biomass. It alters the physical and chemical properties of biomass and improves the enzyme access and effectiveness by:

- Altering or removing lignin and hemicelluloses,
- Changing the crystallinity of cellulose,
- Removing acetyl groups from hemicelluloses,
- Reducing the degree of polymerization in cellulose, and
- Increasing internal surface area and pore volume.

### **1.4 Pretreatment Methods for Bioethanol**

Lignocellulosics mainly consist of cellulose, hemicelluloses and lignin which are bonded together by covalent bonding, various intermolecular bridges, and van der Waals forces forming a complex structure, making it resistant to enzymatic hydrolysis and

insoluble in water.<sup>22, 23</sup> Therefore, an efficient, less energy intensive and cost effective pretreatment method is a necessity for producing ethanol at economically viable cost. Different pretreatment methods are broadly classified into physical, chemical, physiochemical and biological processes.

#### **1.4.1 Physical**

Physical pretreatments such as chipping, grinding, ball milling and colloid milling are mainly done for size reduction, increasing surface area, and mechanical decrystallization of biomass.<sup>24-27</sup> It is not certain that the benefit derived from these mechanical treatments is because of reduction in crystallinity or increase in surface area.<sup>28</sup> The non mechanical methods such as high temperature, freeze/thaw cycles, and irradiation are attempted to change one or more structural features of the cellulose and enhance the hydrolysis. Most of these methods are limited in their effectiveness and often expansive.<sup>21, 24, 29, 30</sup>

#### **1.4.2 Chemical Pretreatments**

Chemical pretreatment employs the use of acid / alkali for fractionating biomass, increasing surface area and pore volume, and swelling cellulose. There may be two types of swelling of cellulose, intercrystalline and intracrystalline. Inercrystalline swelling can be affected by water, whereas intracrystalline swelling requires a chemical agent for breaking the hydrogen bonding of the cellulose. Some of the most commonly used pretreatment methods are discussed below.

*Dilute Acid Pretreatment:* Different acidic reagents such as dilute sulfuric acid, dilute nitric acid, dilute hydrochloric acid, dilute phosphoric acid and peracetic acid have been used for the pretreatment process. Dilute acid pretreatment mainly removes the

hemicellulose fractions from the lignocellulosics. The removal of hemicelluloses increases the porosity in the biomass and, thus, enzymatic accessibility to the cellulosic fractions is increased. Dilute acid is an efficient pretreatment method suitable for most of the lignocellulosic feedstock. Among the other dilute acids (sulfuric acid, hydrochloric, or nitric acids), dilute sulfuric acid (0.5-1.5%) above 160°C was found to be most suitable for the industrial application. The method fractionates majority of hemicelluloses (75-90%). Two approaches for dilute acid pretreatment are followed. In one approach high temperature (more than 160°C) in a continuous flow reactor with low solid loading is used, while in another approach, low temperature batch process is used with high solids loading. The major disadvantage of the process is the removal of acids or neutralization which yields a large amount of gypsum before next step of enzymatic hydrolysis. Although close to theoretical yields can be achieved, the process requires high capital cost coupled with corrosion problems, acid consumption and recovery costs.<sup>21, 24, 31-33</sup>

*Peracetic Acid ( $C_2H_4O_3$ ):* The use of peracetic acid (2-10%) at 25-75°C causes significant delignification of lignocellulosics due to the oxidizing action of peracetic acid. Reduction in crystallinity due to structural swelling and dissolution of crystalline cellulose are observed. The process retains majority of hemicelluloses in solids.<sup>21, 24</sup>

*Concentrated Sulfuric Acid:* Sulfuric acid is strong swelling and a hydrolyzing agent. Intracrystalline swelling of cellulose occurs at acid concentration between 62.5-70% and above 75%, dissolution and decomposition of cellulose takes place. The dissolved cellulose is re-precipitated by the addition of methanol or ethanol. After the treatment with 75% sulfuric acid, degree of polymerization (DP) of treated cellulose drops from 2150 to 300. The re-precipitated cellulose is easily hydrolyzed by acid or enzyme with

high conversions. Sulfuric acid can be reused after the distillation of methanol or ethanol. Large scale testing of this process is still needed to determine the permissible recycling of sulfuric acid.<sup>24</sup>

*Concentrated Phosphoric Acid:* Concentrated phosphoric acid (85%) has been applied earlier as a cellulose solvent. Phosphoric acid causes less degradation of the cellulose than other acids.<sup>34</sup> Recently, a novel method for lignocelluloses fractionation was applied to hardwoods as well as softwoods. The major advantage of the method lies in the moderate process condition (50°C and atmospheric pressure). Fractionation of lignocelluloses into highly reactive amorphous cellulose, hemicelluloses sugars, lignin and acetic acid was achieved. After the pretreatment, Enzymatic hydrolysis of Avicel and alpha-cellulose were completed within 3 h while corn stover and switchgrass were hydrolyzed to the extent of 94%.<sup>24,35</sup>

*Ionic Liquid:* Dissolution of cellulose in ionic liquid and subsequent regeneration as amorphous cellulose with the use of anti-solvent such as water, ethanol, or methanol has attracted some research interest. Hydrolysis of regenerated cellulose is significantly increased and the initial rates of hydrolysis are approximately an order of magnitude higher than that of untreated cellulose.<sup>36</sup> Nearly complete conversion of the carbohydrate fraction into water-soluble products is readily observed at 120°C in ionic liquids, which is much lower than the temperatures typically applied for aqueous-phase hydrolysis.<sup>37</sup> Cost and recycling of ionic liquid are the major disadvantage of the process.

*Alkali Pretreatment:* Among the various chemical pretreatments, alkali pretreatment is most widely used to enhance enzymatic hydrolysis of lignocellulose. Alkali treatment selectively removes majority of lignin and part of hemicelluloses, thus the success of

method depends on the amount of lignin in the biomass. The main reagents used for alkali pretreatment are sodium hydroxide, ammonia, calcium hydroxide, and oxidative alkali ( $\text{NaOH} + \text{H}_2\text{O}_2$  or  $\text{O}_3$ ). Dilute NaOH treatment causes disruption lignin and carbohydrate linkages, swelling of cellulose, removal of lignin and hemicelluloses, increase in surface area and decrease in the DP.<sup>30</sup> The mechanism is considered to be saponification of intermolecular ester bonds cross-linking the hemicelluloses and lignin. The optimum levels range between 5 and 8 g NaOH/100 g substrate. Process depends on the type of substrate. It was observed that digestibility of softwood with high lignin content increased slightly as compared to hardwoods.<sup>25</sup> Considering the cost of chemical, Holtzapple et al. used calcium hydroxide as alkali for pretreating corn stover and poplar, and applied a longer treatment time (few days) and low temperature. Similar to other alkaline pretreatment, calcium hydroxide causes large amount of delignification and increases the hydrolysis rate.<sup>24, 31, 38-40</sup>

*Ammonia:* Treatment with liquid ammonia was first patented in 1905.<sup>24</sup> Ammonia causes a strong swelling action and cellulose changes its crystal structure from cellulose I to cellulose III<sub>1</sub>. Ammonia shows high selectivity for lignin show majority of hemicelluloses is retained in the solids. Relatively low cost and possibility of recycling due to its volatile nature are the major advantages of this process. Two process based on aqueous ammonia known as ammonia recycle percolation (ARP) and soaking in aqueous ammonia (SAA) were used by Kim et al. to improve the hydrolysis of corn stover close to the quantitative maximum. ARP process also enhanced the enzymatic digestibility of poplar wood.<sup>21, 24, 41</sup>

*Organic Solvent:* Pretreatment using organic solvents with mineral acids as catalysts have been reported to an effective method of delignification of biomass. Organic solvents

break attacks the lignin carbohydrate bonds selectively and fractionates the lignin and hemicelluloses. Methanol, ethanol, acetone, ethylene glycol, triethylene glycol and tetrahydrofurfuryl alcohol have been used to dissolve the lignin from the biomass. Organic acids such as oxalic, acetylsalicylic, and salicylic acid can be used as catalysts. Organic solvents should be recycled for the cost effective use. Moreover, removal of organic solvents from the system after pretreatment is necessary because solvents may be inhibitory to the growth of organisms, enzymatic hydrolysis, and fermentation.

#### **1.4.3 Hydrothermal Pretreatment**

Hydrothermal pretreatment uses hot water at elevated pressure (more than saturation pressure) to ensure that water remain in liquid phase. Water acts as a solvent and as a reactant at the same time. Water as reactant is seen as a promising path to green chemistry by providing alternatives to corrosive acids and toxic solvents.<sup>42</sup> Dielectric constant of water decreases with temperature, and water behaves like a more non-polar solvent. Ionization constant of water increases with temperature below critical point. Such changes in properties of water with temperature lead to the cleavage of ether and ester bonds and favor the hydrolysis of hemicelluloses. Hydrothermal treatment of lignocellulosic biomass generates acid that arises from the thermally labile acetyl groups of hemicelluloses and catalyzes the hydrolysis of hemicelluloses and subsequent solubilization. Xylose recovery from biomass can be achieved as high as 88-98%. The structural alterations due to the removal of hemicelluloses increase the accessibility and enzymatic hydrolysis of cellulose. Process liberates organic acids from the biomass, and pH of the reaction medium decreases during the treatment. To avoid the formation of inhibitors, the pH should be kept between 4 and 7 during the pretreatment. Maintaining

the pH between 4 and 7 minimizes the formation of monosaccharides, and therefore also the formations of degradation products that can further catalyze hydrolysis of the cellulosic material during pretreatment.<sup>7, 21, 24, 43-46</sup>

#### **1.4.4 Physiochemical Pretreatments**

Some of the pretreatment methods combine physical and chemical methods. High pressure steaming, with or without rapid decompression (explosion) is considered one of the most successful method option for fractionating wood into its three major components.

*Steam Treatment (Autohydrolysis) and Steam Explosion:* Heating of biomass in the presence of steam-saturated water (about 200°C and 1.5 MPa) leads to organic acid generation. The evolved acid hydrolyzes some of the hemicelluloses and alters the lignin structure. The structural changes in biomass after the treatment enhance its enzymatic digestibility.<sup>21</sup>

If, autohydrolysis is followed by rapid pressure release, the liquid water inside the biomass explosively vaporizes which shatters the biomass in popcorn like effect and thus, increases surface area. This approach combines both chemical and pretreatment into one step. Steam explosion is the widely used method for pretreatment of biomass. The process is conducted typically between temperature 190 to 220°C and pressure 1.2 to 4.1 MPa. Low energy input and negligible environmental effects are the major advantages of the process. However, steam explosion does not always break down all the lignin, requires small particle size, and also produces some inhibitory compounds for further enzymatic hydrolysis and fermentation steps.<sup>21, 24, 47-49</sup> Sometimes the addition of sulfur dioxide or carbon dioxide during steam explosion treatment further improves the

enzymatic hydrolysis of biomass by making the pretreatment environment more acid. SO<sub>2</sub> forms sulfuric acid and CO<sub>2</sub> forms the carbonic acid. The limitation of these methods is the lower yield of hemicellulose sugars.<sup>31</sup>

*Ammonia Fiber Explosion (AFEX):* In AFEX process, a batch of lignocelluloses is contacted with ammonia at high loadings and elevated temperature and pressure. After the reaction, the pressure is explosively released (similar to steam explosion) to disrupt the biomass structure. The physical disruption due to decompression and alkaline hydrolysis improves the enzymatic hydrolysis of biomass. Most of the ammonia (up to 99%) can be recovered for reuse.<sup>21</sup> The AFEX treatment does not solubilize much of the hemicellulose and effectively results in higher sugar yield than acid catalyzed steam explosion. AFEX was found very effective for pretreatment of low lignin substrate (Agriculture residue, herbaceous crops and grasses).<sup>31, 50, 51</sup>

*Supercritical Carbon Dioxide (CO<sub>2</sub>) Pretreatment:* Supercritical carbon dioxide (critical point, 31°C and 7.4 MPa) is nontoxic and relatively cheaper pretreatment agent. The method has several advantages such as low pretreatment temperatures, easy recovery of CO<sub>2</sub>, and high solids loading. Though the process showed good results for Avicel, the low effectiveness for lignocellulosic biomass is the major drawback.<sup>24</sup>

Appendix B summarizes the variety of pretreatment methods and process conditions.

## 1.5 Supercritical Fluid Technology

The unique physiochemical properties of dense supercritical fluids provide an attractive medium for chemical reactions and other processes. Fluids near critical points have solvent power comparable to that of liquids and are much more compressible than

dilute gases. The transport properties of such fluids lie intermediate between gas- and liquid-like. Supercritical fluids are attracting much attention in various fields of science and technology. In the last decades, the number of applications has increased continuously in several areas such as:

- Supercritical critical water and carbon dioxide as an alternative solvents for chemical reactions,
- Supercritical fluid extraction and purification,
- Fine particle production by supercritical antisolvent (SAS) and rapid expansion of supercritical solutions (RESS),
- Supercritical fluid chromatography for analytical applications,
- Supercritical steam cycle technology for power plants.

Supercritical fluids can be advantageously exploited in environmentally benign separation and reaction processes, as well as for new kinds of materials processing. Although laboratory scale studies show excellent results, there are relatively few processes in industrial scale. The high pressure processes are generally expansive to design, built, operate, and maintain. Therefore, scaling up from laboratory to industrial scale of such processes can only be successful if clear benefits can be achieved in terms of high efficiency, conversion ratios, product quality, and cost advantages over the conventional processes.<sup>52-54</sup>

## **1.6 Sub- and Supercritical Water (hydrothermal treatment)**

Water is an ecologically safe and abundantly available solvent in nature. Water has a relatively high critical point (374°C and 22.1 MPa) because of the strong interaction between the molecules due to strong hydrogen bond. Liquid water below the critical point

is referred as subcritical water whereas water above the critical point is called supercritical water. Density and dielectric constant of the water medium play major role in solubilizing different compounds. Water at ambient conditions (25°C and 0.1 MPa) is good solvent for electrolytes because of high dielectric constant 78.5), whereas most organic matters are poorly soluble at this condition.

As water is heated, the H-bonding start weakening, allowing dissociation of water into acidic hydronium ions ( $\text{H}_3\text{O}^+$ ) and basic hydroxide ions ( $\text{OH}^-$ ). Structure of water changes significantly near the critical point because of the breakage of infinite network of hydrogen bonds and water exists as separate clusters with a chain structure.<sup>55</sup> In fact, dielectric constant of water decreases considerably near the critical point, which causes a change in the dynamic viscosity and also increases self-diffusion coefficient of water.<sup>56</sup>

Supercritical water has liquid-like density and gas-like transport properties, and behaves very differently than it does at room temperature. For example, it is highly non-polar, permitting complete solubilization of most organic compounds and oxygen. The resulting single-phase mixture does not have many of the conventional transport limitations that are encountered in multi-phase reactors. However, the polar species present, such as inorganic salts, are no longer soluble and start precipitating. The physiochemical properties of water, such as viscosity, ion product, density, and heat capacity, also change dramatically in the supercritical region with only a small change in the temperature or pressure, resulting in a substantial increase in the rates of chemical reactions. It is interesting to see (Figure 1.4) that the dielectric behavior of 200°C water is similar to that of ambient methanol, 300°C water is similar to ambient acetone, 370°C water is similar to methylene chloride, and 50°C water is similar to ambient hexane.

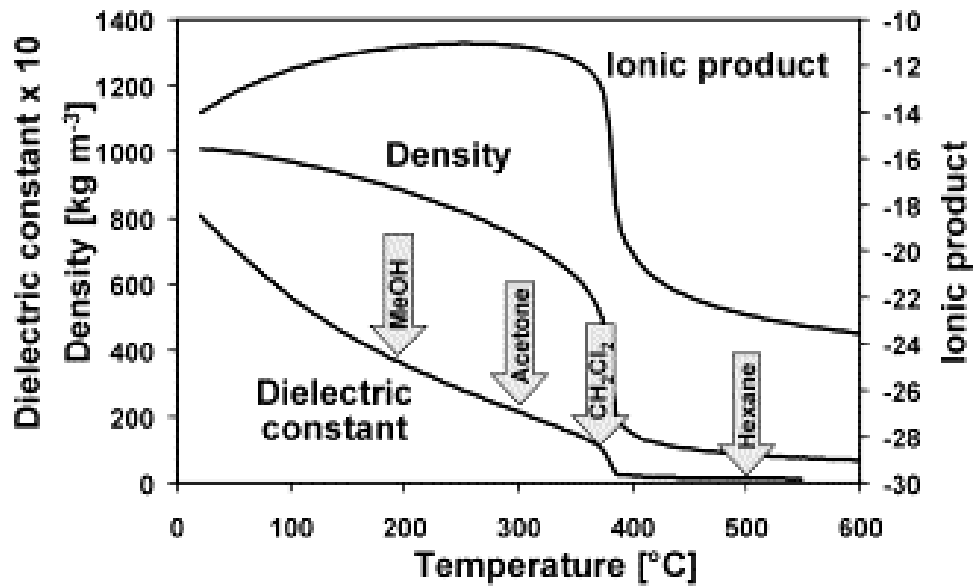


Figure 1.4 Physical properties of water with temperature, at 24 MPa (Kritzer et al.).<sup>57</sup>

In addition to the unusual dielectric behavior, transport properties of water are significantly different than the ambient water as shown in Table 1.2.

Table 1.2 Comparison of ambient and supercritical water.

	Ambient water	Supercritical water
Dielectric constant	78	< 5
Solubility of organic compounds	Very low	Fully miscible
Solubility of oxygen	6 ppm	Fully miscible
Solubility of inorganic compounds	Very high	~ 0
Diffusivity (cm <sup>2</sup> s <sup>-1</sup> )	10 <sup>-5</sup>	10 <sup>-3</sup>
Viscosity (g cm <sup>-1</sup> s <sup>-1</sup> )	10 <sup>-2</sup>	10 <sup>-4</sup>
Density (g cm <sup>-3</sup> )	1	0.2 - 0.9

## **1.7 Sub- and Supercritical Water Technology for Biofuels**

Hydrothermal media, which can be broadly defined as water-rich phase above 200°C (sub- and supercritical water) offers several advantages over other biofuel production methods.<sup>19</sup> Some of the major benefits are

- High energy and separation efficiency (since water remains in liquid phase and the phase change is avoided),
- High throughputs,
- Versatility of chemistry (solid, liquid and gaseous fuels),
- Reduced mass transfer resistance in hydrothermal conditions,
- Improved selectivity for the desired energy products (methane, hydrogen, liquid fuel) or biochemicals (sugars, furfural, organic acids etc),
- Ability to use mixed feedstock as well as wet biomass,
- No need to maintain specialized microbial cultures,
- Products are completely sterilized with respect to any pathogens including biotoxins, bacteria or viruses, and
- Processing of post fermentation residues.

Hydrothermal treatment can be applied to produce solid (biochar), liquid (bioethanol, biocrude), and gaseous (methane, hydrogen) fuels depending on the processing temperature and pressure as shown in Figure 1.5.

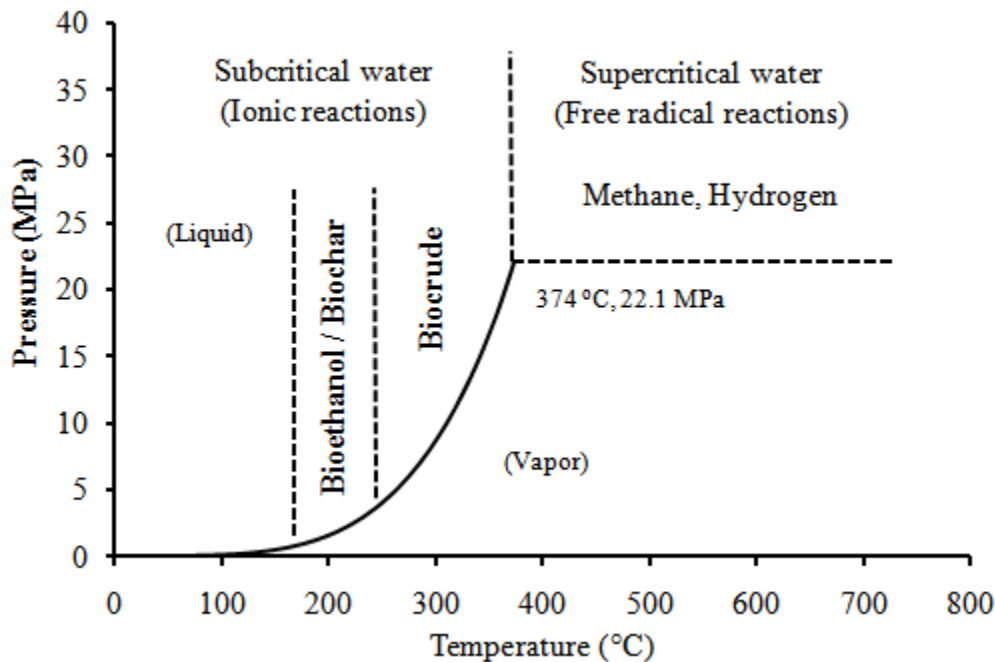


Figure 1.5 Hydrothermal treatment application referenced to pressure-temperature phase diagram of water.

The substantial changes in the physical and chemical properties of water in the vicinity of its critical point can be utilized advantageously for converting lignocellulosic biomass to desired biofuels.<sup>19, 58</sup> In fact, reactions in subcritical and supercritical water also provide a novel medium to conduct tunable reactions for the synthesis of specialty chemicals from biomass.<sup>59</sup>

In the subcritical region, the ionization constant ( $K_w$ ) of water increases with temperature and is about three orders of magnitude higher than that of ambient water (Figure 1.4) and the dielectric constant ( $\epsilon$ ) of water drops from 80 to 20.<sup>60</sup> A low dielectric constant allows subcritical water to dissolve organic compounds, while a high ionization constant allows subcritical water to provide an acidic medium for the hydrolysis reactions. These ionic reactions can be dominant because of the liquid-like

properties of subcritical water. Moreover, the physical properties of water, such as viscosity, density, dielectric constant and ionic product, can be tuned by small changes in pressure and/or temperature in subcritical region.<sup>61-63</sup> In the supercritical region, density of water drops down to lower value. This means that ionic product of water is much lower and ionic reactions are inhibited because of the low relative dielectric constant of water. The lower density favors free-radical reactions, which may be favorable for gasification.<sup>18</sup> The following sections discusses about application of hydrothermal medium properties for biochar, bioethanol, biocrude, and gaseous fuel production.

### 1.7.1 Biochar

Biochar is the carbon rich, high energy density solid product resulting from the advanced thermal degradation of organic materials such as wood, manure, agricultural residues etc. The less fibrous structure and high calorific value of biochar similar to that of coal makes it an excellent candidate for solid fuel. Biochar is highly resistant to decomposition upon land application and has a number of positive effects relating to soil fertility.<sup>64</sup> Pyrolysis and hydrothermal carbonization (HTC) are the two main processes for the production of biochar. Pyrolysis typically utilizes high quality dry biomass for biochar production where air pollution is primary concern during traditional pyrolysis operation due to the emission of volatile compounds. The HTC is an environment friendly and promising process that uses water as solvent. Besides being simple process, HTC has a number of other practical advantages. The HTC process does not require dry biomass and also the final product can be easily filtered from the reaction solution. This way, complicated drying schemes and costly separation procedures are conceptually avoided.

The biomass feedstock typically contains 40-60% oxygen. Therefore, the removal of oxygen from biomass is the major objective for upgrading its energy density during biochar production. This objective can be accomplished by the removal of oxygen by dehydration, which removes oxygen in the form of water, and by decarboxylation, which removes oxygen in the form of carbon dioxide. Thermodynamically, water is fully oxidized compound and has no residual heating value. Therefore, water makes an ideal medium for conducting such reactions. Even in the excess of water, biomass undergoes dehydration reaction at elevated temperature and pressure.<sup>19</sup> As discussed earlier, the ionization constant of water increases with temperature and near-critical point, the amount of dissociation is three times what it would be at normal temperatures and pressures. Due to the increased ionization of water at elevated temperature, the biomass components undergo depolymerization mainly by hydrolysis reactions. The temperature region 180-250°C in the phase diagram of water (Figure 1.5) can effectively be utilized for the production of biochar from biomass. The longer reaction time of the order of several hours is typically needed for the substantial removal of oxygen by dehydration and for the subsequent breakdown of the fibrous structure of biomass. The dehydration of biomass at lower temperature can be accelerated by the addition of small amount of acids.

### **1.7.2 Bioethanol**

Pretreatment of lignocellulosic biomass is viewed as a critical step to make the cellulose accessible to enzymes for achieving an economical yield of fermentable sugars for bioethanol production. As discussed earlier, there are several chemical pretreatment methods are available. But these methods are associated with serious the economic and

environmental constraints due to the heavy use of chemicals.<sup>65, 66</sup> Hydrothermal pretreatment of biomass is a non-toxic, environmentally benign and inexpensive medium for chemical reactions. Process mainly removes hemicelluloses and a part of lignin. The resulting structural change, increased surface area, and increased pore volume of pretreated biomass helps in the acceleration of the rate of enzymatic hydrolysis as well as product yield. The increased ionization constant of water in 180-220°C regions (Figure 1.5) can potentially be used for the fractionation of hemicelluloses. Since, no chemical is used during the process; the hydrolyzate can be combined with biomass fraction after pH conditioning for fermentation.

### 1.7.3 Biocrude

Biocrude is defined as an aqueous carbohydrate solution (oxygenated hydrocarbon) produced from the hydrothermal liquefaction of biomass. Lignocellulosics mainly consist of cellulose, hemicelluloses and lignin. Among that approximately 75% of the dry weight of herbaceous and woody biomass is composed of holocellulose.<sup>67</sup> Hydrolysis of cellulose in hydrothermal medium has been studied extensively. The earlier studies show that subcritical and supercritical water can be used under a variety of conditions to rapidly (order of seconds) liquefy cellulose to sugar and its degradation products.<sup>59, 68, 69</sup> Hemicellulose, an amorphous structure is much more susceptible than cellulose to hydrothermal extraction and hydrolysis. It is easily dissolved in water at temperature about 180°C. Hemicelluloses have been successfully extracted upto 95% of its fraction as monomeric sugar and sugar products in hydrothermal medium in the range of 200-230°C in a very short reaction time.<sup>7, 70</sup> Low activation energy of lignin causes substantial degradation of lignin in hydrothermal medium at temperature below 200°C.

Reaction proceeds through the cleavage of aryl ether linkages, fragmentation, and dissolution.<sup>7</sup> Lignin depolymerization yields low molecular weight fragments having very reactive functional groups such as syringols, guaiacols, catechols and phenols.<sup>71</sup> The density of water within the hydrothermal medium has been found to be a key parameter in deciding the product pathways.<sup>19</sup>

The results of liquefaction studies on model compounds and the actual biomass in hydrothermal medium provides an opportunity for converting biomass to biocrude and other important chemicals. The hydrothermal medium (subcritical water) in the range of 250-350°C regions (Figure 1.5) is a favorable condition for conducting ionic reactions. In general, hydrothermal liquefaction conditions range from 250-380°C, 7 to 30 MPa with liquid water present, often in presence of alkaline catalyst.<sup>19</sup>

Biocrude derived from the direct liquefaction of biomass can be converted to liquid fuel, hydrogen gas or chemicals. Aqueous phase reforming processes have been successfully utilized for converting the biomass derived water soluble carbohydrates to liquid alkanes and hydrogen.<sup>67, 72, 73</sup> Preliminary studies on the conversion of various biomass types into liquid fuels have indicated that hydrothermal liquefaction is more attractive than pyrolysis or gasification. In these studies, typically 25% biomass slurry in water is treated at temperatures of 300–350°C and 12-18 MPa pressures for 5-20 min to yield a mixture of liquid, gas (mainly CO<sub>2</sub>) and water. The liquid is a mixture with a wide molecular weight distribution and consists of various kinds of molecules. A large proportion of the oxygen is removed as carbon dioxide and the resulting biocrude contains only 10-13% oxygen, as compared to 40% in the dried biomass.<sup>74</sup>

Karagoez et al. investigated the distribution of hydrothermal liquefaction (280°

for 15 min) products, i.e. liq., gas and solid from wood (sawdust) and non-wood biomass (rice husk), and major biomass components, i.e. lignin, cellulose produced by and analyzed the liquid hydrocarbons (oils) for the differences in the hydrocarbon composition with respect to feed material. Cellulose showed the highest conversion among the four samples investigated. Sawdust and rice husk had almost similar conversions. Liquid products were recovered with various solvents (ether, acetone, and ethyl acetate) and analyzed by GC-MS. The oil (ether extract) from the hydrothermal treatment of cellulose consisted of furan derivatives whereas lignin-derived oil contained phenolic compounds. The composition of oils (ether extract) from sawdust and rice husk contained both phenolic compounds and furans, however phenolic compounds were dominant. Rice husk derived oil consists of more benzenediols than sawdust derived oil. The volatility distribution of oxygenated hydrocarbons were carried out by C-NP gram and it showed that the majority of oxygenated hydrocarbons from sawdust, rice husk and lignin were distributed at n-C<sub>11</sub>, whereas they were distributed at n-C<sub>8</sub> and n-C<sub>10</sub> in cellulose-derived oil. The gaseous products were carbon dioxide, carbon monoxide, methane in sawdust, rice husk, lignin and cellulose.<sup>75, 76</sup>

Demirbas have reviewed the possible mechanism of liquefaction. Organic materials are converted to liquefied products through a series of physical and chemical changes such as solvolysis, depolymerization, dehydration, and decarboxylation. Solvolysis is a type of nucleophilic substitution where the nucleophile is a solvent molecule. This reaction results in micellar-like substructures of the feedstock. Depolymerization reactions lead to smaller molecules. Decarboxylation and dehydration

leads to new molecules and the formation of carbon dioxide through splitting off of carboxyl groups.<sup>14</sup>

#### 1.7.4 Hydrothermal Gasification

Relatively fast hydrolysis of biomass in hydrothermal medium leads to a rapid degradation of polymeric structure of biomass. The subsequent reactions also are rather fast, which leads to gas formation at relatively lower temperature compared to dry processes.<sup>77</sup> Above the critical point, the lower density of supercritical fluid favors free radical reactions and makes the reaction conditions conducive for the formation of methane and hydrogen gas.<sup>18</sup> Biomass is gasified to mainly methane and carbon dioxide in the presence of an added heterogeneous catalyst in near critical or supercritical water (350-400°C). At higher temperature in supercritical water (Figure 1.5), biomass is converted to hydrogen rich gas without catalyst or with non metal catalysts.<sup>78</sup> As discussed earlier, part of lignin and hemicelluloses fraction of biomass undergo solvolysis within few minutes of the exposure to hydrothermal medium. The hydrothemolysis of remaining biomass fractions occurs at somewhat higher temperature. The initial products subsequently undergo a variety of isomerization, dehydration, fragmentation, and condensation reactions, that ultimately form gas and tars.<sup>79</sup>

### 1.8 Challenges of Hydrothermal Processing

Although in laboratory experiments excellent results have been achieved and the technology possesses many potential benefits over the conventional methods of processing biomass to biofuels or chemicals, there are certain issues, which need to be addressed.

- *Biomass feeding at high pressure:* As a “rule of thumb”, the solid loading in

excess of 15-20 wt% is considered economical on commercial point of view.

Feeding slurries at high pressure is always challenging especially for the lab scale studies since low capacity slurry pumps are rarely available. Pumping slurry at large scale is less of a problem, where progressive cavity or similar pumps are commercially available.

- *Salt precipitation:* Plugging of reactors caused by the precipitation of inorganic salts above supercritical temperature and low density conditions. At room temperature, water is an excellent solvent for most salts. On the other hand, solubility of most salts in very low (typically 1-100 ppm) in supercritical water (low density) and precipitating salts may plug the reactors even at high flow velocities.<sup>80</sup> However, the problem may be used as an opportunity to produce a valuable fertilizer by-product of the process, if managed properly.
- *Corrosion:* The halogens sulfur, or phosphorous present in the organic matters are converted to the respective acids, which may cause severe corrosion on the reactor wall under harsh reaction conditions. The corrosion problem can be reduced or avoided by selecting the right material of construction and or a slightly modified reactor concept.
- *Coking and deactivation of heterogeneous catalyst:* Some catalyst supports degrades or oxidize in hydrothermal conditions. Decline in catalyst activity is also observed with long period of exposure of catalyst during continuous process.<sup>19</sup>

## 1.9 Research Plan

This research study focuses on the fundamental understanding of the reactions involved during hydrothermal treatment (sub- and supercritical water) of lignocellulosic

biomass. A good amount of work has been done on biomass pyrolysis, this knowledge base would be utilized in deciphering the mechanisms, while allowing for the alterations due to the presence of water as a solvent and high pressure. An experimental facility for conducting high temperature and high pressure (sub- and supercritical water) reactions in continuous and semi-continuous flow, and batch mode will be designed and tested. Following main objectives are being pursued in this study to apply hydrothermal treatment technology for biofuels applications:

### **1.9.1 Hydrothermal Pretreatment of Biomass for Bioethanol**

Pretreatment of biomass is an important step in bioethanol production. Subcritical water as an effective pretreatment medium for biomass is gathering considerable attention. However, a clear fundamental understanding is lacking. To compliment, the aim of this study is to carry out a fundamental study on how subcritical water condition affect the structure and enzymatic digestibility of biomass. Cellulose, switchgrass (herbaceous grass), and corn stover (agricultural residue) are chosen for the study. In this work, specifically, the effect of temperature on the cellulose structure and its reactivity with the cellulase enzyme are studied. The study will help in understanding the fate of cellulose molecule during subcritical water pretreatment and will provide key design parameters for optimization of the process.

### **1.9.2 Hydrothermal Liquefaction for Biocrude**

Liquefaction of biomass in hydrothermal medium provides an environmentally benign method for converting biomass to biocrude and other important chemicals. The process requires a fundamental understanding of the reactions involved. Most of the work is done in the batch reactors. Kinetics obtained from the batch reactor often can give

misleading information on the design for industrial level continuous reactors. The main aim of this study is to examine the possibilities of maximizing hydrolysis products (sugar) yields from the liquefaction of cellulose and switchgrass (an energy crop) in a flow reactor.

Another objective of this study is to examine the effect of alkali on the liquefaction temperature and also, examine the behavior of solid residues for understanding the nature of thermochemical liquefaction. In heterogeneous catalysis, high surface is obtained by reducing particle or pore size. One can think about using nanoparticles of alkali as catalysts, but these particles will dissolve in the ambient feed water and the later precipitate to form large particles during the heating. A method for in-situ generation of catalyst nanoparticles in supercritical water, using antisolvent precipitation concept will be applied as shown in Figure 1.6. The method has already been successfully tested for sodium carbonate.<sup>81</sup> The concept will be applied to the biomass liquefaction in hydrothermal reactor as shown below:

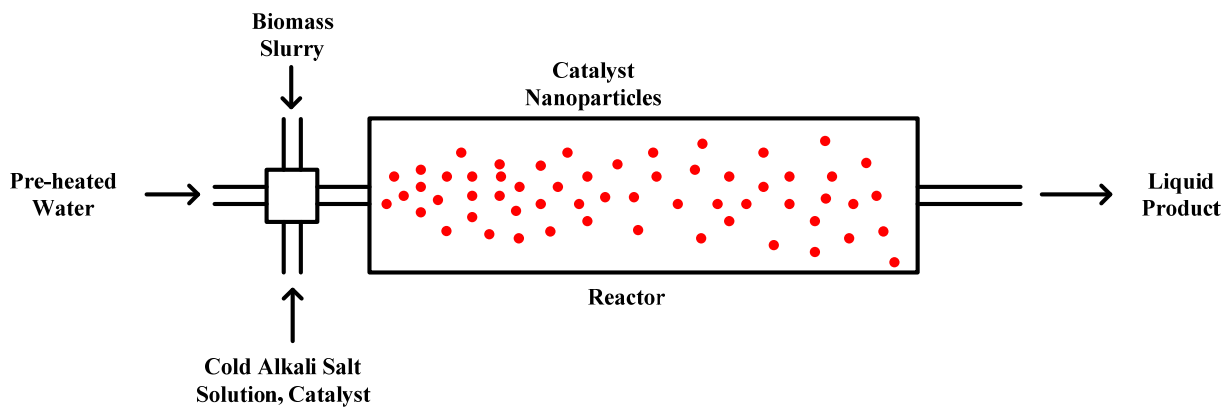


Figure 1.6 Generation of in-situ alkali catalyst nanoparticles in hydrothermal reactor.

The solution of alkali salt in ambient water is injected directly to the reactor. Due

to the insolubility in supercritical water, the alkali salts precipitate out rapidly as nanoparticles. The key is rapid precipitation due to the high diffusivity of the supercritical water and sudden heating upon mixing. The produced nanoparticles will provide a high surface area. In addition, the newly generated alkali particle surface is highly catalytic due to the high surface roughness.

### **1.9.3 Hydrothermal Carbonization for Biochar**

The hydrothermal carbonization process, a traditional but recently revived method, presents superior characteristics that make it a promising route of wide potential application for converting biomass to biochar. The conversions of biomass in hydrothermal conditions are widely examined process with the aim for the recovery of liquid or gaseous fuel intermediates (e.g. Glucose, 5-hydroxymethylfurfural, methane, hydrogen etc.) from biomass. The solid residues from such process are mostly treated as undesirable by-products. However, the acceleration of coalification in HTC process by a factor of  $10^6$ - $10^9$  under rather soft conditions, down to a scale of hours, makes it a considerable, technically-attractive alternative for the sequestration of carbon from biomass on large and ultra-large scales. Essentially, all forms of biomass can be converted to biochar. Forest thinning, herbaceous grasses, crop residues, manure, and paper sludge are some of the potential feedstock. Presence of inorganic trace elements (K, Ca, Si, P etc) and lignin content can affect the biochar yield.<sup>82</sup>

In general, biochar is produced by heating biomass dispersion in water around 200°C in a closed reaction vessel in the presence of a weak acid catalyst for 4-24 h. Under acidic conditions and below 200°C, most of the original carbon stays bound to the final structure. In this work, switchgrass, a major energy crop, is processed by HTC

method for high energy density biochar production. Besides optimizing the process parameters for producing high energy density product, the research work will focus on enhancing the rate of coalification / dehydration. The process can provide a promising route for carbonaceous functional materials and higher energy density fuel for use in a variety of applications.

## 1.10 References

1. Farrell, A. E.; Plevin, R. J.; Turner, B. T.; Jones, A. D.; O'Hare, M.; Kammen, D. M., Ethanol can contribute to energy and environmental goals. *Science* **2006**, 311, 506-508.
2. Pastircakova, K., Determination of trace metal concentrations in ashes from various biomass materials. *Energy Edu. Sci. Technol.* **2004**, 13, 97-104.
3. <http://www-cta.ornl.gov/data/chapter1.shtml>. (Feb, 2010)
4. Perlack, R. D.; Wright, L. L.; Turhollow, A. F.; Graham, R. L.; Stokes, B. J.; Erbach, D. C. *Biomass as feedstock for a bioenergy and bioproducts industry: The technical feasibility of a billion-ton annual supply*; US Department of Energy US Department of Agriculture: 2005.
5. <http://www.nrel.gov>. (Feb, 2010).
6. Jarvis, M., Chemistry: Cellulose stacks up. *Nature* **2003**, 426, 611-612
7. Bobleter, O., Hydrothermal degradation of polymers derived from plants. *Prog. Polym. Sci.* **1994**, 19, 797–841.
8. Meister, J. J., Chemical modification of lignin. In *Chemical modification of lignocellulosic materials*, Hon, D. N.-S., Ed. Marcel Dekker Inc.: 1996; pp 129-157.

9. Olsson, L.; Jorgensen, H.; Krogh, K. B. R.; Roca, C., Bioethanol production from lignocellulosic material. In *Polysaccharides: Structural diversity and functional versatility*, second ed.; Dumitriu, S., Ed. Marcel Dekker: 2005; pp 957-993.
10. Falkehag, S. I., Synthesis of phenolic polymer. *Appl. Polym. Symp.* **1975**, 28, 247-257.
11. Zhang, B.; Huang, H.-J.; Ramaswamy, S., Reaction Kinetics of the hydrothermal treatment of lignin. *Appl Biochem Biotechnol* **2008**, 147, 119-131.
12. Knill, C. J.; Kennedy, J. F., Cellulosic biomass-derived products. In *Polysaccharides: Structural diversity and functional versatility*, Dumitriu, S., Ed. Marcel and Dekker: 2005; pp 937-956.
13. Balat, M., Mechanisms of thermochemical biomass conversion processes, Part 1: Reactions of pyrolysis. *Energy Sources, Part A* **2008**, 30, 620-635.
14. Demirbas, A., Mechanisms of liquefaction and pyrolysis reactions of biomass. *Energy Conversion and Management* **2000**, 41, 633-646.
15. Ni, M.; Leung, D. Y. C.; Leung, M. K. H.; Sumathy, K., An overview of hydrogen production from biomass. *Fuel Processing Technology* **2006**, 87, 461-472.
16. Jong, W. d., Sustainable hydrogen production by thermochemical biomass processing. In *Hydrogen Fuel: Production, transport and storage*, Gupta, R. B., Ed. CRC Press: 2009; pp 185-225.
17. Galkin, A. A.; Lunin, V. V., Subcritical and supercritical water: a universal medium for chemical reactions. *Russian chemical reviews* **2005**, 74, (1), 21-35.
18. Kruse, A.; Gawlik, A., Biomass conversion in water at 330-410 °C and 30-50 MPa: Identification of key compounds for indicating different chemical reaction

- pathways. . *Ind. Eng. Chem. Res.* **2003**, 42, 267-269.
19. Peterson, A. A.; Vogel, F.; Lachance, R. P.; Froling, M.; Michael Jerry Antal, J.; Tester, J. W., Thermochemical biofuel production in hydrothermal media:A review of sub- and supercritical water technologies. *Energy and Environmental Science* **2008**, 1, 32-65.
20. Ghosh, T. K.; Roychoudhury; Ghosh, P., Simultaneous saccharification and fermentation (SSF) of lignocellulosics to ethanol under vacuum cycling and step feeding. *Biotechnol. Bioeng.* **1984**, 26, 377-381.
21. Sierra, R.; Smith, A.; Granda, C.; Holtzapple, M. T., Producing fuels and chemicals from lignocellulosic biomass. *Chemical Engineering Progress* August, 2008, pp S10-S18.
22. O'Sullivan, A. C., Cellulose: the structure slowly unravels. *Cellulose* **1997**, 4, (3), 173-207.
23. Schacht, C.; Zetzl, C.; Brunner, G., From plant materials to ethanol by means of supercritical fluid technology. *Journal of Supercritical Fluids* **2008**, 46s (3), 299-321.
24. Laxman, R. S.; Lachke, A. H., Bioethanol from lignocellulosic biomass, Part 1: Pretreatment of the substrates. In *Handbook of plant-based biofuels*, Pandey, A., Ed. CRC Press: 2008; pp 121-139.
25. Millet, M. A.; Baker, A. J.; Scatter, L. D., Physical and chemical pretreatment for enhancing cellulose saccharification. *Biotech. Bioeng. Symp.* **1976**, 6, 125-153.
26. Caufield, D. F.; Mooer, W. E., Effect of varying crystallinity of cellulose on enzymic hydrolysis. *Wood Science and Technology* **1974**, 6, (4), 375–379.
27. Sintsyn, A. P.; Gusakov, A. V.; Vlasenko, E. Y., Effect of structural and physico-

- chemical features of cellulosic substrates on the efficiency of enzymatic hydrolysis. *Appl. Biochem. Biotechnol.* **1991**, 30, 43-59.
28. Chang, V. S.; Holtapple, M. T., Fundamental factors affecting biomass enzymatic reactivity. *Applied Biochemistry and Biotechnology* **2000**, 84, 5-37.
29. Chang, M. M.; Chou, T. Y. C.; Tsao, G. T., Structure, Pretreatment and Hydrolysis of Cellulose. *Adv. In Biochem. Eng.* **1981**, 20, 15-42.
30. Fan, L. T.; Lee, Y. H.; Gharpuray, M. M., The nature of lignocellulosics and their pretreatments for enzymatic hydrolysis. *Adv. Biochem. Eng.* **1982**, 23, 157-187.
31. Gupta, R. Alkaline pretreatment of biomass for ethanol production and understanding the factors influencing the cellulose hydrolysis. Auburn University, Auburn, 2008.
32. Grohmann, K. R.; Torget, R.; Himmel, M., Dilute acid pretreatment of biomass at high solids concentrations. *Biotechnology and Bioengineering Symposium* **1985**, 15, 59-80.
33. Torget, R.; Himmel, M.; Grohmann, K., Dilute-acid pretreatment of two short-rotation herbaceous crops. *Applied Biochemistry and Biotechnology* **1992**, 34/35, 115-123.
34. Welseth, C. S., Influence of fine structure of cellulose on the action of cellulases. *TAPPI* **1952**, 35, 233-238.
35. Zhang, Y.-H. P.; Ding, S.-Y.; Mielenz, J. R.; Cui, J.-B.; Elander, R. T.; Laser, M.; Himmel, M. E.; McMillan, J. R.; Lynd, L. R., Fractionating recalcitrant lignocellulose at modest reaction conditions. *Biotech. Bioeng.* **2007**, 97, 214-223.
36. Dadi, A. P.; Varanasi, S.; Schall, C. A. In *A novel inic liquid pretreatment strategy*

*to achieve enhanced cellulose saccharification kinetics*, AIChE Annual meeting, San Francisco, CA, 2006; AIChE: San Francisco, CA, 2006.

37. Sievers, C.; Valenzuela-Olarte, M. B.; Marzialetti, T.; Musin, I.; Agrawal, P. K.; Christopher; Jones, W., Ionic-Liquid-Phase Hydrolysis of Pine Wood. *Ind. Eng. Chem. Res.* **2009**, 48, (3), 1277-1286.
38. Playne, M. J., Increased digestibility of bagasse by pretreatment with alkalis and steam explosion. *Biotechnol. Bioeng.* **1984**, 26, 426-433.
39. Chang, V. S.; Nagwani, M.; Kim, C. H.; Holtzapple, M. T., Oxidative lime pretreatment of high-lignin biomass. *Applied Biochemistry and Biotechnology* **2001**, 94, 1-28.
40. Karr, W. E.; Holtzapple, T., Using lime pretreatment to facilitate the enzymatic hydrolysis of corn stover. *Biomass & Bioenergy* **2000**, 18, 189-199.
41. Yoon, H. H.; Wu, Z. W.; Lee, Y. Y., Ammonia-recycled percolation process for pretreatment of biomass feedstock. *Appl. Biochem. Biotechnol.* **1995**, 51-52, 5-19.
42. Hashaikeh, R.; Fang, Z.; Butler, I. S.; Hawari, J.; Kozinski, J. A., Hydrothermal dissolution of willow in hot compressed water as a model for biomass conversion. *Fuel* **2007**, 86, 1614-1622.
43. Kohlmann, K. L.; Westgate, P. J.; Sarikaya, A.; Velayudhan, A.; Weil, J.; Hendricson, R.; Ladisch, M. R., Enhanced enzyme activities on hydrated lignocellulosic substrates. In *American Chemical Society National Meeting*, ACS Symposium series No. 618: 1995; Vol. 207, pp 237-255.
44. Mosier, N.; Hendrickson, R.; Ho, N.; Sedlak, M.; Ladisch, M. R., Optimization of pH controlled liquid hot water pretreatment of corn stover. *Bioresour. Technol.* **2005a**, 96,

1986-1993.

45. Weil, J. R.; Brewer, M.; Hendrickson, R.; Sarikaya, A.; Ladisch, M. R., Continuous pH monitoring during pretreatment of yellow poplar wood sawdust by pressure cooking in water. *Appl. Biochem. Biotechnol.* **1997**, 68, 21-40.
46. Hendriks, A. T. W. M.; Zeeman, G., Pretreatments to enhance the digestibility of lignocellulosic biomass. *Bioresource Technology* **2008**.
47. Overend, R. P.; Chornet, E., Fractionation of lignocellulosics by steam-aqueous pretreatments. *Philosophical Transactions of the Royal Society of London* **1987**, A321, 523-536.
48. Grous, W. R.; Converse, A. O.; Grethlien, H. E., Effect of steam explosion treatment on pore size and enzymatic hydrolysis of poplar. *Enzyme Microb. Technol.* **1986**, 8, 274-280.
49. Duff, S. J. B.; Murray, W. D., Bioconversion of forest products industry waste cellulosics to fuel ethanol: a review. **1996**, 55, 1-33.
50. Dale, B. E.; Leong, C. K.; Pham, T. K.; Esquivel, V. M.; Rios, I.; Latimer, V. M., Hydrolysis of lignocellulosics at low enzyme levels: application of the AFEX process. *Bioresource Technology* **1996**, 56, (1), 111-116.
51. Foster, B. L.; Dale, B. E.; Doran-Peterson, J. B., Enzymatic hydrolysis of ammonia-treated sugar beet pulp. *Appl. Biochem. Biotechnol.* **2001**, 91, (3), 269-282.
52. Wellig, B. Transpiring wall reactor for supercritical water oxidation. Swiss Federal Institute of Technology, Zurich, 2003.
53. Savage, P. E.; Gopalan, S.; Mizan, T. I.; Martino, C. J.; Brock, E. E., Reactions at supercritical conditions - applications and fundamentals. *AIChE J.* **1995**, 41, (7), 1723-

1778.

54. Eckert, C. A.; Knutson, B. L.; Dobenedetti, P. G., Supercritical fluids as solvents for chemical and materials processing. *Nature* **1996**, 383, (6598), 313-318.
55. Kalinichev, A. G; Churakov, S. V., Size and topology of molecular clusters in supercritical water: a molecular dynamics simulation. *Chem. Phys. Letters* **1999**, 302, 411-417.
56. Marcus, Y., On transport properties of hot liquid and supercritical water and their relationship to the hydrogen bonding. *Fluid Phase Equilibr.* **1999**, 164, 131-142.
57. Kritzer, P.; Dinjus, E., An assessment of supercritical water oxidation (SWO). Existing problems, possible solutions and new reactor concepts. *Chemical Engineering Journal (Amsterdam, Netherlands)* **2001**, 83, (3), 207-214.
58. Dinjus, E.; Kruse, A., Hot compressed water-a suitable and sustainable solvent and reaction medium? *Journal of physics: condensed matter* **2004**, 16, S1161-S1169.
59. Matsumura, Y.; Sasaki, M.; Okuda, K.; Takami, S.; Ohara, S.; Umetsu, M.; Adschariri, T., Supercritical water treatment of biomass for energy and material recovery. *Combust. Sci. and Tech.* **2006**, 178, 509-536.
60. Tester, J. W.; Holgate, H. R.; Armellini, F. J.; Webley, P. A.; Killilea, W. R.; Hong, G. T.; Barner, H. E. In *Supercritical water oxidation technology – process development and fundamental research*, In Emerging technologies in hazardous waste management III, Washington D.C., 1993; American Chemical Society: Washington D.C., 1993; pp 35-76.
61. Franck, E. U., Fluids at high pressures and temperatures. *Pure Appl. Chem.* **1987**, 59, (1), 25-34.
62. Miyoshia, H.; Chena, D.; AkaiT., A novel process utilizing subcritical water to

recycle soda-lime-silicate glass. *Journal of Non-Crystalline Solids* **2004**, 337, ( 3), 280-282.

63. Savage, P. E., Organic chemical reactions in supercritical water. *Chemical Reviews* **1999**, 99, 603-621.
64. Bruun, S.; Luxhoi, J., Is biochar production really carbon-negative? *Environmental Science & Technology* **2008**, 1388.
65. Hsu, T.-A., *Pretreatment of biomass. Handbook on bioethanol: Production and Utilization* Taylor and Francis, Washington, DC: 1996.
66. Sun, Y.; Cheng., J. J., Hydrolysis of lignocellulosic material for ethanol production: A review. *Bioresource Technology* **2002**, 83, 1-11.
67. Huber, G. W.; Cheda, J. N.; Barrett, C. J.; Dumesic, J. A., Production of liquid alkanes by aqueous processing of biomass derived carbohydrates. *Science* **2005**, 308, 1446-1450.
68. Sasaki, M.; Kabyemela, B.; Malaluan, R.; Hirose, S.; N.Takeda; Adschiri, T.; Arai, K., Cellulose hydrolysis in subcritical and supercritical water. *J. Supercritical Fluids* **1998**, 13, 261-268.
69. Deguchi, S.; K. Tsujii; Horikoshi, K., Crystalline-to-amorphous transformation of cellulose in hot and compressed water and its implications for hydrothermal conversion. *Green Chem.* **2008**, 10, 191-196.
70. Mok, W. S.; Antal, M. J., Uncatalyzed solvolysis of whole biomass hemicellulose by hot compressed liquid water. *Ind. Eng. Chem. Res.* **1992**, 31, 1157-1161.
71. Fang, Z.; Sato, T.; Jr., R. L. S.; Inomata, H.; Arai, K.; Kozinski, J. A., Reaction chemistry and phase behaviour of lignin in high-temperature and super critical water.

*Bioresource Technology* **2008**, 99, 3424-3430.

72. Huber, G. W.; Iborra, S.; Corma, A., Synthesis of transportation fuels from biomass: Chemistry, catalysts, and engineering. *Chem. Rev.* **2006**, 106, 4044.
73. Valenzuela, M. B.; Jones, C. W.; Agrawal, P. K., Batch aqueous reforming of woody biomass. *Energy & Fuels* **2006**, 20, 1744-1752.
74. Gourdiaan, F.; Peferoen, D., Liquid fuels from biomass via a hydrothermal process. *Chemical Engineering Science* **1990**, 45, 2729-2734.
75. Karagoz, S.; Bhaskar, T.; Muto, A.; Sakata, Y., Hydrothermal upgrading of biomass: Effect of  $K_2CO_3$  concentration and biomass/water ratio on product distribution. *Bioresource Technology* **2006**, 97, 90-98.
76. Karagoez, S.; Bhaskar, T.; Muto, A.; Sakata, Y., Comparative studies of oil compositions produced from sawdust, rice husk, lignin and cellulose by hydrothermal treatment. *Fuel* **2005**, 84, (7-8), 875-884.
77. Kruse, A., Hydrothermal biomass gasification. *J. of Supercritical Fluids* **2009**, 47, (3), 391-399.
78. Elliott, D. C., Catalytic hydrothermal gasification of biomass. *Biofuels, Bioproducts and Biorefining* **2008**, 2, 254-265.
79. Matsumura, Y.; Minowa, T.; Potic, B.; Kersten, S. R. A.; Prins, W.; Swaaij, W. P. M. V.; Beld, B. V. D.; Elliott, D. C.; Neuenschwander, G. G.; Kruse, A.; Jr., M. J. A., Biomass gasification in near- and super-critical water: Status and prospects *Biomass and Bioenergy* **2005**, 29, (4), 269-292
80. Kritzer, P.; Dinjus, E., An assessment of supercritical water oxidation (SCWO): Existing problems, possible solutions and new reactor concepts. *Chemical Engineering*

*Journal* **2001**, 83, 207-214.

81. Muthukumaraa, P.; Gupta, R. B., Sodium-carbonate assisted supercritical water oxidation of chlorinated waste. *Ind. Eng. Chem. Res.* **2000**, 39, 4555-4563.

82. Amonette, J., An introduction to Biochar: Processes, Properties, and Applications.

In *Harvesting Clean Energy 9, Special Workshop*, Billings, MT, 2009.

## 2. Cellulose Pretreatment in Subcritical Water: Effect of Temperature on Molecular Structure and Enzymatic Reactivity

### 2.1 Abstract

Microcrystalline cellulose (MCC) was pretreated with subcritical water in a continuous flow reactor for enhancing its enzymatic reactivity with cellulase enzyme. Cellulose/water suspension was mixed with subcritical (i.e., pressurized and heated) water and then fed into the reactor maintained at a constant temperature and pressure. After the reaction, product was immediately cooled in a double-pipe heat exchanger. The solid portion of the product (i.e., treated MCC) was separated and tested for molecular structure and enzymatic reactivity. Experiments were conducted at temperatures ranging from 200 to 315 °C, at 27.6 MPa, and for 3.4 to 6.2 seconds reaction times.

The treated MCC was characterized for degree of polymerization ( $DP_v$ ) by viscosimetry, and crystallinity by X-ray diffraction (XRD). In addition, differential scanning calorimetry and scanning electron microscopy (SEM) analyses were carried out to study any transformation in the cellulose structure. As expected,  $DP_v$  of cellulose steadily decreased with increase in the pretreatment temperature, with a rapid drop occurring above 300 °C. On the other hand, XRD analysis did not show any decrease in crystallinity upon pretreatment but, partial transformation of cellulose I to cellulose II structure was noticed in the MCC treated at  $\geq 300$  °C. Enzymatic reactivity was increased after the treatment at  $\geq 300$  °C.

## 2.2 Introduction

Discovered more than 150 years ago, cellulose is the most abundant organic matter on the earth and perhaps is the most studied polymer.<sup>1</sup> For its utilization as transportation fuel, the major research focus is to convert the cellulose into monomeric sugar, which can be economically fermented to ethanol. Lignocellulosic biomass, a class that includes straw, perennial grasses, plant stalks, and woody biomass is an attractive renewable source of holocellulose.<sup>2</sup> Lignocellulosics mainly consist of cellulose, hemicelluloses and lignin which are bonded together by covalent bonding, various intermolecular bridges, and van der Waals forces forming a complex structure, making it resistant to enzymatic hydrolysis and insoluble in water.<sup>1, 3</sup> Cellulose is an unbranched chain of anhydroglucose ( $C_6H_{10}O_5$ ) linked head to tail by  $\beta$ -glycosidic linkages (Jarvis, 2003).<sup>4</sup> The  $\beta$ -linkages in cellulose form linear chains that are highly stable and resistant to chemical attack because of the high degree of intra and intermolecular hydrogen bonding. There are six known polymorphs of cellulose (I, II, III<sub>I</sub>, III<sub>II</sub>, IV<sub>I</sub>, and IV<sub>II</sub>) which can also interconvert. Cellulose I, also termed as native cellulose, has parallel arrangement of chains and is the only polymorph that occurs naturally. Cellulose II is converted through mercerization or solubilization-regeneration of native or other celluloses. Cellulose II is thermodynamically more stable structure with an antiparallel arrangement of the strands and some inter-sheet hydrogen bonding. Cellulose III<sub>I</sub> and III<sub>II</sub> can be obtained from Cellulose I and II, respectively, by treatment with liquid ammonia or some amines, whereas polymorphs IV<sub>I</sub> and IV<sub>II</sub> can be obtained from heating cellulose III<sub>I</sub> and III<sub>II</sub>, respectively, to 206°C in glycerol.<sup>1, 5-7</sup> Two decades ago, it was reported that native cellulose exists as a mixture of two crystalline forms I <sub>$\alpha$</sub>  and I <sub>$\beta$</sub> , having triclinic and

monoclinic unit cells, respectively.<sup>8</sup> Cellulose I <sub>$\alpha$</sub>  is thermodynamically less stable, as shown by its conversion to cellulose I <sub>$\beta$</sub>  by annealing at 260°C. In both crystalline forms, cellobiose is the repeating unit with a strong intra-chain H-bond from 3-OH to the preceding ring O5, whereas the inter-chain H-bonding and packing of the crystal are slightly different in the two forms.<sup>9</sup>

Biomass pretreatment with acid or alkali followed by enzymatic saccharification is a conventional method to produce fermentable sugars for ethanol production. However, this treatment is associated with the serious economic and environmental constraints due to the heavy use of chemicals.<sup>10, 11</sup> Supercritical (>374°C, >22.1 MPa) and subcritical water have attracted much attention because of their suitability as a non-toxic, environmentally benign and inexpensive media for chemical reactions. Supercritical water technology provides a novel method to quickly convert cellulose to sugar and to conduct tunable reactions for the synthesis of specialty chemicals from biomass.<sup>12</sup> The solvent property of sub- and super critical water has been discussed in chapter 1 (section 1.6). In the subcritical region, the ionization constant ( $K_w$ ) of water increases with temperature and is about three orders of magnitude higher than that of ambient water (Figure 2.1). On the other hand, the dielectric constant ( $\epsilon$ ) of water drops from 80 to 20, which help solubilize the organic compounds in subcritical water. Therefore subcritical water potentially provides an acidic medium for the hydrolysis of cellulose.<sup>13-15</sup>

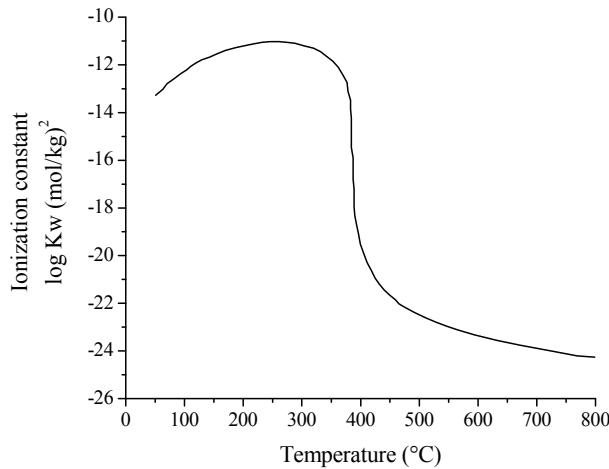


Figure 2.1 Ionization constant ( $K_w$ ) of water as a function of temperature at 25MPa.<sup>16</sup>

Experimental studies have been conducted on cellulose hydrolysis in subcritical and supercritical water in the temperature ranging 320-400°C and residence time ranging 0.05 to 10.0 seconds. The results showed that cellulose can be effectively converted to hydrolysis products (i.e., oligosaccharides, cellobiose and monosaccharides) and aqueous decomposition products of glucose (i.e., levoglucosan, 5-hydroxymethyl furfural, erythrose, glycolaldehyde, and dihydroxyacetone) in a fraction of a second within a flow type reactor.<sup>17-22</sup> The hydrolysate (water-soluble portion) and precipitate obtained by supercritical water treatment were treated with alkali or wood charcoal for reducing inhibitory effects of the various decomposition compounds of cellulose on enzyme activity and fermentation. High efficiency of ethanol production was achieved and the studies concluded that supercritical water treatment could be a promising pretreatment for ethanol production from lignocellulosic biomass.<sup>23-25</sup>

Hydrolysis of cellulose in supercritical water is very sensitive to residence time. A High residence time enhances the formation of organic acids such as acetic acid, formic acid and lactic acid. Formation of acids makes the reaction medium more acidic, which is

conducive for further degradation of hydrolysis products. Indeed after hydrolysis of cellulose in water at 320°C and 25 MPa for 9.9 s, more than half of the cellulose was converted to organic acids.<sup>21</sup> The solid cellulose-like residues have been inevitably observed in all the studies because of the rapid change in the polarity of water in going from reaction condition to room temperature. These residues have been reported to have less viscosity-average degree of polymerization ( $DP_v$ ) with no significant change in crystallinity as compared to untreated cellulose.

Supercritical water treatment requires additional process of alkaline or wood charcoal treatment for reducing the inhibitory effect of degradation products present in aqueous solution. To avoid, the degradation products, the use of hot compressed (subcritical) water as an effective pretreatment medium for biomass is gathering considerable attention. However, a clear fundamental understanding is lacking. The early fundamental work in this area was performed by Bobleter and co-workers in which they established that hemicelluloses could be completely solubilized from the lignocellulosic biomass, together with lignin.<sup>26-29</sup> To compliment, the aim of this study is to carry out a fundamental study on how subcritical water conditions affect cellulose structure and digestibility.

In this study, pretreatment of microcrystalline cellulose (MCC) was carried out in subcritical water in the temperature range of 200-315°C. Treated MCC samples are characterized by the use of XRD, SEM, and DSC techniques to investigate the structural changes.  $DP_v$  of the samples was measured to examine the polymer chain length. In this work, specifically, the effect of temperature on the cellulose structure and its reactivity with the cellulase enzyme are studied. The study will help understand the fate of cellulose

molecule during subcritical water pretreatment and will provide key design parameters for optimization of the process.

### 2.3 Experimental Section

*Materials:* Microcrystalline cellulose powder (size 20 µm, product number 310697) and high purity standard reagents for HPLC analysis were purchased from Sigma Aldrich. De-ionized water was used for preparing cellulose slurry.

*Apparatus:* Figure 2.2 shows the schematic of the apparatus used for the experiments. It consists of high-pressure liquid pumps, a cellulose slurry feeder, an electrical tubular furnace, a water-cooled double tube heat exchanger, a backpressure regulator, and a phase separator.

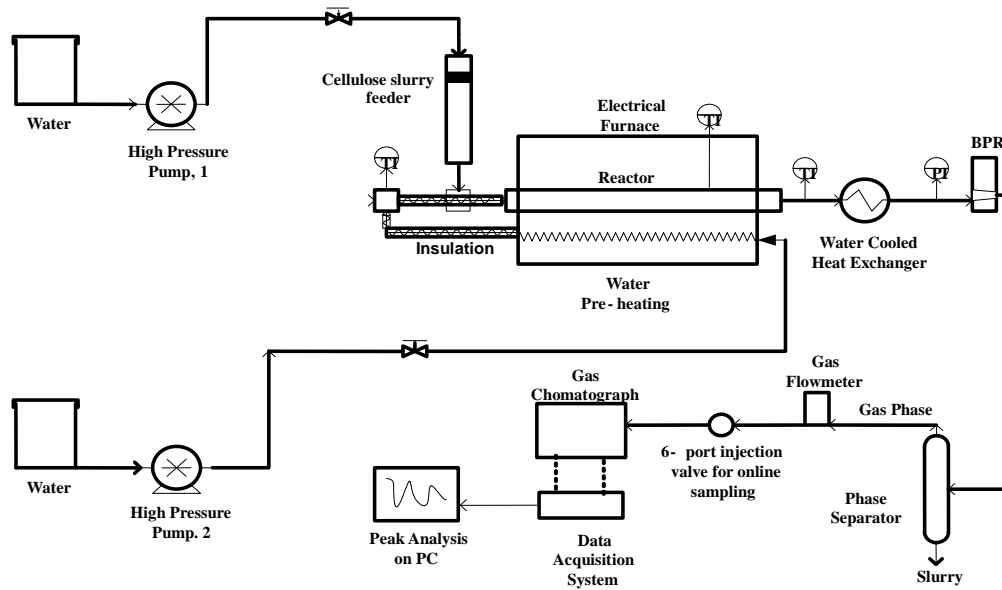


Figure 2.2 Apparatus for cellulose pretreatment in subcritical water.

Reactor was a high-pressure 14" long Inconel 600 tube having 0.25" OD, 0.11"ID and 2.2 ml volume. A custom designed piston-operated high-pressure slurry feeder (0.57" ID, 20" long) was used to supply cellulose slurry at desired flow rate. Real time temperature

of the reaction zone was measured using a 1/16" thermocouple placed 3" inside the reactor from outlet end. This thermocouple measured reaction zone temperature with accuracy of  $\pm 0.1^{\circ}\text{C}$ . There were three additional thermocouples installed at different locations in the apparatus. Real time temperature indicated by the thermocouple placed inside the reaction zone was used for all the analyses. Reactor pressure was maintained using a backpressure regulator.

*Experimental Procedure:* MCC was added to continuously stirred hot water ( $70^{\circ}\text{C}$ ) to prepare 24.1 wt% slurry and charged to the slurry feeder. It was observed that 24.1 wt% of cellulose suspension in hot water did not settle appreciably in a similar diameter tube for an hour, hence any agitation was not required in the slurry feeder.

At the start, temperature and pressure of the reaction zone were established under water flow. Then, slurry was pumped at a desired flow rate and mixed with 8 fold (mass basis) of preheated water prior to the reactor. Products coming out of the reactor were rapidly cooled in the heat exchanger, and collected in the phase separator after depressurization. Periodic liquid samples were collected, centrifuged at 3400 rpm to remove any solids and analyzed for total organic carbon (TOC) in the Shimadzu TOC-Vcsn analyzer. Products collected during the steady state phase of experiment were stored at  $4^{\circ}\text{C}$ .

MCC was treated with subcritical water at temperatures ranging from 200 to  $315^{\circ}\text{C}$  at a constant pressure 27.6 MPa and residence times ranging from 3.4 to 6.2 seconds. The experiments were divided into two groups (Table 2.1) as: (I) 200- $275^{\circ}\text{C}$ , and (II) 300- $315^{\circ}\text{C}$ . One experiment from group I (run 5) and two experiments from group II (run 7 and run 9) were conducted in triplicates to confirm the reproducibility of

the cellulose conversion by measuring the total organic contents (TOC) in the supernatant.

Table 2.1 Summary of experimental conditions (at 27.6 MPa).

Run	Reactor temperature, (°C)	Residence time, (s)	TOC of liquid product, (ppm)	pH of liquid product	$\ln R_0$
Group I, 200-275°C					
Run 1	200	4.1	667	6.4	4.1
Run 2	200	6.2	735	6.5	4.5
Run 3	253	3.9	510	5.5	7.6
Run 4	251	5.8	596	5.0	7.9
Run 5	275	3.7	568	4.4	9.1
Run 6	274	5.6	1151	4.0	9.4
Group II, 300-315°C					
Run 7	300	3.5	3992	3.8	10.7
Run 8	303	5.2	4309	3.4	11.3
Run 9	315	3.4	4945	3.3	11.7

Multiple samples were collected and analyzed for TOC values during each experiment to confirm the steady state. The relative standard deviation for runs 5, 7, and 9 were 4.1, 6.6, and 5.3%, respectively. Regression analysis of enzymatic hydrolysis data was carried out with Design of experiment software (DOE PRO 2007).

The residence time ( $t$ ) in the reactor was calculated using pure water density at the

reaction temperature and pressure (i.e. fluid phase in the reaction zone is assumed to be pure water for the simplicity of calculations) as

$$t = \frac{V}{F \left( \frac{\rho_{\text{pump}}}{\rho_{P_1, T_1}} \right)} \quad [1]$$

where,  $V$  (2.2 ml) is reactor volume,  $F$  is the combined volumetric flow rate of pumps 1 and 2,  $\rho_{\text{pump}}$  is the density of water at pump condition (25°C, 27.6 MPa), and  $\rho_{P_1, T_1}$  is the density of water at reactor condition (e.g.,  $T_1$  and  $P_1$ ).

Reynolds number, which varied from 900 to 1700, was calculated assuming pure water. Therefore, considering the small diameter tube, relatively high Reynolds number, use of very fine cellulose powder (size 20 µm), short residence time (3.4 to 6.2 s) and dilute feed (2.7 wt%) in reactor, ideal plug flow reactor was assumed for the study.

The severity factor ( $R_0$ ) has been used by several researchers to measure the combined effect of temperature and residence time in hot water treatment of biomass processes.<sup>26, 30, 31</sup> The severity index is defined as

$$R_0 = t \times \exp \left\{ \frac{T - 100}{14.75} \right\} \quad [2]$$

where  $t$  is the residence time in minutes and  $T$  is temperature in °C. The logarithmic values of  $R_0$  are listed in Table 2.1.

## 2.4 Product Analyses

After completion of the experiment, solids from the product slurry were separated by centrifugation, which was then freeze dried, weighed and taken for different analyses as follows:

*Viscosity Average Degree of Polymerization (DP<sub>v</sub>):* DP<sub>v</sub> of MCC and treated samples

were calculated from the intrinsic viscosity of pulp dissolved in cupriethylenediamine (CED) by viscosimetry as per TAPPI method using <sup>32</sup>

$$(DP_v) = \{(1.65 \eta_{pulp} - 116 y)/x\}^{1.111} \quad [3]$$

where  $x$  and  $y$  are the weight fractions of cellulose and the hemicelluloses in the pulp, respectively,  $\eta_{pulp}$  is the inherent viscosity of cellulosic pulp. Since, pure cellulose was used in the study, no correction was needed for the presence of hemicelluloses or other compounds, and hence the value of  $y$  was taken as zero.

*X-Ray Diffraction Analysis:* Rigaku Miniflex powder X-ray diffractometer equipped with a Cu K $\alpha_1$  radiation source at 30 kV voltages, 15 mA current and a miniflex goniometer was used for the XRD analysis. Diffraction patterns were collected in the  $2\theta$  range of 10-28° at a scan speed of 1°/min. and step size of 0.01°. Table 2.2 compares the diffraction angle of different planes in Cellulose I and Cellulose II.

Table 2.2 Lattice planes of cellulose I and II and the diffraction angles in XRD spectra.

	Plane	Angle, $2\theta$ (°)
Cellulose I	101	14.7
	<b>101</b>	16.8
	021	20.5
	002	22.7
Cellulose II	101	12.1
	<b>101</b>	20.0
	002	21.9

The crystallinity index ( $CI$ ) for cellulose I was determined <sup>33</sup> by

$$CI = (I_{002} - I_{18.5^\circ}) / I_{002} \quad [4]$$

where  $I_{002}$  is the peak intensity corresponding to (002) lattice plane of cellulose molecule,

and  $I_{18.5^\circ}$  is the peak intensity observed at  $2\theta$  equal to  $18.5^\circ$ .

*Enzymatic Hydrolysis:* Enzymatic hydrolysis of all the untreated and treated MCC samples were carried out simultaneously in 35 ml kmax test tubes with rubber stoppers on the top. The protocol used was similar to the NREL Laboratory Analytical Procedure (LAP) No. 009,<sup>34</sup> where a total liquid volume of 10 ml was used instead of 100 ml. Cellulase commercial enzyme (brand name: Spezyme CP) used in this study was provided by Genencor International Inc. (Palo Alto, CA). Two enzyme loadings were used for each substrate: 3.5 FPU/g and 60 FPU/g. Each test tube contained 0.1 g oven dried MCC substrate, 1 ml diluted enzyme (with equivalent activity of 3.5 FPU/g or 60 FPU/g), 0.07 ml of antibiotics (0.04 ml tetracycline solution + 0.03 ml of cycloheximide solution) and 0.05 N sodium citrate buffer (rest of the volume) for maintaining the pH (4.8) in the reaction. Magnetic stirrer was used for mixing of the reactant in the test tube. All the test tubes were placed in the incubator which maintained constant reaction temperature of 50°C. Samples were collected after 1 and 24 h for measurement of glucose and cellobiose concentration in the liquid. Sugar concentrations were measured using HPLC with a Bio-Rad Aminex HPX-87P column. The reported enzymatic digestibility is the ratio of glucan equivalent of glucose + cellobiose found in the liquid and initial glucan loading (0.1 g). Glucan equivalent of glucose and cellobiose is calculated as  $(0.9 \times \text{solubilized glucose amount}) + (0.95 \times \text{solubilized cellobiose amount})$ .

*Scanning Electron Microscopy (SEM):* The samples were prepared onto adhesive carbon tape on an aluminum stub followed by sputter coating of gold. Surface morphology of the sample was studied using an environmental scanning electron microscopy system (Zeiss EVO 50).

*Differential Scanning Calorimetry (DSC) Analysis:* DSC analysis was performed using a TA instruments, model DSC Q2000. Samples (7-10 mg) were placed in an open aluminum pan while an empty pan was placed in the reference cell. Heating rate was 10°C/min from 25 to 350°C. Nitrogen was used as inert gas for removing all oxygen from the DSC chamber prior to the heating.

*Liquid Analysis:* Carbon content in the supernatant liquid was determined by using TOC analyzer. Hydrolysis products (monomers and oligomers) and degradation products in liquid samples were determined by following the National Renewable Energy Laboratory, biomass laboratory analytical procedure (described in technical report-NREL/TP-510-42623). The analysis was performed using a HPLC with Bio-Rad Aminex HPX-87P lead-based column, refractive index detector, water mobile phase, and column temperature of 85°C.<sup>35</sup>

## 2.5 Results and Discussion

Results were divided in two groups based on the reaction temperature range used and the reactivity of the cellulose to cellulase enzyme. Group I experiments represent the pretreatment of MCC in the temperature range 200-274°C and group II represents those in the temperature range 300-315 °C. Both groups of experiments were conducted at 27.6 MPa pressure. Table 2.1 shows the details of the process parameters, TOC, pH value of the liquid products and the degree of severity of the treatment. In general, solids recovered after subcritical water treatment became fluffier and turned off white in group II runs. Liquid products collected during group I experiments were colorless and slightly acidic, but the liquid from group II runs were yellowish and more acidic (pH 3.3-3.4). There was no improvement in enzymatic digestibility of group I samples even though

severity factor ( $\ln R_0$ ) was increased from 4.1 to 9.4, on the contrary, group II samples showed significant rise in enzymatic reactivity (Table 3.3).

Table 2.3 Enzymatic digestibility of MCC, group I, and group II samples.

Run	Enzyme loading			
	3.5 FPU		60 FPU	
	Digestibility (%)		Digestibility (%)	
	1 hour	24 hours	1 hour	24 hours
MCC	7.9	47.2	45.0	75.0
Group I				
Run 1 (200°C)	6.4	40.0	36.0	68.3
Run 2 (200°C)	6.7	40.1	46.1	81.1
Run 3 (253°C)	5.1	37.3	28.5	65.4
Run 4 (251°C)	5.3	38.5	31.1	69.4
Run 5 (275°C)	6.3	40.9	31.6	70.9
Run 6 (274°C)	6.2	42.2	34.7	74.2
Group II				
Run 7 (300°C)	11.1	48.5	44.4	85.0
Run 8 (303°C)	13.0	54.6	50.1	90.3
Run 9 (315°C)	22.0	68.1	60.1	90.6

As expected, conversion of MCC to water-soluble products increased with severity factor. Characterization and enzymatic digestibility of recovered solids and liquid products are discussed as follows:

### 2.5.1 Solids Analysis

*DP<sub>v</sub> Analysis:* DP<sub>v</sub> analyses for both group I and group II samples, representing the entire temperature range of this study, are shown in Figure 2.3.

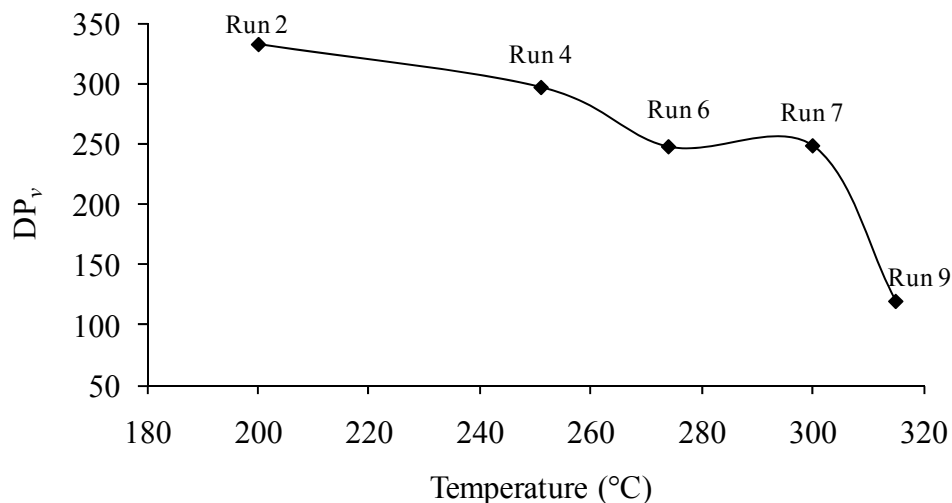


Figure 2.3 Degree of polymerization (DP<sub>v</sub>) versus pretreatment temperature.

The DP<sub>v</sub> of untreated MCC was 327. It decreased with temperature as expected, but reduced rapidly for treatment above 300°C. Runs 6 and 7 show almost similar DP<sub>v</sub>, but there was a distinct difference in the physical appearance of these two powders. Run 6 powder looked white like MCC, while run 7 appeared to be off white and fluffier than the MCC. The depolymerization of MCC during subcritical water treatment at different temperatures can be interpreted to proceed in the following two steps:

*Step 1:* At lower pretreatment temperatures (group I), water hydrolyzed mostly the amorphous region of MCC, which caused increase in the percentage crystallinity of the remaining samples, and slightly decreased DP<sub>v</sub>.

*Step 2:* At higher pretreatment temperatures (group II), intermolecular hydrogen bonding between the cellulose molecules weakens, which is followed by the cleavage of

glycosidic linkages due to the increased accessibility of water molecules to the reactive sites.

Therefore, reaction at higher temperatures ( $>300^{\circ}\text{C}$ ) caused the rapid decline of  $\text{DP}_v$ , increased solubility of cellulose in water, and rapid conversion of cellulose to monomers and the degradation products. Liquid analysis of group II experiments showed that more than 30% of cellulose converts to water soluble products. Compositions of these products in liquid are discussed in the liquid analysis section.

*XRD Analysis:* Figures 2.4 and 2.5 show the XRD pattern for group I and II samples. The intensity distribution in the region of interest (diffraction angle,  $2\theta = 18^{\circ}$  to  $24^{\circ}$ ) usually displays two peaks. The peak at  $20^{\circ}$  is due to (021) line in cellulose I and (10 $\bar{1}$ ) line in cellulose II. The other peak at 22-22.7° is due to the contribution from (002) line of both the polymorphs. Using the XRD data, crystallinity of the solids (Table 2.4) was determined by Equation 4. Here, each data is derived from a single run; for future work, it is recommended that multiple runs should be conducted for each pretreatment condition to ensure statistically significant variation in the crystallinity.

Table 2.4 Crystallinity of samples by XRD analysis.

Run	Crstallinity (%)
MCC	77.8
Group I	
Run 1	79.3
Run 2	79.3
Run 3	82.7
Run 4	82.5
Run 5	81.9
Run 6	81.4
Group II	
Run 7	81.2
Run 8	82.2
Run 9	83.6

MCC crystallinity was 77.8% and increased with the treatment temperature and residence time. The maximum TOC value in liquid product of group I sample was 1151 ppm (run 6), which indicated that there was no significant hydrolysis of MCC at 274°C or below by subcritical water in the studied range of residence time. Increase in TOC and crystallinity were mainly because of the hydrolysis and removal of the amorphous region of MCC. Therefore, it can be concluded that hydrolysis occurred mainly at the crystal surface with no minimal swelling or dissolution of MCC. Hence, it is not surprising to see that XRD patterns for MCC and group I samples are similar (Figure 2.4).

TOC values for group II samples were 3992 ppm (run 7) or above, which confirmed the sharp rise in the rate of hydrolysis of MCC in this group. As the treatment temperature increases, density and dielectric constant of water decreases. Water becomes more non-polar and becomes an excellent solvent for organic compounds.<sup>15</sup> Moreover, higher temperature increases the reactivity and kinetic energy of cellulose molecules.

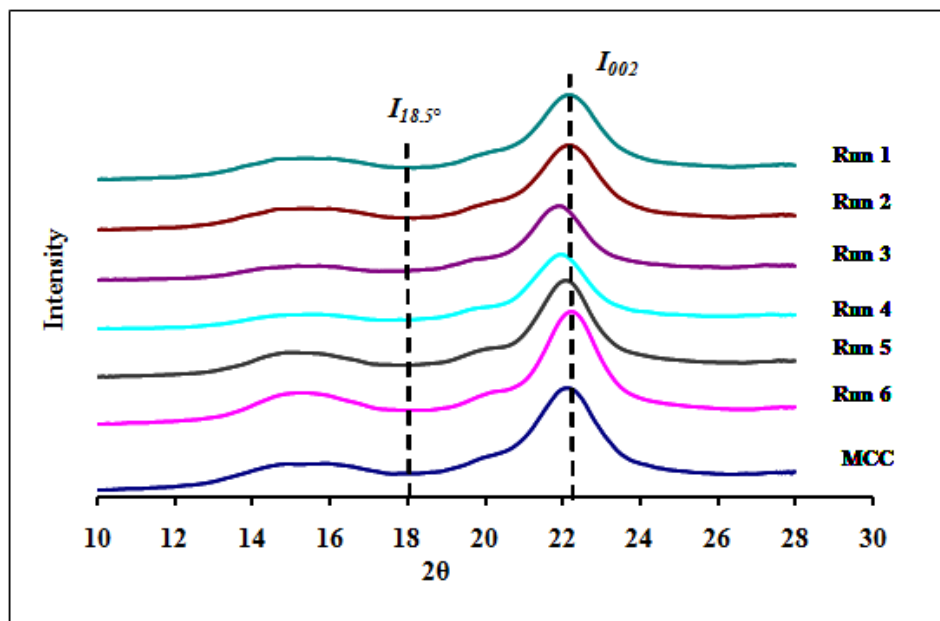


Figure 2.4 XRD results for MCC and group I samples.

Therefore, a high temperature results in weakening of intermolecular hydrogen bonds. A

change in the reaction condition enhances the partial dissolution of cellulose in water.

Figure 2.5 shows the gradual shift of diffraction peak of (002) lattice plane from  $2\theta$  angle of  $22.1^\circ$  to a slightly lower angle.

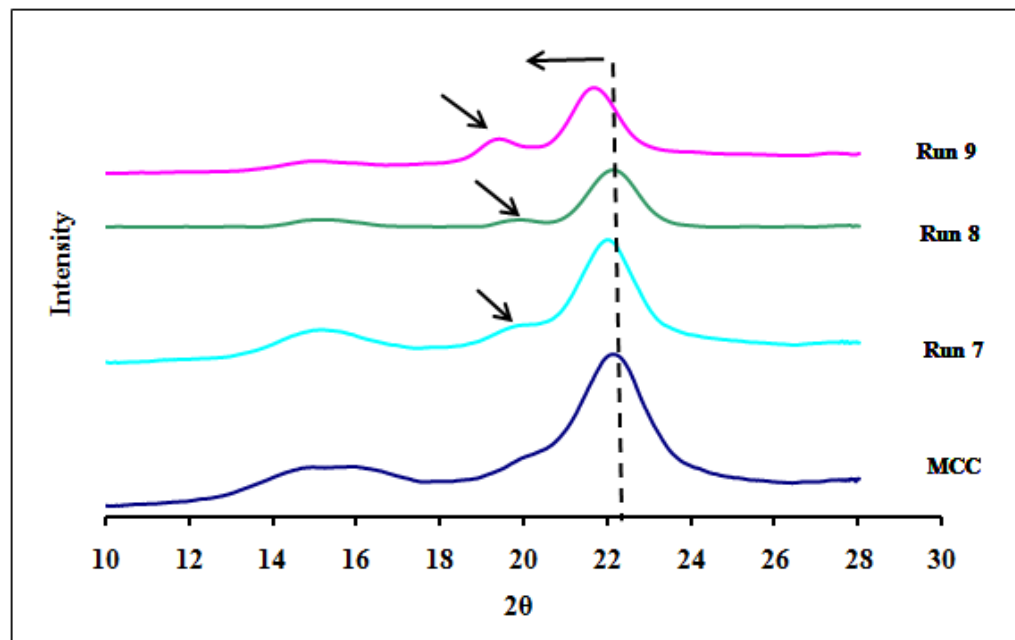


Figure 2.5 XRD results for original MCC and group II samples.

Onset of a new peak at  $2\theta$  of  $19.4^\circ$  is seen in group II samples. This peak is more prominent in run 9, whereas it was very small in runs 7 and 8. Peak at about  $20^\circ$  angle is assigned to the  $(10\bar{1})$  lattice plane of cellulose II.<sup>36</sup> Based on the XRD pattern of group II samples, it can be concluded that cellulose started swelling around the crystal surface of MCC at the high temperature. This swollen region should be hydrolyzed to water-soluble saccharides and the degradation products. Yields of these products are discussed in the liquid analysis section. Cellulose II has antiparallel arrangement of chains and a more stable structure with a low energy crystalline arrangement.<sup>37</sup> After the reaction, products are rapidly cooled to the room temperature. Due to the sudden cooling, swollen part of cellulose around the crystal surface recrystallizes to cellulose II, which is the

thermodynamically more favorable crystal arrangement. Therefore, XRD of group II samples shows the presence of cellulose II. The ratio between the peak intensities at angle about  $2\theta = 20^\circ$  and  $002$  ( $I_{20^\circ} / I_{002}$ ) have been used for estimating the ratio of cellulose I cellulose II in a mixture. The ratio ( $I_{20^\circ} / I_{002}$ ) for MCC (Cellulose I) is 0.37, which upon processing increased to 0.44 for run 9. By using the method and the calibration curve developed by Gjonnes et al. cellulose II percentage in the run 9 was estimated to be 8.9%, where  $I_{20^\circ} / I_{002}$  of 100% cellulose II was considered 1.16.<sup>36</sup>

Reaction at the temperatures studied here is mainly heterogeneous and occurs at the crystal surface with partial swelling or dissolution of MCC. With increase in the temperature, polarity of water decreases considerably, making the reaction medium more homogeneous and conducive for swelling and dissolution of cellulose. Consequently, part of the undissolved cellulose precipitated as crystal II polymorph. Consistent to our observation, Sasaki et al. have also reported the production of cellulose II from native cellulose by near- and supercritical water solubilization.<sup>38, 39</sup>

*Enzymatic Digestibility:* As shown in Table 2.3, enzymatic digestibility of untreated and treated MCC was carried out with two different cellulase loadings (3.5 FPU and 60 FPU). Hydrolysis with a low enzyme loading measures the enzymatic reactivity of cellulose, while those with the high enzyme loading indirectly measure the total digestible cellulose. Regression analysis of enzymatic hydrolysis data was carried out with Design of Experiment software (DOE PRO 2007 from Digital Computation). Figures 6a-d show the surface plots for different enzymatic digestibility values with respect to the reaction temperature and treatment time.

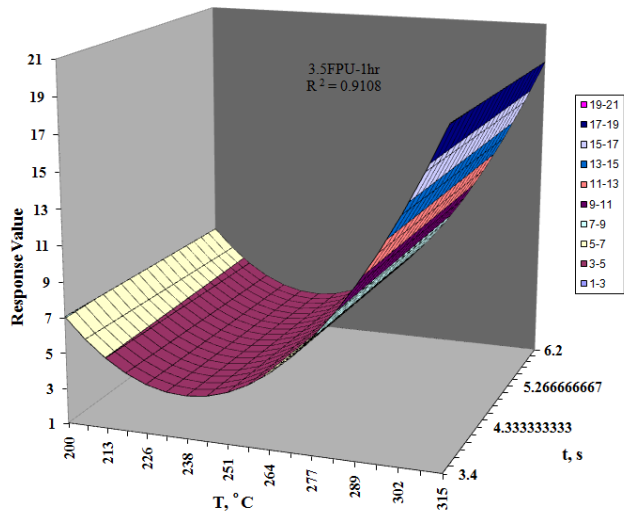


Figure 2.6a Plot after regression analysis of enzymatic hydrolysis data at 3.5 FPU and after 1 h.

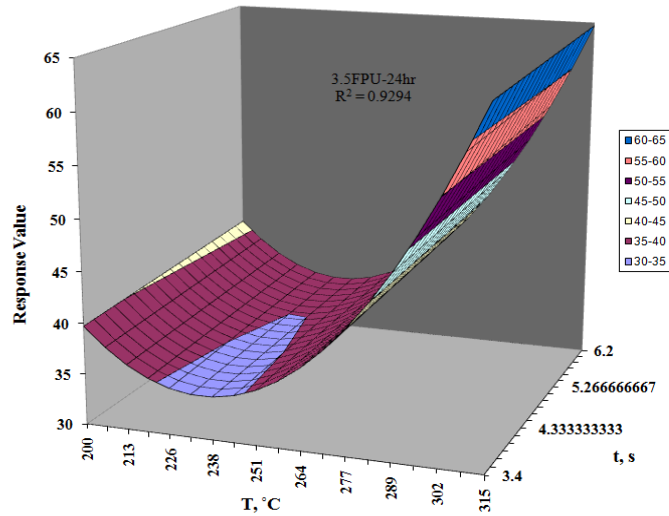


Figure 2.6b Plot after regression analysis of enzymatic hydrolysis data at 3.5 FPU and after 24 h.

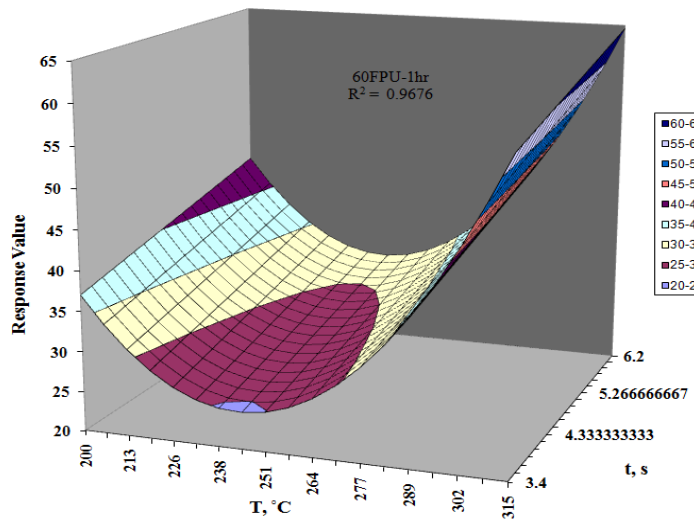


Figure 2.6c Plot after regression analysis of enzymatic hydrolysis data at 60 FPU and after 1 h.

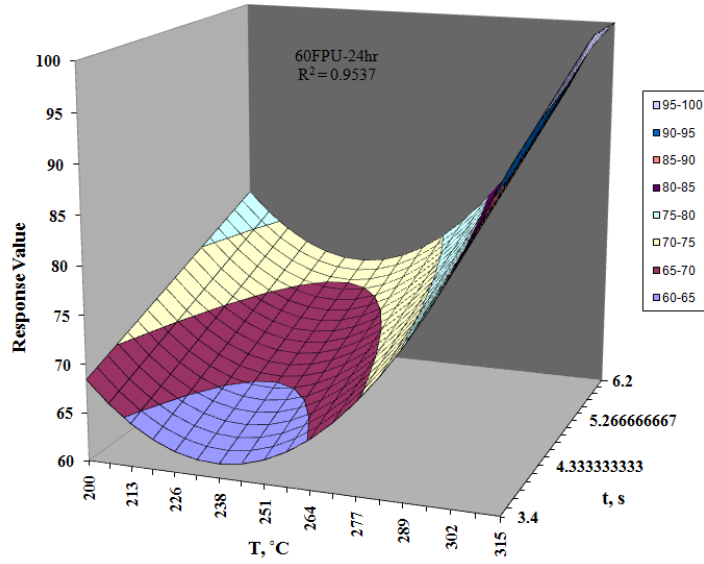


Figure 2.6d Plot after regression analysis of enzymatic hydrolysis data at 60 FPU and after 24 h.

As evident, enzymatic reactivity (with 3.5 FPU/ g cellulose) of treated solid is not much affected by the reaction time but is mainly a function of reaction temperature. But

overall enzymatic reactivity (with 60 FPU/ g cellulose) of treated solid is a function of both reaction temperature as well as time. At, a constant temperature, enzymatic digestibility of the treated solid increases with the reaction time.

Interestingly, it is found that MCC treated in the low temperature range (200-275°C) shows a lower enzymatic reactivity than the untreated MCC. There are two plausible reasoning for this behavior: (a) a slight increase in crystallinity, and (b) a reduction in  $DP_v$  of MCC upon pretreatment. If the crystallinity and enzyme accessibility are the main resistances for decreased hydrolysis for these treated samples, that should have been overcome in higher enzyme loading of 60 FPU where enzyme is supplied in excess. But even with very high enzyme loading, extent of hydrolysis for treated MCC samples from runs 1-6 is lower than that for untreated MCC, with the exception of run 2. This suggests that it is not the difference in crystallinity that is causing the lower hydrolysis but probably some other molecular characteristics such as  $DP_v$ . As indicated elsewhere,<sup>40</sup> enzymatic hydrolysis of lower  $DP_v$  amorphous cellulose substrate leads to slightly lower hydrolysis rate. Similar trends are shown here with crystalline substrates.

Another interesting point here is that this trend does not hold true when MCC is treated at high temperatures (over 300°C). Even though the  $DP_v$  of these treated MCC substrates is much lower than those treated at lower temperatures, MCC obtained from runs 7-9 have higher hydrolysis rates. As discussed earlier, with XRD plot of different treated MCC at higher temperature, transformation of cellulose I to cellulose II is suspected. Transformation in cellulose structure might be a factor leading to the higher enzymatic reactivity of these samples.

*SEM Analysis:* MCC and solid samples from runs 5, 7 and 9, which were pretreated at

different temperatures (275, 300, and 315 °C, respectively), were taken for SEM analysis (Figures 2.7a-d). The surface of MCC before subcritical water treatment, shown in Figure 2.7a, is marked by some boundary edges and does not show the presence of any pores, trenches or surface cracks. Figures 2.7b-d show the images of samples produced in runs 5, 7 and 9. Here, cracks and trenches can be clearly seen on the surface of the samples. These cracks, trenches and kinks are very prominent in all images of treated samples seen at about 30,000X magnification. Though surface cracks or trenches are seen in the images, they are not evenly distributed over the surface of samples. From the several images taken at different magnifications of these samples (not shown here), presence of steps and terrains was confirmed. These surface modifications might have occurred as a result of mild hydrolysis over the crystal surface, whereas cracks are seen, perhaps be due to the removal of amorphous region from MCC after subcritical water treatment.

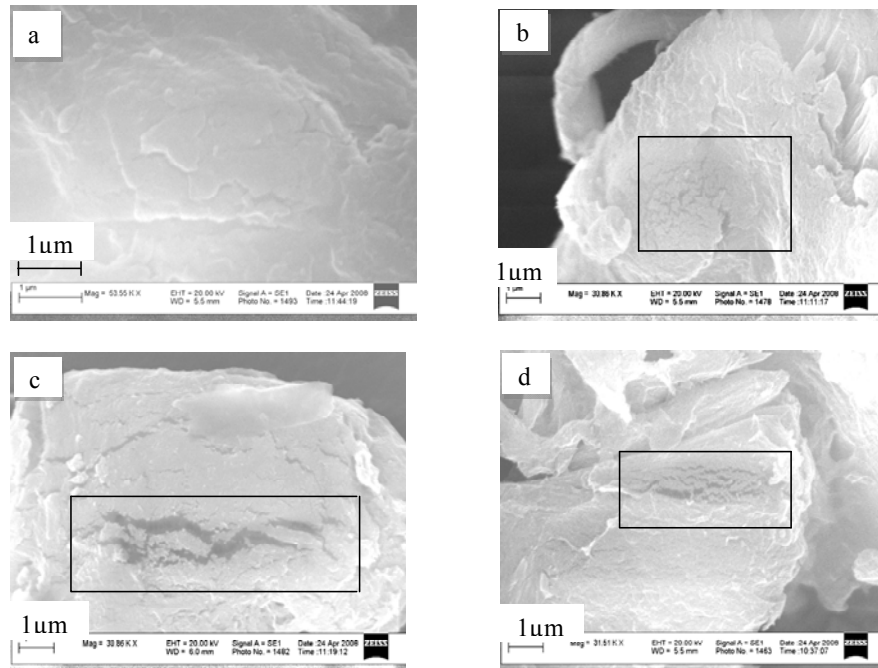


Figure 2.7 SEM images of samples: (a) MCC, (b) run 5, (c) run 7, and (d) run 9.

*DSC Analysis:* DSC thermograms MCC and samples from run 6, 7, and 9 are shown in Figure 2.8. Despite having different  $DP_v$ , the samples follow similar endothermic heating path and show the endotherm minima in the range of 324-331°C, indicating no change in thermal stability of the samples after subcritical water treatment. With the removal of the amorphous region and subsequently, slight increase in percentage crystallinity as observed in XRD, it is expected to increase the thermal stability of the treated cellulose. Studies also show that endotherm minimum temperature decreases with  $DP_v$ .<sup>41</sup>

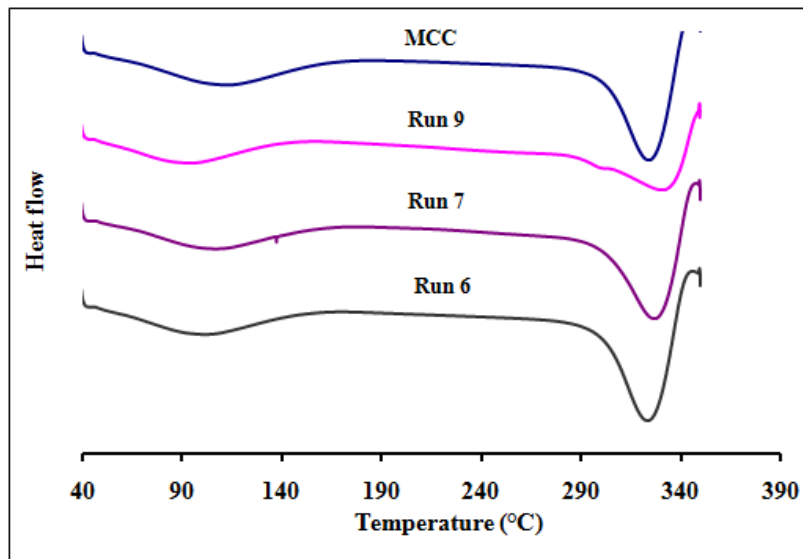


Figure 2.8 DSC thermograms of MCC, group I (run 6) and group II (run 7 and 9) samples.

As discussed earlier,  $DP_v$  of the samples decreased with temperature and reduced to one third of its initial value in case of run 9. In our study,  $DP_v$  did decrease, but it still remained substantially high ( $>100$ ), and so, lowering of endotherm minimum below 327°C was not observed. There was no exothermic reaction and also no indication of glass transition temperature up to 350°C. The observations of thermograph support the fact that there was no substantial change in thermal properties of the samples.

### 2.5.2 Liquid Analysis

Table 2.1 shows that TOC values of liquid products from various runs. TOC increased rapidly with rise in temperature above 275°C and more than 30% of cellulose was converted to hydrolysis or degradation products in group II experiments. Clear liquid recovered after centrifugation was analyzed by HPLC for oligosaccharides, monomers and degradation products. In this study, we defined (a) hydrolysis products as the combination of oligomers (>2 monomer units), cellobiose, glucose, and fructose, and (b) degradation products as glycoaldehyde, D-fructose, anhydroglucose, and 5-HMF.

pH of the liquid products varied from 4.0-6.5 in group I experiments, while 3.3-3.4 in group II experiments (Table 2.1). Low pH values confirm the presence of organic acids (e.g. formic acid, lactic acid). The liquid samples from group I having cellulose conversion less than 10% did not show the presence of hydrolysis products during HPLC analysis. Liquid samples from group II (runs 8 and 9) which were treated at almost same severity factor, but at different temperatures were analyzed. The yields of different products present in the liquid were calculated based on the input of 2.7 wt% of MCC and are listed in Table 2.5. These samples primarily showed the presence of hydrolysis products, along with a comparatively small amount of degradation products.

Table 2.5 Yields of different compounds in the liquid product.

Run	Hydrolysis products (%)				Degradation products (%)		
	Olg	CB	Glu	Fr	GA	AG	HMF
Run 8	16.1	2.8	5.0	0.5	0.8	0.9	0.9
Run 9	20.0	4.1	3.7	0.4	0.7	0.6	0.6

Hydrothermal degradation of cellulose is a heterogeneous and pseudo-first-order reaction for which detailed chemistry and mechanism have been proposed.<sup>28, 29, 42, 43</sup> A simplified reaction scheme is shown in Figure 2.9.

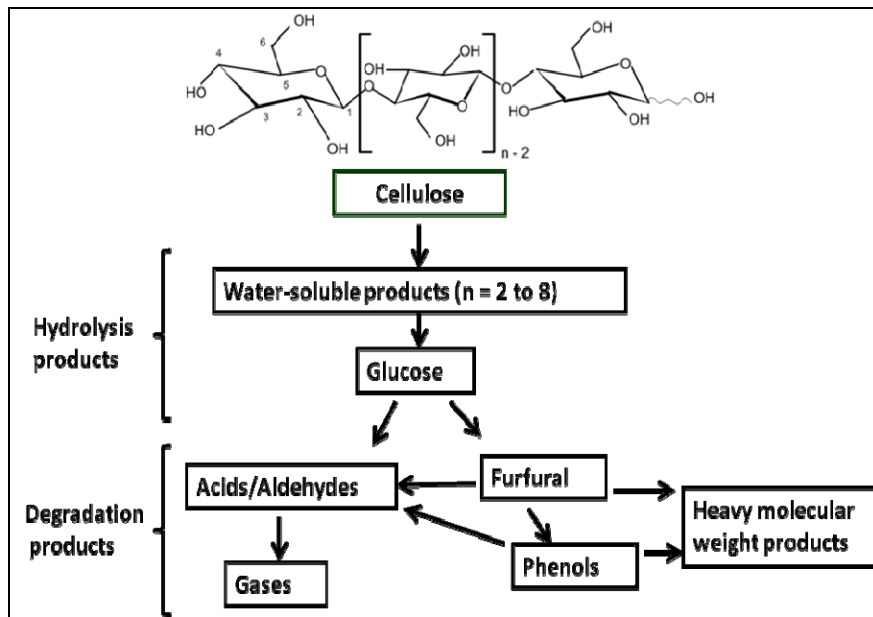


Figure 2.9 Simplified reaction scheme of cellulose in subcritical water.<sup>44</sup>

As discussed earlier, the ionization constant of water increases with temperature and near-critical point, the amount of dissociation is three times what it would be at normal temperatures and pressures. Under such a severe condition, glycosidic linkages of cellulose are broken and cellulose starts to convert to water soluble compounds and further to glucose. Glucose molecules are unstable at high temperature and so part of the glucose further converts to its degradation products such as glycoaldehyde, HMF, organic acids etc. which makes the reaction medium more acidic. Once organic acids are formed in the reaction mixture, it provides necessary acidity for further degradation of the converted hydrolysis products, as an autocatalytic process. Indeed, after hydrolysis of cellulose in water at 320 °C and 25 MPa for 9.9 s, more than half of the cellulose was converted to organic acids.<sup>20</sup> The detailed mechanism of cellulose hydrolysis and product

composition in subcritical and supercritical water above 300°C has been discussed in a separate study.<sup>45</sup> Liquid composition of group II samples clearly indicate that cellulose converted to hydrolysis products (oligomers and monomers) and a portion further degraded to the aqueous degradation products of glucose, including glycoaldehyde, fructose, anhydroglucose, and 5-HMF.

Based on the results, it is clear that subcritical water can be used as an effective pretreatment media for lignocellulosic biomass without degrading or losing the significant amount of glucan, and also for increasing the accessibility to enzymes. Throughout this study, crystallinity of cellulose was observed to increase with treatment temperature while  $DP_v$  decreased. But enzymatic digestibility improved only after considerable lowering of  $DP_v$ . These findings support the theory that to improve the enzymatic digestibily, it is not necessary to bring down the crystallinity, rather improving the accessibility of enzymes and lowering the  $DP_v$  are more important factors.

## 2.6 Conclusion

The percentage crystallinity of microcrystalline cellulose (MCC) slightly increased after the subcritical water pretreatment in a continuous flow reactor for a short residence time (3.4 - 6.2 s) and remained high (> 81%) throughout the treatment range (200-315°C). Under the reaction condition, cellulose conversion to water soluble products during pretreatment was considerably low (<10 wt.%) at lower treatment temperatures (group I). The enhancement in enzymatic digestibility of cellulose (initial and total digestibility, both) was observed for the samples pretreated at higher temperatures ( $\geq 300^\circ\text{C}$ ). In fact, MCC pretreated at 315 °C showed nearly three-fold increase in the initial enzymatic reactivity as compared to the untreated MCC at 3.5

FPU/g of glucan enzyme loading. On the other hand, cellulose pretreated at lower temperature ( $\leq 275^{\circ}\text{C}$ ) had slightly lower digestibility as compared to the untreated MCC. The viscosity average degree of polymerization of cellulose though reduced after the pretreatment, it decreased rapidly at  $315^{\circ}\text{C}$ . The onset of cellulose I to cellulose II polymorph formation was noticed in XRD spectra for samples pretreated at  $\geq 300^{\circ}\text{C}$ . The development of surface cracks and trenches were also observed in the SEM images. Improvement in the enzymatic reactivity may be attributed to the partial transformation of cellulose I to cellulose II polymorph and some other structural changes in cellulose at higher temperature.

## 2.7 Acknowledgments

Author is thankful for the financial supports from the National Science Foundation (grant NSF-CBET-0828269) and Alabama Center for Paper and Bioresource Engineering. Additionally, the authors are thankful to Rajeev Kumar (CE-CERT, University of California, Riverside) for help in  $DP_v$  analyses.

## 2.8 Nomenclature

Olg: Oligomers

CB: Cellobiose

Glu: Glucose

Fr: D-Fructose

GA: Glycoaldehyde dimer

AG: 1,6 Anhydro-beta glucose

HMF: 5-Hydroxymethyl –2-furaldehyde

## 2.9 References

1. O'Sullivan, A. C., Cellulose: the structure slowly unravels. *Cellulose* **1997**, 4, (3), 173-207.
2. Chornet, E.; Overend, R. P., Liquid fuels from lignocellulosics. *Biomass* **1987**, 257-269.
3. Schacht, C.; Zetzl, C.; Brunner, G., From plant materials to ethanol by means of supercritical fluid technology. *Journal of Supercritical Fluids* **2008**, In Press, 23.
4. Jarvis, M., Chemistry: Cellulose stacks up. *Nature* **2003**, 426, 611-612
5. Marchessault, R. H.; Sarko, A., X-Ray Structure of Polysaccharides. *Advances in Carbohydrate Chemistry* **1967**, 22, 421-482.
6. Sarko, A., What is the crystalline structure of cellulose ? *Tappi* **1978**, 61, 59-61.
7. Sarko, A., Cellulose - how much do we know about its structure? *Wood and Cellulosics: Industrial utilization, biotechnology, structure and properties* **1987**, (J.F.Kennedy ed.), 55-70.
8. Atalla, R. H.; Vanderhart, D. L., Native Cellulose: A Composite of Two Distinct Crystalline Forms. *Science* **1984**, 223, (4633), 283 - 285.
9. Sinnott, M. L., *Chapter 4: Primary structure and conformation of oligosaccharides and polysaccharides*. RSC publishing: 2007.
10. Hsu, T.-A., *Pretreatment of biomass. Handbook on bioethanol: Production and Utilization* Taylor and Francis, Washington, DC: 1996.
11. Sun, Y.; Cheng., J. J., Hydrolysis of lignocellulosic material for ethanol production: A review. *Bioresource Technology* **2002**, 83, 1-11.
12. Matsumura, Y.; Sasaki, M.; Okuda, K.; Takami, S.; Ohara, S.; Umetsu, M.;

- Adschiri, T., Supercritical water treatment of biomass for energy and material recovery. *Combust. Sci. and Tech.* **2006**, 178, 509-536.
13. Franck, E. U., Fluids at high pressures and temperatures. *Pure Appl. Chem.* **1987**, 59, (1), 25-34.
14. Miyoshia, H.; Chena, D.; AkaiT., A novel process utilizing subcritical water to recycle soda-lime-silicate glass. *Journal of Non-Crystalline Solids* **2004**, 337, ( 3), 280-282.
15. Savage, P. E., Organic chemical reactions in supercritical water. *Chemical Reviews* **1999**, 99, 603-621.
16. Tester, J. W.; Holgate, H. R.; Armellini, F. J.; Webley, P. A.; Killilea, W. R.; Hong, G. T.; Barner, H. E. In *Supercritical water oxidation technology – process development and fundamental research*, In Emerging technologies in hazardous waste management III, Washington D.C., 1993; American Chemical Society: Washington D.C., 1993; pp 35-76.
17. Ehara, K.; Saka, S., A comparative study on chemical conversion of cellulose between the batch-type and flow-type systems in supercritical water. *Cellulose* **2002**, 9, 301-311.
18. Ehara, K.; Saka, S., Decomposition behavior of cellulose in supercritical water, subcritical water, and their combined treatments. . *J. Wood Sci.* **2005**, 51, 148–153.
19. Matsumura, Y.; Minowa, T.; Potic, B.; Kersten, S. R. A.; Prins, W.; Swaaij, W. P. M. V.; Beld, B. V. D.; Elliott, D. C.; Neuenschwander, G. G.; Kruse, A.; Jr., M. J. A., Biomass gasification in near- and super-critical water: Status and prospects *Biomass and Bioenergy* **2005**, 29, (4), 269-292
20. Sasaki, M.; Kabyemela, B.; Malaluan, R.; Hirose, S.; N.Takeda; Adschiri, T.;

- Arai, K., Cellulose hydrolysis in subcritical and supercritical water. *J. Supercritical Fluids* 1998 **1998**, 13, 261-268.
21. Sasaki, M.; Fang, Z.; Fukushima, Y. N.; Adschari, T.; Arai, K., Dissolution and hydrolysis of cellulose in subcritical and supercritical water. *Ind. Eng. Chem. Res.* **2000**, 39, 2883-2890.
22. Sakai, T.; Shibata, M.; Miki, T.; Hirosue, H.; Hayashi, N., Reaction model of cellulose decomposition in near-critical water and fermentation of products. *Bioresource Technology* **1996**, 197-202.
23. Hisashi, M.; Toshiki, N.; Katsunobu, E.; Shiro, S., Fermentability of Water-Soluble Portion to Ethanol Obtained by Supercritical Water Treatment of Lignocellulosics *Applied Biochemistry and Biotechnology* **2005**, 124, (1-3), 963-972.
24. Shiro, S.; Hisashi, M., Bioethanol production from lignocellulosics using supercritical water *ACS symposium series* **2007**, 954, 422-433.
25. Nakata, T.; Miyafuji, H.; Saka, S., Bioethanol from cellulose with supercritical water treatment followed by enzymatic hydrolysis *Applied Biochemistry and Biotechnology* **2006**, 130, (1-3), 476-485.
26. Allen, S. G.; Kam, L. C.; Zemann, A. J.; M. J. Antal, J., Fractionation of Sugar Cane with Hot, Compressed, Liquid Water. *Ind. Eng. Chem. Res.* **1996**, 35, (8), 2709 - 2715.
27. Bobleter, O.; Bonn, G.; Concin, R., Hydrothermolysis of biomass-production of raw material for alcohol fermentation and other motor fuels. *Alt. Energy Sour.* **1983**, 3, 323-332.
28. Bobleter, O., Hydrothermal degradation of polymers derived from plants. *Prog.*

*Polym. Sci.* **1994**, 19, 797–841.

29. Mok, W. S.; Antal, M. J., Uncatalyzed solvolysis of whole biomass hemicellulose by hot compressed liquid water. *Ind. Eng. Chem. Res.* **1992**, 31, 1157-1161.
30. Overend, R. P.; Chornet, E., Fractionation of lignocellulosics by steam-aqueous pretreatments. *Philosophical Transactions of the Royal Society of London* **1987**, A321, 523-536.
31. Rogalinski, T.; Ingram, T.; Brunner, G., Hydrolysis of lignocellulosic biomass in water under elevated temperatures and pressures. *Journal of Supercritical Fluids* **2007**.
32. Perez, D. d. S.; van, A. R. P., Determination of cellulose degree of polymerization in chemical pulps by viscosimetry. *7th EWLP conference* **2002**, 393-396.
33. Segal, L.; Creely, J. J.; Martin, A. E.; Conrad, C. M., An empirical method for estimating the degree of crystallinity of native cellulose using the X-ray diffractometer. *Textile Res. J.* **1959**, 29, 786–794.
34. Larry, B.; Robert, T., Enzymatic saccharification of lignocellulosic biomass,LAP-09. [http://www.eere.energy.gov/biomass/analytical\\_procedures.html](http://www.eere.energy.gov/biomass/analytical_procedures.html) **1996**.
35. Sluiter, A.; Hammes, B.; Ruiz, R.; Scarlata, C.; Sluiter, J.; Templeton, D., Determination of sugars, byproducts, and degradation products in liquid fraction process samples. *NREL Biomass Program, Laboratory Analytical Procedure (LAP)* **2006**.
36. Norman, J. G. a. N., X-ray investigation on cellulose II and mixtures of cellulose I and II: A method for characterizing and determining the relative contents of the new modifications. *Acta Chem. Scand.* **1960**, 14, (3), 683-688.
37. Simon, I. G., L.; Scheraga, H.A.; Manley, R.S.J., Structure of Cellulose. Part 2. Low-Energy Crystalline Arrangements. *Macromolecules* **1988**, 21, 990-998.

38. Sasaki, M.; Adschariri, T.; Arai, K., Production of cellulose II from native cellulose by near- and supercritical water solubilization. *J Agric Food Chem.* **2003** 51, (18), 5376-81.
39. Sasaki, M.; Adschariri, T.; Arai, K., Kinetics of cellulose conversion at 25 MPa in sub- and Supercritical water. *AIChE J.* **2004**, 50, (1), 192–202.
40. Gupta, R.; Lee, Y. Y., Cellulase reaction mechanism with pure cellulosic substrates. *Biotechnology and Bioengineering* **2008**.
41. Bouchard, J.; Abatzoglou, N.; Chornet, E.; Overend, R. P., Characterization of depolymerized cellulosic residues. *Wood Science and Technology* **1989**, 23, (4), 343-355.
42. Mok, W. S. L.; M.J., A. J.; Varhegyi, G, Productive and parasitic pathways in dilute-acid-catalyzed hydrolysis of cellulose. *Ind. Eng. Chem. Res.* **1992**, 31, 94-100.
43. Schwald, W.; Bobleter, O., Hydrothermolysis of cellulose under static and dynamic conditions at high temperatures. *J. Carbohydr. Chem.* **1989**, 8, (4), 565-578.
44. Kruse, A.; Gawlik, A., Biomass conversion in water at 330-410 °C and 30-50 MPa: Identification of key compounds for indicating different chemical reaction pathways. *Ind. Eng. Chem. Res.* **2003**, 42, 267-269.
45. Kumar, S.; Gupta, R. B., Hydrolysis of Microcrystalline Cellulose in Subcritical and Supercritical Water in a Continuous Flow Reactor. *Industrial and Engineering Chemistry Research* **2008**, 47, (23), 9321-9329.

### 3. Hydrothermal Pretreatment of Switchgrass and Corn Stover for Production of Ethanol and Carbon Microspheres

#### 3.1 Abstract

Pretreatment of biomass is viewed as a critical step to make the cellulose accessible to enzymes and for an adequate yield of fermentable sugars in ethanol production. Recently, hydrothermal pretreatment has attracted much attention as a non-toxic, environmentally benign and inexpensive media for chemical reactions. The hydrothermal pretreatment of switchgrass and corn stover was conducted in a flow through reactor to enhance and optimize the enzymatic digestibility. More than 80% of glucan digestibility was achieved by pretreatment at 190°C. Addition of small amount of K<sub>2</sub>CO<sub>3</sub> (0.45-0.9 wt%) can enhance the pretreatment and allow use of a lower temperature. Switchgrass pretreated at 190°C only with water had higher internal surface area than that pretreated in the presence of K<sub>2</sub>CO<sub>3</sub>, but both the biomasses showed similar glucan digestibility. In comparison to switchgrass, corn stover required milder pretreatment conditions. The liquid hydrolyzate generated during pretreatment was converted into carbon microspheres by hydrothermal carbonization, providing a value-added byproduct. The carbonization process is further examined by GC-MS analysis to understand the mechanism for microsphere formation.

### 3.2 Introduction

Lignocellulosic biomass has emerged as a potential renewable biomass resource for the bioethanol production<sup>1, 2</sup>. Biomass, which mainly contains cellulose, hemicelluloses, and lignin biopolymers, can be used as fuel by direct combustion or by first gasifying and then burning the gas. However, being only renewable resource which can be converted to liquid fuel for transportation, there is a great deal of interest in converting these resources to bioethanol and other chemicals. The concept is to hydrolyze the cellulose and hemicelluloses to recover C<sub>5</sub> and C<sub>6</sub> sugars and then ferment the sugars to bioethanol.<sup>3</sup> The recovered lignin in the process which has relatively higher heating value in the range of 24-26 MJ/kg is typically used for generating steam or providing the process heat. Switchgrass, a summer perennial grass native to North America that grows on marginal land, is considered to be a major lignocellulosic biomass crop of interest for the second generation biofuels. The advantages of switchgrass as energy crop include low requirement of chemical inputs and the use of marginal land which does not compete with the food production. The switchgrass plants are immense biomass producer that can reach heights of  $\geq$ 10 feet and provide 6-8 dry-ton/acre/year (as compared to 2.5 tons/acre/year for hay) with a high cellulosic content.<sup>4</sup>

The biochemical pathways which can be realized at a very moderate process conditions using cellulase enzyme to convert holocelluloses to fermentable sugars are the most promising ones for large scale bioethanol production. But, the efficiency of this technology is limited due to the complex chemical structure of lignocellulose biomass and the inaccessibility of  $\beta$ -glycosidic linkages to cellulase enzymes because of the low surface area and small size of pores in multicomponent structure. Hence, pretreatment is

nowadays viewed as a critical step in lignocellulose processing. Pretreatment alters both the structural barrier (removal of lignin and hemicelluloses) and physical barrier (surface area, crystallinity, pore size distribution, degree of polymerization) which help in improving the accessibility of enzyme for hydrolysis.<sup>5-7</sup> The pretreatment enhances the rate of production and the yield of monomeric sugars from biomass. But the pretreatment is among the most costly step in the bioethanol conversion process as it may account for up to 40% of the processing cost. Moreover, it also affects the cost of upstream and downstream processes.<sup>8-11</sup> Hence, an efficient, less energy intensive and cost effective pretreatment method is a necessity for producing ethanol at an economically viable cost. Different pretreatment methods are broadly classified into physical, chemical, physiochemical and biological processes. The conventional pretreatment, by using acids or alkalis, is associated with the serious economic and environmental constraints due to the heavy use of chemicals and chemical resistant materials.<sup>12-14</sup>

Recently, hydrothermal pretreatment employing subcritical water has attracted much attention because of its suitability as a non-toxic, environmentally benign and inexpensive media for chemical reactions.<sup>15, 16</sup> One of the most important benefit of using water instead of acid as pretreatment media is that there is no need of acid recovery process and related solid disposal and handling cost.<sup>14, 17</sup> Liquid water, below the critical point is conducive for conducting ionic reactions. Ambient water is polar, has extensive network of H-bonding, and does not solubilize most organics. As water is heated, the H-bonds start weakening, allowing dissociation of water into acidic hydronium ions ( $\text{H}_3\text{O}^+$ ) and basic hydroxide ions ( $\text{OH}^-$ ). Below the critical point, the ionization constant of water increases with temperature and is about three orders of magnitude higher than that of

ambient water. Also, the dielectric constant of water decreases with temperature. A low dielectric constant allows liquid water to dissolve organic compounds, while a high ionization constant provides an acidic medium for the hydrolysis of biomass components via the cleavage of ether and ester bonds and favor the hydrolysis of hemicelluloses.<sup>18-21</sup> The structural alterations due to the removal of hemicelluloses increase the accessibility and enzymatic hydrolysis of cellulose. Enzyme accessibility is increased as a result of the increase in mean pore size of the substrate which enhances the probability of the hydrolysis of glycosidic linkage.<sup>22</sup>

Hydrothermal pretreatment is typically conducted in the range of 150-220°C. The temperature range, aiming for the fractionation of hemicelluloses, are decided based on the fact that at temperature below 100°C less/small extent of hydrolytic reaction is observed whereas cellulose hydrolysis and degradation become significant above 210°C.<sup>23, 24</sup> Ether bonds of the hemicelluloses are most susceptible to breakage by the hydronium ions. Depending on the operational conditions, hemicelluloses are depolymerized to oligosaccharides and monomers, and the xylose recovery from biomass can be as high as 88-98%. For example, Suryawati et al. has reported 90% removal of hemicelluloses from Kanlow switchgrass at 200°C.<sup>25</sup> Acetic acid is also generated from the splitting of thermally labile acetyl groups of hemicelluloses. In further reactions, the hydronium ions generated from the autoionization of acetic acid also acts as catalyst and promotes the degradation of solubilized sugars. In fact, the formations of hydronium ions from acetic acid is much more than from water.<sup>23, 24</sup>

The low pH (< 3) of the medium causes the precipitation of solubilized lignin and also catalyzes the degradation of hemicelluloses. To avoid the formation of inhibitors, the

pH should be kept between 4 and 7 during the pretreatment. This pH range minimizes the formation of monosaccharides, and therefore the formations of degradation products that can further catalyze hydrolysis of the cellulosic material during pretreatment.<sup>6, 22, 26-30</sup> Maintaining the pH near neutral (5-7) helps in avoiding the formation of fermentation inhibitors during the pretreatment.

In general, the concentrations of solubilized products are lower in hydrothermal pretreatment compared to the steam pretreatment.<sup>26</sup> Since the hot compressed water is used instead of steam, the latent heat of evaporation is saved which makes it easier to apply for a continuous process.<sup>31</sup> Earlier, Yang and Wyman have reported that flow through process fractionated more hemicelluloses and lignin from corn stover as compared to batch system under the conditions of similar severity.<sup>32</sup> In a flow through system, the product is continuously removed from the reactor which reduces the risk on condensation and precipitation of lignin components, making the biomass less digestible. The soluble lignin are very reactive at the pretreatment temperature and if not removed rapidly part of these compounds re-condense and precipitate on the biomass.<sup>33, 34</sup>

The main objective of this work is to carry out the hydrothermal pretreatments of Auburn switchgrass and corn stover in a flow through reactor to enhance and optimize the enzymatic digestibility. Another objective is to maintain the pH of liquid hydrolyzate near to neutral (5-6) by conducting alkali salt ( $K_2CO_3$ ) assisted hydrothermal pretreatment. The purpose was to retain hemicelluloses, fractionate lignin to minimize the loss of carbohydrates in liquid. Hence, the effect of pretreatment temperature (150-190°C) and addition of  $K_2CO_3$  (0-0.9 wt%) is studied. The enzymatic digestibility of the resulting pretreated biomass is investigated with cellulase and  $\beta$ -glucosidase enzymes. In

addition, the changes in crystallinity, surface area, and surface morphology are examined by X-ray diffraction (XRD), BET surface area measurement, and electron microscopy (SEM), respectively.

As discussed earlier, the liquid hydrolyzate byproduct from pretreatment contains several compounds resulting from the partial solubilization of lignin besides hydrolysis of hemicelluloses. Depending upon the pretreatment temperature, 25-45% of the initial biomass carbon is solubilized in hydrolyzate, mostly in the form of sugars from hemicelluloses, degradation products such as furfural, lignin derived phenolic compounds, and carboxylic acids. These degradation compounds are the potential inhibitors during fermentation.<sup>22</sup> Fermentation of cellulose (C<sub>6</sub> sugar) for bioethanol production is a well-established process which is carried out by using Baker's yeast *Saccharomyces cerevisiae*. However, yeast or the high ethanol yielding bacterium *Zymomonas mobilis* cannot ferment multiple sugar substrates e.g. xylose and arabinose to ethanol.<sup>35</sup> To maximize the yield of ethanol from lignocellulosic biomass, it is proposed that liquid hydrolyzate containing sugars from hemicelluloses should be co-fermented with cellulosic sugars.<sup>36</sup> Though many pentose-utilizing strains such as *Escherichia coli*, *Pichia stipitis*, and *Zymomonas mobilis* have been developed, the detoxification of hydrolyzate are needed.<sup>37</sup> Detoxification of hydrolyzate improves their fermentability, however, the cost associated in the process is often higher than the benefit.<sup>38</sup> Furthermore, genetically engineered microorganisms which can utilize all sugars in hydrolyzate are still in developmental stage.<sup>37</sup> Depending upon the type of aqueous pretreatment, pH of liquid hydrolyzate may vary. The dilute concentration of sugars in liquid hydrolyzate is another challenge.

In this work an alternate pathway is developed to recover soluble organic carbon in liquid hydrolyzate. Hydrolyzate is subjected to hydrothermal carbonization to produce carbon microsphere byproduct. The properties of microspheres are analyzed by calorimetry, SEM and FTIR. The reaction mechanism involved in hydrothermal carbonization is studied using gas chromatography and mass spectrometry of the hydrolyzate.

### 3.3 Experimental Section

*Materials:* Switchgrass was locally grown at Auburn University in a test plot (Prof. David I. Bransby, Department of Agronomy and Soil) and corn stover was obtained from National Renewable Energy Laboratory (NREL, Colorado). Both feedstocks were reduced to (+) 60 mesh to (-) 20 mesh size before utilization. Moisture content of both the feedstocks was 8-9 wt%. The composition analysis of switchgrass and corn stover are shown in Table 3.1.

Table 3.1 Feedstock composition (oven dry basis).

Components	Switchgrass	Corn stover
	wt%	wt%
Cellulose	38.9	34.5
Hemicelluloses	28.9	27.7
Klason lignin	30.4	16.5
Acid soluble lignin	1.3	1.3
Ash	3.0	5.6

The selected lot of Auburn switchgrass contained unexpectedly high lignin content. Potassium carbonate ( $K_2CO_3$ ) and high purity standard reagents for HPLC analysis were purchased from Sigma Aldrich. De-ionized water was used for all the experiments.

*Apparatus:* Figure 3.1 shows the schematic of the hydrothermal pretreatment apparatus. It consists of two high-pressure liquid pumps, an electrical tubular furnace, a water-cooled double tube heat exchanger, a backpressure regulator, and a phase separator. Reactor is a 0.57" ID, 65 ml volume high-pressure stainless steel tube.

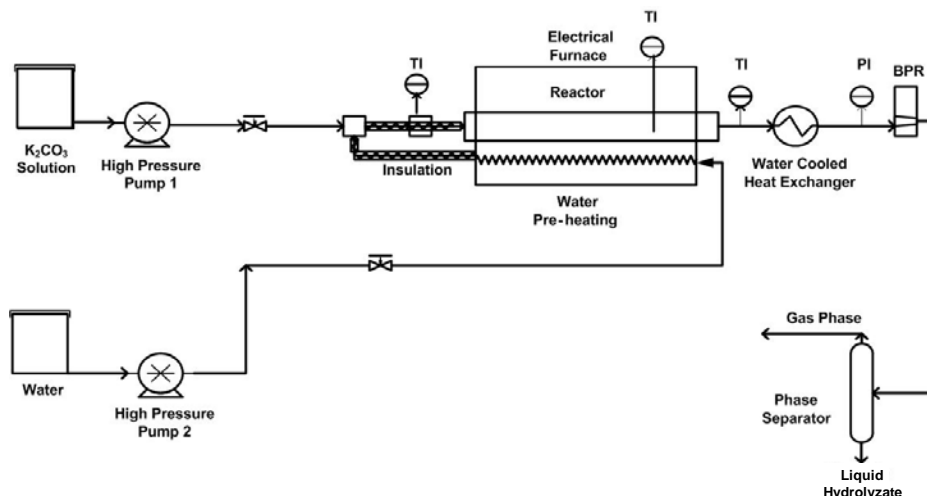


Figure 3.1 Apparatus for the hydrothermal pretreatment of biomass.

Temperature of the reaction zone was measured using a 1/16" thermocouple placed inside the biomass bed from the inlet. There were three additional thermocouples installed at different locations in the apparatus. Real time temperature indicated by the thermocouple placed inside the reaction zone was used for all the analyses. Reactor pressure was maintained using a backpressure regulator.

*Experimental Procedure:* Study was conducted in a flow through scheme in the apparatus shown in Figure 3.1. In a typical experiment, reactor was placed inside the furnace after

packing with 11.0 g of biomass. Moisture of the biomass (switchgrass or corn stover) was measured before charging into the reactor. A stainless steel frit (2 µm pore size) was placed in the reactor outlet to prevent the entrainment of fine solids with the liquid stream. Water and K<sub>2</sub>CO<sub>3</sub> solution was pumped using high pressure pumps 1 and 2 (Figure 3.1) and total liquid inlet flow rate was maintained 2.5 ml/min for the duration of study. Pretreated biomass retained in the reactor was washed with water to neutral pH in the reactor during the cooling cycle and collected for the solid composition analysis and subsequent enzymatic hydrolysis. Experiments were conducted using pure water and K<sub>2</sub>CO<sub>3</sub> (0-0.9 wt%) dissolved in water for temperature range of 150-190°C (Table 3.2).

Table 3.2 Pretreatment details conducted at 3.4 MPa and 20 min steady operation time and the weight loss of switchgrass after pretreatment (oven dry basis).

Switchgrass	Temperature (°C)	K <sub>2</sub> CO <sub>3</sub> (wt%)	Weight loss (wt%)
Run 1	150	0	17.0
Run 2	150	0.6	17.8
Run 3	150	0.9	17.1
Run 4	175	0	34.0
Run 5	175	0.9	35.0
Run 6	190	0	40.0
Run 7	190	0.9	50.0
Corn stover			
Run 8	150	0	25.6
Run 9	150	0.45	34.4
Run 10	190	0.45	50.0

After completing the desired (20 minute) steady operation, heating was stopped and reactor was rapidly cooled to below 50°C. In a flow through process, biomass is subjected to a typical temperature cycle as shown in Figure 3.2.

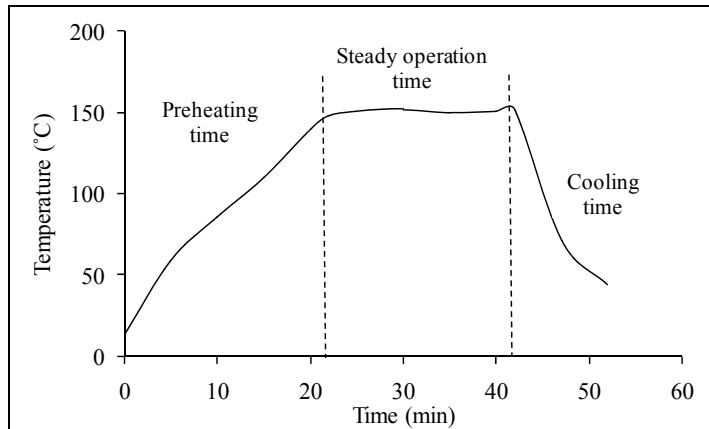


Figure 3.2 Typical temperature cycle during pretreatment process.

The liquid products collected during all three stages of operation - preheating, steady operation, and cooling/washing - were analyzed for total organic carbon (TOC) content. Liquid samples were centrifuged at 3600 rpm before analyzing TOC to remove suspended solids. The gaseous products which were appreciably low in the temperature range of study were vented without analysis.

Hydrothermal carbonization experiments were conducted in a 45 ml batch reactor (Figure 3.3).

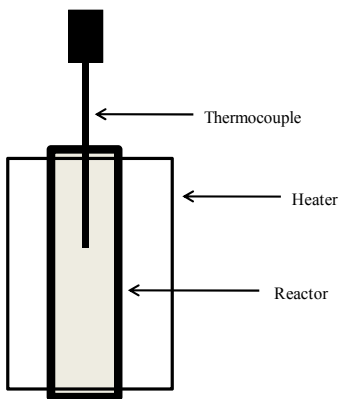


Figure 3.3 Batch reactor for hydrothermal carbonization process.

The liquid hydrolyzate was charged to reactor and heated to 200°C for the desired reaction time under autogeneous pressure condition. After the reaction, reactor was rapidly cooled to ambient condition and the precipitated solids were recovered using centrifuge. Obtained powder was washed with water, freeze dried for 48 h and preserved for further characterization. The liquid fraction recovered after centrifugation was analyzed for the TOC content to determine the conversion of organic carbon into powder and gaseous fraction. Again, at the studied temperature condition (200°C), gaseous products were appreciably low and so were not collected.

Since, liquid hydrolyzate comprised of mainly sugar compounds, glucose solution of equivalent TOC value was also used as model compound for the similar experiments and the results were compared. Table 3.3 shows the details of experiment conducted for hydrothermal carbonization.

Table 3.3 Details of hydrothermal carbonization experiments.

Run no	Input Solution	Time (h)
Run I	Liquid hydrolysate	1
Run II	Liquid hydrolysate	2
Run III	Liquid hydrolysate	4
Run IV	Glucose	1
Run V	Glucose	2
Run VI	Glucose	4

Liquid hydrolyzate collected during the hydrothermal pretreatment experiments (run 6) typically contained 1.1-1.2 wt% of organic carbon and this solution was used for the carbonization study.

*Experimental and analytical accuracy:* All the thermocouples ( $\pm 0.1^\circ\text{C}$ ) were calibrated before the start of experiment. High precision HPLC pumps (Chrome Tech, USA) were used for the liquid flow. Pump flow rates were calibrated before every experiment and showed less than 1% variation. Multiple liquid samples were collected and analyzed for TOC and pH values during every experiment. Pretreatment experiments were duplicated or done in triplicates to confirm the reproducibility of the data. Composition analysis of solids after the pretreatment experiment was done in duplicates as per the NREL standard procedures. The standard deviation of the reported values of solid composition in biomass is less than 3%. Enzymatic digestibility is also performed as per NREL standard procedures using duplicate samples within the error of  $\pm 5\%$ .

### **3.4 Product Characterization**

#### 3.4.1 Pretreatment

Pretreated switchgrass and corn stover were analyzed for carbohydrate and lignin composition, and enzymatic hydrolysis published in NREL technical report NREL/TP-510-42618 ([www.eere.energy.gov/biomass/analytical\\_procedures.html](http://www.eere.energy.gov/biomass/analytical_procedures.html)).

*Chemical composition of pretreated solids/liquid:* Composition analysis of solid biomass was done as per NREL laboratory analytical procedures (LAP) “Preparation of samples for compositional analysis,” “Determination of structural carbohydrates and lignin in biomass”, and “Determination of ash in biomass”. Pretreatment liquor was analyzed for different monomer and oligomer sugars as per NREL LAP: “Determination of sugars, byproducts and degradation products in liquid fraction process samples.” HPLC with Bio-Rad Aminex HPX-87P column was employed for determination of sugar concentrations in liquid samples while Bio-Rad Aminex HPX-87H column was used for acids and degradation products.

*Enzymatic hydrolysis of pretreated solids:* Enzymatic hydrolyses of the original and pretreated biomasses were carried out in 125 ml flasks with rubber stoppers on the top. The protocol used was similar to the NREL LAP “Enzymatic saccharification of lignocellulosic biomass.” Cellulase commercial enzyme (Spezyme CP, Genencor) with initial loading of 15 FPU/g glucan and  $\beta$ -glucosidase (Novo 188<sup>®</sup>, Novozyme) 30 CBU/g glucan were used for the study. Other test conditions were maintained as per the protocol: 0.05 N sodium citrate buffers were used and the initial pH was maintained as 4.8. Antibiotics tetracycline and cyclohexamide were used to avoid contamination. Flasks were placed in an incubator which maintained constant reaction temperature of 50°C at

150 rpm. Liquid samples were collected every 1, 12, 24, and 72 h of hydrolysis and then were placed in boiling water for 5 minutes to kill the reaction. Then the samples were centrifuged for 10 minutes at 14000 rpm to remove solids and analyzed for released glucose in the liquid phase by HPLC with Bio-Rad Aminex HPX-87P column and refractive index detector. The enzymatic digestibility is calculated as the ratio of glucan equivalent of glucose + cellobiose in the liquid phase to the initial glucan loading (1 g). Glucan equivalent of glucose and cellobiose is calculated as  $0.9 \times$ solubilized glucose amount +  $0.95 \times$ solubilized cellobiose amount. Though, periodic hydrolysis samples were collected as discussed earlier only 72 h glucan digestibility data are discussed in the study for all the pretreatment conditions.

*XRD analysis:* Rigaku Miniflex powder X-ray diffractometer equipped with a Cu K $\alpha_1$  radiation source at 30 kV voltages, 15 mA current and a miniflex goniometer was used for the XRD analysis. Diffraction patterns were collected in the  $2\theta$  range of 10-35° at a scan speed of 1°/min. and step size of 0.01°. The cellulose crystallinity index (*CI*) in the switchgrass was determined<sup>39</sup> by

$$CI = (I_{002} - I_{AM}) / I_{002} \quad [1]$$

where  $I_{002}$  is the peak intensity corresponding to (002) lattice plane of cellulose molecule, and  $I_{AM}$  is the peak intensity observed at  $2\theta$  equal to 18°.  $I_{002}$  represents both crystalline and amorphous material while  $I_{AM}$  represents amorphous material only.

*BET surface area measurement:* Surface area is a measure of the exposed surface of a solid sample on the molecular scale. The method of Brunauer, Emmett, and Teller (BET) is used to determine the total surface area of materials. Raw and pretreated switchgrass

samples were analyzed for the BET surface area using Krypton as adsorptive gas by multi-point analysis method at Micromeritics Analytical Services (Norcross, GA).

*Electron microscopy:* The untreated and pretreated samples were prepared on adhesive carbon tape on an aluminum stub followed by sputter coating of gold. Surface morphology of the sample was studied using an environmental scanning electron microscopy system (Zeiss EVO 50).

#### 3.4.2 Hydrothermal Carbonization:

After hydrothermal carbonization of hydrolyzate (and glucose solution for comparison) product liquid and solid were separated. Solids were characterized using SEM (Zeiss EVO 50), FTIR (Nicolet IR100), elemental carbon analysis, and calorimetry (IKA-C200 Calorimeter). Liquids were analyzed by TOC and GC-MS as following. Agilent model HP-5 column with 5% phenyl methyl siloxane (30 m long, 0.25 mm diameter, 0.25  $\mu$ m film thickness) was utilized for identifying the compounds in liquid samples. Oven was programmed as: 45°C (hold 5 min) and ramped up (rate 5°C/min) to 250°C (hold 8 min). Injector was kept at 250°C in split mode (split ratio 50:1) with helium as carrier gas. Sample volume was 0.2  $\mu$ l and compounds were identified using NIST library of mass spectra.

### **3.5 Results and Discussion**

#### 3.5.1 Pretreatment

*Hydrothermal pretreatment:* Figure 3.4 shows the percentage removal (oven dry basis) of hemicelluloses and lignin from switchgrass upon pretreatment 3.4 MPa and 20 min of steady operation time (run 1,4 and 6) and varying temperature.

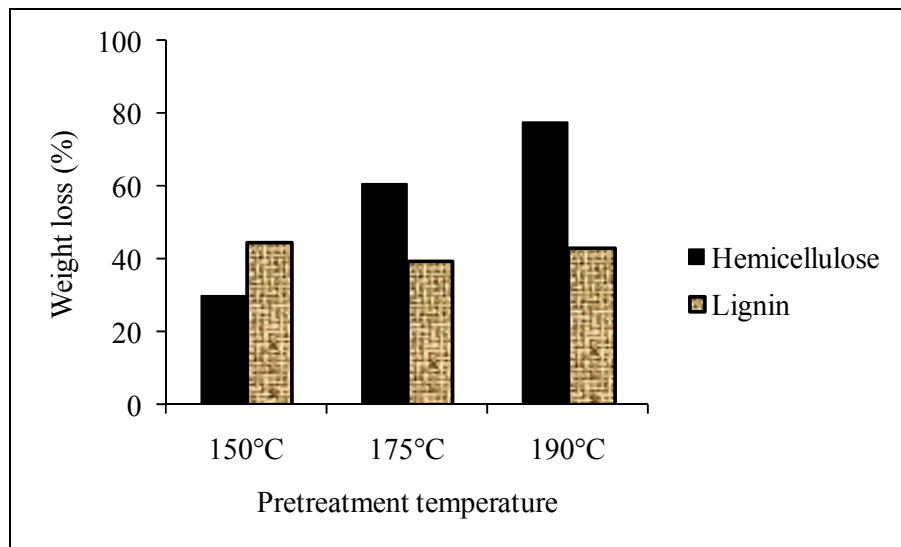


Figure 3.4 Percentage removal of hemicelluloses and lignin with temperature for the switchgrass pretreated at 3.4 MPa and 20 min steady operation time.

It was observed that hemicelluloses hydrolysis to water soluble products increased from 30% to 77% as the pretreatment temperature increased from 150 to 190°C. Part of the lignin (~40%) was also solubilized, but it remained nearly constant in the temperature range of 150-190°C. And pH of the liquid hydrolyzate varied between 3.5 to 4.5 depending on the pretreatment temperature. Typically, pH liquid hydrolyzate decreases with increase in temperature due to the increased formation of organic acids.<sup>40</sup> Low activation energy of lignin causes partial degradation of lignin in hydrothermal medium at temperature below 200°C.<sup>26, 41</sup> The ether bonds in lignin start breaking above 150°C in a weakly acidic medium.<sup>42</sup> Cellulose remained stable at below 190 °C and about 10% of weight loss was observed at 190°C. Cellulose composition in washed pretreated solid biomass was increased to 51-58 wt% compared to 38.9 wt% in native switchgrass. These results are in agreement with those for Almo and Kanlow switchgrass.<sup>25, 43</sup> In general, cellulose hydrolysis is mainly observed above 210°C in hydrothermal medium.

Hemicelluloses are the most susceptible in hydrothermal medium because of hydronium ions generated from water autoionization. Hemicelluloses possess side groups, including acetic acid, pentoses, hexuronic acids, and deoxyhexoses. The lower stability of hemicelluloses is mainly due to the fact that their side chains reduces the aggregation of their molecules and inhibits the formation of H-bonds.<sup>26</sup>

Figure 3.5 shows the 72 h glucan digestibility for pretreated switchgrass. The untreated switchgrass has almost negligible enzymatic reactivity.

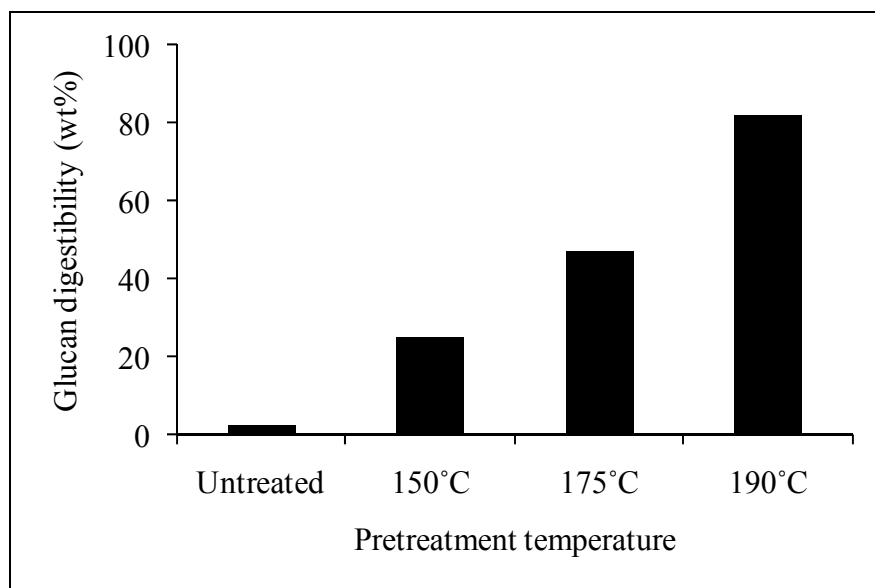


Figure 3.5 Glucan digestibility (72 h) of hydrothermally pretreated switchgrass.

However, as a result of partial removal of hemicelluloses and lignin during the pretreatment, physical and chemical properties of switchgrass are altered. The pretreatment helped in improving the enzyme accessibility and effectiveness for cellulose hydrolysis by increasing the internal surface area and pore volume. As a result, cellulose depolymerization to sugars substantially enhanced. Glucan digestibility of switchgrass

pretreated at 150°C was still low (25%) but with the increase of pretreatment temperature, more than 82% of digestibility could be achieved.

*Alkali salt ( $K_2CO_3$ ) assisted hydrothermal pretreatment:* Figure 3.6 shows the effect of  $K_2CO_3$  addition during the hydrothermal pretreatment at 150°C.

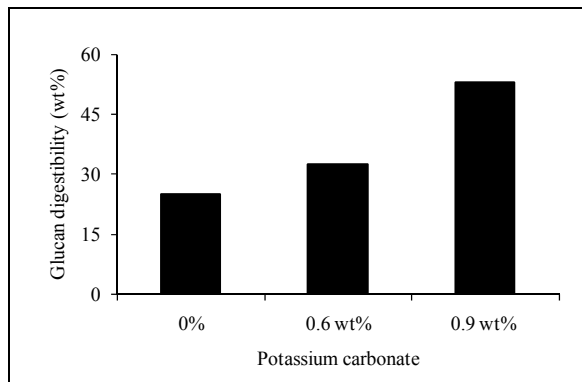


Figure 3.6 Glucan digestibility (72 h) of switchgrass pretreated at 150°C in the presence of  $K_2CO_3$ .

With the addition of 0.9 wt%  $K_2CO_3$  in water during pretreatment, enzymatic digestibility of the substrate doubled compared to that without  $K_2CO_3$ . On the component basis, more than 40% of lignin was removed during run 3, and nearly 90% of hemicelluloses were retained in solid fraction. In runs 2 and 3, which are conducted in the presence of  $K_2CO_3$ , pH of liquid hydrolyzate increased to 7 as compared to 5 in run 1 (i.e., without  $K_2CO_3$ ). As expected, the hydrolysis of hemicelluloses could be minimized mainly due to the relatively low temperature and near neutral pH. Alkali has selectivity towards lignin and cause lignin degradation by breaking aryl ether linkages which constitutes approximately 50-70% of total linkages. On the other hand, diaryl ethers and carbon-carbon bonds are relatively stable. Hydroxyl ion catalyzes the cleavage of ether linkages in the lignin and thus liberating the soluble phenolics in the liquid. The breakage

of these bonds increases the hydrophilicity of lignin. Alkaline medium also causes the solvation of hydroxyl groups in carbohydrates which in turn swells the sugar residue, thus increasing the diffusivity of reagent through the capillaries.<sup>44</sup> These all combined factors would help in increasing the effective adsorption of enzyme molecule on pretreated biomass and thus increasing the accessibility and digestibility of carbohydrate fraction in the biomass.<sup>45, 46</sup> Figure 3.7 compares the SEM images of raw and the pretreated switchgrass (run 3), where additional pores created after the pretreatment can be seen.

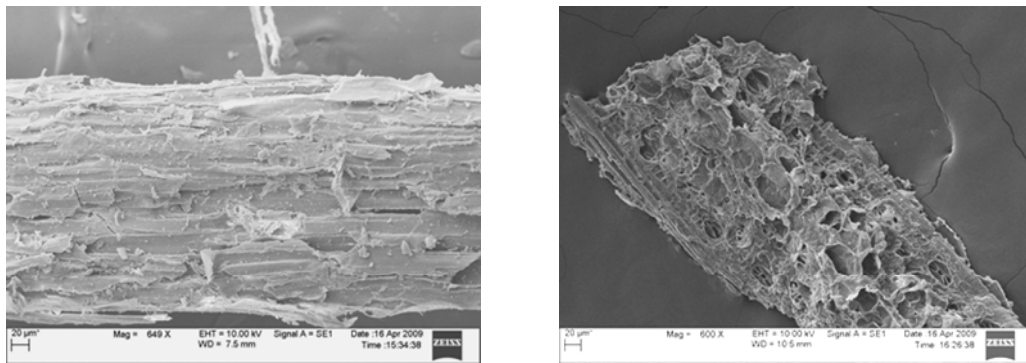


Figure 3.7 SEM images of untreated and pretreated (run 3) switchgrass taken at 600X magnification.

Figure 3.8 shows the effect of pretreatment temperature on the enzymatic digestibility of pretreated switchgrass. These samples were pretreated in the presence of 0.9 wt% of  $K_2CO_3$  at 3.4 MPa and 20 min steady operation time.

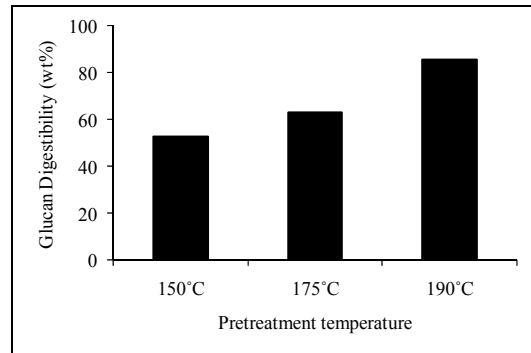


Figure 3.8 Glucan digestibility (72 h) of  $\text{K}_2\text{CO}_3$  (0.9 wt%) assisted hydrothermally pretreated switchgrass.

Glucan digestibility increased with pretreatment temperature and 85.5% of glucan digestibility could be achieved in run 7. This was marginally higher compared to run 6. To understand the phenomena, it is important to observe the Figure 3.9 which shows the component wise weight loss during runs 3, 5 and 7.

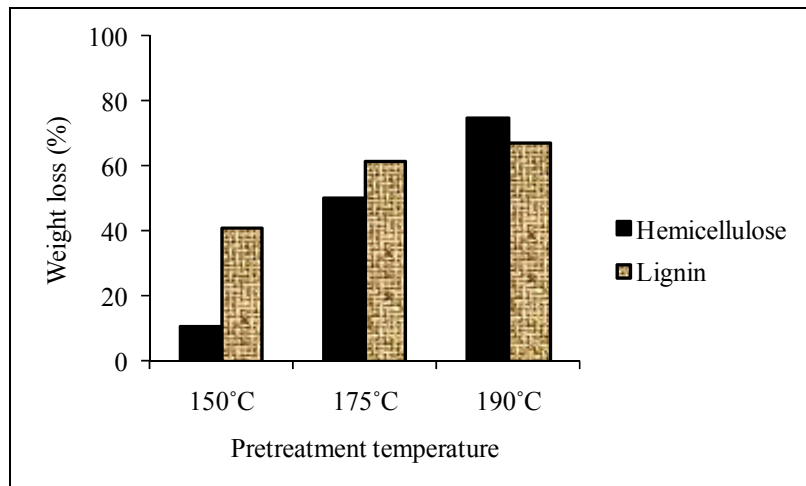


Figure 3.9 Percentage removal of hemicelluloses and lignin with temperature for the switchgrass pretreated in the presence of 0.9 wt% of  $\text{K}_2\text{CO}_3$ .

Though delignification increased from 40.8 to 67.3% in these experiments, hemicelluloses were also hydrolyzed substantially during these runs. Percentage removals

of hemicelluloses were 10.5, 50, and 75% for the runs 3, 5, and 7, respectively. Liquid pH for run 7 dropped down to 5. Increase in pretreatment temperature increases the delignification as well as hemicelluloses loss from the solids. Hemicelluloses are known to undergo numerous physical and chemical changes such as swelling, dissolution, saponification, reprecipitation, peeling and glycosidic cleavage reactions at higher temperature in the presence of hydroxyl ions.<sup>44</sup> Presence of several biomass derived components in the reaction medium makes the chemistry very complex.

If we compare the glucan digestibility of the run 6 to run 7, it can be concluded that at the higher pretreatment temperature, hydrothermal treatment alone can enhance the enzymatic digestibility of pretreated switchgrass higher than 80%. Figure 3.10 and 3.11 compares the overall material balance based on the 100 kg oven dry switchgrass for run 6 and 7.

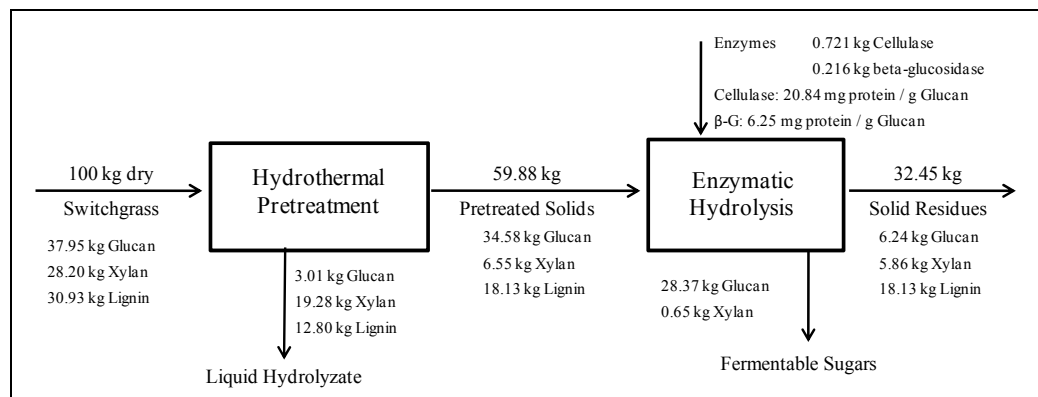


Figure 3.10 Material balance for hydrothermally pretreated switchgrass (run 6) at 190°C.

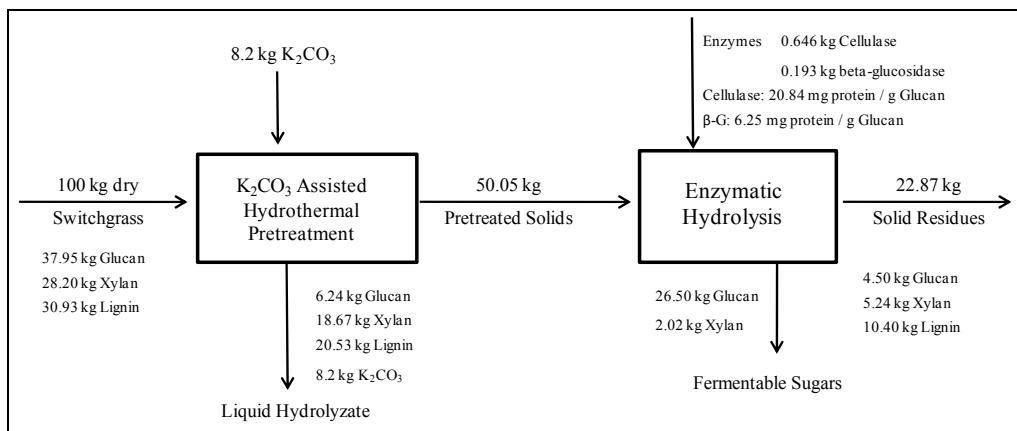


Figure 3.11 Material balance for  $\text{K}_2\text{CO}_3$  assisted hydrothermally pretreated switchgrass (run 7) at 190°C.

Presence of  $\text{K}_2\text{CO}_3$  supported the delignification even at lower temperature (150-175°C), and so the enzymatic digestibility of switchgrass was comparatively higher than that of hydrothermal pretreatment. Pressure is another important factor, which may be considered. Constant pressure 3.4 MPa, which is higher than the vapor pressure of water in the range of study (150-190°C) was chosen in this study to maintain water in liquid phase. Previous studies on the effect of pressure have reported that the influence of pressure on hydrolysis of biomass is normally limited to keeping water in liquid phase at the operating temperature.<sup>47</sup> In fact, ionization constant of water shows small dependence on pressure (ionization slightly increases with increasing pressure).<sup>48</sup> But, pressure and temperature can be used to influence the density and transport properties (viscosity, thermal conductivity, and diffusivity) of hydrothermal medium. Change in pressure mainly influences the density-dependent physical properties such as partition coefficient and dielectric constant.<sup>49</sup> To understand the effect of pressure during pretreatment, an experiment (not shown in Table 3.2) at higher pretreatment pressure (13.8 MPa) keeping

other process parameters same as run 3 was conducted using switchgrass. The glucan digestibility after pretreatment increased from 53% (run 3) to 71.2%. It was observed that the overall weight loss after pretreatment increased with pretreatment pressure from 17.1 to 39.4%. On the component basis, removal of hemicelluloses and lignin both increased substantially, whereas almost no loss (< 5%) of cellulose was observed.

*BET surface area:* The purpose of the pretreatment is to remove resistance in biomass which limits the enzyme accessibility to cellulosic sites. Enzymatic hydrolysis of lignocellulosic biomass is limited by several factors such as crystallinity of cellulose, degree of polymerization, available surface area and the lignin content.<sup>22, 50</sup> Among these factors, the accessible surface area is regarded as one of the most important factors affecting the effectiveness of enzymatic digestibility.<sup>35</sup> After the pretreatment, internal surface area may increase because of following changes: (i) due to the fragmentation and development of cracks (Figure 3.7), (ii) removal of hemicelluloses and lignin which diminishes shielding effects and opens up additional pores.<sup>35</sup> To understand the changes in switchgrass internal surface area after the pretreatment, samples from run 6 and run 7 were analyzed for the BET surface area. It is observed that internal surface area of pretreated switchgrass increased by 3 to 5 folds (Table 3.4).

Table 3.4 BET surface area of untreated switchgrass and pretreated samples from run 6 and run 7.

Biomass	BET surface area (m <sup>2</sup> /g)
Untreated switchgrass	0.8251
Pretreated switchgrass, Run 6	4.4184
Pretreated switchgrass, Run 7	2.8300

An interesting and contradicting observation is that though pretreated switchgrass from run 6 has 55% more internal surface area than that of run 7, their glucan digestibility are comparable. Notably, the lignin content in run 6 and run 7 solids are 30.3 and 20.8%, respectively. Nonproductive and irreversible adsorption of enzymes to lignin is often claimed to be responsible for the need for high enzyme loadings.<sup>51</sup> Lignin limits the rate and extent of enzymatic hydrolysis due to its shielding effect. If only the internal surface area is the reason, run 6 pretreated sample should have higher digestibility than run 7, which not the case here. This suggests that it is not just the internal surface area or lignin content in pretreated biomass affecting enzymatic digestibility of the substrate but probably some other molecular characteristics such as degree of polymerization, crystallinity, and other internal rearrangement of the structure are also responsible.

*XRD pattern:* Figure 3.12 shows the XRD pattern of untreated switchgrass and pretreated switchgrass from runs 6 and 7.

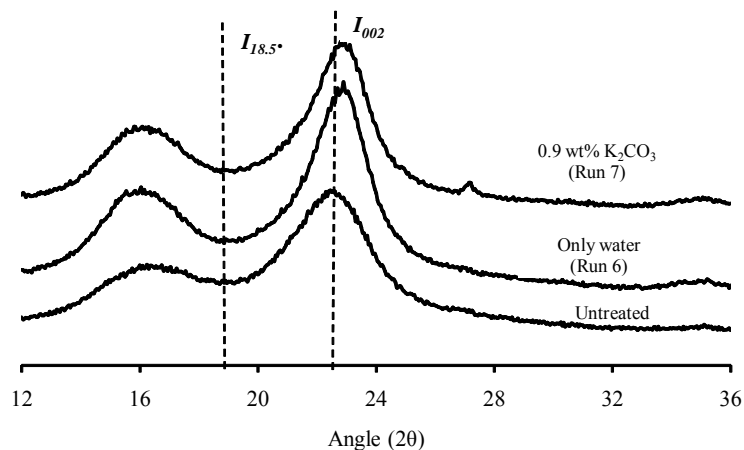


Figure 3.12 XRD patter of untreated and pretreated (run 6 and 7) switchgrass.

The untreated switchgrass has a broader peak ( $I_{002}$ ) with cellulose crystallinity of 53.5%. Peak ( $I_{002}$ ) became sharper after the pretreatment and also percentage crystallinity increased. The crystallinity of cellulose in runs 6 and 7 samples were almost same and was 67.1 and 67.6%, respectively. Increase in percentage crystallinity may be attributed to the hydrolysis and removal of the amorphous part of cellulose during pretreatment.<sup>52</sup>

*Comparison with corn stover:* The composition of lignocellulosic biomass is a key factor affecting efficiency of biofuel production during conversion processes. The structural and chemical compositions of lignocelluloses are highly variable because of genetic and environmental influences and their interactions. Nevertheless the chemical composition of switchgrass and corn stover is relatively similar (Table 3.1) except the fact that the switchgrass used in this study had much higher lignin content than corn stover. Figure 3.13 compares the glucan digestibility of corn stover pretreated in different process condition.

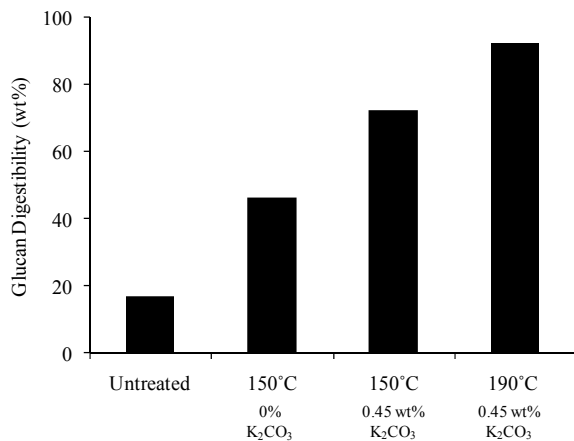


Figure 3.13 Glucan digestibility (72 h) of untreated and pretreated corn stover.

Interestingly, corn stover required less severe pretreatment than switchgrass. Corn stover pretreated at 190°C had 92.6% of glucan digestibility even though K<sub>2</sub>CO<sub>3</sub> concentration in water was only 0.45 wt%. Under the similar pretreatment condition, switchgrass (run 7) pretreated in the presence of 0.9 wt% K<sub>2</sub>CO<sub>3</sub> had only 85.5% of digestibility. The SEM images of corn stover (Figure 3.14) reveal the fact that even untreated corn stover has relatively more porous structure and also morphologically it shows more structural changes than switchgrass after the pretreatment.

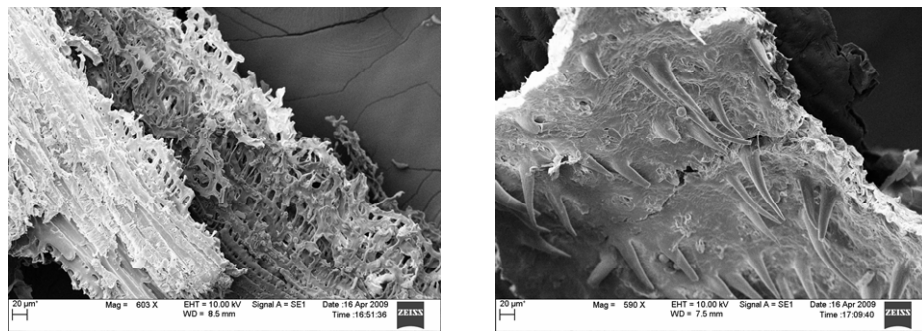


Figure 3.14 SEM images of untreated and pretreated (run 8) corn stover taken at 600X magnification.

### 3.5.2 Hydrothermal Carbonization:

At present, co-fermentation of liquid hydrolyzate for ethanol production is the major focus of research. The challenges associated with the detoxification and development of pentose-utilizing strains for co-fermentation has already been discussed in introduction section. On the other hand, there have been very few studies conducted on the development of alternate pathway for utilizing the liquid hydrolyzate excluding the studies on hydrogen production through dark fermentation and on biogas production through anaerobic digestion.<sup>36</sup> However, the hydrogen yield obtained by dark fermentation is relatively low (approximately 20-30% of the energy content in the organic matter) while the remaining organic matter is converted to volatile fatty acids.<sup>36</sup>

The biogas production by anaerobic digestion has the possibility to utilize all types of organic molecules however; setting up another bioreactor for the purpose may bring some additional cost to the process. Hydrothermal carbonization of liquid hydrolyzate is another potential alternative, where majority of organic content of the liquid hydrolyzate can be recovered as carbon rich microspheres.<sup>53</sup> The process is typically conducted at 180-200°C, so there is no additional heat requirement since hydrothermal pretreatment is also conducted in the similar range for achieving the optimal enzymatic digestibility of pretreated biomass. Table 3.5 shows the typical sugar composition of liquid hydrolyzate collected at 190°C during experiment run 6.

Table 3.5 Sugar compounds analyzed by HPLC in liquid hydrolyzate collected at 190°C during run 6.

Compounds	Before hydrolysis	After hydrolysis
	g/L	g/L
Cellobiose	0.5	-
Glucose	0.7	2.7
Xylose	2.6	18.1
Galactose	0.4	1.8
Arabinose	1.1	2.4
Furfural	1.1	-
Acetic acid	1.5	-

Xylose is the major component besides the host of other inhibitory compounds present in the liquid. GC-MS analysis of the sample confirmed the presence of several other phenolic compounds such as furfural, 2,3-dihydrobenzofuran, 2-furancarboxaldehyde, benzaldehyde 3-hydroxy-, 1,4-benzenediol 2-methyl-, vanillin etc.

It can be seen that by carbonizing this liquid at 200°C for just 2 h, nearly 60% of the organic compounds (based on TOC) could be precipitated as solids (Figure 3.15).

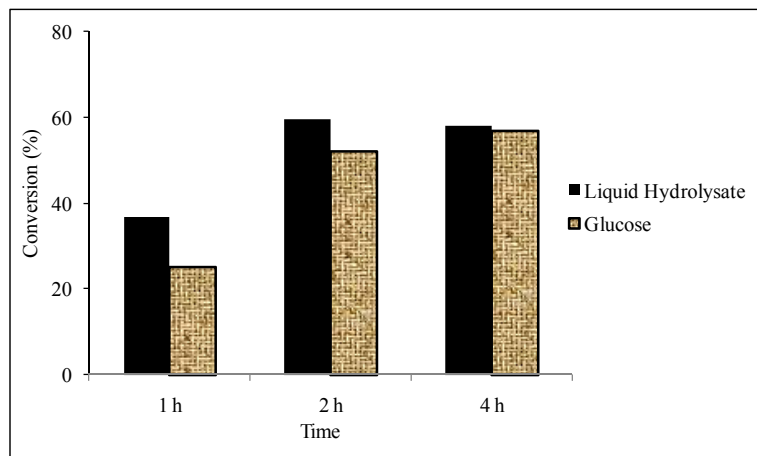


Figure 3.15 Percentage conversion of liquid hydrolyzate (based on TOC of input) of run 6 and glucose solution.

Though, maintaining the temperature for 4 h (Table 3.3, run III), the conversion did not increase. Similar results were observed when glucose solution was used for comparison. The precipitated solids were globular with their diameter ranging from 0.2-2  $\mu\text{m}$  (Figure 3.16).

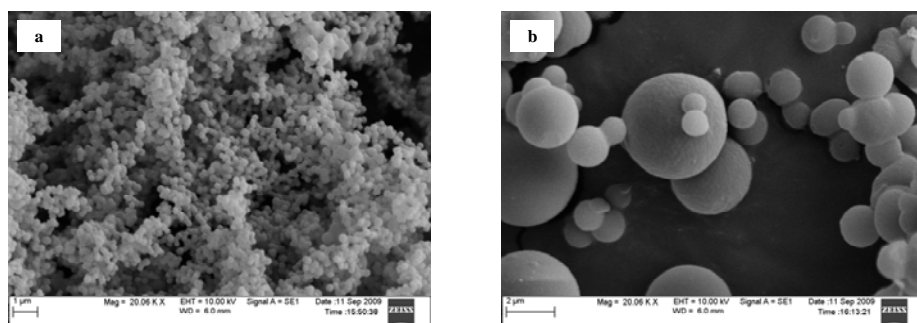


Figure 3.16 SEM images (at 20,000X magnifications) of carbon microspheres produced from (a) glucose solution and (b) liquid hydrolyzate of run 6.

The microspheres produced from glucose solution (Figure 3.16a) were mostly of uniform size but they were much finer (submicron size, 0.2-0.4  $\mu\text{m}$ ) compared to the

microspheres obtained from the liquid hydrolyzate. This may be mainly because of the many phenolic compounds present in liquid which also contributed in polymerization process. These microspheres appeared brown and were fluffy. Elemental carbon in microspheres produced in run II and run V were 64.88 and 66.06%, respectively. Titirici et al. had also studied the hydrothermal carbonization of carbohydrate model compounds such as glucose and xylose. Their study reported the elemental carbon in the microsphere as 64.47 and 68.58% from glucose and xylose, respectively.<sup>54</sup> The HHV of these carbon rich microspheres from run II was 24.8 MJ/kg which is comparable to lignin's HHV (24-26 MJ/kg).

Glucose conversion to its degradation products and the carbon microspheres was almost complete (99%) just in an hour of reaction time. Only traces (~1%) of glucose was observed in the output liquid from run IV. The concentration of acetic acid in liquid product was found to increase with reaction times, i.e run VI had higher acetic acid concentration than run IV. GC-MS spectra of the liquid samples from runs IV, V, and VI are shown in Figure 3.17.

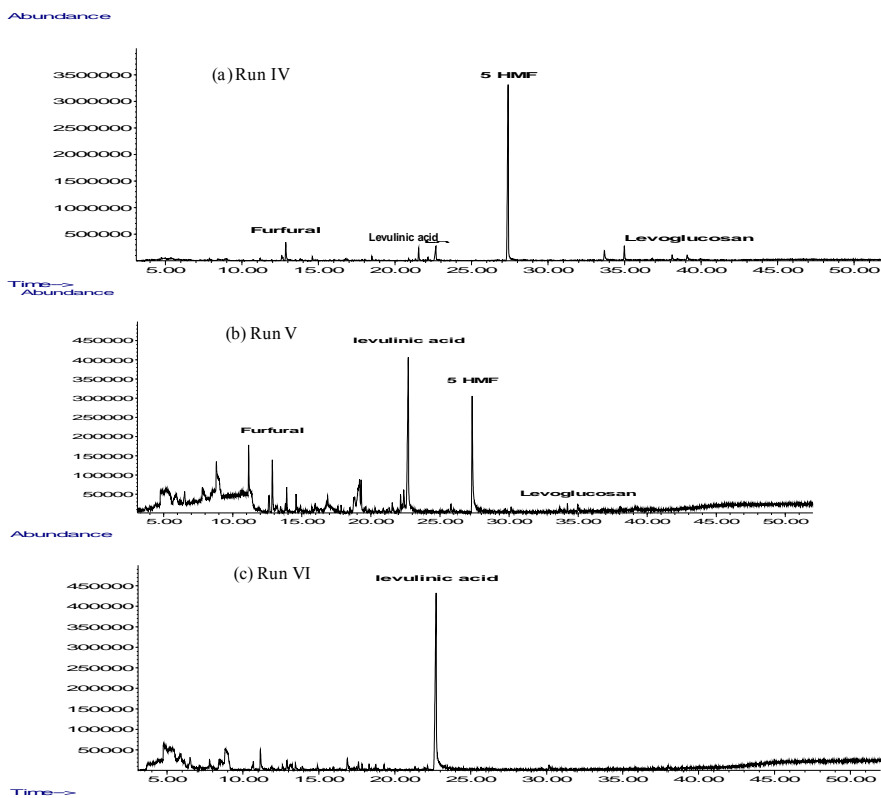


Figure 3.17 GC-MS spectra of liquid product from (a) run IV, (b) run V, and (c) run VI.

Some of the key compounds identified in the output liquid from glucose experiments and their trend for run IV, V, and VI (based on GC-MS spectra) are shown in Table 3.6.

Table 3.6 Key compounds identified in the product liquid from run IV, V, and VI and their trend with reaction time.

No.	Compounds	Retention time (min)	Trend
1	Furfural	12.86	Initially increased (run IV) and then started decreasing. Not observed in (run VI)
2	pentanoic acid, 4-oxo-, (levulinic acid)	22.67	Increased with reaction time i.e. from run IV to run VI
3	2-Furancarboxaldehyde, 5-(hydroxymethyl)- (SHMF)	27.39	Initially increased (run IV) and then started decreasing. Not observed in (run VI)
4	1,6-Anhydro-.beta.-D-glucopyranose (levoglucosan)	34.99	Initially increased (run IV) and then started decreasing. Not observed in (run VI)

It is interesting to note from Figure 3.17 that the ring compounds (e.g. furfural, 5HMF, and levoglucosan) started to disappear with increase in reaction time from 1 h to 4 h (run IV, V, and VI), whereas concentration of organic acids (e.g. levulinic acid) increased. In the run VI (Figure 3.17c), none of the ring compounds discussed in Table 6 are present. Glucose in hydrothermal medium at relatively low temperature (180-200°C) range undergoes mainly dehydration and partial fragmentation (C-C bond breaking) reactions. The intermediate compounds are mainly furan like compounds, organic acids and aldehydes.<sup>55</sup> Furan like ring compounds may undergo polymerization via aldol condensation to form soluble polymers. Aromatization of soluble polymers takes place under the reaction condition and when the aromatic clusters in aqueous solution reach the critical super-saturation point, they precipitate as carbon rich microspheres.<sup>56</sup> Figure 3.18 shows the simplified reaction scheme of glucose to carbon rich microspheres in hydrothermal medium.

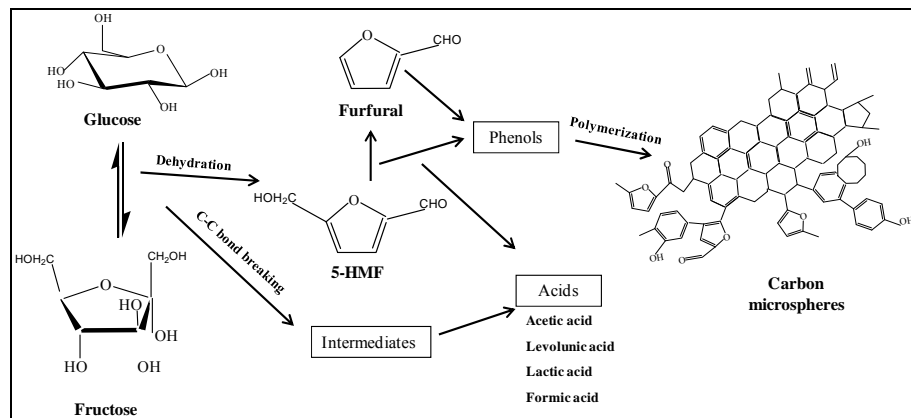


Figure 3.18 Simplified reaction pathway of glucose during hydrothermal carbonization reactions.<sup>54, 56, 58</sup>

The carbon rich microspheres produced in run II and V were further analyzed by FTIR to understand the presence of functional groups. Figure 3.19 compares the FTIR spectra from run II and V. Also, Table 3.7 shows the position of IR absorption bands and their assignments for the solid samples from run II and V.

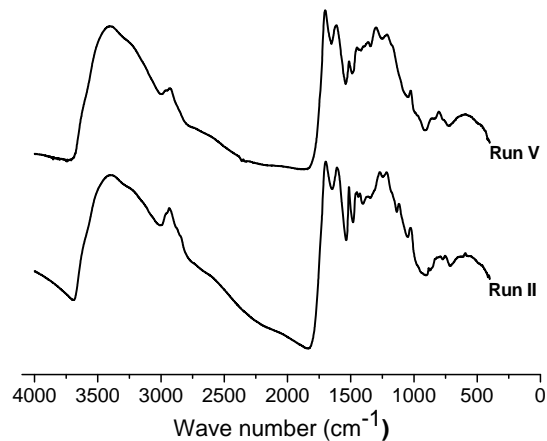


Figure 3.19 FTIR spectra of solids recovered in run II and V.

Table 3.7 Functional groups in the FTIR spectra of carbon rich microspheres from run II and V.<sup>59</sup>

Position of the bands, cm <sup>-1</sup>	Functional group	Belongs
3405	O-H stretching	Run II and V
2930-2850	CH, CH <sub>2</sub> stretching	Run II and V
1680-1580	C=C stretching	Run II and V
1510	Benzene ring stretching	Run II and V
1456	C-O-H stretching	Run II and V
1428	C-C-H stretching	Run II and V
1375-1317	C-H bending	Run II and V
1281	C-C-H stretching	Run II and V
1235	C-O-H stretching	Run II and V
1112	C-O-H stretching	Run II and V
1056	C-O stretching	Run II and V
897	Alienation Zone β-bond absorption	Run V
803	C=H Benzene ring stretching	Run II
700-400	C-H bending	-

The broad absorbance peak of O–H stretching vibration between 3,200 and 3,600 cm<sup>-1</sup> indicate the presence of water impurities and other polymeric O–H in the solids. The presence of alkanes was indicated by the strong absorbance peak of C–H vibration at 2,930 cm<sup>-1</sup> and the C–H deformation vibration at 1,460 cm<sup>-1</sup>. The absorbance peak at 1,700 cm<sup>-1</sup> represented the C=O stretching vibration indicating the presence of ketones and aldehydes. The presence of both O–H and C=O stretching vibrations also indicated the presence of carboxylic acids and their derivative esters. The possible presence of alkenes was indicated by the absorbance peaks between 1,680 and 1,580 cm<sup>-1</sup>. The peaks between 1,300 and 950 cm<sup>-1</sup> were due to the presence of primary, secondary, and tertiary alcohols, phenols, ethers, and esters showing the C–O stretching and O–H deformation vibration. Absorbance peaks between 900 and 650 cm<sup>-1</sup> indicated the possible presence of single, polycyclic, and substituted aromatic groups. The presence of aromatic rings (900 and 650 cm<sup>-1</sup>) and C=O stretching as well as C–O stretch indicated the presence of aromatic esters. The results were confirmed by the peaks 1281, 1428 and 1513cm<sup>-1</sup> in the FTIR. At the same time, 1600 and 1700 cm<sup>-1</sup>, the peaks of polymeric product were also shown in the spectra. The results proved that the carbon rich solids were composed of the aromatics and polymeric product which are produced in the hydrothermal carbonization process.<sup>57</sup>

Microspheres which are fine and easy to compact seem to have good solid fuel value based on their elemental carbon and HHV. These powders can be mixed and co-fired with lignin. The study have shown that just by maintaining the liquid hydrolyzate temperature for another two hours, nearly 60% of the organic matters can be converted as high energy density powders. The product liquid after this process mainly contains the

organic acids. Though the results only from run 6 liquid hydrolyzate are discussed here, carbonization of liquid hydrolyzate from run 7 yielded the similar results. This confirms that liquid hydrolyzates recovered after aqueous pretreatment processes can be used potentially for recovering soluble carbons as high energy density products.

### 3.6 Conclusion

Switchgrass can be pretreated effectively in a flow through reactor in hydrothermal medium. Enzymatic digestibility of pretreated biomass depends on the pretreatment temperature. Addition of small amount of  $K_2CO_3$  increased the glucan digestibility even at low temperatures (150-175°C). At a higher pretreatment temperature (190°C), the study showed that even though switchgrass pretreated just with water had more internal surface area than that pretreated in the presence of  $K_2CO_3$ , both the substrate had almost similar glucan digestibility. Therefore, it is not only the internal surface area, but many other factors such as degree of polymerization, structural rearrangements, lignin content after pretreatment are responsible in improving the sugar yields. Corn stover required milder pretreatment conditions than switchgrass.

An alternative pathway for the utilization of liquid hydrolyzate is developed, where dissolved sugars can be recovered as carbon rich microspheres by hydrothermal carbonization. Sugars ( $C_5$  and  $C_6$ ) degrade to furan based intermediates (ring compounds) and organic acids during the process. Ring compounds further undergo condensation polymerization and precipitate as carbon rich microspheres. The energy densities of these solids are comparable to that of lignin, which make them suitable as solid fuels. The hydrothermal carbonization process can potentially be used to recover valuable byproduct with a good energy value.

### **3.7 Acknowledgments**

Author is thankful for the financial supports from the National Science Foundation (grant NSF-CBET-0828269) and Alabama Center for Paper and Bioresource Engineering. In addition, the authors are thankful to Prof. David I. Bransby for supplying switchgrass, and to Mr. Ramesh V. Pallapolu, Prof. Sushil Ashikari, and Mrs. Suchithra T. Gopakumar for help with some analyses.

### **3.8 References**

1. Taherzadeh, M. J.; Karimi, K., Enzyme based hydrolysis processes for ethanol from lignocellulosic materials: A review. *BioResources* **2007**, 2, (4), 707-738.
2. Perlack, R. D.; Wright, L. L.; Turhollow, A. F.; Graham, R. L.; Stokes, B. J.; Erbach, D. C. *Biomass as feedstock for a bioenergy and bioproducts industry: The technical feasibility of a billion-ton annual supply*; US Department of Energy US Department of Agriculture: 2005.
3. Petchpradab, P.; Yoshida, T.; Charinpanitkul, T.; Matsumura, Y., Hydrothermal Pretreatment of Rubber Wood for the Saccharification Process. *Ind. Eng. Chem. Res.* **2009**, 48, (9), 4587-4591.
4. Rinehart, L., Switchgrass as a bioenergy crop. [www.attra.ncat.org](http://www.attra.ncat.org) **2006**.
5. Mosier, N.; Wyman, C.; Dale, B.; Elander, R.; Lee, Y. Y.; Holtzapfel, M.; Ladisch, M., Features of promising technologies for pretreatment of lignocellulosic biomass. *Bioresource Technology* **2005**, 96, (6), 673-686.

6. Laxman, R. S.; Lachke, A. H., Bioethanol from lignocellulosic biomass, Part 1: Pretreatment of the substrates. In *Handbook of plant-based biofuels*, Pandey, A., Ed. CRC Press: 2008; pp 121-139.
7. Gupta, R.; Lee, Y. Y., Mechanism of cellulase reaction on pure cellulosic substrates. *Biotechnology and Bioengineering* **2008**, 102, (6), 1570-1581.
8. Zhang, Y.-H. P.; Berson, E.; Sarkanyen, S.; Dale, B. E., Sessions 3 and 8: Pretreatment and Biomass Recalcitrance: Fundamentals and Progress. *Appl Biochem Biotechnol* **2009**, 153, 80-83.
9. Wyman, C. E.; Dale, B. E.; Elander, R. T.; Holtzapple, M.; Ladisch, M. R.; Lee, Y. Y., Coordinated development of leading biomass pretreatment technologies. *Bioresour. Technol.* **2005**, 96, 1959-1966.
10. Lynd, L. R., Overview and evaluation of fuel ethanol from cellulosic biomass: technology, economics, the environment, and policy. *Ann Rev Energy Environ* **1996**, 21, 403-465.
11. Pérez, J. A.; Ballesteros, I.; Ballesteros, M.; Sáez, F.; Negro, M. J.; Manzanares, P., Optimizing Liquid Hot Water pretreatment conditions to enhance sugar recovery from wheat straw for fuel-ethanol production. *Fuel* **2008**, 87, 3640-3647.
12. Hsu, T.-A., *Pretreatment of biomass. Handbook on bioethanol: Production and Utilization* Taylor and Francis, Washington, DC: 1996.
13. Sun, Y.; Cheng, J. J., Hydrolysis of lignocellulosic material for ethanol production: A review. *Bioresource Technology* **2002**, 83, 1-11.
14. Diaz, M. J.; Cara, C.; Ruiz, E.; Romero, I.; Moya, M.; Castro, E., Hydrothermal pre-treatment of rapeseed straw. *Bioresour. Technol.* **2010**, 101, (2010), 2428-2435.

15. Kumar, S.; Gupta, R.; Lee, Y. Y.; Gupta, R. B., Cellulose pretreatment in subcritical water: Effect of temperature on molecular structure and enzymatic reactivity. *Bioresour. Technol.* **2009**, 101, (2010), 1337-1347.
16. Matsumura, Y.; Sasaki, M.; Okuda, K.; Takami, S.; Ohara, S.; Umetsu, M.; Adschariri, T., Supercritical water treatment of biomass for energy and material recovery. *Combust. Sci. and Tech.* **2006**, 178, 509-536.
17. Kadam, K. L.; Chin, C. Y.; Brown, L. W., Continuous biomass fractionation process for producing ethanol and low-molecular-weight lignin. *Environmental Progress & Sustainable Energy* **2009**, 28, (1), 89-99.
18. Franck, E. U., Fluids at high pressures and temperatures. *Pure Appl. Chem.* **1987**, 59, (1), 25-34.
19. Miyoshia, H.; Chena, D.; AkaiT., A novel process utilizing subcritical water to recycle soda-lime-silicate glass. *Journal of Non-Crystalline Solids* **2004**, 337, (3), 280-282.
20. Savage, P. E., Organic chemical reactions in supercritical water. *Chemical Reviews* **1999**, 99, 603-621.
21. Kumar, S.; Gupta, R. B., Biocrude Production from Switchgrass using Subcritical Water. *Energy & Fuels* **2009**, 23, (10), 5151-5159.
22. Hendriks, A. T. W. M.; Zeeman, G., Pretreatments to enhance the digestibility of lignocellulosic biomass. *Bioresour. Technol.* **2009**, 100, (1), 10-18.
23. Heitz, M.; Carrasco, F.; Rubio, M.; Chauvette, G.; Chornet, E.; Jaulin, L.; Overend, R. P., Generalized correlations for aqueous liquefaction of lignocellulosics. *Can. J. Chem. Eng.* **1986**, 64, 647-650.

24. Garrote, G.; Dominguez, H.; Parajo, J. C., Hydrothermal processing of lignocellulosic materials. *Holz als Roh- und Werkstoff* **1999**, 57, (1999), 191-202.
25. Suryawati, L.; Wilkins, M. R.; Bellmer, D. D.; Huhnke, R. A.; Maness, N. O.; Banat, I. M., Simulteneous sacchrification and fermentation of Kanlow Switchgrass pretreated by hydrothermolysis using Kluyveromyces marxianus IMB4. *Biotechnology and Bioengineering* **2008**, 101, (5), 894-902.
26. Bobleter, O., Hydrothermal degradation of polymers derived from plants. *Prog. Polym. Sci.* **1994**, 19, 797–841.
27. Sierra, R.; Smith, A.; Granda, C.; Holtzapple, M. T., Producing fuels and chemicals from lignocellulosic biomass. *Chemical Engineering Progress* August, 2008, pp S10-S18.
28. Kohlmann, K. L.; Westgate, P. J.; Sarikaya, A.; Velayudhan, A.; Weil, J.; Hendricson, R.; Ladisch, M. R., Enhanced enzyme activities on hydrated lignocellulosic substrates. In *American Chemical Society National Meeting*, ACS Symposium series No. 618: 1995; Vol. 207, pp 237-255.
29. Mosier, N.; Hendrickson, R.; Ho, N.; Sedlak, M.; Ladisch, M. R., Optimization of pH controlled liquid hot water pretreatment of corn stover. *Bioresour. Technol.* **2005a**, 96, 1986-1993.
30. Weil, J. R.; Brewer, M.; Hendrickson, R.; Sarikaya, A.; Ladisch, M. R., Continuous pH monitoring during pretreatment of yellow poplar wood sawdust by pressure cooking in water. *Appl. Biochem. Biotechnol.* **1997**, 68, 21-40.
31. kobayashi, N.; Okada, N.; Hirakawa, A.; Sato, T.; J.Kobayashi; Hatano, S.; Itaya, Y.; Mori, S., Characteristics of solid residues obtained from hot-compressed-water

treatment of woody biomass. *Industrial and Engineering Chemistry Research* **2009**, 48, 373-379.

32. Yang, B.; Wyman, C. E., Effect of xylan and lignin removal by batch and flow through pretreatment on the enzymatic digestibility of Corn Stover Cellulose. *Biotech. Bioeng.* **2004**, 86, (1), 88-95.
33. Liu, C.; Wyman, C. E., The effect of flow rate of compressed hot water on xylan, lignin and total mass removal from corn stover. *Ind. Eng. Chem. Res.* **2003**, 42, 5409-5416.
34. Rogalinski, T.; Ingram, T.; Brunner, G., Hydrolysis of lignocellulosic biomass in water under elevated temperatures and pressures. *Journal of Supercritical Fluids* **2008**, 47, (1 ), 54-63
35. Olofsson, K.; Bertilsson, M.; Lidén, G., A short review on SSF – an interesting process option for ethanol production from lignocellulosic feedstocks. 1: 7 (doi: 10.1186/1754-6834-1-7). *Biotechnology for Biofuels* **2008**, 1, (7), 1-14.
36. Kaparaju, P.; Serrano, M.; Angelidaki, I., Effect of reactor configuration on biogas production from wheat straw hydrolysate. *Bioresour. Technol.* **2009**, 100, 6317-6323.
37. Klinke, H. B.; Thomsen, A. B.; Ahring, B. K., Inhibition of ethanol-producing yeast and bacteria by degradation products produced during pre-treatment of biomass. *Appl. Microbiol Biotechnol* **2004**, 66, 10-26.
38. Palmqvist, E.; Hahn-Hagerdal, B., Fermentation of lignocellulosic hydrolyzates. II. Inhibitors and mechanism of inhibition. *Bioresour. Technol.* **2000b**, 74, 25-33.

39. Segal, L.; Creely, J. J.; Martin, A. E.; Conrad, C. M., An empirical method for estimating the degree of crystallinity of native cellulose using the X-ray diffractometer. *Textile Res. J.* **1959**, 29, 786-794.
40. Negro, M. J.; Manzanares, P.; Ballesteros, I.; Oliva, J. M.; Cabanas, A.; Ballesteros, M., Hydrothermal pretreatment conditions to enhance ethanol production from poplar biomass. *Applied Biochemistry and Biotechnology* **2003**, 105-108, 87-100.
41. Lai, Y.-Z., Chemical Degradation. In *Wood and Cellulosic Chemistry*, David N.-S. Hon, N. S., Ed. Marcel Dekker, Inc.: New York . Basel, 2001; pp 443-512.
42. Rodríguez, A.; Moral, A.; Sánchez, R.; Requejo, A.; Jiménez, L., Influence of variables in the hydrothermal treatment of rice straw on the composition of the resulting fractions. *Bioresour. Technol.* **2009**, 100, 4863-4866.
43. Suryawati, L.; Wilkins, M. R.; Bellmer, D. D.; Huhnke, R. A.; Maness, N. O.; Banat, I. M., Effect of hydrothermolysis on ethanol yield from Alamo switchgrass using a thermotolerant yeast. In *2007 ASABE Annual International Meeting*, American Society of Agricultural and Biological Engineers: Minneapolis, Minnesota, 2007; Vol. Paper Number: 077071, St. Joseph, Mich.:ABASE, pp 1-13.
44. Gupta, R. Alkaline pretreatment of biomass for ethanol production and understanding the factors influencing the cellulose hydrolysis. Auburn University, Auburn, 2008.
45. Carr, M. E.; Doane, W. M., Modification of wheat straw in a high- shear mixer. *Biotech. and Bioeng.* **1984**, 26, 1252-1257.

46. Detroy, R. W.; Lindenfelser, L. A.; Orton, W. L., Bioconversion of wheat straw to ethanol: Chemical modification, enzymatic hydrolysis, and fermentation. *Biotech. and Bioeng.* **1981**, 23, 1527-1535.
47. Schacht, C.; Zetzl, C.; Brunner, G., From plant materials to ethanol by means of supercritical fluid technology. *Journal of Supercritical Fluids* **2008**, 46s (3), 299-321.
48. [http://en.wikipedia.org/wiki/Self-ionization\\_of\\_water](http://en.wikipedia.org/wiki/Self-ionization_of_water) Self-ionization of water. (Jan 19, 2010),
49. Rezaei, K.; Temelli, F.; Jenab, E., Effects of pressure and temperature on enzymatic reactions in supercritical fluids. *Biotechnology Advances* **2007**, 25, 272-280.
50. Chang, V. S.; M. T, H., Fundamental factors affecting biomass enzymatic reactivity. *Applied Biochemistry and Biotechnology* **2000**, 84-86, 5-37.
51. Kumar, R.; Wyman, C. E., Access of cellulase to cellulose and lignin for poplar solids produced by leading pretreatment technologies. *Biotechnol. Prog.* **2009**, 25, (3), 807-819.
52. Kumar, S.; Gupta, R.; Lee, Y. Y.; Gupta, R. B., Cellulose pretreatment in subcritical water: Effect of temperature on molecular structure and enzymatic reactivity. *Bioresour. Technol.* **2010**, 101, 1337-1347.
53. Titirici, M.-M.; Thomas, A.; Antonietti, M., Back in the black: hydrothermal carbonization of plant material as an efficient chemical process to treat the CO<sub>2</sub> problem. *New J. Chem.* **2007**, 31, 787-789.
54. Titirici, M.-M.; Antonietti, M.; Baccile, N., Hydrothermal carbon from biomass: a comparision of the local structure from poly- to monosaccharides and pentoses/hexoses. *Green Chem.* **2008**, 10, 1204-1212.

55. Knez̄ević, D.; Swaaij, W. P. M. v.; Kersten, S. R. A., Hydrothermal Conversion of Biomass: I, Glucose Conversion in Hot Compressed Water. *Ind. Eng. Chem. Res.* **2009**, 48, 4731-4743.
56. Sevilla, M.; Fuertes, A. B., The production of carbon materials by hydrothermal carbonization of cellulose. *Carbon* **2009**, 47, 2281-2289.
57. Almendros, G.; Sanj, J.; Sobrados, L., Characterization of synthetic carbohydrate-derived humic-like polymers. *The Science of the Total Environment* **1989**, 81-82, 91-98.
58. Chuntanapum, A.; Matsumura, Y., Formation of Tarry Material from 5-HMF in Subcritical and Supercritical Water. *Ind. Eng. Chem. Res.* **2009**, 48, (22), 9837-9846.
59. Baeza, J.; Freer, J., Chemical characterization of wood and its components. In *Wood and cellulosic chemistry*, second ed.; Hon, D. N.-S.; Shiraishi, N., Eds. Marcel Dekker, Inc.: New York. Basel, 2001; pp 275-384.

## 4. Hydrolysis of Microcrystalline Cellulose in Subcritical and Supercritical Water in a Continuous Flow Reactor

### 4.1 Abstract

For cellulosic ethanol production, efficient hydrolysis of crystalline cellulose to easily fermentable sugars is important. Focus of this study is to maximize the yield of cellulose hydrolysis in subcritical and supercritical water at practically achievable reaction times. Microcrystalline cellulose is treated with subcritical and supercritical water in temperature range 302 to 405°C, at pressure 27.6 MPa, and residence times of 2.5 to 8.1 s. Cellulose-water slurry of 2.7 wt% after mixing with preheated water is rapidly heated to the reaction temperature and then the reaction product is rapidly cooled in a continuous reactor. Cellulose partially dissolves in subcritical water at 302°C and completely dissolves at 330°C. About 65% of cellulose converts to the oligomers and monomers at 335°C in 4.8 s, and also at 354°C in 3.5 s. Upon increase in the reaction time or temperature to supercritical region, oligomers and monomers partially degrade to glycoaldehyde dimer, D-fructose, 1, 3 dihydroxyacetone dimer, anhydroglucose, 5-HMF and furfural. The effect of temperature, pressure, and reaction time on formation of various products is studied. In addition, the effect of a base catalyst, K<sub>2</sub>CO<sub>3</sub>, is examined. The catalyst increases cellulose gasification in the temperature range studied (302-333°C).

## 4.2 Introduction

Ethanol from lignocellulosic biomass is an attractive and renewable fuel for transportation. Globally, the means to utilize this abundantly available resource in a cost-effective way is a major research focus. Cellulose, a linear polymer of anhydroglucose units is one of the three major components of lignocellulosic biomass. Acid/alkali pre-treatment of biomass followed by enzymatic hydrolysis is a conventional method to produce glucose from cellulose. Glucose can be used to synthesize various specialty chemicals or fermented to produce ethanol. Supercritical water, an environmentally benign solvent for organic matters, can be used under a variety of conditions to rapidly convert cellulose to sugar or to convert biomass into a bio-crude. Bio-crude, which contains only 10-13% oxygen provides excellent opportunities for conversion of biomass to a transportable form of energy.<sup>1</sup> Also, reactions in subcritical and supercritical water provide a novel medium to conduct tunable reactions for the synthesis of specialty chemicals from biomass.<sup>2</sup>

Density and dielectric constant of the water medium play major role in soubilizing organic compounds in subcritical and supercritical water. Dielectric constant of water near the critical point decreases considerably, which enhances the solubility of organic compounds.<sup>3</sup> Direct observation of phase behavior of cellulose-water system in a diamond anvil cell showed that at higher temperatures (300-320°C) cellulose particles disappeared with increasing transparency, and shrinking rate was significantly increased with temperature above 300°C.<sup>4</sup> Recently, it was shown that crystalline cellulose undergoes transformation to an amorphous state in subcritical water, which is followed by complete dissolution at temperature between 330-340°C at 25 MPa.<sup>5, 6</sup>

Most of the work on cellulose decomposition in sub- or supercritical water has been done in the batch reactors. Due to the formation of gaseous products during the reactions, it becomes difficult to maintain the constant density of the reaction medium and so, kinetics obtained from the batch reactor often can give misleading information on the design for industrial level continuous reactors. Also, difficulty arises when one wants to limit the reaction time to few seconds. In addition, catalytic effects of the wall are not translated accurately to the continuous reactor. A comparative study on conversion of cellulose between batch-type and flow-type systems in supercritical water concluded that flow type systems can hydrolyze cellulose with minimum pyrolyzed products, whereas batch-type systems give higher yields of the pyrolyzed products due to the longer treatment time.<sup>7</sup> It has been reported that combined process of short supercritical water treatment followed by subcritical water treatment increases the yield of hydrolyzed products.<sup>8</sup>

In context to studies in batch reactors, Minowa et al.<sup>9, 10</sup> conducted hydrolysis of cellulose with and without catalyst. Using a conventional autoclave, slurry solutions of cellulose were heated in a nitrogen atmosphere to various temperatures between 200-350°C. Results indicate that decomposition of cellulose increased with reaction temperature. Temperatures of 240°C and below lead to the formation of water-soluble products. Temperatures above 260°C leads to the formation of oil, char, and gas. At temperatures above 260°C non-recoverable char begins to form decreasing the carbon in the liquid phase. The maximum oil yield was obtained at 280°C; increasing temperature leads to increase in the char and gas formation but decrease in the oil yields, indicating a secondary decomposition of oil to char and gas. Based on the same product distribution

obtained from glucose and cellulose decomposition, it was concluded that cellulose decomposition starts with hydrolysis step. Sakaki et al.<sup>11</sup> reported nearly 80 wt% conversion of cellulose to water soluble products with glucose yields 40% within 15 s by heating the cellulose and water mixture in a sealed reactor above 355°C.

Sasaki et. al.<sup>4, 12</sup> developed a high-pressure slurry feeder to feed the cellulose water slurries in a flow reactor and studied the decomposition of microcrystalline cellulose in subcritical and supercritical water (320-400°C, and 0.05-10.0 s). It was reported that 75% yield of hydrolysis products were obtained in supercritical water, while aqueous decomposition products of glucose were the main products in subcritical water. Cellobiose degradation in sub- and super-critical water in a flow apparatus proceeds via the hydrolysis of the glycosydic bond and via pyrolysis of the reducing end.<sup>13</sup>

The results of earlier studies in flow reactors show that a higher hydrolysis product yield can be achieved by treating cellulose with supercritical water in a fraction of a second residence time. To develop the process for large scale applications, it is necessary to optimize both from process point of view (e.g., temperature, pressure, residence time etc.) and engineering point of view (e.g., feeding, heating, etc.)<sup>2</sup> Cellulose being a poor conductor of heat will require some innovative heating techniques for heating to the reaction temperature in such a short time. Therefore, the main aim of this study is to examine the possibilities of maximizing hydrolysis products yield from the hydrolysis of crystalline cellulose at a relatively lower temperature and at a practically achievable residence time in a continuous flow apparatus.

Lignocellulosic biomass naturally contains alkali metals such as K, Ca and Na, which can increase the rate of gas formation at the supercritical water temperatures. At

less than 350°C, it has been reported that cellulose or wood can be liquefied in subcritical water in presence of Na<sub>2</sub>CO<sub>3</sub>.<sup>14</sup> Also, direct liquefaction of wood in the presence of K<sub>2</sub>CO<sub>3</sub> exhibits a marked catalytic effect.<sup>14, 15</sup> Sinag et al. reported that hydrolysis of glucose in the presence of K<sub>2</sub>CO<sub>3</sub> at residence time in the range of 1.6-6.3 minutes leads to increased gas formation. The gaseous products mainly consist of hydrogen, carbon dioxide, methane and smaller amount of carbon monoxide.<sup>16, 17</sup> Carbohydrate structures of the solid residues start to disappear at liquefaction temperatures of 290-300°C in the presence of Na<sub>2</sub>CO<sub>3</sub>. Above 300°C the amount of methane shows a highly upward trend indicating an increasing carbonization.<sup>18</sup>

The second objective of this study is to examine the effect of heterogeneous catalyst (K<sub>2</sub>CO<sub>3</sub>) in flow reactor on the liquefaction temperature and also, examine the behavior of solid residues for understanding the nature of thermochemical liquefaction when cellulose is used. Dielectric constant of water decreases from 78.5 at 25°C to 5 in the near critical region which causes reduced solubility of inorganic compounds, as a result alkali salts precipitates as fine powder. These fine particles provide a high surface area during the heterogeneous reactions.<sup>19</sup> The effect of catalysis on the decomposition of cellulose is examined in the temperature range of 302-330°C in subcritical water.

### 4.3 Experimental Section

*Materials:* Microcrystalline cellulose powder (size 20 µm, degree of polymerization 229, Product Number 310697), K<sub>2</sub>CO<sub>3</sub>, high purity standard reagents used for HPLC analysis (see Table 4.1) were purchased from Sigma Aldrich. De-ionized water was used for preparing cellulose slurry.

Table 4.1 HPLC standards used for analysis of liquid products.

No.	Chemicals	Formula	Conc., (g/l)	MW
1	Cellobiose	C <sub>12</sub> H <sub>22</sub> O <sub>11</sub>	2	342
2	Glucose	C <sub>6</sub> H <sub>12</sub> O <sub>6</sub>	2	180
3	Glycoaldehyde,dimer	C <sub>4</sub> H <sub>8</sub> O <sub>4</sub>	1	120
4	D- Fructose	C <sub>6</sub> H <sub>12</sub> O <sub>6</sub>	2	180
5	1,3 Dihydroxyacetone,dimer	C <sub>6</sub> H <sub>12</sub> O <sub>6</sub>	2	180
6	1,6 Anhydro - beta glucose	C <sub>6</sub> H <sub>10</sub> O <sub>5</sub>	1	162
7	5-(hyroxymethyl)-furaldehyde	C <sub>6</sub> H <sub>6</sub> O <sub>3</sub>	1	126
8	Furfural	C <sub>5</sub> H <sub>4</sub> O <sub>2</sub>	2	96

*Apparatus:* Figure 4.1 shows the schematic of apparatus used for the experiments. It consists of high-pressure liquid pumps, a cellulose slurry feeder, an electrical tubular furnace, a water-cooled double tube heat exchanger, a backpressure regulator, and a phase separator. Reactor is a high-pressure 14" long Inconel 600 tube having 0.25" OD, 0.11" ID and 2.18 mL volume. Specially designed piston operated high-pressure slurry feeder (0.57" ID, 20" long) was used to supply cellulose slurry at desired flow rate. Real time temperature of the reaction zone was measured using a 1/16" thermocouple placed 3" inside the reactor from outlet end. This thermocouple measures the reaction zone temperature with accuracy of  $\pm 0.1^{\circ}\text{C}$ . There are three additional thermocouples installed at different locations in the apparatus. Real time temperature indicated by the thermocouple placed inside the reaction zone was used for all the analyses. Reactor pressure was maintained using a Stra-val backpressure regulator.

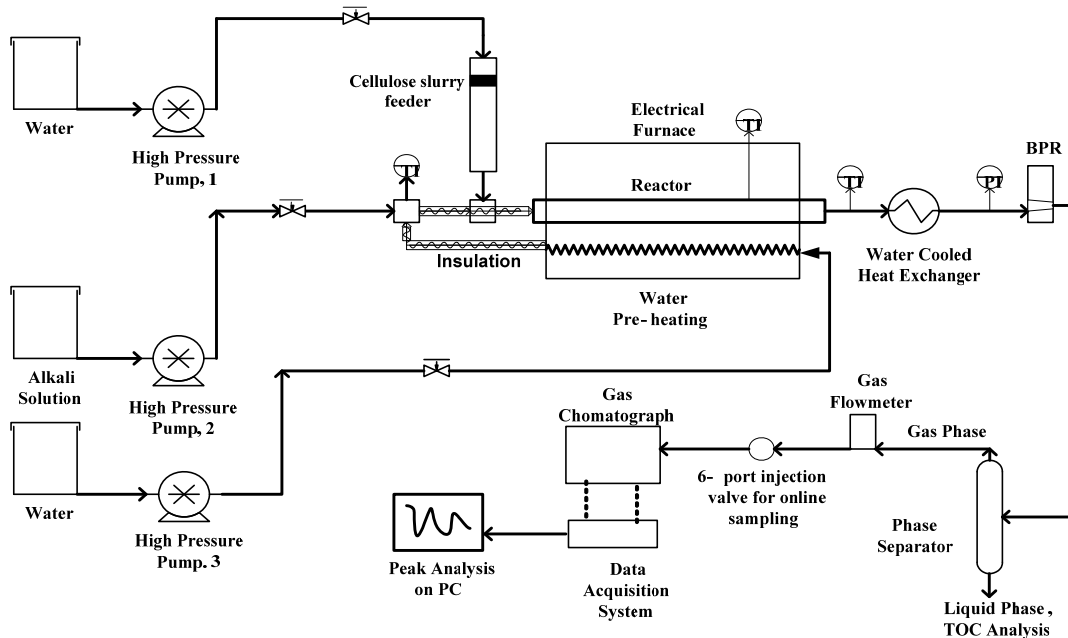


Figure 4.1 Apparatus for cellulose hydrolysis in subcritical and supercritical water.

*Experimental Procedure:* Microcrystalline cellulose (MCC) was added to continuously stirred hot water (70°C) to prepare 24.1 wt% slurry, which was charged in the slurry feeder. It was observed that 24.1 wt% of cellulose suspension in hot water did not settle appreciably in a similar diameter tube for an hour, which helped us in avoiding the requirement of any agitation in the slurry feeder.

At the start, temperature and pressure of the reaction zone are established under water flow. Then, slurry is pumped at desired flow rate and mixed with 8 fold (mass basis) of preheated water prior to entering the reactor. Products coming out of the reactor are cooled in the heat exchanger, depressurized in the back pressure regulator and collected in the phase separator. Periodic liquid samples are collected, centrifuged at 3400 rpm to remove any solids and analyzed for total organic carbon (TOC) in Shimadzu TOC-Vcsn analyzer.

MCC was treated with subcritical and supercritical water at temperatures ranging

from 302 to 405°C, at a constant pressure 27.6 MPa and residence times of 2.5 to 8.1 s. Experiments using K<sub>2</sub>CO<sub>3</sub> catalyst were conducted at 302°C (5.2 s) and 330°C (4.8 s) temperature. The catalyst was introduced as 8 wt% solution in ambient water, pumped to the mixing point as shown in the Figure 4.1.

The experiments were divided into four groups as: (1) 302-335°C, (2) 350-366°C, (3) 376-405°C, and (4) 302, 330°C in the presence of K<sub>2</sub>CO<sub>3</sub>. One experiment from each group was repeated to confirm the reproducibility of the cellulose conversion by measuring the total organic contents (TOC). Multiple samples were collected and analyzed for TOC values during each experiment to confirm the steady state. TOC value varied within ± 2% during the reaction. Liquid products collected during the steady state phase of experiment are stored in the refrigerator for chromatographic (HPLC) analyses. Yields were calculated based on the 2.7 wt % of pure cellulose input to the reactor.

The residence time (*t*) in the reactor was calculated using pure water density at the reaction temperature and pressure (i.e. fluid phase in the reaction zone is assumed to be pure water for the simplicity of calculations) as

$$t = \frac{V}{F \left( \frac{\rho_{\text{pump}}}{\rho_{P_1, T_1}} \right)}$$

where, *V* (2.18 ml) is reactor volume, *F* is the combined volumetric flow rate of pumps 1, 2 and 3,  $\rho_{\text{pump}}$  is the density of water at pump condition (25°C, 27.6MPa), and  $\rho_{P_1, T_1}$  is the density of water at reactor condition (e.g., *T*<sub>1</sub> and *P*<sub>1</sub>).

#### 4.4 Product Analyses

Residual solids from the product were separated by centrifugation, oven dried at 70°C, weighed and taken for analysis. Carbon content in the supernatant liquid was

determined by TOC analyzer. Hydrolysis products (monomers and oligomers) and degradation products in liquid samples were determined by following the National Renewable Energy Laboratory, biomass laboratory analytical procedure (described in technical report-NREL/TP-510-42623). The analysis was done using HPLC having Bio-Rad Aminex HPX-87P (lead based) column, refractive index detector, water mobile phase, and column temperature of 85°C. Additionally analysis was done using Bio-Rad Aminex HPX-87H column, refractive index detector, 0.01 N sulfuric acid mobile phase and column temperature of 65°C.<sup>20</sup>

Solid residues collected during the catalytic experiments were oven dried and analyzed for elemental carbon using Elementar Vario Macro CNS analyzer.<sup>21</sup>

#### 4.5 Results

Four groups of experiments were performed in the continuous reactor at constant pressure 27.6 MPa and residence time ranging from 2.5 to 8.1 s, at (1) 302-335°C, (2) 350-366°C, (3) 376-405°C, and (4) 302, 330°C in the presence of K<sub>2</sub>CO<sub>3</sub>. At temperature 275°C or below cellulose conversion to water soluble products were not significant (< 10%) for the 3-6 s residence time. Longer residence times would be needed to hydrolyse cellulose in lower temperature range which promotes rapid degradation of converted hydrolysis products. Cellulose conversion increased sharply above 275°C. Therefore hydrolysis study was mainly focused at higher temperatures in the range 302-405°C. The products from cellulose hydrolysis in subcritical and supercritical water were identified and quantified in different runs as shown in Table 4.2.

Table 4.2 Liquid products yield from cellulose treatment in subcritical and supercritical water at 27.6 MPa.

Run	T (°C)	t (s)	TOC (ppm)	Hydrolysis products (%)				Degradation products (%)				
				Olig	CB	Glu	Fr	GA	DA	AG	HMF	FUR
Group 1, 303-335 °C												
1	303	5.2	4309	16.3	2.8	5.0	0.4	0.8	0.0	0.9	0.9	0.0
2	330	8.1	11880	10.5	0.6	26.7	4.8	10.1	0.0	5.5	7.9	3.1
3	332	4.8	11770	18.0	6.2	37.6	4.9	6.5	0.4	7.0	4.1	1.5
4	333	3.5	6306	24.7	7.7	14.6	1.1	1.7	0.3	2.4	1.3	0.4
5	335	4.7	10390	29.6	5.7	27.9	3.6	4.8	0.3	5.1	3.5	1.2
Group 2, 350-366 °C												
6	350	7.5	10580	7.0	0.3	18.3	2.9	10.8	0.9	4.2	5.0	2.1
7	354	3.5	11970	21.3	5.9	32.9	4.8	6.5	0.5	6.4	3.3	1.2
8	355	4.4	11310	0.0	0.0	4.9	1.1	20.4	1.2	1.0	4.7	2.4
9	366	3.3	11660	11.6	0.9	29.4	6.7	13.7	0.9	6.8	4.6	1.9
Group 3, 376-405 °C												
10	376	3.7	12670	3.5	0.0	11.6	0.0	16.0	1.3	1.6	8.6	4.0
11	377	6.2	9962	0.0	0.0	0.3	0.0	17.7	0.5	0.0	7.4	0.2
12	384	6.6	12250	0.0	0.0	4.1	0.9	17.7	0.5	0.2	9.9	5.1
13	387	3.1	10640	0.0	0.0	0.5	0.0	22.0	1.1	0.0	5.0	2.8
14	405	2.5	11380	0.0	0.0	0.0	0.0	20.3	0.5	0.0	7.6	4.1

Figure 4.2, 4.3, and 4.4 show the yield of hydrolysis products, glucose and 5-HMF for runs 1-14. Here, product yields were calculated based on 2.7 wt% of pure cellulose input in the reactor at 27.6 MPa.

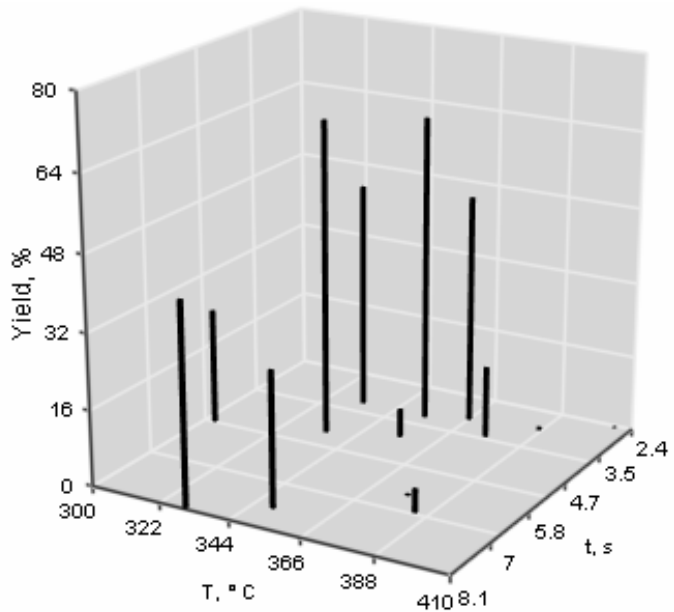


Figure 4.2 Yield of hydrolysis products obtained from cellulose treatment in subcritical and supercritical water at 27.6 MPa.

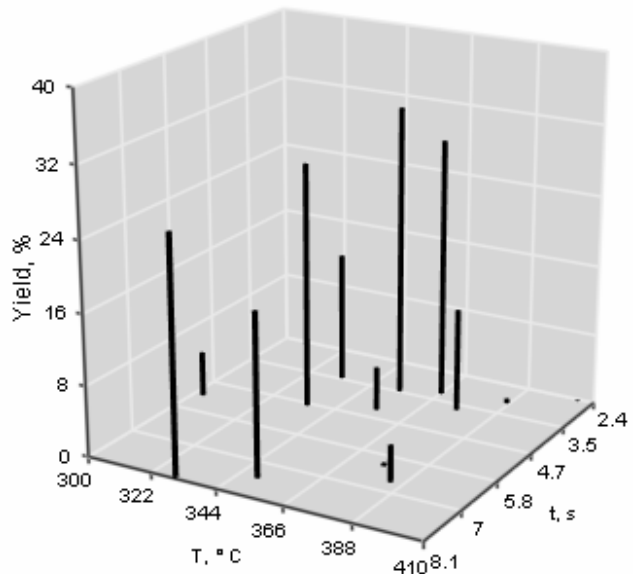


Figure 4.3 Yield of glucose obtained from cellulose treatment in subcritical and supercritical water at 27.6 MPa.

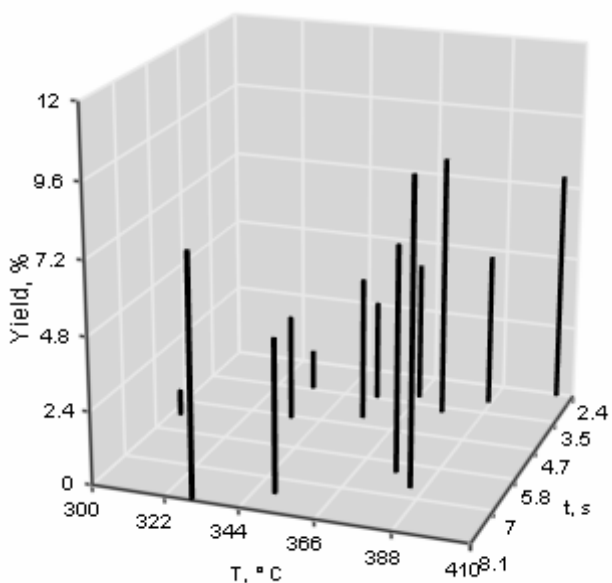


Figure 4.4 HMF yield in liquids obtained from cellulose treatment in subcritical and supercritical water at 27.6 MPa.

In this study, we defined (a) hydrolysis products as the combination of oligomers ( $>2$  monomer units), cellobiose, glucose, and fructose, and (b) degradation products as glycoaldehyde, D-fructose, 1,3 dihydroxyacetone, anhydroglucose, 5-HMF, and furfural. These products are quite similar to those obtained by Sasaki et al.<sup>4</sup> HPLC chromatographs show the presence of pyruvaldehyde, glyceraldehydes and erythrose in most of the liquid products, these intermediate products were not quantified due to lack of accurate calibration. The organic acid (e.g., formic acid, lactic acid and acetic acid) presence were confirmed by HPLC analysis in Bio-Rad Aminex HPX-87H column, but were not quantified.

Figure 4.5 shows that the TOC of liquid product increased rapidly with rise in temperature from 302 to 330°C, and more than 90% of cellulose was converted to hydrolysis or degradation products above 330°C, except for run 4 (333°C, 3.48 s).

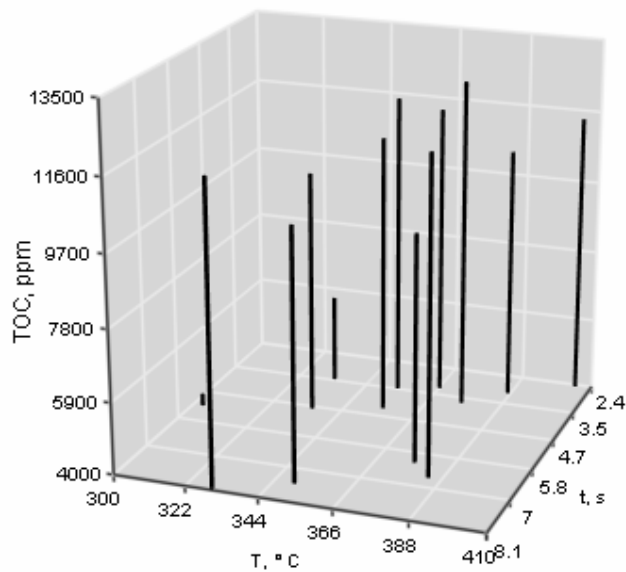


Figure 4.5 TOC in liquid products obtained from cellulose treatment in subcritical and supercritical water at 27.6 MPa.

The nine quantified compounds in 14 runs are compiled in Table 4.3. It is observed that as percentage of other compounds (OC), which is defined in Table 4.3 as the difference between TOC and total identified carbon (mmol/l), increases with increase in temperature or residence time. The OC are mostly organic acids, which is confirmed by the low pH (2.3 to 3) for all the runs.

Table 4.3 Carbon balance in the liquid products obtained from subcritical and supercritical treatment of cellulose at 27.6 MPa.

Samples	Olg	CB	Glu	Fr	GA	DA	AG	HMF	FUR	Total identified		
										carbon mmol/l	TOC mmol/l	OC %
Run 1	153.0	26.3	45.0	7.0	4.0	0.0	9.3	11.0	0.0	255.5	359.1	28.9
Run 2	98.9	5.6	238.7	90.3	43.0	0.0	54.8	100.5	43.2	675.0	990.0	31.8
Run 3	169.1	57.9	335.7	58.0	44.0	3.7	69.6	51.9	20.3	810.1	980.8	17.4
Run 4	231.9	72.3	130.7	15.0	9.7	2.3	24.1	16.7	5.7	508.3	525.5	3.3
Run 5	278.2	54.0	249.0	43.0	32.3	3.0	51.1	44.3	16.7	771.6	865.8	10.9
Run 6	65.6	2.8	163.7	96.3	26.3	7.7	41.8	63.8	29.7	497.7	881.7	43.5
Run 7	200.5	55.6	293.7	58.5	43.2	4.2	63.6	42.4	16.4	778.1	997.5	22.0
Run 8	0.0	0.0	44.1	182.1	9.5	10.9	9.7	60.4	34.0	350.7	942.5	62.8
Run 9	109.1	8.1	262.3	122.7	60.0	7.7	67.7	58.6	26.6	722.7	971.7	25.6
Run 10	33.3	0.0	104.0	142.7	17.7	11.3	15.5	109.5	55.7	489.8	1055.8	53.6
Run 11	0.0	0.0	2.3	158.4	0.0	4.6	0.0	94.1	2.6	262.1	830.2	68.4
Run 12	0.0	0.0	36.4	158.6	8.1	4.7	1.6	126.2	70.8	406.4	1020.8	60.2
Run 13	0.0	0.0	4.2	196.1	0.0	9.7	0.0	64.3	38.7	313.0	886.7	64.7
Run 14	0.0	0.0	0.0	181.2	0.0	4.3	0.0	96.5	57.1	339.1	948.3	64.2

\* Carbon percentage in oligomers is considered same as that of cellobiose

Solids from all the runs were oven dried at 70°C, before analysis. Solids from runs 1, 3, 4 and 5 were brown fluffy, whereas from others were black. The elemental carbon in the solids from run 1 was 41.9%.

*Experiment Group 1 (302-335°C):* Runs 3, 5 (Table 4.2), conducted at almost the same process conditions, show reproducible results in terms of hydrolysis product yield, which are 66.7% and 65.8%, respectively. HPLC chromatograph from run 5 is shown in Figure 4.6.

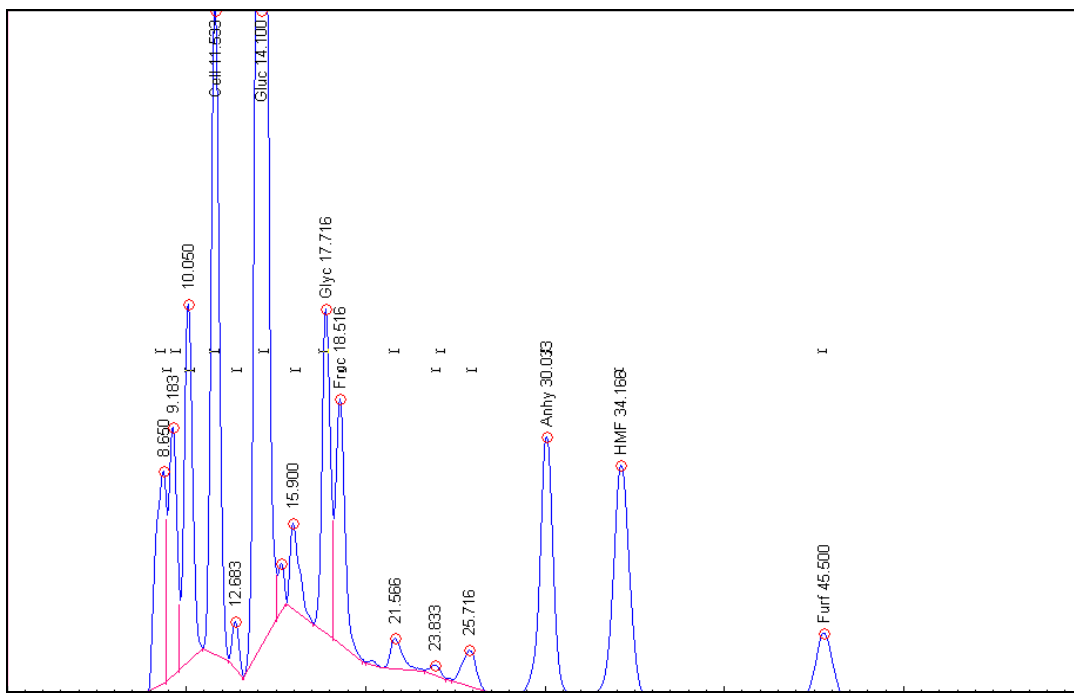


Figure 4.6 HPLC chromatograph of run 5 (335°C, and 4.7 s residence time).

Glucose yield in run 3 is 37.6%. OC (Table 4.3) for runs 3 and 5 were 17.4 and 10.9%, respectively. 5-HMF and furfural yields in product liquid were almost same for both the runs. Liquid products of run 3 and 5 were hazy, and turned turbid even after the centrifuging. Residual solids were brown, fluffy and sticky. Degradation products yield in run 1 is minimum among all the runs, but it has higher yield of OC because of the comparatively longer residence time (5.2 s), as organic acids increase with the increase in residence time. Run 4 conducted at relatively low residence time (3.5 s) had only 3.3% of OC as shown in Table 4.3.

*Experiment Group 2 (350-366°C):* For the experiments conducted in this temperature range, run 7 (354°C, 3.5 s) had the highest hydrolysis products yield (64.9%) and glucose yield (32.9%). HPLC chromatograph from run 7 is shown in Figure 4.7.

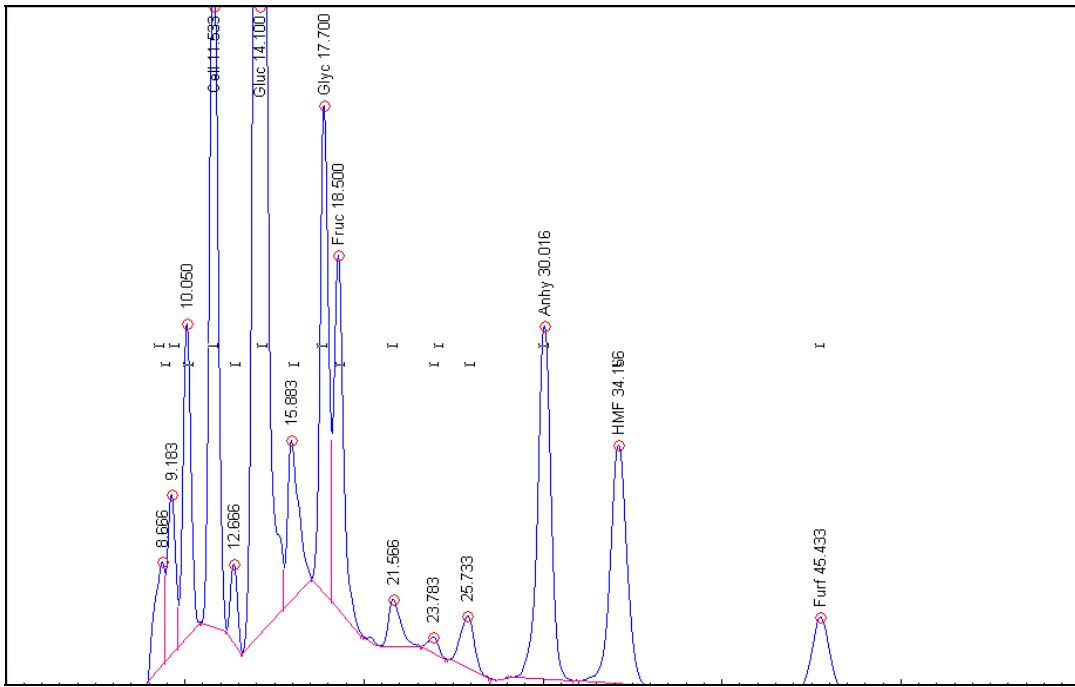


Figure 4.7 HPLC chromatograph of run 7 with (354°C, and 3.5 s residence time).

This experiment was duplicated to verify the reproducibility. Liquid products were clear yellowish liquid having very little solids. Increase in residence time from 3.5 to 4.4 s for run 8 resulted in a rapid decline in yield of hydrolysis products, which again decreased for run 9, where reactor temperature was increased from 354 to 366°C. OC yields for runs 7 and 9, shown in Table 3.5 were 22.0% and 25.6%, respectively.

*Experiment Group 3 (376-405°C):* Degradation products were the main products for the experiments conducted in supercritical water. The highest hydrolysis products and glucose yields were 15.2% and 11.6% respectively, in run 10 (376 °C, 3.7 s). HPLC chromatograph of run 14 is shown in Figure 4.8.

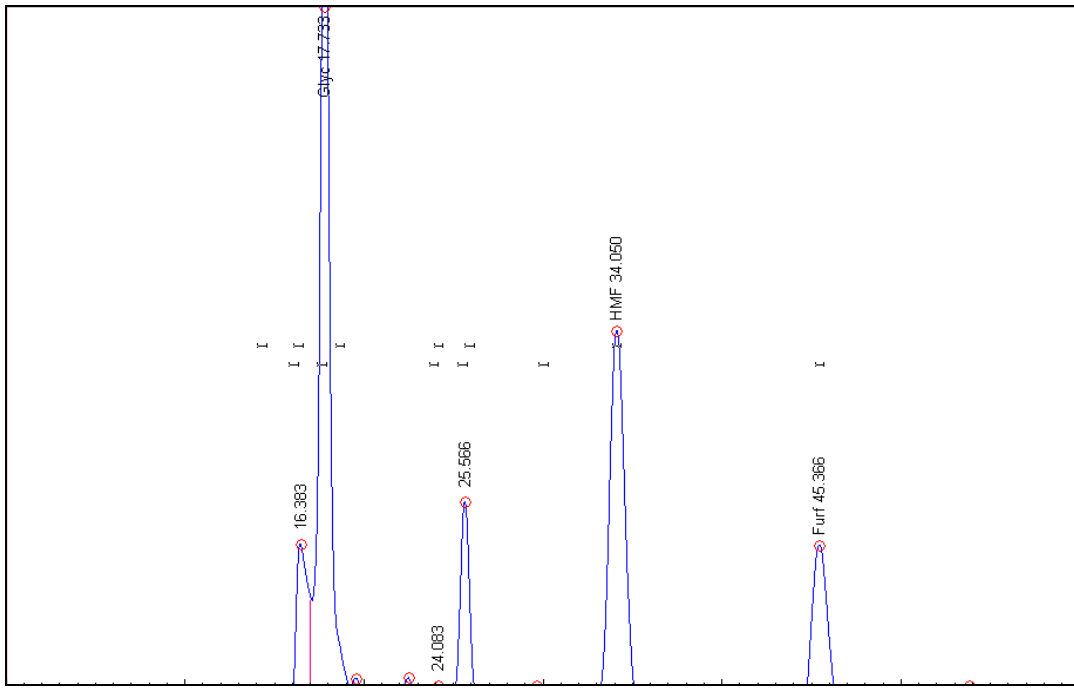


Figure 4.8 HPLC chromatograph of run 14 (405 °C, and 2.5 s residence time).

Glycoaldehyde dimer was the major product among the entire identified products. OC yield (Table 4.4) increased to more than 50%, due to increase in the organic acids formation. Liquid products in supercritical range were almost clear, yellowish liquid with very little solids.

*Experiment Group 4 (302 and 330°C with K<sub>2</sub>CO<sub>3</sub> catalyst):* For these experiments, Table 4.4 shows the process parameters and the results in terms of carbon balance. Notably, the gas formation is high in the presence of K<sub>2</sub>CO<sub>3</sub>. Gas flow almost doubled, when K<sub>2</sub>CO<sub>3</sub> concentration was increased from 0.22 wt% (run C1) to 0.44 wt% (run C2) at 302°C.

Table 4.4 Experimental conditions of cellulose runs in presence of catalyst  $K_2CO_3$  in subcritical water.

Run	T, (°C)	t, (s)	$K_2CO_3$ (wt%)	TOC, (Liquid products) ppm	Liquefaction	Elemental	Unconverted	Carbon in
					(Organic carbon in liquid products) %	Carbon* % in solid residues (1)	carbon as solid residue, (2)	gaseous products, [100-(2)-(1)]
								%
C1	302	5.2	0.22	2230	18.5	41.9	65.5	16.0
C2	302	5.2	0.44	3343	27.7	40.9	37.1	35.2
C3	330	4.8	0.13	2503	21.0	41.2	35.6	43.4

\* Based on elemental analysis in Elementar Vario Macro CNS analyzer

In run C3, 43.4 wt% of input carbon goes to gaseous products at 330°C, 4.8 s in presence of 0.13 wt% of  $K_2CO_3$ . Figure 4.9 shows the photographs of liquid products obtained from run 1 (in absence of catalyst at 303°C) and those from runs C1 and C2, which were conducted in presence of 0.22 wt% and 0.44 wt% of  $K_2CO_3$ , respectively.

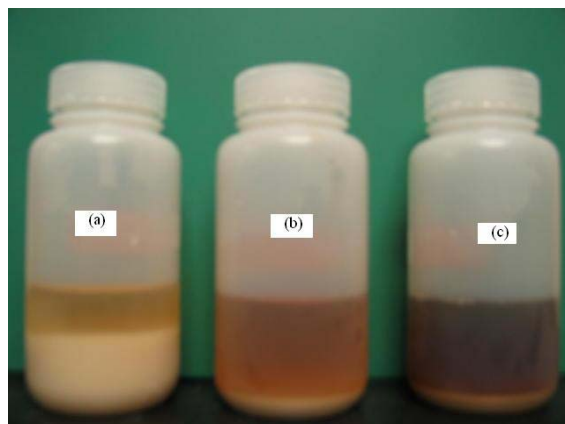


Figure 4.9 Products obtained at 302°C, 5.2 s, 27.6 MPa in the presence of  
(a) 0%  $K_2CO_3$ , (b) 0.22%  $K_2CO_3$ , and (c) 0.44%  $K_2CO_3$ .

Color of liquid turned light yellowish to brownish with the increase of  $K_2CO_3$ . Solids from runs C1 and C2 were dense, but the carbon analysis did not show rise in %carbon. Liquid products, from runs C1 and C2, show small peaks for glycoaldehyde

dimer in HPLC analysis. However, no such peaks were observed for run C3. Small peaks due to formic acid and acetic acid were observed in all the three runs, but were not quantified.

#### 4.6 Discussion

Structure of water changes significantly near the critical point because of the breakage of infinite network of hydrogen bonds and water exists as separate clusters with a chain structure.<sup>22</sup> In fact, dielectric constant of water decreases considerably near the critical point, which causes a change in the dynamic viscosity and also increases self-diffusion coefficient of water.<sup>23</sup> These properties of supercritical water provide a completely different homogeneous reaction atmosphere. Hot compressed water acts as both reactant and reaction medium. Water as reactant leads to hydrolysis reactions; rapidly degrading the polymeric structure of cellulose to hydrolysis products, instead of pyrolysis. The intermediates formed during the decomposition reactions show a high solubility in sub- and supercritical water; hence reaction steps are mainly homogeneous.<sup>24</sup> Diffusion related problems such as mass transfer through the interface are not encountered in homogeneous reaction.<sup>3</sup>

Hydrothermal degradation of cellulose in 200-300°C range is a heterogeneous and pseudo-first-order reaction for which detailed chemistry and mechanism were proposed by Antal and coworkers.<sup>25-30</sup> The models are based on the sequence cellulose → glucose → decomposition products, in which hydrolysis to glucose is an important step. It is assumed that the unconverted cellulose retains its chemical integrity with the extent of the hydrolysis.<sup>31</sup> Results of the studies clearly indicate that cellulose converts to hydrolysis products (oligomers and monomers) and then further degrades to aqueous

degradation products of glucose, producing glycoaldehyde, fructose, 1,3 dihydroxyacetone, anhydroglucose, 5-HMF and furfural.

In a very recent study, it has been observed that crystalline to amorphous transition of cellulose is observed between 320-330°C at 25 MPa and cellulose is completely dissolved above 340°C.<sup>5, 6</sup> Hydrolysis products are intermediate products in cellulose decomposition in subcritical and supercritical water and they convert further to various degradation products, if allowed a higher residence time. To minimize degradation, most of the studies have been conducted for a very short residence times, typically less than a second.<sup>4, 7</sup> However, this extremely short residence time may not be enough for crystalline to amorphous transformation of cellulose.<sup>6</sup>

All of our studies in subcritical water were conducted for the residence time 3.3-8.1 s. For the runs 3 and 5, residence times were 4.8 and 4.7 s, respectively, which appear to be sufficient for the crystalline to amorphous transformation of cellulose. Therefore, a yield of hydrolysis products as high as 66.8% was achieved in this region. Glucose molecules are unstable at high temperature and immediately degrade to conversion products. Earlier study of glucose reactions in hot compressed water (200-500°C, 4-40 MPa) in a batch-type reactor has shown that more than 80% of the glucose was consumed above 300°C and 60 s heating period. Gasification of glucose was promoted with increasing temperature and the heating rate.<sup>32</sup>

Optimizing the residence time in this temperature zone may further increase the hydrolysis products yields. By increasing the reactor temperature from 335 to 354°C and reducing the residence time from 4.7 to 3.5 s achieved similar yields of hydrolysis products. In our observation, yields of hydrolysis products depend on the temperature and

residence times at which crystalline to amorphous transformation of cellulose is completed in subcritical water, and the yield of degradation products may be minimized by optimizing the residence time around this temperature. A longer residence time enhances the degradation rate of converted hydrolysis products. For example, in a recent study, majority of water soluble compounds from cellulose decomposition in subcritical water at 300-310°C for the residence time 0.5-1.5 min were converted to degradation products, and the yield of hydrolysis products such as oligomers, glucose was less than 20%.<sup>33</sup> In our study, pH of all the liquid products varied between 2.3 to 3. Acidic medium is conducive for the degradation of converted hydrolysis products at the reaction temperatures studied here. Once organic acids are formed in the reaction mixture, it provides necessary acidity for further degradation of the converted hydrolysis products, as an autocatalytic process. Indeed after hydrolysis of cellulose in water at 320°C and 25 MPa for 9.9 s, more than half of the cellulose was converted to organic acids.

Sasaki et al.<sup>4</sup> reported that cellobiose was derived from cellulose by supercritical water treatment. However, in runs 10-14, other oligosaccharides, which differ from the results of Sasaki et al., were apparently obtained from cellulose. These oligosaccharides decreased and glucose degradation products (glycoaldehyde, fructose, 1,3-dihydroxyacetone, anhydroglucose, 5-HMF and furfural) increased upon the prolonged treatment (2.5-6.6 s). The liquid products obtained in this region are transparent yellow with almost 100% cellulose conversion.

Among the identified products (runs 10-14) in supercritical region, glycoaldehyde dimer is the major product yield. It is known that the reducing ends of oligosaccharides

are fragmented to erythrose and glycoaldehyde in supercritical water. Low supercritical water density favors retro-aldol condensation of glucose.<sup>34, 35</sup> Main reaction pathway of glucose decomposition in subcritical and supercritical water explains the formation routes for degradation products, such as glycoaldehyde, erythrose, glyceraldehydes, dihydroxyacetone, pyruvaldehyde, 1,6 anhydrous glucose, 5-HMF, furfural and lactic acid.<sup>13, 36</sup> In fact, 5-HMF was observed to increase with temperature and residence time.

*Effect of K<sub>2</sub>CO<sub>3</sub> catalyst:* Addition of alkali metal salts (e.g. KHCO<sub>3</sub>, KOH, Na<sub>2</sub>CO<sub>3</sub>, K<sub>2</sub>CO<sub>3</sub>) reduces coke formation and catalyzes the water-gas shift reaction.<sup>37</sup> For example, the addition of KHCO<sub>3</sub> leads to an increase in gas formation and a decrease in the amount of carbon monoxide due to water-gas shift reaction.<sup>16</sup> Also, methane formation is dominant at relatively low temperatures in catalytic gasification of cellulose in supercritical water.<sup>38</sup> We also observed the increased formation of gas in presence of K<sub>2</sub>CO<sub>3</sub>, based on carbon balance. Biomass contains about 0.5 wt% potassium and other alkalis such as Ca and Na. Therefore, gasification of biomass in supercritical water will be enhanced by the presence of these natural elements. It has been reported that carbohydrate structure of solid residues start to disappear at liquefaction temperature of 290-300°C and according to elemental analysis, the carbon content of the solid residues increases significantly.<sup>18</sup> Since the residence time in our study was short (4.8-5.2 s), carbonization of solids might not have started. With the increase in the concentration of K<sub>2</sub>CO<sub>3</sub>, color of the liquid turned dark. Conversion of cellulose to liquid products without K<sub>2</sub>CO<sub>3</sub> in similar conditions (run 1) was higher than the conversion in presence of K<sub>2</sub>CO<sub>3</sub> (runs C1- C3), use of much lower concentration of K<sub>2</sub>CO<sub>3</sub> may improve liquefaction of cellulose at low temperatures.

#### **4.7 Conclusion**

Crystalline cellulose can be successfully converted to monomers (mainly glucose) and oligomers by hydrolysis in subcritical water. Earlier studies show that high yields of hydrolysis products (65-77%) are mainly obtained in supercritical water (at 400°C, 25 MPa) between 0.1-0.5 s residence times in a continuous flow reactor. Some of the studies suggest a combination of supercritical and subcritical water treatment of cellulose to obtain a high yield of hydrolysis products.

More than 90% of the cellulose converts to water soluble products above 330 °C. Reaction medium becomes acidic, which is conducive for the degradation of converted oligomers and monomers (i.e., hydrolysis products) at the reaction temperature. Thus optimizing the residence time and rapid cooling after the reaction are key to minimizing the degradation. Our findings show that a high yield of hydrolysis products can be achieved at comparatively lower temperature (335°C) in subcritical water. For example, upto 66.8% of crystalline cellulose can be converted to hydrolysis products at 335°C and 27.6 MPa in merely 4.7 second reaction time. With increase in the reaction time, the hydrolysis products degrade to glycoaldehyde, fructose, 1,3 dihydroxyacetone, anhydroglucose, 5-HMF and furfural. Yield of glycoaldehyde, a retro-aldol condensation product of glucose, increases with a decrease in the density of supercritical water, and the yield of degradation products, 5-HMF and organic acids, increases with temperature and residence time. In supercritical water conditions, studied here, more than 80% of the cellulose converts into the degradation products and organic acids.

Use of K<sub>2</sub>CO<sub>3</sub> catalyst in the reaction mixture during depolymerization of cellulose in subcritical water substantially enhances the gas formation. However, during

the short residence time (4.8-5.2 s), carbonization of residue solid does not occur.

#### **4.8 Acknowledgment**

Author is thankful for the financial supports from the U.S. Department of Energy (grant DE-FC26-05424.56) and Alabama Center for Paper and Bioresource Engineering. Additionally, the authors are thankful for technical discussions and assistance from Prof. Y. Y. Lee and Prof. Ayhan Demirbas.

#### **4.9 Products Nomenclature**

Olg: Oligomers

CB: Celllobiose

Glu: Glucose

Fr: D-Fructose

GA: Glycoaldehyde dimer

DA: 1,3 Dihydroxyacetone dimer

AG: 1,6 Anhydro - beta glucose

HMF: 5-Hydroxymethyl –2-furaldehyde

FUR: Furfural

OC: Other compounds

#### 4.10 References

1. Gourdian, F.; Peferoen, D., Liquid fuels from biomass via a hydrothermal process. *Chemical Engineering Science* **1990**, 45, 2729-2734.
2. Matsumura, Y.; Sasaki, M.; Okuda, K.; Takami, S.; Ohara, S.; Umetsu, M.; Adschari, T., Supercritical water treatment of biomass for energy and material recovery. *Combust. Sci. and Tech.* **2006**, 178, 509-536.
3. Galkin, A. A.; Lunin, V. V., Subcritical and supercritical water: a universal medium for chemical reactions. *Russian chemical reviews* **2005**, 74, (1), 21-35.
4. Sasaki, M.; Fang, Z.; Fukushima, Y. N.; Adschari, T.; Arai, K., Dissolution and hydrolysis of cellulose in subcritical and supercritical water. *Ind. Eng. Chem. Res.* **2000**, 39, 2883-2890.
5. Deguchi, S.; Tsujii, K.; Horikoshi, K., Cooking cellulose in hot and compressed water. *Chem. Commun.* **2006**, 3293-3295.
6. Deguchi, S.; K. Tsujii; Horikoshi, K., Crystalline-to-amorphous transformation of cellulose in hot and compressed water and its implications for hydrothermal conversion. *Green Chem.* **2008**, 10, 191-196.
7. Ehara, K.; Saka, S., A comparative study on chemical conversion of cellulose between the batch-type and flow-type systems in supercritical water. *Cellulose* **2002**, 9, 301-311.
8. Ehara, K.; Saka, S., Decomposition behavior of cellulose in supercritical water, subcritical water, and their combined treatments. *J. Wood Sci.* **2005**, 51, 148–153.
9. Minowa, T.; Zhen, F.; Ogi, T., Cellulose decomposition in hot-compressed water with alkali or nickel catalyst. *J. Supercritical Fluids* **1997**, 13, 253-259.

10. Minowa, T.; Zhen, F.; Ogi, T.; Varhegyi, G., Decomposition of cellulose and glucose in hot-compressed water under catalyst-free conditions. *J Chem. Eng. Japan* **1998**, 31, 131-134.
11. Sakaki, T.; Shibata, M.; Miki, T.; Hirosue, H.; Hayashi, N., Reaction model of cellulose decomposition in near-critical water and fermentation of products. *Bioresource Technology* **1996**, 197-202.
12. Sasaki, M.; Kabyemela, B.; Malaluan, R.; Hirose, S.; N.Takeda; Adschari, T.; Arai, K., Cellulose hydrolysis in subcritical and supercritical water. *J. Supercritical Fluids* **1998** **1998**, 13, 261-268.
13. Kabyemela, B. M.; Takigawa, M.; Adschari, T.; Malaluan, R. M.; Arai, K., Mechanism and Kinetics of Cellobiose Decomposition in Sub- and Supercritical Water. *Ind. Eng. Chem. Res.* **1998**, 37, 357-361.
14. Ogi, T.; Yokayama, S.; Koguchi, T., Direct liquefaction of wood by catalyst (Part 1). *Sekiyu Gakkaishi* **1985**, 28, 239-245.
15. Yokayama, S.; Ogi, T.; Koguchi, K.; Murakami, M.; Suzuki, A., Direct liquefaction of wood by catalyst (Part 2). *Sekiyu Gakkaishi* **1986**, 29, 262-266.
16. Sinag, A.; Kruse, A.; Schwarzkopf, V., Key compounds of the hydrolysis of glucose in supercritical water in the presence of K<sub>2</sub>CO<sub>3</sub>. *Ind. Eng. Chem. Res.* **2003**, 42, 3516-3521.
17. Sinag, A.; Kruse, A.; Schwarzkopf, V., Formation and degradation pathways of intermediate products formed during the hydrolysis of glucose as a model substance for wet biomass in a tubular reactor. *Eng. Life Sci.* **2003**, 3, 469-473.

18. Szabo, P.; Minowa, T.; Ogi, T., Liquefaction of cellulose in hot compressed water using sodium carbonate. Part 2: thermogravimetric-mass spectrometric study of the solid residues. *J. Chem. Eng. of Japan* **1998**, 31, 571-576.
19. Muthukumaraa, P.; Gupta, R. B., Sodium-carbonate assisted supercritical water oxidation of chlorinated waste. *Ind. Eng. Chem. Res.* **2000**, 39, 4555-4563.
20. Sluiter, A.; Hammes, B.; Ruiz, R.; Scarlata, C.; Sluiter, J.; Templeton, D., Determination of sugars, byproducts, and degradation products in liquid fraction process samples. *NREL Biomass Program, Laboratory Analytical Procedure (LAP)* **2006**.
21. Wright, A. F.; Bailey, J. S., Organic carbon, total carbon, and total nitrogen determinations in soils of variable calcium carbonate contents using a Leco CN-2000 dry combustion analyzer. *Communications in soil science and plant analysis* **2001**, 32, 3243-3258.
22. Kalinichev, A. G.; Churakov, S. V., Size and topology of molecular clusters in supercritical water: a molecular dynamics simulation. *Chem. Phys. Letters* **1999**, 302, 411-417.
23. Marcus, Y., On transport properties of hot liquid and supercritical water and their relationship to the hydrogen bonding. *Fluid Phase Equilibr.* **1999**, 164, 131-142.
24. Kruse, A.; Gawlik, A., Biomass conversion in water at 330-410 °C and 30-50 MPa: Identification of key compounds for indicating different chemical reaction pathways. *Ind. Eng. Chem. Res.* **2003**, 42, 267-269.
25. Bobleter, O., Hydrothermal degradation of polymers derived from plants. *Prog. Polym. Sci.* **1994**, 19, 797–841.

26. Schwald, W.; Bobleter, O., Hydrothermolysis of cellulose under static and dynamic conditions at high temperatures. *J. Carbohydr. Chem.* **1989**, 8, (4), 565-578.
27. Mok, W. S. L.; M.J., A. J.; Varhegyi, G., Productive and parasitic pathways in dilute-acid-catalyzed hydrolysis of cellulose. *Ind. Eng. Chem. Res.* **1992**, 31, 94-100.
28. Mok, W. S.; Antal, M. J., Uncatalyzed solvolysis of whole biomass hemicellulose by hot compressed liquid water. *Ind. Eng. Chem. Res.* **1992**, 31, 1157-1161.
29. Antal, J. M. J.; Mok, W. S. L.; Richards, G. N., Mechanism of formation of 5-(hydroxymethyl)-2-furfuraldehyde from D-fructose and sucrose. *Carbohydr. Res.* **1990**, 199, 91-109.
30. Antal, J. M. J.; Leesomboon, T.; Mok, W. S. L.; Richards, G. N., Mechanism of formation of 2-furaldehyde from D-xylose. *Carbohydr. Res.* **1991**, 217, 71-85.
31. Bouchard, J.; Abatzoglou, N.; Chornet, E.; Overend, R. P., Characterization of depolymerized cellulosic residues. *Wood Science and Technology* **1989**, 23, (4), 343-355.
32. Watanabe, M.; Aizawa, Y.; Iida, T.; Levy, C.; Aida, T. M.; Inomata, H., Glucose reactions within the heating period and the effect of heating rate on the reactions in hot compressed water. *Carbohydrate Research* **2005**, 340, 1931-1939.
33. Xiuyang, L.; Sakoda, A.; Motoyuki, S., Kinetics and product distributions of cellulose decomposition in near critical water. *J. Chem. Ind. and Eng. China* **2001**, 52, (6), 556-559.
34. Sasaki, M.; Furukawa, M.; Adschari, T.; Arai, K., Kinetics and mechanism of cellobiose hydrolysis and retro-aldol condensation in subcritical and supercritical water. *Ind. Eng. Chem. Res.* **2002**, 42, 6642-6649.

35. Sasaki, M.; Goto, K.; Tajima, K.; Adschiri, T.; Arai, K., Rapid and selective retro-aldol condensation of glucose to glycolaldehyde in supercritical water. *Green Chem.* **2002**, 4, 285-287.
36. Sasaki, M.; Hattori, H.; Arai, K., Rapid and selective productions of valuable chemical intermediates from cellulose using supercritical water. *Cellulose Commun.* **2003**, 10, 63-68.
37. Hao, X. H.; Guo, L. J.; Mao, X.; Zhang, X. M.; Int., X. J. C., Hydrogen production from glucose used as a model compound of biomass gasified in supercritical water. *J. Hydrogen Energy* **2003**, 28, 55-64.
38. Guan, Y.; Pei, A.; Lie-jin, P.; Guo, L., Hydrogen production by catalytic gasification of cellulose in supercritical water. *J. Chem. Eng. of Chinese Univ.* **2007**, 21, 436-441.

## 5. Biocrude Production from Switchgrass using Subcritical Water

### 5.1 Abstract

Subcritical water is an environmentally attractive solvent for organic matters and can be used to liquefy biomass to biocrude, which is a mixture of oxygenated hydrocarbons of varying molecular weights. Liquefaction of switchgrass in subcritical water is studied using a semi-continuous reactor in the temperature range of 235-260°C. Subcritical water is pumped through a tubular reactor packed with switchgrass particles of 40-60 mesh size. Effects of reaction temperature and catalysis by K<sub>2</sub>CO<sub>3</sub> are examined. Potassium carbonate significantly enhances the hydrolysis of macromolecular components of switchgrass into water soluble products. More than 50 wt% of organic carbon available in switchgrass was converted to biocrude after 20 min of steady operation at 235°C in the presence of 0.15 wt% of K<sub>2</sub>CO<sub>3</sub>. At the high temperature (260°C), dehydration of biomass was favored over hydrolysis reactions. Based on chromatography and mass spectrometry analyses, biocrude contains lignin derived products, sugars and its decomposition products. Based on the infrared spectroscopy and electron microscopy of residue solid, the subcritical water treatment causes complete breakdown of lignocellulosic structure of switchgrass. In fact, the residue solid mainly contained lignin fractions.

## 5.2 Introduction

The increased demand for energy, and concerns about climate change and energy security have led to an explosion in interest in alternative and renewable energies. Among the several renewable energy options available, biomass is the only renewable source, which is capable of producing petroleum compatible products.<sup>1</sup> In recent years, U.S. government has sponsored numerous research studies and demonstration projects, for developing abundantly available biomass resources of the country for biofuels applications. The major focus is on non-food resources or so called second generation biofuels from lignocellulosic biomass, which is mainly composed of cellulose, hemicelluloses, and lignin. Switchgrass, a summer perennial grass native to North America that grows on marginal land, is considered to be a major energy crop of interest for the second generation biofuels. The advantages of switchgrass as energy crop include low requirement of chemical inputs and the use of marginal land which does not compete with the food production. The switchgrass plants are immense biomass producer that can reach heights of  $\geq 10$  feet and provide 6-8 dry-ton/acre/year yield (as compared to 2.5 tons/acre/year for hay) with a high cellulosic content.<sup>2,3</sup>

In the subcritical region, the ionization constant ( $K_w$ ) of water increases with temperature and is about three orders of magnitude higher than that of ambient water (Figure 5.1) and the dielectric constant ( $\epsilon$ ) of water drops from 80 to 20.<sup>4</sup> A low dielectric constant allows subcritical water to dissolve organic compounds, while a high ionization constant allows subcritical water to provide an acidic medium for the hydrolysis of biomass components.<sup>5-7</sup>

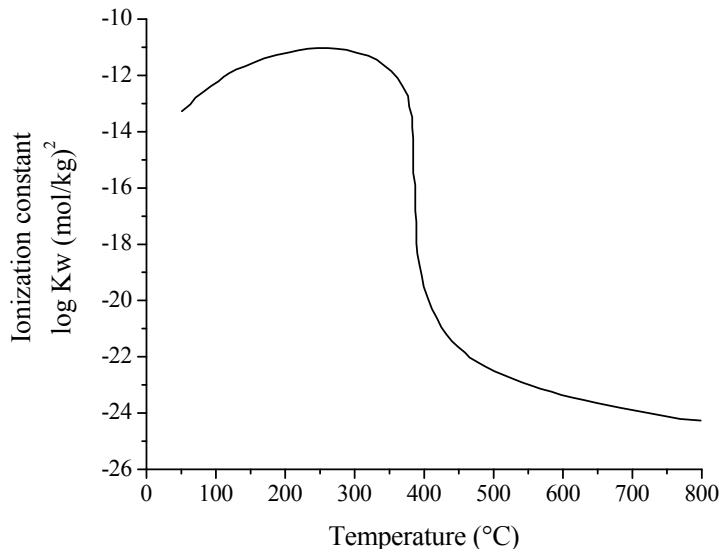


Figure 5.1 Ionization constant ( $K_w$ ) of water as a function of temperature at 25 MPa.<sup>4</sup>

Although the dielectric constant of subcritical is low enough for organics to be soluble, it remains high enough to allow salt dissolution.<sup>8</sup>

There are several competing pathways for converting the biomass to liquid fuel, chemicals, and/or hydrogen (Figure 5.2). Among them, hydrothermal (subcritical) liquefaction process has attracted much attention due its versatility to utilize mixed biomass feedstock without any pretreatment or drying, at a comparatively low temperature. Since water is used both as a reactant and as the reaction medium, the moisture content of biomass is not an issue. Moreover, biomass residue generated from the any other process can be utilized to produce biocrude.<sup>9</sup> Liquefaction of biomass in subcritical water proceeds through a series of structural and chemical transformations involving<sup>10</sup>

- Solvolysis of biomass resulting in micellar-like structure
- Depolymerization of cellulose, hemicelluloses, and lignin

- Chemical and thermal decomposition of monomers to smaller molecules

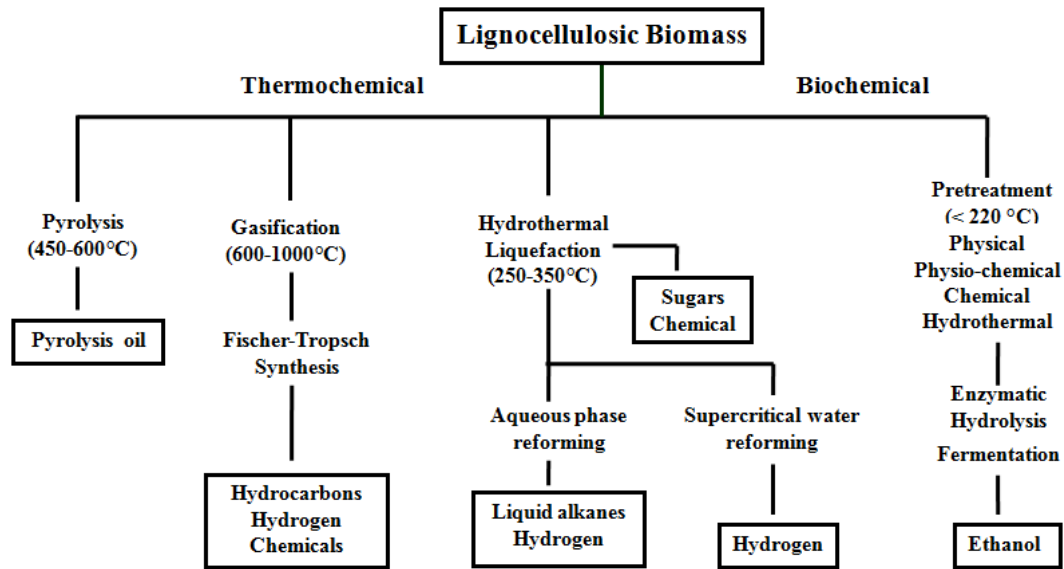


Figure 5.2 Major pathways for the conversion of biomass to biofuels.

In this study, biocrude is defined as the solubilized fraction of biomass after subcritical water treatment. Biocrude, which is an aqueous carbohydrate solution derived from the direct liquefaction of biomass can be converted to liquid fuel, hydrogen, or chemicals. For example, Huber et. al. produced liquid alkanes by aqueous phase processing of carbohydrates derived from biomass.<sup>11</sup> In another study, hydrogen was produced by aqueous-phase reforming of woody biomass in a batch reactor using two step processes: hydrolysis of biomass using sulfuric acid followed by reforming in the presence of Pt/Al<sub>2</sub>O<sub>3</sub> catalyst.<sup>12</sup> Glucose, a biocrude component, was catalytically reformed in supercritical water to produce hydrogen with yields as high as 12 mol of H<sub>2</sub>/mol of glucose reaching the stoichiometric limit.<sup>13</sup>

Bobleter et al., in their pioneering work, have developed hydrothermal process for pretreatment of biomass and subsequent enzymatic hydrolysis.<sup>14-16</sup> Several studies have been conducted using model compounds such as cellulose, hemicelluloses and lignin in

sub-and supercritical water. Minowa et al.<sup>17, 18</sup> conducted hydrolysis of cellulose with and without catalyst. Using a conventional autoclave, water/cellulose slurry was heated in a nitrogen atmosphere to various temperatures between 200-350°C. Results indicate that decomposition of cellulose increases with the reaction temperature. For example, reactions below 240°C lead to the formation of water-soluble products, and those above 260°C lead to the formation of oil, char, and gas products. Hydrolysis of microcrystalline cellulose in subcritical and supercritical water (320-400°C, and 0.05-10.0 seconds) in a continuous reactor were conducted to produce upto 75% yield of hydrolysis products (glucose and oligomers) along with aqueous decomposition products of glucose.<sup>19-21</sup> Most of the hemicelluloses together with lignin was solubilized in hot compressed water using a tubular percolating reactor in the pretreatment of biomass.<sup>22</sup> Conversion of lignin model compound under hydrothermal conditions have also been studied earlier.<sup>23, 24</sup> Majority of previous studies have focused mainly on model compounds and have established the reaction kinetics and reaction pathways of such compounds in hydrothermal medium. However, lignocellulosic biomass is mainly a mixture of cellulose (38-50 wt%), hemicelluloses (23-32 wt%), and lignin (15-25 wt%) which are held together by covalent bonding, various intermolecular bridges, and van der Waals forces forming a complex structure.<sup>25, 26</sup> These components interact with each other in reaction medium and lead to a very complex chemistry. The presence of different inorganic salts in biomass can also influence the reaction pathways.<sup>27</sup> For example, Karagoz et al. and Midgett observed enhanced hydrothermal upgrading of biomass in batch reactor for the producing oils using alkali catalyst.<sup>28-31</sup> However, there are not many studies conducted with the real biomass particularly with the energy crops except a recent study by Cheng

et al. on the rapid conversion of switchgrass in subcritical water in a batch reactor in the temperature range of 250-350°C and pressure of 20 MPa.<sup>32</sup>

The main aim of this study is to explore the possibility of depolymerizing the entire holocellulose and lignin fraction of switchgrass in subcritical water to produce biocrude, and converting them to sugar and lignin derived components, in a semi-continuous reactor. Effects of temperature and K<sub>2</sub>CO<sub>3</sub> on the decomposition of switchgrass are examined. The major objective is to understand the decomposition reaction of switchgrass in subcritical water and characterization of biocrude for identifying the formation of value-added chemicals. In addition, the physical and chemical characteristics of the solid residue are investigated.

### 5.3 Experimental Section

*Materials:* Alamo switchgrass (*panicum virgatum* species), moisture content 7.78%, and size + 60 to - 40 mesh (0.25 to 0.42 mm) was used in this study. The composition analysis of switchgrass is shown in Table 5.1. The higher heating value (HHV) of the switchgrass was measured in IKA C200 calorimeter as 17.10 MJ/kg. Potassium carbonate (K<sub>2</sub>CO<sub>3</sub>) and high purity standard reagents for HPLC analysis were purchased from Sigma Aldrich. De-ionized water was used for conducting the experiments.

Table 5.1 Composition (wt%) of switchgrass.

Glucan	Xylan	Galactan	Arabinan	Klason Lignin	Acid soluble lignin	Ash	Acetic acid
39.5	22.4	1.4	2.9	22.2	1.3	2.2	4.1
C	N	Ca	K				
44.61	0.74	0.22	0.57				

*Apparatus:* Figure 5.3 shows the schematic of the biocrude production apparatus. It consists of two high-pressure liquid pumps, an electrical tubular furnace, a water-cooled double tube heat exchanger, a backpressure regulator, and a phase separator. Reactor was a 0.57" ID, 20" long high-pressure stainless steel tube.

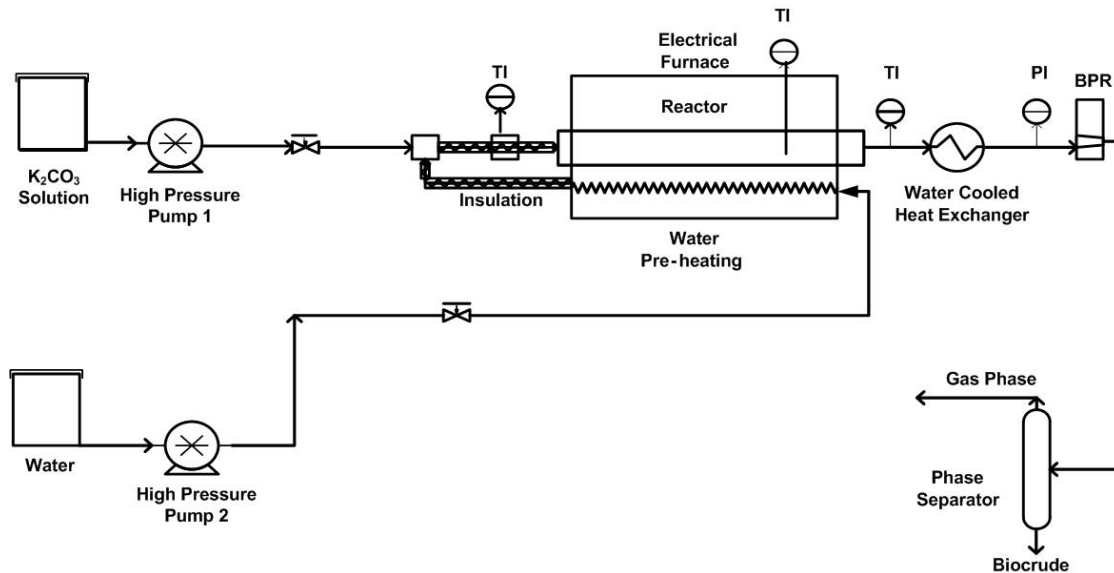


Figure 5.3 Apparatus for biocrude production.

Temperature of the reaction zone was measured using a 1/16" thermocouple placed inside the biomass bed from the inlet. This thermocouple measured reaction zone temperature with accuracy of  $\pm 0.1^\circ\text{C}$ . There were three additional thermocouples installed at different locations in the apparatus. Real time temperature indicated by the thermocouple placed inside the reaction zone was used for all the analyses. Reactor pressure was maintained using a backpressure regulator. All the thermocouples were calibrated before the start of experiment. High precision HPLC pumps (Chrome Tech, USA) were used for the liquid flow. Pump flow rates were calibrated before every experiment. Multiple samples were collected and analyzed for TOC values during each experiment.

*Experimental Procedure:* In a typical experiment, reactor was placed inside the furnace after packing with 13 g of switchgrass. A stainless steel frit (pore size 2  $\mu\text{m}$ ) was placed in the reactor outlet to prevent the entrainment of fine solids with the liquid stream. Water and  $\text{K}_2\text{CO}_3$  solution was pumped using high pressure pumps 1 and 2 (Figure 5.3) and total liquid inlet flow rate was maintained 1.5 ml/min for the entire study. Experiments were conducted using only water and also adding  $\text{K}_2\text{CO}_3$  solution for some experiments in the temperature range of 235-260°C. The typical heating cycle of the process is shown in Figure 4. After completing the desired steady operation time ( $t$ ) of steady operation, heating was stopped and reactor was rapidly cooled to below 50°C. Biocrude produced at the reaction temperature was collected from the phase separator and stored at 4°C. The liquid products collected during all three stages of operation (Figure 5.4) i.e. preheating, steady operation, and cooling/washing period were analyzed for total organic carbon (TOC) content.

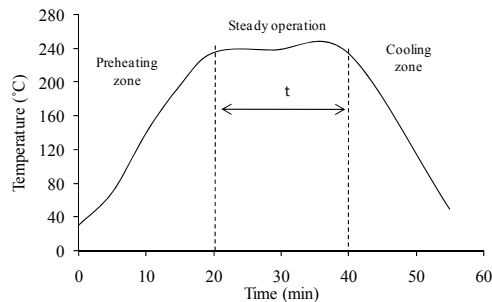


Figure 5.4 Heating profile in a typical experiment.

Gaseous products were noticeably low (< 10 wt.%) at 235°C. The gaseous products were vented without analysis. As per the Cheng et al. study the gas yield was 17.2 wt% at 250°C.<sup>32</sup> Biomass residue remained in the reactor was washed with de-ionized water and dried for the further analysis.

Two groups of experiments were conducted as listed in Table 5.2. Group I experiments were conducted at 260°C, 23.5 MPa in subcritical water and also in the presence of 0.5 wt% of K<sub>2</sub>CO<sub>3</sub>. Group II experiments were conducted at 235°C and 13.8 MPa.

Table 5.2 Experiment details of various runs.

Run No.	Temperature (°C)	Steady operation time (min)	K <sub>2</sub> CO <sub>3</sub> (wt%)	Switchgrass weight loss dry basis (wt%)
Group I ( at 23.5 MPa)				
1	260	50	0	82.0
2	260	25	0.50	81.9
Group II (at 13.8 MPa)				
3	235	90	0	65.0
4	235	80	0.15	69.7
5	235	20	0	61.9
6	235	5	0.15	42.3
7	235	10	0.15	59.6
8	235	20	0.15	70.8*

\* Relative standard deviation (RSD) is 5.3%

#### 5.4 Product Separation

Reaction products were separated into three components named as aqueous phase, solid precipitates, and biochar as per the scheme shown in Figure 5.5. In this study, the aqueous phase (water soluble fraction) and the solid precipitates are collectively called as Biocrude.

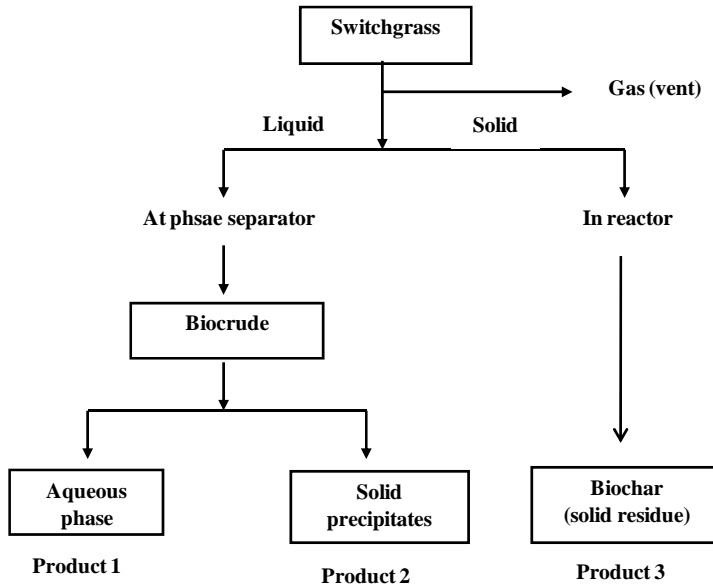


Figure 5.5 Products separation scheme.

*Aqueous Phase (Product 1):* After removing the suspended solids by centrifugal separation, aqueous phase samples collected at the reaction temperature were analyzed for organic carbon. Sugar and degradation products were determined as per the NREL biomass laboratory analytical procedure (described in technical report-NREL/TP-510-42623). Ultraviolet (UV) spectra were collected in the range of 200-400 nm. Sample was also taken for gas chromatography-mass spectroscopy (GC-MS) for identifying the phenolic compounds.

*Solid precipitates (Product 2):* Because of the change in property of water, some of the compounds soluble in subcritical condition were precipitated as fine solids upon cooling to ambient temperature. These fine solids, named solid precipitates were separated by centrifugation and dried in oven at 105°C to the constant weight. Solid precipitate was analyzed for the carbohydrate composition as per the earlier discussed procedure for biochar.

*Biochar (Product 3):* The residue solids collected from reactor after water washing at the end of experiment were named biochar. Biochar was analyzed for carbohydrates compositions by chemical analysis, and further characterized by X-ray diffraction, FT-IR, and SEM techniques. Composition analysis was performed as per the National Renewable Energy Laboratory (NREL) biomass laboratory analytical procedure (described in technical report-NREL/TP-510-42618).

## 5.5 Product Characterization

*TOC analysis:* After separating the suspended solids from liquid by centrifugation, liquid samples were analyzed for TOC in Shimadzu TOC-Vcsn analyzer, and an average of analyses is reported in this work.

*High pressure liquid chromatography (HPLC):* Monomers and oligomers of sugars and its degradation products in aqueous phase samples were determined as per the NREL biomass laboratory analytical procedure (described in technical report-NREL/TP-510-42623). The analysis was done using HPLC having Bio-Rad Aminex HPX-87P (lead based) column, refractive index detector, water mobile phase, and column temperature of 85°C. Additionally, analysis was done using Bio-Rad Aminex HPX-87H column, refractive index detector, 0.01 N sulfuric acid mobile phase and column temperature of 65°C.<sup>33</sup>

*GC-MS analysis:* Agilent model HP-5 column with 5% phenyl methyl siloxane (30 m long, 0.25 mm diameter, 0.25 µm film thickness) was utilized. Oven was programmed as: 45°C (hold 5 min) and ramped up (rate 5°C/min) to 250°C (hold 8 min). Injector was kept at 250°C in split mode (split ratio 50:1) with helium as carrier gas. Sample volume was 0.2 µl and compounds were identified using NIST library of mass spectra.

*XRD pattern:* Rigaku Miniflex powder X-ray diffractometer equipped with a Cu K $\alpha_1$  radiation source at 30 kV voltages, 15 mA current and a miniflex goniometer was used for the XRD analysis. Diffraction patterns were collected in the 2 $\theta$  range of 10-35° at a scan speed of 1°/min. and step size of 0.01°. The cellulose crystallinity index ( $CI$ ) in the switchgrass was determined<sup>34</sup> by

$$CI = (I_{002} - I_{AM}) / I_{002} \quad [1]$$

where  $I_{002}$  is the peak intensity corresponding to (002) lattice plane of cellulose molecule, and  $I_{AM}$  is the peak intensity observed at 2 $\theta$  equal to 18°.  $I_{002}$  represents both crystalline and amorphous material while  $I_{AM}$  represents amorphous material only.

*FT-IR spectra:* Infrared spectra of the samples were obtained using the FT-IR model Avatar 360, Nicolet. The sample discs were prepared by mixing 3 mg of oven dried (at 105°C) sample with 200 mg of spectroscopy grade KBr in an agate mortar. The final spectra were composed of 64 scans performed in the range of 4000 and 400 cm<sup>-1</sup> with 2 cm<sup>-1</sup> resolution.

*SEM:* The samples were prepared onto adhesive carbon tape on an aluminum stub followed by sputter coating of gold. Surface morphology of the sample was studied using an environmental scanning electron microscopy system (Zeiss EVO 50).

## 5.6 Results

The initial experiments (Group I) were conducted at 260°C, 23.5 MPa in subcritical water and also in the presence of K<sub>2</sub>CO<sub>3</sub>. Eighty two percent (oven dry basis) of the switchgrass was solubilized in run 1, and the maximum TOC value in the biocrude was observed as 31,520 ppm within 10 minutes of steady operation. With the use of merely 0.5 wt% K<sub>2</sub>CO<sub>3</sub>, TOC in the biocrude increased to 44,500 ppm and 81.9% of the

switchgrass was solubilized in 25 minutes of steady operation (run 2). Therefore, the use of  $K_2CO_3$  showed the marked catalytic effect on switchgrass decomposition. But the use of catalyst at this temperature frequently plugged the reactor because of the rapid formation of char-like solids at the frit (reactor outlet), due to the dehydration and pyrolysis reactions favored at the high temperature along with the catalytic effect of  $K_2CO_3$ . Therefore, subsequent studies were conducted at less severe conditions, i.e. at 235°C and 13.8 MPa.

Figure 5.6 shows the TOC profile in the aqueous phase with steady operation time for the studies conducted at 235°C with liquid flow rate 1.5 ml/min (runs 3 and 4).

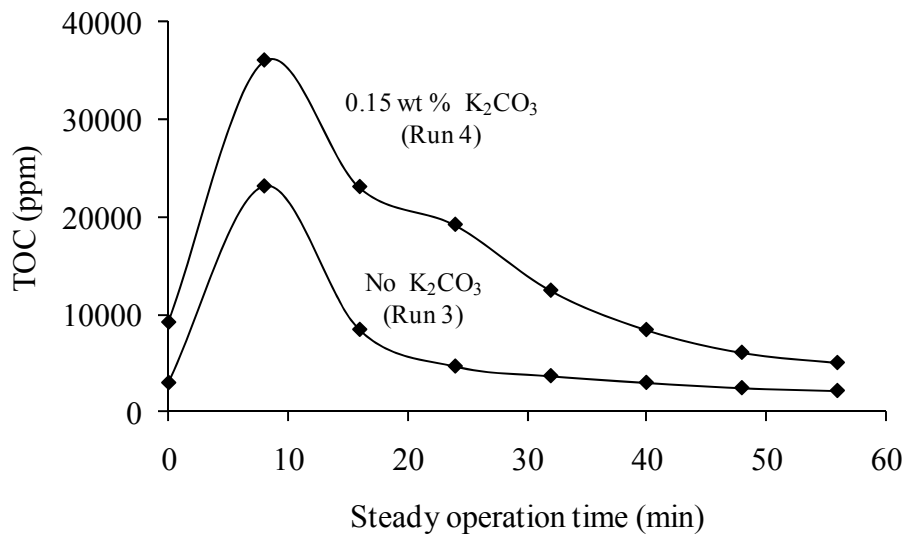


Figure 5.6 Total organic content (TOC) of aqueous phase versus steady operation time.

The rate of decomposition of switchgrass increased significantly with the use of 0.15 wt% of  $K_2CO_3$  (run 4) where the maximum TOC value in aqueous phase, observed within 10 minutes of reaction time, was increased by more than 55%. It was observed that the TOC profile in the followed a bell shaped curve. TOC started increasing rapidly in the initial 10 min of the steady operation and then decreased with the depletion of

switchgrass in the reactor. Run 1-4 experiments were either conducted at higher temperature 260°C or for a very long steady operation time. These experiments provided the basis for optimizing the parameters based on the switchgrass conversion (%wt loss) and operational difficulties at higher temperature in flow reactor. To investigate further for the rate of solubilization of switchgrass at 235°C in presence of 0.15 wt% K<sub>2</sub>CO<sub>3</sub>, separate experiments were conducted for the 5, 10 and 20 min of steady operation (runs 5-8). Figure 5.7 shows the percentage weight loss of switchgrass with steady operation time in subcritical water in the presence of K<sub>2</sub>CO<sub>3</sub> for runs 6, 7, and 8.

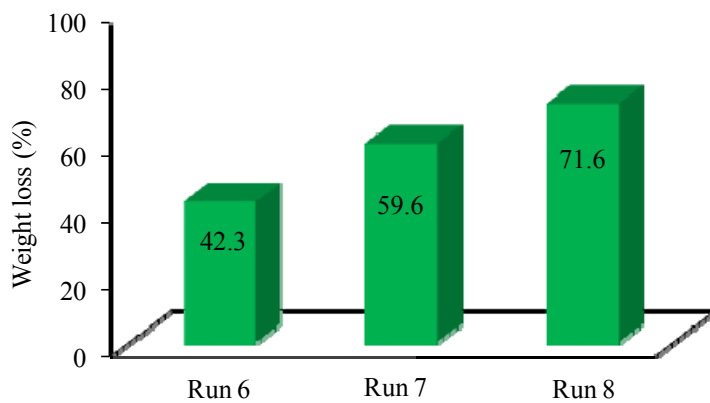


Figure 5.7 Conversion of switchgrass (weight loss) for runs 6, 7, and 8.

The weight loss increased steadily and 71.6% of the switchgrass was solubilized after 20 minutes of steady operation in run 8. Triplicates of run 8 were conducted to confirm the reproducibility of the results and the average value of weight loss (run 8) is shown in Table 5.2; the relative standard deviation of in weight loss was 5.3%. Aqueous phase and solid precipitates from runs 5-8 were separated to determine the biocrude yield. Table 5.3 shows the yields of biocrude from switchgrass conversion for the runs 5-8 based on the organic carbon in liquid product and solid precipitate. More than 50 wt%

(run 8) of carbon present in switchgrass could be converted to biocrude in the presence of  $K_2CO_3$  at 235°C.

Table 5.3 Biocrude yield from switchgrass conversion (wt%, carbon basis).

Run no.	Aqueous	Solid	Biocrude
	Phase	Precipitate*	yield
	(1)	(2)	(1) + (2)
Run 5	31.8	7.2	39.0
Run 6	31.4	16.4	47.8
Run 7	32.4	14.6	47.0
Run 8	36.9	14.2	51.1

\* Carbon in solid precipitate was considered as 66.67 wt%.

Cheng et al.'s study on switchgrass conversion in subcritical water using a batch apparatus showed that percentage weight loss of switchgrass based on initial mass varied between 41.3 - 54.8 wt% at 250°C depending upon the reaction time (1-60 s). Conversion increased with temperature to 64.6 - 78.9 wt% at 300°C.<sup>32</sup> The results of the different products as per the Figure 5.4 products separation scheme follow.

*Aqueous Phase (Product 1):* The pH of the aqueous phase ranged from 3 to 5 throughout the study depending on the use of  $K_2CO_3$ , and the liquid product appeared dark in color. Table 5.3 shows the percentage of carbon in switchgrass converted to water soluble compounds (aqueous phase). On the basis of carbon balance, 31.8 wt% of switchgrass (run 5) was converted to aqueous phase in the absence of  $K_2CO_3$ . With the use of  $K_2CO_3$ , switchgrass decomposition to water-soluble products increased to 36.9 wt% (run 8).

Similar effect was observed, when steady operation at 235°C was increased from 5 to 20 min in the presence of K<sub>2</sub>CO<sub>3</sub>. The TOC value in aqueous phase during steady operation reaches to nearly 4 wt% (equivalent to 10 wt% of glucose solution) in the presence of 0.15 wt% of K<sub>2</sub>CO<sub>3</sub>. Continuous liquefaction of biomass in subcritical water at large scale, where progressive cavity pumps can be used for feeding the biomass slurry continuously may provide even higher carbon concentration in aqueous phase. The aqueous phase from run 8 collected at steady operation was analyzed for the sugar compounds and organic acids by HPLC. Figure 5.8 shows the composition analysis of aqueous phase.

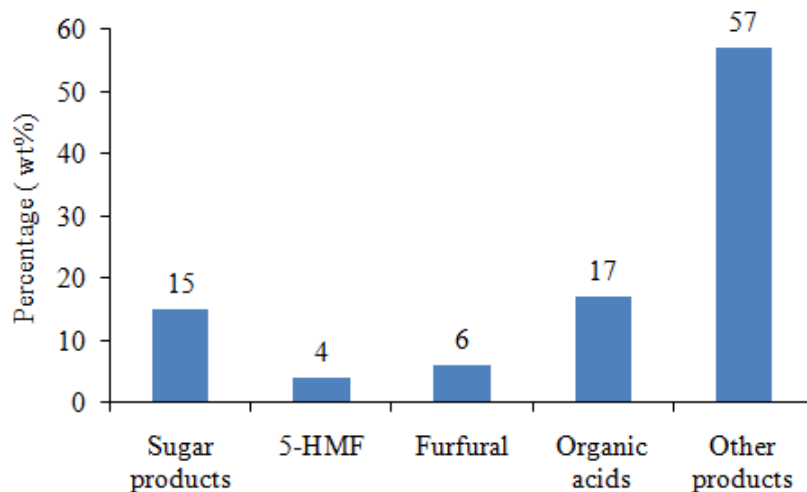


Figure 5.8 Composition of aqueous phase from run 8 by HPLC analysis.

The total oligomers and monomers of five carbon and six carbon sugars were 15 wt%. More than 25 wt% of the compounds was composed of sugar degradation products (5-hydroxymethyl-2-furaldehyde (5-HMF), and furfural) and organic acids (lactic, formic, and acetic acids). GC-MS analysis was conducted for identifying the products

which could not be identified by HPLC analysis. Table 5.4 lists some of the important compounds identified with more than 85% of confidence level.

Table 5.4 Identified compounds in biocrude from run 8 by GC-MS analysis (> 85% of confidence level).

No.	GC Retention time (minutes)	Compound	Area (%)	Quality (%)
1	9.0	Furfural	10.5	86
2	21.0	1,2-benzenediol	3.8	94
3	21.6	2,3-Dihydrobenzofuran	2.6	86
4	21.9	2-Furancarboxaldehyde	30.2	94
5	24.3	2-Methoxy-4-vinylphenol	2.3	93
6	24.9	1,4-Benzenediol, 2-methyl-	2.1	96
7	25.3	Phenol, 2,6-dimethoxy-	1.5	96
8	25.4	Benzaldehyde, 4-hydroxy-	1.4	95
9	26.5	Vanillin	3.0	97
10	29.7	Homovanillyl alcohol	1.0	87
11	32.6	Benzaldehyde, 4-hydroxy-3,5-dimethoxy-	1.0	91

Furfural and 2-furancarboxaldehyde showed a large peak and they contributed 10.5% and 30.2% of the peak area, respectively. Other compounds identified in GC-MS are mainly phenolics which might have been derived from the lignin depolymerization. The UV spectra of aqueous phase from runs 5 and 8 showed the strong absorption at 202 and 280 nm, which is the characteristic of lignin or lignin derivatives.<sup>35</sup>

*Solid precipitates (Product 2):* The composition analysis of the solid precipitate (run 8) indicated only 23.3 wt% of sugar components in the precipitate and majority were the lignin. XRD spectrum of solid precipitate from run 8 is compared with that of untreated switchgrass in Figure 5.9.

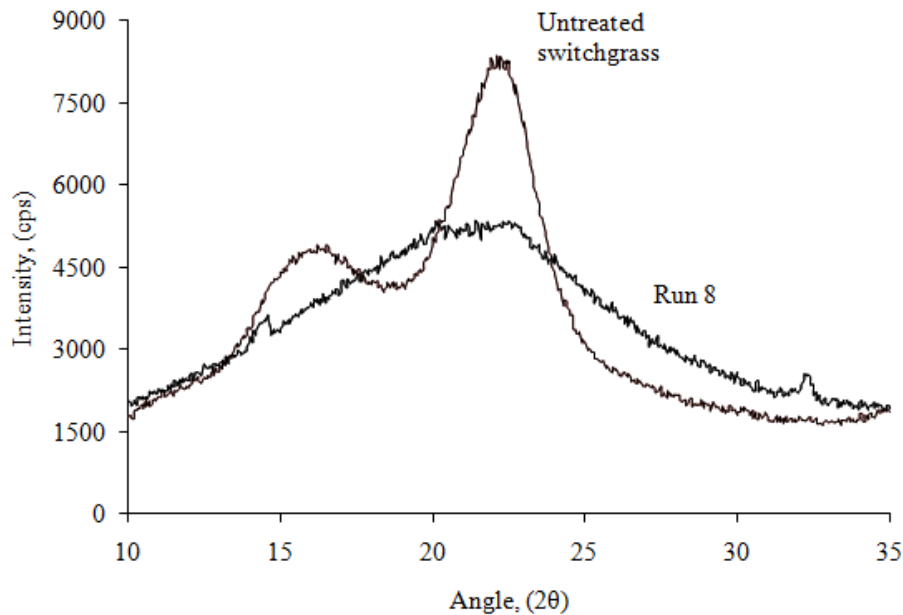


Figure 5.9 XRD patterns for untreated switchgrass and solid precipitate from run 8.

The distinct sharp crystalline cellulosic peak ( $I_{002}$ ) was absent in the solid precipitate, which confirms that it contained mainly less crystalline or amorphous components. Table 5.3 shows the amount of solid precipitates collected in runs 5-8. Since, majority of solid precipitate contained lignin compounds, carbon percentage in solid precipitate was considered to be 66.67 wt% for calculating the yield.<sup>36</sup> Solid precipitate yield was 7.2 wt% in run 5, which almost doubled (14.2 wt%) with the use of  $K_2CO_3$  in case of run 8. Heating value of the oven dried solid precipitate (runs 5 and 8) was measured by IKA C 200 calorimeter using Isoperibol measuring procedure. The HHV of solid precipitates from runs 5 and 8 were 25.1 and 26.2 MJ/kg, respectively.

Solid precipitates seem to be formed via re-condensation process and precipitated as water insoluble fine particles.

*Biochar (Product 3):* The solid residue had two distinct colors. The solids remained in the initial 15% of the reactor length appeared to be less reacted with light color similar to the original switchgrass, whereas solid collected near the outlet of the reactor was completely black and char like. The char-like solid (biochar) from runs 6 and 8 were analyzed for carbohydrates and lignin contents. As expected, biochar contained only cellulose and lignin fractions, and no hemicelluloses were detected. Biochar from runs 6 and 8 contained 33 and 32 wt% cellulose, respectively. These samples were further investigated for structural transformations.

Figure 5.10 compares x-ray diffraction patterns of biochar from runs 6 and 8 with untreated switchgrass. The untreated switchgrass has a broader peak ( $I_{002}$ ) with cellulose crystallinity of 51.6%. The peaks became sharper after the subcritical water treatment due to the increase in the crystallinity to 56.9% and 64.3% for biochar from runs 6 and 8, respectively.

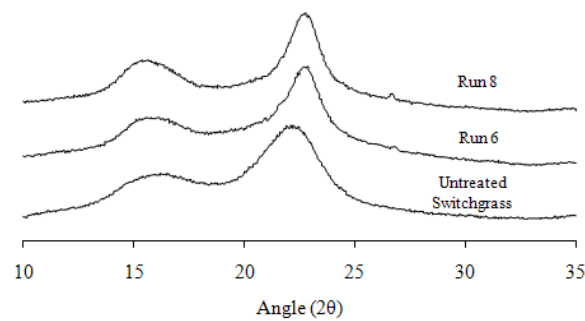


Figure 5.10 XRD pattern of untreated switchgrass and biochars from runs 6 and 8.

The FT-IR spectrum of biochar from run 8 is compared with that of untreated switchgrass in Figure 5.11. Table 5.5 shows the position of IR absorption bands and their assignments.

Table 5.5 Position of infrared absorption bands of switchgrass.<sup>32, 37, 38</sup>

Position of the band, $\text{cm}^{-1}$	Functional group
1740	C=O stretch, unconjugated (xylan)
1635	Adsorbed water
1600	Aromatic skeletal vibration plus CO stretch
1510	Benzene ring stretching (lignin)
1425	$\text{CH}_2$ shearing (cellulose), $\text{CH}_2$ bending (lignin)
1370	CH bending (cellulose, Hemicelluloses)
1330	Phenolic OH (syringical nuclei)
1270	C–O–C stretching in alkyl aromatic (lignin)
1166	C–O–C asymmetry stretching (cellulose, Hemicelluloses)
1053	C–O stretching (cellulose and Hemicelluloses)
893	$\beta$ -anomers or $\beta$ -linked (cellulose)

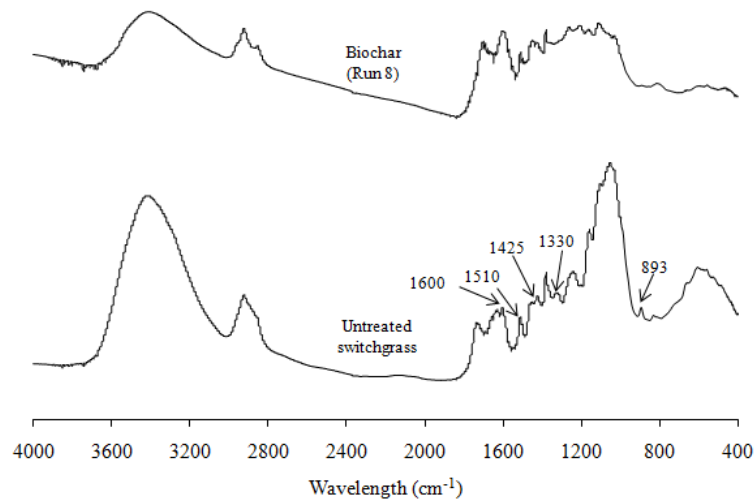


Figure 5.11 FT-IR spectra of untreated switchgrass and biochar from run 8.

The remarkable changes of absorbance peaks mainly appeared in the range of 1800 - 650 cm<sup>-1</sup>. Absorbance peak at 1740 cm<sup>-1</sup> which represents the C=O stretching vibration indicating the presence of unconjugated xylan (hemicelluloses component) is absent in biochar spectra. The peaks at 1425, 1510 and 1600 cm<sup>-1</sup> typically used for the lignin evaluation did not change. Peak at 1330 cm<sup>-1</sup> phenolic OH syringical nuclei is also absent in the biochar. In biochar, peak at 1166 cm<sup>-1</sup>, typical of C–O–C asymmetry stretching in ester group, becomes less sharp, and a sharper peak at 1270 cm<sup>-1</sup> due to guaiacyl nuclei of lignin plus CO stretch is observed. The peak at 893 cm<sup>-1</sup> is characteristic of β-anomers or β-linked glucose polymers and the peak at 1053 cm<sup>-1</sup> is C–O stretching. These peaks are present in the untreated switchgrass but are absent in biochar. Further, the absence of peak around 1635 cm<sup>-1</sup>, which indicates the adsorbed moisture, suggested that the lignocellulosic structure of switchgrass was totally broken after the treatment.<sup>32, 37, 38</sup>

SEM images of untreated switchgrass and biochar from run 8 are shown in Figure 5.12a-b. These images further confirm the disruption of lignocellulosic matrix after the treatment. Small globular particles can be seen precipitated over thin fibers.

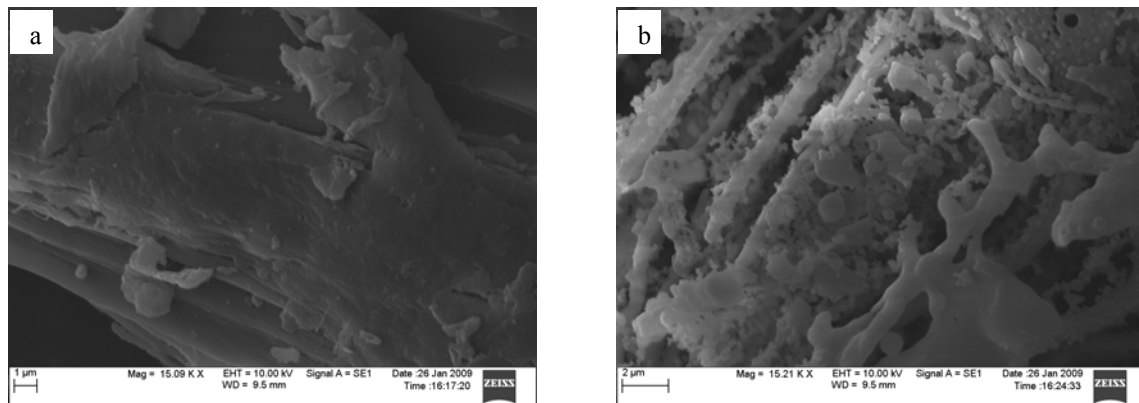


Figure 5.12 SEM image of (a) untreated switchgrass, and (b) biochar from run 8.

## 5.7 Discussion

The ionization constant of water increases with temperature and reaches a maximum near 250°C where it is about 1000-fold that at ambient temperature. Therefore, subcritical water in the 220-300°C region offers opportunities both as a benign solvent and as a self-neutralizing catalyst. Here, water acts as both a reactant and the reaction medium. Water as reactant leads to hydrolysis reactions and rapidly degrades the polymeric structure of biomass to water-soluble products. As explained earlier, switchgrass is composed mainly of hemicelluloses, cellulose and lignin, which are arranged in a complex manner within the natural feedstock. The chemical structure of these polymers is different and so is their individual reactivity as described below.

Hemicelluloses possess side groups, including acetic acid, pentoses, hexuronic acids, and deoxyhexoses, which are responsible for the solubility in water and/or alkali. These side groups reduce aggregation of hemicelluloses molecules making them more susceptible to chemical degradation than cellulose. Hemicelluloses in alkali medium undergo both physical changes and chemical reactions including swelling, dissolution, saponification, reprecipitation, peeling, and glycosidic cleavage. Most of the hemicelluloses along with considerable part of lignin are dissolved in water at 180°C. In the hydrothermal pretreatment of Kanlow switchgrass, more than 90% of hemicelluloses were solubilized at 200°C.<sup>39</sup> Low activation energy of lignin causes substantial degradation of lignin in hydrothermal medium at temperature below 200°C. Reaction proceeds through the cleavage of aryl ether linkages, fragmentation, and dissolution.<sup>14, 40</sup> Lignin depolymerization yields low molecular weight fragments having very reactive functional groups such as syringols, guaiacols, catechols and phenols.<sup>41</sup>

Cellulose, which exists as a mixture of two crystalline forms  $I_\alpha$  and  $I_\beta$  is an unbranched chain of anhydroglucose linked head to tail by  $\beta$ -glycosidic linkages.<sup>42, 43</sup> The  $\beta$ -linkages in cellulose form linear chains that are highly stable and resistant to chemical attack because of the high degree of intra- and inter-molecular hydrogen bonding. Hydrothermal degradation of cellulose is a heterogeneous and pseudo-first-order reaction for which detailed chemistry and mechanism have been proposed.<sup>14, 22, 44, 45</sup> Cellulose converts to hydrolysis products (oligomers and monomers) and the aqueous degradation products of glucose, including glycoaldehyde, fructose, anhydroglucose, 5-HMF, and furfural. The presence of alkali catalyzes degradation reactions via numerous side reactions, and comparatively lower monomer sugar (< 30%) was obtained after the treatment of cellobiose with 0.1N NaOH.<sup>46</sup>

As observed in this work,  $K_2CO_3$  acted as a catalyst in the decomposition of switchgrass during the subcritical water treatment. With the hydrolytic cleavage of glycosidic linkages, catalyst also promoted the endwise depolymerization reactions (peeling) of hemicelluloses and cellulose molecules, leading to the formation of organic acids. The autohydrolysis reactions with the generation of organic acids enhance the degradation of cellulose and lignin. Alkali in the reaction medium acts as hydrolytic reagent for the disintegration of macromolecular lignin in biomass.<sup>14</sup> In hydrothermal reaction medium, most of the hemicelluloses and part of the lignin are removed below 200°C, thus increasing the accessibility of water to cellulose molecules and remaining free lignin, which were initially associated with hemicelluloses. At the higher temperature, dehydration reactions starts competing with the hydrolysis reactions; though hydrothermal media has excess water in the reactor.<sup>8</sup> For example, experiments at 260°C

(Group I) mainly promoted the dehydration reaction and so, reactor was frequently plugged due to the presence of char-like solids at the reactor outlet.

In the case of Group II experiments, hydrolysis reactions were favored over dehydration. The presence of small amount of catalyst (0.15 wt% K<sub>2</sub>CO<sub>3</sub>), in fact, acted like a molecular scissor in breaking down the complex polymeric structure of biomass to water soluble products by hydrolysis and peeling reaction. Cellulose and hemicelluloses depolymerize to their respective monomeric sugar units and forms a homogeneous medium in hydrothermal conditions. Under the reaction condition these sugars start degrading, via several reaction pathways, to organic acids, aldehydes, furfural, phenols and also the heavy molecular weight compounds.<sup>47</sup> Lignin decomposition products have very reactive functional groups. Therefore, part of these compounds might again be cross-linked with the available organic acids and re-condense together to form high-molecular-weight, water-insoluble fragments. In fact, SEM image (Figure 12b) of biochar obtained in run 8 confirms the re-condensation process and globular particles can be seen deposited over the thin fibrous structure. Re-condensed particles over the fibers could have limited the accessibility of water molecules to the remaining cellulose. Temperatures above 200-220°C induce faster lignin solubilization, and the solubilized lignin is subjected to re-condensation because of longer reaction time.<sup>48</sup> Reaction kinetics of the hydrothermal treatment of lignin obtained from different sources was studied in detail by Zhang et al. Switchgrass residue obtained after two-stage dilute acid hydrolysis process was also used in the study. The liquid yield from the switchgrass residue treated at 374°C was 29.7 wt%.<sup>49</sup>

Due to the numerous side reactions in the presence of alkali salts, it is difficult to obtain a high sugar yield<sup>46</sup> and nearly impossible to quantify or even identify all substances formed during conversion of biomass;<sup>27, 50</sup> therefore, only key compounds are analyzed for representing the different reaction pathways. Liquid composition from run 8 sample clearly indicates that cellulose and hemicellulose fractions of switchgrass were initially converted to hydrolysis products (oligomers and monomers). Since these products are not stable at high temperature for a long residence time, the major part of these products were further degraded to the aqueous degradation products of sugars, including glycoaldehyde, fructose, anhydroglucose, 5-HMF and furfural.

Lignin is an aromatic polymer mainly built of phenylpropanoid precursors, which is a rich source of phenolic compounds. Several phenolic compounds such as 1,2 benzenediol, vanillin, and others (Table 4) were identified in the aqueous phase. The yield of phenols increases with temperature and degradation rate of phenols is slower than the other aqueous products such as 5-HMF, furfurals.<sup>51</sup> Typically, aromatic compounds are assumed to originate from lignin precursors during hydrothermal treatment of biomass. But, earlier study with model compounds such as fructose, 5-HMF, and cellulose in hydrothermal medium has shown that aromatics can also be formed from sugar compounds.<sup>52, 53</sup> The GC-MS result (run 8) showed the presence of low molecular weight compounds (C<sub>5</sub>-C<sub>9</sub>). Furfural and 2-furancarboxaldehyde formed the major components among the identified compounds. The compounds identified in aqueous products are in agreement with Cheng et al.'s study.<sup>32</sup> Most of the compounds are oxygenated hydrocarbons of five to nine carbon atoms. Carbon percentages in these compounds vary from 40% (for sugars) to 66.7% (for furfural).

Biochar from runs 6 and 8 still composed nearly 32 wt% of cellulose, which suggest that the complete hydrolysis of cellulose was not be achieved in these experiments. The cellulose crystallinity in the biochar increased mainly due the removal of amorphous portion of cellulose and some structural rearrangements after the treatments. Increased crystallinity may also reduce the accessibility of water molecules. As discussed earlier, FT-IR spectra of biochar (run 8) showed the presence of peaks used for the lignin evaluation, whereas peaks typical of polysaccharides were either absent or became weak.

## 5.8 Conclusion

Switchgrass can be effectively liquefied to produce biocrude in subcritical water at a comparatively low temperature (235°C) in a flow reactor. Biocrude is composed of aqueous phase (water-soluble compound) and solid precipitates. The aqueous phase contains oligomers and monomers of five and six carbon sugars, degradation products (5-HMF and furfural), organic acids (lactic, formic and acetic acid), 2-furancarboxaldehyde and other phenolic products containing 5 to 9 carbon atoms. Solid precipitates seem to be formed via re-condensation process and precipitated as water insoluble fine particles due to the decrease in the solubility upon cooling. A small amount of potassium carbonate can catalyze the liquefaction, which can be used to lower the severity of the reaction conditions, and to enhance the decomposition of biomass to water-soluble products. The residual solid (i.e., biochar) contained mainly lignin fractions and a small amount of cellulose. Based on the infrared spectroscopy and electron microscopy, it was confirmed that subcritical water treatment leads to a breakdown of lignocellulosic structure. Char-

like color of residue biomass is caused by partial dehydration of switchgrass even in hydrothermal medium.

### 5.9 Acknowledgment

Author is thankful for the financial supports from the National Science Foundation (grant NSF-CBET-0828269) and Alabama Center for Paper and Bioresource Engineering. In addition, the authors thank Prof. Sushil Adhikari for GC-MS analysis, Ms. Urvi Kothari for HPLC analysis, Mr. Brian Schwieker for the assembly of the apparatus, and Prof. Y.Y. Lee for fruitful discussions.

### 5.10 References

1. Perlack, R. D.; Wright, L. L.; Turhollow, A. F.; Graham, R. L.; Strokes, B. J.; Erbach, D. C., Biomass as a feedstock for a bioenergy and bioproducts industry: The technical feasibility of a billion-ton annual supply. *A Joint report sponsored by US department of energy and US department of agriculture* **2005**, 78.
2. Bransby, D. Switchgrass profile.  
<http://bioenergy.ornl.gov/papers/misc/switchgrass-profile.html>. (May 10, 2009),
3. Rinehart, L., Switchgrass as a bioenergy crop. [www.attra.ncat.org](http://www.attra.ncat.org). (May 10, 2009)
4. Tester, J. W.; Holgate, H. R.; Armellini, F. J.; Webley, P. A.; Killilea, W. R.; Hong, G. T.; Barner, H. E. In *Supercritical water oxidation technology – process development and fundamental research*, In Emerging technologies in hazardous waste management III, Washington D.C., 1993; American Chemical Society: Washington D.C., 1993; pp 35-76.

5. Franck, E. U., Fluids at high pressures and temperatures. *Pure Appl. Chem.* **1987**, 59, (1), 25-34.
6. Miyoshia, H.; Chena, D.; AkaiT., A novel process utilizing subcritical water to recycle soda-lime-silicate glass. *Journal of Non-Crystalline Solids* **2004**, 337, ( 3), 280-282.
7. Savage, P. E., Organic chemical reactions in supercritical water. *Chemical Reviews* **1999**, 99, 603-621.
8. Patrick, H. R.; Griffith, K.; Liotta, C. L.; Eckert, C. A., Near critical water: A benign medium for catalytic reactions. *Ind. Eng. Chem. Res.* **2001**, 40, 6063-6067.
9. Peterson, A. A.; Vogel, F.; Lachance, R. P.; Froling, M.; Michael Jerry Antal, J.; Tester, J. W., Thermochemical biofuel production in hydrothermal media:A review of sub- and supercritical water technologies. *Energy and Environmental Science* **2008**, 1, 32-65.
10. Chornet, E.; Overend, R. P., Biomass liquefaction: An overview. In *Fundamentals of Thermochemical Biomass Conversion*, Overend, R. P.; Milne, T. A.; Mudge, L. K., Eds. Elsevier Applied Science: New York, 1985; pp 967-1002.
11. Huber, G. W.; Cheda, J. N.; Barrett, C. J.; Dumesic, J. A., Production of liquid alkanes by aqueous processing of biomass derived carbohydrates. *Science* **2005**, 308, 1446-1450.
12. Valenzuela, M. B.; Jones, C. W.; Agrawal, P. K., Batch aqueous reforming of woody biomass. *Energy & Fuels* **2006**, 20, 1744-1752.
13. Byrd, A. J.; Pant, K. K.; Gupta, R. B., Hydrogen production from glucose using Ru/Al<sub>2</sub>O<sub>3</sub> catalyst in supercritical water. *Ind. Eng. Chem. Res.* **2007**, 46, 3574-3579.

14. Bobleter, O., Hydrothermal degradation of polymers derived from plants. *Prog. Polym. Sci.* **1994**, 19, 797–841.
15. Bobleter, O.; Niesner, R.; Rohr, M., The hydrothermal degradation of cellulosic matter to sugars and their fermentative conversion to protein. *J. Appl. Polym. Sci.* **1976**, 20, 2083.
16. Bobleter, O.; Bonn, G.; Concin, R., Hydrothermolysis of biomass-production of raw material for alcohol fermentation and other motor fuels. *Alt. Energy Sour.* **1983**, 3, 323-332.
17. Minowa, T.; Zhen, F.; Ogi, T., Cellulose decomposition in hot-compressed water with alkali or nickel catalyst. *J. Supercritical Fluids* **1997**, 13, 253-259.
18. Minowa, T.; Zhen, F.; Ogi, T.; Varhegyi, G., Decomposition of cellulose and glucose in hot-compressed water under catalyst-free conditions. *J. Chem. Eng. Japan* **1998**, 31, 131-134.
19. Sasaki, M.; Fang, Z.; Fukushima, Y. N.; Adschiri, T.; Arai, K., Dissolution and hydrolysis of cellulose in subcritical and supercritical water. *Ind. Eng. Chem. Res.* **2000**, 39, 2883-2890.
20. Sasaki, M.; Kabyemela, B.; Malaluan, R.; Hirose, S.; N.Takeda; Adschiri, T.; Arai, K., Cellulose hydrolysis in subcritical and supercritical water. *J. Supercritical Fluids* **1998**, 13, 261-268.
21. Kumar, S.; Gupta, R. B., Hydrolysis of Microcrystalline Cellulose in Subcritical and Supercritical Water in a Continuous Flow Reactor. *Industrial and Engineering Chemistry Research* **2008**, 47, (23), 9321-9329.

22. Mok, W. S.; Antal, M. J., Uncatalyzed solvolysis of whole biomass hemicellulose by hot compressed liquid water. *Ind. Eng. Chem. Res.* **1992**, 31, 1157-1161.
23. Saisu, M.; Sato, T.; Watanabe, M.; Adschiri, T.; Arai, K., Conversion of lignin with supercritical water-phenol mixtures. *Energy & Fuels* **2003**, 17, 922-928.
24. Wahyudiono; Kanetake, T.; Sasaki, M.; Goto, M., Decomposition of a lignin model compound under hydrothermal conditions. *Chem. Eng. Technol* **2007**, 30, (8), 1113-1122.
25. O'Sullivan, A. C., Cellulose: the structure slowly unravels. *Cellulose* **1997**, 4, (3), 173-207.
26. Schacht, C.; Zetzl, C.; Brunner, G., From plant materials to ethanol by means of supercritical fluid technology. *Journal of Supercritical Fluids* **2008**, 46s (3), 299-321.
27. Behrendt, F.; Neubauer, Y.; Oevermann, M.; Wilmes, B.; Zobel, N., Direct liquefaction of biomass. *Chem. Eng. Technol* **2008**, 31, (5), 667-677.
28. Karagoz, S.; Bhaskar, T.; Muto, A.; Sakata, Y.; Uddin, M. A., Low temperature hydrothermal treatment of biomass: Effect of reaction parameters on products and boiling point distributions. *Energy & Fuels* **2004**, 18, 234-241.
29. Karagoz, S.; Bhaskar, T.; Muto, A.; Sakata, Y., Effect of Rb and Cs carbonates for production of phenols from liquefaction of wood biomass. *Fuel* **2004**, 83, 2293-2299.
30. Karagoz, S.; Bhaskar, T.; Muto, A.; Sakata, Y., Hydrothermal upgrading of biomass: Effect of  $K_2CO_3$  concentration and biomass/water ratio on product distribution. *Bioresource Technology* **2006**, 97, 90-98.

31. Midgett, J. S. Assessing a hydrothermal liquefaction processing using biomass feedstocks. Louisiana State University And Agricultural and Mechanical College, Baton Rouge, 2005.
32. Cheng, L.; Ye, X. P.; He, R.; Liu, S., Investigation of rapid conversion of switchgrass in subcritical water. *Fuel Processing Technology* **2009**, *90*, 301-311.
33. Sluiter, A.; Hammes, B.; Ruiz, R.; Scarlata, C.; Sluiter, J.; Templeton, D., Determination of sugars, byproducts, and degradation products in liquid fraction process samples. *NREL Biomass Program, Laboratory Analytical Procedure (LAP)* **2006**.
34. Segal, L.; Creely, J. J.; Martin, A. E.; Conrad, C. M., An empirical method for estimating the degree of crystallinity of native cellulose using the X-ray diffractometer. *Textile Res. J.* **1959**, *29*, 786-794.
35. Ando, H.; Sakaki, T.; Kokusho, T.; Shibata, M.; Uemura, Y.; Hatake, Y., Decomposition behaviour of plant biomass in hot-compressed water. *Ind. Eng. Chem. Res.* **2000**, *39*, 3688-3693.
36. <http://www.nrel.gov/biomass/glossary.html#L>.
37. Baeza, J.; Freer, J., Chemical characterization of wood and its components. In *Wood and cellulosic chemistry*, second ed.; Hon, D. N.-S.; Shiraishi, N., Eds. Marcel Dekker, Inc.: New York. Basel, 2001; pp 275-384.
38. Kobayashi, N.; Okada, N.; Hirakawa, A.; Sato, T.; J.Kobayashi; Hatano, S.; Itaya, Y.; Mori, S., Characteristics of solid residues obtained from hot-compressed-water treatment of woody biomass. *Industrial and Engineering Chemistry Research* **2009**, *48*, 373-379.

39. Suryawati, L.; Wilkins, M. R.; Bellmer, D. D.; Huhnke, R. A.; Maness, N. O.; Banat, I. M., Simultaneous saccharification and fermentation of Kanlow Switchgrass pretreated by hydrothermolysis using Kluyveromyces marxianus IMB4. *Biotechnology and Bioengineering* **2008**, 101, (5), 894-902.
40. Lai, Y.-Z., Chemical Degradation. In *Wood and Cellulosic Chemistry*, David N.-S. Hon, N. S., Ed. Marcel Dekker, Inc.: New York . Basel, 2001; pp 443-512.
41. Fang, Z.; Sato, T.; Jr., R. L. S.; Inomata, H.; Arai, K.; Kozinski, J. A., Reaction chemistry and phase behaviour of lignin in high-temperature and super critical water. *Bioresource Technology* **2008**, 99, 3424-3430.
42. Jarvis, M., Chemistry: Cellulose stacks up. *Nature* **2003**, 426, 611-612
43. Atalla, R. H.; Vanderhart, D. L., Native Cellulose: A Composite of Two Distinct Crystalline Forms. *Science* **1984**, 223, (4633), 283 - 285.
44. Schwald, W.; Bobleter, O., Hydrothermolysis of cellulose under static and dynamic conditions at high temperatures. . *J. Carbohydr. Chem.* **1989**, 8, (4), 565-578.
45. Mok, W. S. L.; M.J., A. J.; Varhegyi, G., Productive and parasitic pathways in dilute-acid-catalyzed hydrolysis of cellulose. *Ind. Eng. Chem. Res.* **1992**, 31, 94-100.
46. Bobleter, O., Hydrothermal degradation and fractionation of saccharides and polysaccharides In *Polysaccharides: Structural diversity and functional versatility*, Dumitriu, S., Ed. Marcel Dekker: 2005; pp 893-936.
47. Kruse, A.; Gawlik, A., Biomass conversion in water at 330-410 °C and 30-50 MPa: Identification of key compounds for indicating different chemical reaction pathways. . *Ind. Eng. Chem. Res.* **2003**, 42, 267-269.

48. Kim, T. H.; Lee, Y. Y., Pretreatment and fractionation of corn stover by ammonia recycle percolation process *Bioresource Technology* **2005**, 96, (18), 2007-2013.
49. Zhang, B.; Huang, H.-J.; Ramaswamy, S., Reaction Kinetics of the hydrothermal treatment of lignin. *Appl Biochem Biotechnol* **2008**, 147, 119-131.
50. Loppinet-Serani, A.; Aymonier, C.; Cansell, F., Current and foreseeable applications of supercritical water for energy and the environment. *ChemSusChem* **2008**, 1, 486-503.
51. Bühler, W.; Dinjus, E.; Ederer, H. J.; Kruse, A.; Mas, C., Ionic reactions and pyrolysis of glycerol as competing reaction pathways in near- and supercritical water. *Journal of Supercritical Fluids* **2002**, 22, 37–53.
52. Luijkx, G. C. A.; Rantwijk, F. V.; Bekkum, H. V., Hydrothermal formation of 1,2,4-benzenetriol from 5-hydroxymethyl-2-furaldehyde and D-fructose. *Carbohydrate Research* **1993**, 242, 131-139.
53. Nelson, D. A.; Molton, P. M.; Russell, J. A.; Hallen, R. T., Application of direct thermal liquefaction for the conversion of cellulosic biomass. *Ind. Eng. Chem. Prod. Res. Dev.* **1984**, 23, (3), 471-475.

## 6. Production of Biochar from Switchgrass by Hydrothermal Carbonization

### 6.1 Abstract

Hydrothermal carbonization (HTC), a traditional but recently revived process using hot compressed water, is a promising route for converting biomass to biochar. HTC of switchgrass, a major energy crop, is studied to produce the high energy density biochar in a batch reactor at 200-280 °C. The effects of temperature, residence time, and pressure are examined. The obtained biochar is characterized for molecular structure by FTIR, XRD, and SEM analyses. The results indicate that temperature plays an important role in the conversion of switchgrass to biochar. At the higher temperatures, the lignocellulosic crosslink structure of switchgrass is broken and biochar having a high energy density is obtained. Also, the micro-crystalline structure of cellulosic components present in switchgrass is destroyed and biochar contained mainly amorphous fractions as confirmed by the XRD spectra. The liquid fraction recovered after the HTC of switchgrass, termed biocrude, was further subjected to HTC in the temperature range of 200-280°C to recover soluble carbon fractions. The sugar and its degradation products present in biocrude precipitated as uniform carbon rich microspheres (biotar particles) as a result of polycondensation and dehydration reactions. The results demonstrate that the HTC process can provide a promising route for high energy density (28 MJ/kg) solid fuel and carbonaceous functional materials for use in a variety of applications.

## 6.2 Introduction

Depletion of fossil fuels and environmental concerns are prompting search for alternative and renewable energy resources. Various options include wind, hydro/oceanic, geothermal, solar, and biomass energies, among which biomass is the only renewable source capable of directly producing solid, liquid and gaseous fuels. Additional advantage of biomass utilization is in its wider distribution in the world which may eliminate the regional dependence for the energy sources. Biomass is the CO<sub>2</sub> neutral, as during the growth and utilization process of biomass, same amount of carbon dioxide and other forms of carbon is absorbed and released, respectively. Hence, the concentration of carbon dioxide in the atmosphere theoretically remains constant in this cycle.<sup>1</sup> The conversion of biomass to biofuels can be realized in several pathways such as pyrolysis, gasification, fermentation and hydrothermal reaction.<sup>2</sup> Hydrogen,<sup>3</sup> ethanol,<sup>4</sup> organic acid,<sup>5-7</sup> biofuel,<sup>8</sup> and biochar<sup>9</sup> are produced in different processes. Recently, the research attention was focused on the conversion of biomass to biochar which has higher heating value (HHV) typically over 28 kJ/g and is richer in carbon content as compared to raw biomass. Biochar is defined here as the non-liquefied carbonaceous solid product having a high energy density resulting from the thermal treatment of biomass. Table 6.1 compares some of the advantages of biochar as solid fuels to biomass.

Table 6.1 Comparison of biomass and biochar as solid fuel.

Biomass	Biochar
High moisture retention	Low moisture retention and easily dried
Low heating value, so high transportation cost	High heating value, so less (\$)/MJ cost during transportation
Perishable on storage	Not perishable, and can be stored longer
Fibrous and so, difficult material handling	Friable, easier to compact and handle
Poor compatibility with coal for co-firing	Better compatibility with coal for co-firing

In nature, coal is formed from plant material undergoing heat and pressure treatment over millions of years. The acceleration of coalification of biomass by a factor of  $10^6$ - $10^9$  in hydrothermal medium under milder process conditions can be a considerable and technically-attractive alternative for biochar production.<sup>10</sup> Essentially, all forms of biomass can be converted to biochar. Forest thinning, herbaceous grasses, crop residues, manure, and paper sludge are some of the potentially attractive feedstocks.

The enhanced transportation and solubilization properties of sub- and supercritical water (hydrothermal medium) play an important role in the transformation of biomass to high energy density fuels and functional materials.<sup>11</sup> Here, water acts as reactant as well as reaction medium which helps in performing hydrolysis, depolymerization, dehydration and decarboxylation reactions. The proton-catalyzed mechanism, direct nucleophilic attack mechanism, hydroxide ion catalyzed mechanism, and the radical mechanism play important roles in the conversion of biomass in hydrothermal medium.<sup>12, 13</sup> Under the umbrella of hydrothermal process, the conversion of a variety of biomass to chemicals, including organic monomer, biofuel, hydrogen, and biochar have been studied widely. Through hydrothermal carbonization, a carbon-rich black solid as insoluble product is obtained from biomass in 180–350°C range.<sup>10, 14</sup>

The earliest research focused on the analyzing the changes in O/C and H/C atomic ratio to understand the chemical transformations taking place during HTC.<sup>15</sup> For example, Marta et al. studied the hydrothermal carbonization of three different saccharides (glucose, sucrose, and starch) at temperatures ranging from 170 to 240 °C. The result showed that a carbon-rich solid product made up of uniform spherical micrometer-sized particles of diameter 0.4–6 mm range could be synthesized by

modifying the reaction conditions. The formation of the carbon-rich solid through the HTC of saccharides was the consequence of dehydration, condensation, polymerization and aromatization reactions. In a recent study, the same group of researchers used cellulose as starting material and successfully established that highly functionalized carbonaceous materials can be produced by HTC from cellulose in the range of 220 to 250°C.<sup>16</sup> The formation of this material follows essentially the path of a dehydration process, similar to that previously observed for the hydrothermal transformation of saccharides such as glucose, sucrose or starch. In another recent study, Titirici et al. compared hydrothermal carbons synthesized from diverse monomeric sugars and their derivatives (5-hydroxymethyl-furfural-1-aldehyde (HMF) and furfural) under hydrothermal conditions at 180°C with respect to their chemical structures. The results showed that type of sugars has an effect on the structure of carbon rich solids.<sup>17</sup> Majority of the research studies have utilized monomeric sugars instead of real biomass as model compounds for understanding the reaction mechanism and the structural differences in solids formed from the diverse sugar sources in HTC process.

The traditional method for biochar production from biomass sources is slow pyrolysis, where dry biomass is used for the purpose in the range of 500 to 800°C. Antal Jr. and coworkers has developed another method for charcoal production which is named as flash carbonization. The process is conducted at elevated pressure by the ignition and control of a flash fire within a packed bed of biomass.<sup>18</sup> Considering the relatively high energy consumption needed in the pyrolysis process, hydrothermal carbonization process which is typically conducted in subcritical water below 300°C might be an economical

and efficient option for biochar production. The process is particularly important since it can utilize the wet biomass.

In this work our primary interest is the production of carbonaceous functional materials and higher energy density solid fuels. Our work relates to a process for the hydrothermal carbonization of biomass in shorter residence time (order of minutes to few hours) and moderate temperature condition. The effect of reaction temperature and pressure in the range of 200-280°C and 2-8 MPa, respectively are studied for understanding the carbonization of an energy crop switchgrass. The liquid product (biocrude) from HTC process is a complex mixture organic compounds soluble in water,<sup>2,19</sup> mainly resulting from the decomposition sugars and acid soluble lignin. In this work, biocrude is also investigated as a source for producing biotar particles (a carbon rich solid) in hydrothermal medium, by polymerization of the organic compounds in biocrude. The FTIR, XRD and SEM analytical techniques were used to characterize the products and to understand the transformation process during HTC. The higher heating value (HHV) of the products are also evaluated and discussed.

### **6.3 Experimental Section**

*Materials:* Auburn grown switchgrass (chopped to 5-10 mm long size) having moisture content of 7-8 wt% was used for the study. The main physical and chemical properties of the switchgrass are listed in the Table 6.2. De-ionized water was used for conducting the experiments.

Table 6.2 Main physical and chemical properties of switchgrass.

Properties	Mass
Moisture (%)	2.6
Lignin (%)	23.5
Cellulose (%)	39.5
Hemicellulose (%)	26.7
Carbon (%)	44.6
HHV(kJ/g)	17.1

*Apparatus and procedure:* Hydrothermal carbonization of switchgrass was carried out in a batch apparatus (Figure 6.1). The reactor was a high pressure stainless steel tube having an internal volume of 65.0 cm<sup>3</sup> (internal diameter 14.5 mm).

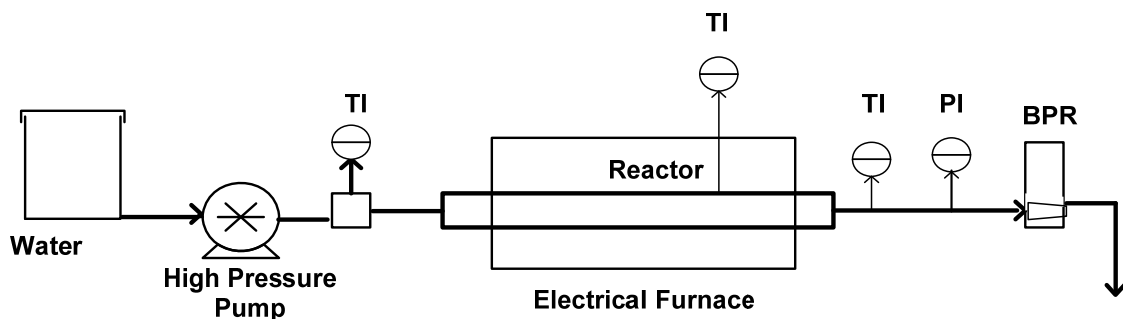


Figure 6.1 Apparatus for HTC process.

The study was conducted for the temperature range of 200-280°C and reaction times of 0.5-4.0 h as described in Table 3. To maintain the water in liquid phase during the reaction, water fill was fixed at 75% of reactor volume. In a typical run, the desired amount of switchgrass and water was charged into the reactor and sealed. The reactor was heated up to a reaction temperature in an electric furnace. After the desired residence time, the reactor was rapidly cooled to quench the reaction. The residence time was defined as the time at reaction temperature excluding preheating and cooling time. The

preheating and cooling time typically varied between 10-15 minutes. To study the effect of pressure on biochar formation at constant temperature, reactor pressure was increased to desired pressure by pumping water into the reactor. Similarly, the reactor was filled with biocrude obtained after the HTC process of switchgrass for experiments related to biotar particles production.

The solid products (biochar and biotar) recovered after the HTC processes were washed with deionized water and oven dried. The biochar samples were characterized for molecular structure by infra-red spectroscopy (FTIR), X-ray diffraction (XRD) and scanning electron microscopy (SEM) techniques. The higher heating value of biochar was analyzed using a calorimeter. Liquid products were analyzed for total organic carbon (TOC) content and for the organic compounds by high performance liquid chromatography (HPLC) before subjecting to the second stage HTC process for producing biotar particles.

*Product Separation Scheme:* Figure 6.2 shows the two stage process and the product separation scheme. In the first stage, biochar is produced after HTC process using switchgrass as starting material. The biotar particles are recovered during the second stage HTC process where biocrude from the first stage HTC is used as starting material. Gaseous products which were appreciably low in both the stages were vented out.

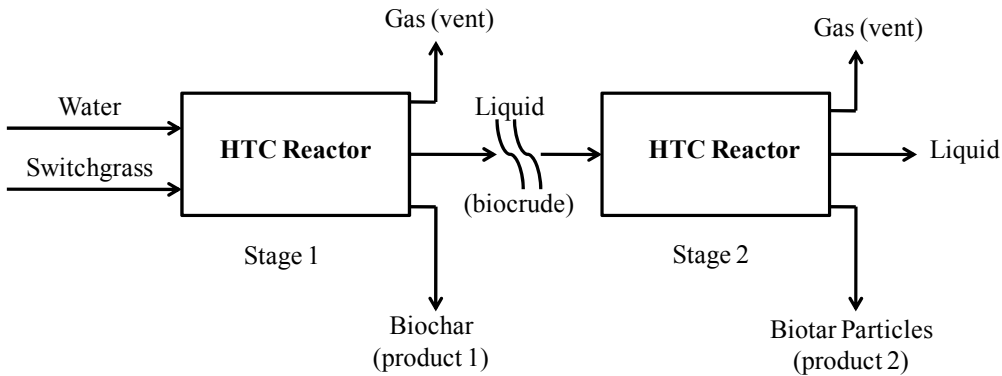


Figure 6.2 Products separation scheme in two stage HTC process.

#### 6.4 Product Characterization

*SEM analysis:* The biochar samples were prepared onto adhesive carbon tape on an aluminum stub followed by sputter coating of gold. Surface morphology of the sample was studied using an environmental scanning electron microscopy system (Zeiss EVO 50).

*XRD analysis:* Rigaku Miniflex powder X-ray diffractometer equipped with a Cu  $\text{K}\alpha_1$  radiation source at 30 kV voltages, 15 mA current and a miniflex goniometer was used for the XRD analysis. Diffraction patterns were collected in the  $2\theta$  range of 10-35° at a scan speed of 1°/min. and step size of 0.01°.

*FTIR analysis:* Infrared spectra (4000–400  $\text{cm}^{-1}$ ) were recorded by a Nicolet IR100 FTIR spectrometer which was equipped with a TGS/PE detector and a silicon beam splitter with 1  $\text{cm}^{-1}$  resolution. The sample discs were prepared by mixing oven dried (at 105°C) sample with spectroscopy grade KBr in an agate morter.

*HHV analysis:* The higher heating value of sample was determined by IKA-C200 Calorimeter. The samples were dried (at 105°C) and compressed as small pellet for HHV analysis.

*HPLC analysis:* Liquid analysis was performed with an HPLC system equipped with a refractive index detector. Two columns were used in the HPLC analysis. Monomers and oligomers of sugars were determined by Bio-Rad Aminex HPX-87P (lead based) column, water mobile phase, and column temperature of 85°C. The other column was Bio-Rad Aminex HPX-87H column with IR detector, to identify polar compounds with a polar functional group (-OH, -C=O, -COOH) and separate more intermediate products expect sugars. The column was held at 65°C. The element containing 0.01mol/L H<sub>2</sub>SO<sub>4</sub> was applied at a flow rate of 1.0 ml/min. The peak identification was accomplished by comparison of sample peak retention times with those of standard solutions of pure compounds.

*TOC analysis:* The total organic carbon concentration (TOC) in clear liquid products, obtained after centrifugation at 3600 rpm, was measured using a TOC analyzer (Shimadzu TOC 5000A).

## 6.5 Results and Discussions

Table 6.3 shows the details of the experiment conditions, biochar yield, and HHV of biochar.

Table 6.3 Experiment summary and results.

Run	Temperature (°C)	Reaction Time (h)	Pressure (MPa)	Biochar Yield (wt%)	Biochar HHV (kJ/g)
1	200	2.0	17.2	59.8	21.5
2	200	2.0	27.6	66.7	20.9
3	200	4.0	17.2	63.2	21.5
4	200	4.0	27.6	60.6	21.8
5	230	2.0	17.2	48.9	26.9
6	230	2.0	27.6	45.6	24.3
7	230	4.0	17.2	52.8	25.7
8	230	4.0	27.6	49.1	25.4
9	200	4.0	2.4	66.4	20.3
10	230	4.0	4.1	37.8	23.5
11	260	4.0	6.5	28.4	25.9
12	280	4.0	8.3	19.0	28.1
13	280	0.5	7.2	20.7	24.7
14	280	1.0	7.2	19.2	28.3

In general, biochar yield (wt%) decreased with increase in temperature, whereas HHV of biochar showed opposite trend. Qualitatively, the biochar produced at higher temperatures retains less moisture and is more fragile and could easily be powdered just by hand. The results are discussed in following sections:

***Effect of residence time and pressure:*** Experiments at the temperature 200°C and 230°C were conducted to study the effect of residence time and pressure on the carbonization of switchgrass. The residence time and pressure varied were changed from 2 to 4 h and 17.6 and 27.2 MPa at these temperatures. Figures 6.3 and 6.4 show the yield (wt%) and HHV of biochar.

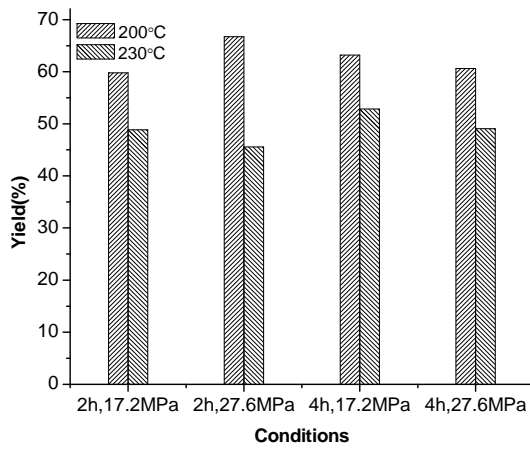


Figure 6.3 Yield (wt%) of obtained biochar at 200°C and 230°C.

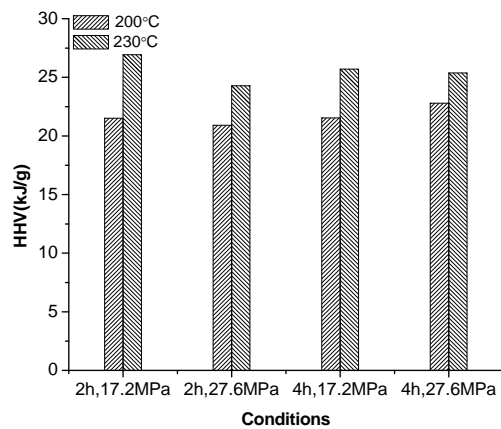


Figure 6.4 HHV of obtained biochar at 200°C and 230°C.

The results of runs 2 and 4 (Table 6.3) showed that at constant pressure and temperature, the yield of biochar decreased from 66.7 to 60.6 wt% with residence time whereas heating value of biochar increased from 20.9 to 21.8 kJ/g. Increase in the temperature to 230°C produced higher HHV of biochar, the range of 24.3-26.9 kJ/kg (run 5-8). As expected, the yield of biochar showed the descending trend with temperature. But even with 4 h of residence time at 230°C, the HHV of biochar was just comparable to lignin's higher heating value (24-26 kJ/g). These results confirm that lignocellulosic

structure of switchgrass was not decomposed at 200-230°C range and the increase in heating value may be mainly attributed to the removal of amorphous components (hemicelluloses and part of lignin) from switchgrass. It can be concluded that higher residence time though favored the carbonization process; the rate of carbonization was still slower due to the moderate temperature condition.

The set of experiments represented by run 9, 3, and 4 were conducted to investigate the effect of pressure in the range of 2.4-27.6 MPa at 200°C and at 4 h residence time. There is gradual decrease in biochar yield, from 66.4% (run 9) to 60.6 wt% (run 4). The heating value of biochar increased marginally with pressure from 20.3 kJ/g (run 9) to 21.8 kJ/g (run 4). It is important to note that even after more than ten fold rise in pressure, the increase in heating value was less than 10% when comparing run 9 to run 4. Even at 230°C (run 10), the HHV of biochar obtained under autogeneous pressure was 23.5 kJ/g which is slightly lower than the data under controlled pressure.

The increased pressure of the reaction medium keeps water in liquid phase and influences mainly the density dependent physical properties of water.<sup>20</sup> At 200°C, the density of water which is 0.86 g/ml at 2.4 MPa increases slightly with pressure to 0.88 g/ml at 27.6 MPa (source: National Institute of Standards and Technology). Therefore, effect of pressure in this temperature range is not pronounced except it helps in improving the contact between biomass components and water molecules.

Switchgrass contains more than 40 wt% oxygen. The major objective of HTC is the deoxygenation of biomass. The removal of oxygen can be achieved most readily by dehydration reaction, which removes oxygen in the form of water, and by decarboxylation, which removes oxygen in the form of carbon dioxide.<sup>21</sup> Hence, higher

reaction temperature should favor HTC more than the increased residence time or pressure.

**Effect of temperature:** To examine the effect of temperature on biochar production from switchgrass further experiments at the residence times 4.0 h (runs 9-12) were performed. The effects of temperature from 200 to 280°C were investigated and the results are shown in the Figures 6.5 and 6.6.

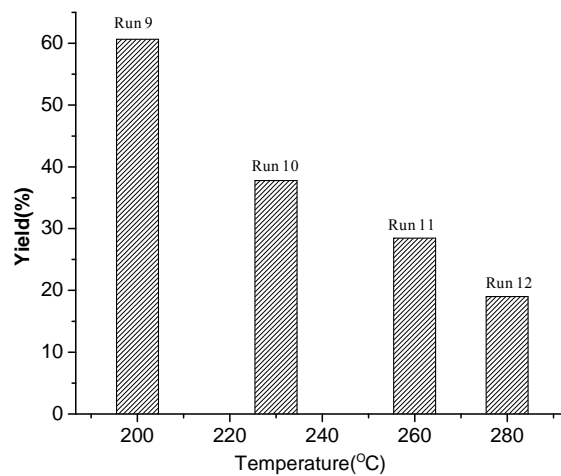


Figure 6.5 Yield (wt%) of obtained biochar at 200-280°C.

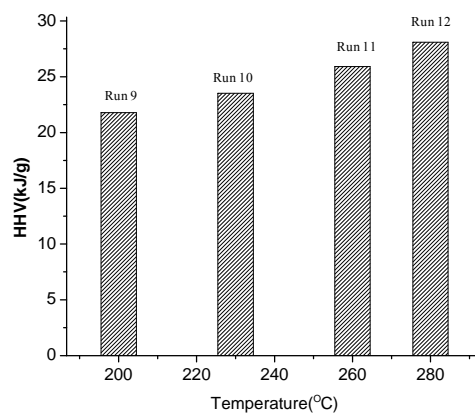


Figure 6.6 HHV of obtained biochar at 200-280°C.

The reactor pressure was autogenous and was higher than the vapor pressure of water due to the formation of gaseous products during the reaction. As expected, the influence of temperature was noteworthy. With increase in temperature, biochar became richer in carbon content indicated by its higher heating value. For example, the HHV value reached to 28.1 kJ/g at 280°C (run 12), which is comparable to bituminous grade coal. Though biochar yield (wt%) decreased with temperature.

To quantify the amount of energy being retained in solid biochar with respect to the initial energy input from switchgrass, energy conversion ratio (ECR) is defined as:

$$ECR = \frac{\text{dry mass of biochar} \times \text{HHV of biochar}}{\text{dry mass of switchgrass} \times \text{HHV of switchgrass}}$$

The *ECR* for the runs 10-12 was 52.4%, 43.0%, and 31.2% at 230, 260, and 280°C, respectively. The results indicate that energy conversion efficiency decreases with the temperature. Hence, temperature can play an important role in optimizing the *ECR* and HHV of biochar.

Figures 6.7 and 6.8 show the biochar yield and HHV with residence time at 280°C under autogeneous pressure (runs 12-14).

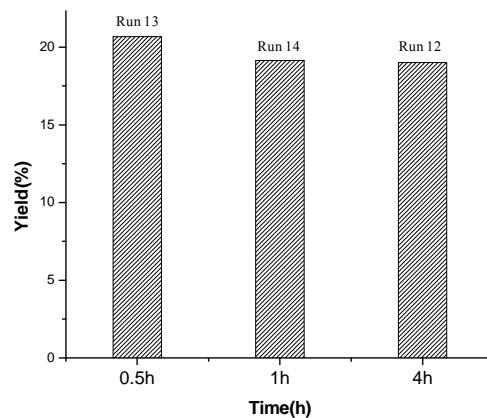


Figure 6.7 Yield (wt%) of obtained biochar at 280°C.

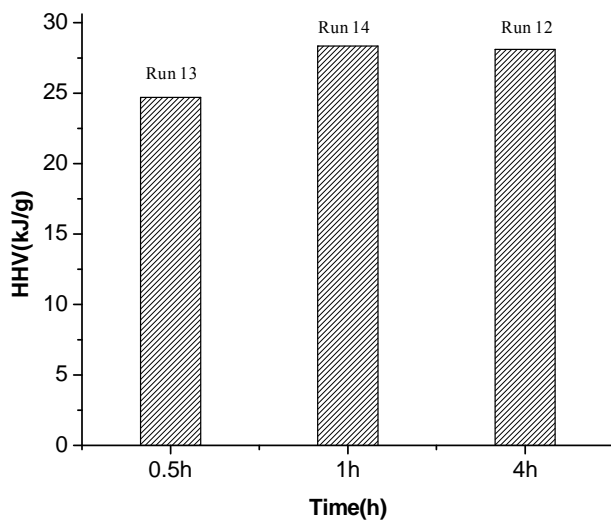


Figure 6.8 HHV of obtained biochar at 280°C.

Interestingly, the yield of biochar and HHV for run 12 and 14 did not change appreciably after increasing the residence time from 1 to 4 h. The biochar yield for run 13 was higher but the HHV was unexpectedly lower when compared to run 12 or 14. Switchgrass yielded less biochar during run 14 (1 h and 280°C) than during run 11 (4 h and 260°C), but the HHVs for obtained biochar were 28.4 and 25.9 kJ/g, respectively. These results show that the temperature plays a key role for the conversion of switchgrass to biochar. The higher temperature favors the dehydration of polymeric components of biomass including cellulose. In fact, dehydration reactions start competing with the hydrolysis reactions; even though hydrothermal media has excess water in the reactor.<sup>22</sup>

Biochar yield can be further optimized by increasing the selectivity towards dehydration and decarboxylation reactions. The hydrolysis needs to be suppressed which causes the loss of organic carbon as water soluble compounds in liquid product (biocrude). The second part of this study discusses about the process to recover these

water soluble compounds as biotar particle again by conducting reactions in hydrothermal medium.

**Biochar characterization:** The switchgrass and biochar are characterized by FTIR in the near IR region (wave number: 4000-400 cm<sup>-1</sup>). Typical FTIR spectra of switchgrass and biochar are shown in Figure 6.9 and the various band assignments are listed in Table 6.4. The FTIR spectrum of biochar was somewhat similar to that of switchgrass and the peaks of lignin were remained in the biochar. These results indicate that the biochar has lignin-like molecular structure. The appearance of absorption peaks at 1,060 and 1,160 cm<sup>-1</sup> in the samples produced at 200°C (run 9) and 230°C (run 8) confirmed that switchgrass was not decomposed completely under these reaction conditions.

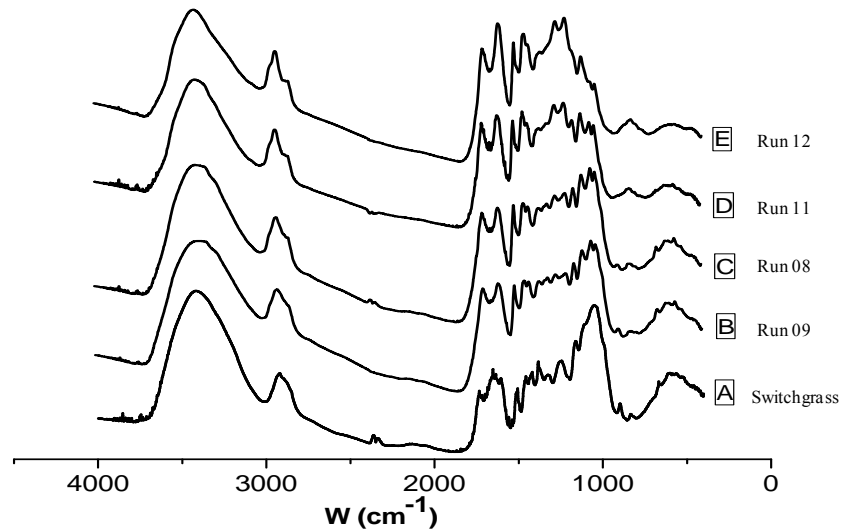


Figure 6.9 FTIR spectra of switchgrass and biochar, reaction time 4 h:  
Switchgrass (A), biochar from HTC at 200°C (B), biochar from HTC at 230°C (C), biochar from HTC at 260°C (D), biochar from HTC at 280°C (E).

Table 6.4 FTIR spectra of the switchgrass and biochar.

Position of the bands (cm <sup>-1</sup> )	Functional group
3401	O–H stretching
2920	CH, CH <sub>2</sub> stretching
1700	Carbonyl C=O stretching (polyxylose)
1600	C=C stretching
1513	Benzene ring stretching (lignin)
1424	CH <sub>2</sub> shearing (cellulose), CH <sub>2</sub> bending (lignin)
1383	CH bending (cellulose, semi-cellulose)
1267	C–O–C stretching in alkyl aromatic (lignin)
1160	C–O–C asymmetry stretching (cellulose, semi-cellulose)
1060	C–O stretching (cellulose and semi-cellulose)

The spectra of switchgrass and the samples from runs 8 and 9 were similar as confirmed the presence of absorption peaks attributed to the hemicelluloses and cellulose components of switchgrass. As for 260°C (run 11) and 280°C (run 12), the FTIR spectra have peaks for the biochar which are different than switchgrass or lower temperature biochar. This difference suggests that the aromatic ring started to recombine at the higher temperatures. The possible presence of alkenes was indicated by the absorbance peaks between 1,680 and 1,580 cm<sup>-1</sup>. The ether linkages around 1,200 cm<sup>-1</sup> and 1,000 cm<sup>-1</sup> between the cellulose skeleton units were hydrolyzed for the biochar samples produced at 260°C to 280°C.<sup>23-26</sup> It is noted that cellulose, which has four OH groups in its unit structure, exhibited a higher hydrolysis conversion to the aqueous sample due to its facile solvation and decoagulation with sub-critical water. Macropores located within the cellulose structure are readily altered during cross-linking, whereas the associated mesopores are much more stable. The particle size and porosity of the substrates should be taken into account for the comparison of their hydrolysis reactivity, although they may

be relatively minor factors compared to their different chemical structures and intra- and intermolecular interactions through the functional groups.<sup>24</sup> More detailed information and experimental data on such physical factors are necessary for the confirmation. As the skeleton structure of switchgrass, the lignin was remained in the biochar when the treatment temperature increased from 200°C to 280°C. The results were confirmed by the lignin peaks 1265, 1424 and 1513cm<sup>-1</sup> in the spectra. At the same time, 1600 and 1700 cm<sup>-1</sup>, the peaks of polymeric product are also present. The FTIR results prove that the biochar was composed of lignin and polymeric products produced during HTC.

The SEM images (Figure 6.10) suggest that biochar has smaller particle size and different microstructure than switchgrass.

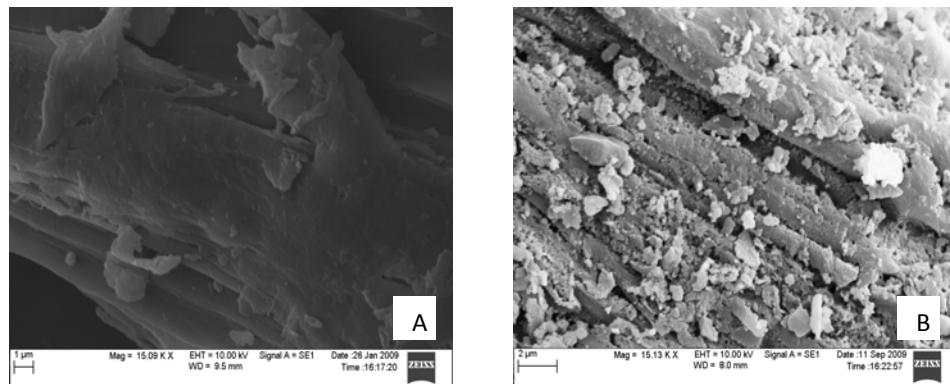


Figure 6.10 SEM images of switchgrass (A), and biochar (B) from run 11.

The images show that the lignocellulosic structure of switchgrass was destroyed in HTC process.<sup>2, 27</sup> Compared to lignin, the microcrystal structure of cellulose is relatively easier to change at higher temperatures as also demonstrated by FTIR analysis.

The XRD patterns for biochar from run 12 (280°C, 4.0 h) and switchgrass are compared in Figure 6.11.

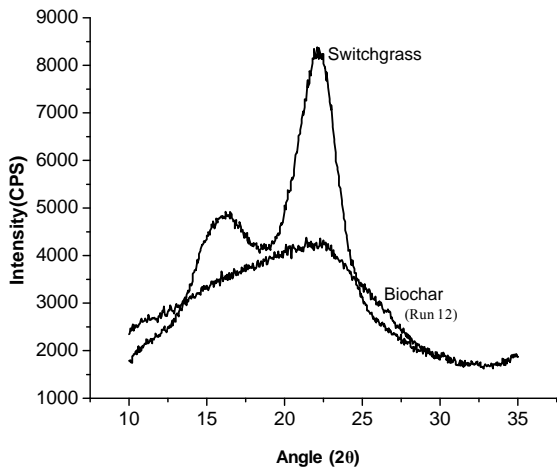


Figure 6.11 XRD images of untreated switchgrass and biochar obtained at 280°C, 4 h.

The distinctly sharp crystalline cellulosic peak (at  $2\theta = 22.7^\circ$ ) due to the crystal structure of cellulose is present in switchgrass, but is absent in biochar.<sup>28</sup> The XRD pattern of biochar from run 12 confirmed that it contained mainly amorphous components. Hence, cellulose microcrystalline feature converted to non-crystal structure during HTC process. The element analysis of the biochar (run 12) indicate that its carbon content was over 70 wt%. The results of HHV for different samples listed in Table 3.3 conclude that O/C ratio starts decreasing with the treatment temperature from about 0.90 for the untreated switchgrass to 0.32 for hydrothermally produced biochar at 280°C, due to deoxygenation. With the breakdown of lignocellulosic structure and removal of some oxygen from the structure, the moisture retention capacity of the product biochar is significantly reduced. Qualitatively, it was observed that biochar was a fluffy, less hydrophilic, and high energy density powder, which can be easily compacted.

**HTC of biocrude to produce biotar particles:** Typically, the TOC value of biocrude ranged between 1-1.5 wt%. The main sugar and organic acid in biocrude obtained at

different temperature are listed in Table 6.5, with the main hydrolysis product being glucose, acetic acid, lactic acid, HMF and furan, etc.

Table 6.5 The main sugar and acid in biocrude.

Composition	200°C	230°C	260°C	280°C
Glucose (g/L)	2.71	1.18	0.36	0.28
Lactic acid (g/L)	3.21	3.52	3.56	2.67
Acetic acid (g/L)	-	0.64	1.10	0.88
HMF (g/L)	-	-	-	0.66
Furan (g/L)	-	-	-	1.88

With the increase in temperature, the amount of glucose decreases whereas amounts of organic acids increase. It is well known that a low temperature is favorable for the production of sugars from the hydrolysis of hemicelluloses and cellulose, and these sugars further transform to organic acids at higher temperatures.

Biocrude obtained from the HTC of switchgrass at 200-280°C were again subjected to the hydrothermal conditions at 200°C for 2 h in a batch reactor. The dissolved organic carbon started precipitating as biotar particles. The conversion efficiency of carbon from biocrude to biotar particles based on TOC value was shown in the Figure 6.12.

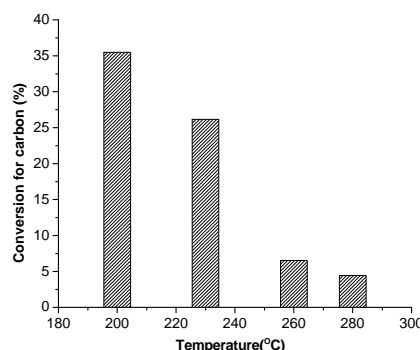


Figure 6.12 Conversion efficiency of carbon from biocrude.

As for the biocrude obtained at 200°C, the conversion efficiency of carbon was 35.5%. The value decreases to mere 4.4% when the biocrude obtained at 280°C from run 12 was used. The conversion efficiency of carbon for biocrude obtained from 230°C and 260°C were 26.2% and 6.5%, respectively. The experimental data indicated that biocrude produced at lower temperature is favorable for the transformation of carbon to biotar particles due to the presence sugars. In the reaction condition, the sugars are expected to partially convert to ring compound (furans) which further precipitate through polycondensation process as biotar particles. The SEM images of biotar particles obtained at 200°C are shown in Figure 6.13. The biotar particles are globules of about 2  $\mu\text{m}$  in size.

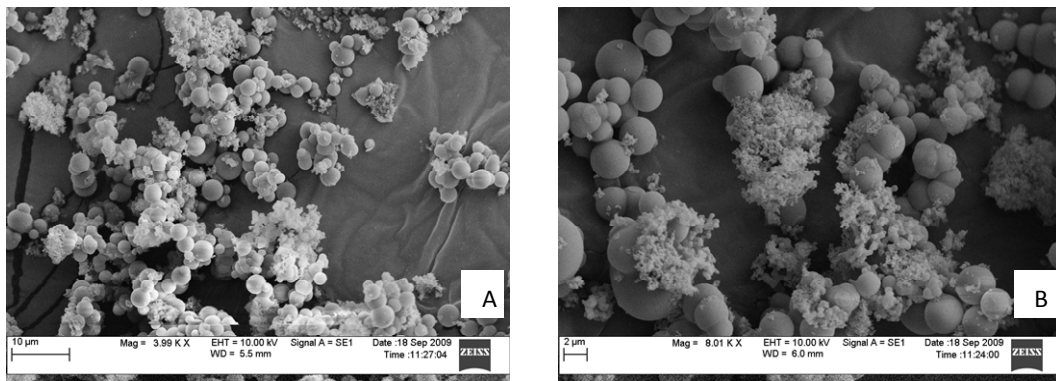


Figure 6.13 SEM images of biotar particles obtained at 200°C, 2 h.

Comparing biochar from switchgrass to biotar from biocrude processes, it is obvious different formation mode can provide various product properties. The biochar can potentially be used as high energy density solid fuel. On the other hand, due to the homogeneous characteristics, biotar particles can be utilized for producing carbonaceous functional materials.

## **6.6 Conclusion**

Switchgrass was converted to biochar by hydrothermal carbonization at 200-280°C. Compared with the reaction time and pressure, the temperature plays an important role in the conversion. With increase in temperature, biochar yield decreases but the heating value increases. Based on infrared spectroscopy and electron microscopy of biochar, complete breakdown of lignocellulosic crosslink structure of switchgrass was realized at higher temperatures and biochar contained mainly lignin fractions. Based on x-ray diffraction, microcrystalline component is converted to non-crystalline components. The HHV of biochar produced at 280°C in just 1 h of HTC was comparable to the bituminous grade coal.

Biotar microparticles can be produced from HTC of biocrude. Biocrude produced at a lower temperature is favorable for the biotar production where sugar compounds present in the biocrude undergoes polycondensation and dehydration processes resulting in carbon rich microspheres. The biotar microparticles are globular and uniform in particle size.

## **6.7 Acknowledgments**

Author is thankful for the financial supports from the National Science Foundation (grant NSF-CBET-0828269) and Alabama Center for Paper and Bioresource Engineering.

## 6.8 References

1. Matsumura, Y.; Sasaki, M.; Okuda, K.; Takami, S.; Ohara, S.; Umetsu, M.; Adschiri, T., Supercritical water treatment of biomass for energy and material recovery. *Combust. Sci. and Tech.* 2006, 178, 509-536.
2. Kumar, S.; Gupta, R. B., Biocrude Production from Switchgrass using Subcritical Water. *Energy & Fuels* 2009, 23, (10), 5151-5159.
3. Lee, I.; Kim, M.; Ihm, S., Gasification of glucose in supercritical water. *Ind. Eng. Chem. Res.* 2002, 41, 1182-1188.
4. Motonobu, G.; Ryusaku, O.; Tsutomu, H., Hydrothermal conversion of municipal organic waste into resources. *Bioresource Technology* 2004, 93, 279-284.
5. Kishida, H.; Jin, F.; Zhou, Z., Conversion of glycerin into lactic acid by alkaline hydrothermal reaction. *Chemistry Letters* 2005, 34, (11), 1560-1561.
6. Kong, L. Z.; Li, G. M.; Wang, H., Hydrothermal catalytic conversion of biomass for lactic acid production. *Journal of Chemical Technology & Biotechnology* 2008, 83, 383-388.
7. Lourdes, C.; David, V., Formation of organic acids during the hydrolysis and oxidation of several wastes in sub- and supercritical water. *Ind. Eng. Chem. Res.* 2002, 41, 6503-6509.
8. Selhan, K.; Thallada, B.; M. Akinori Low-temperature catalytic hydrothermal treatment of wood biomass: analysis of liquid products. *Chemical Engineering Journal* 2005, 108, 127-13.

9. Abdullah, H.; Wu, H. W., Biochar as a fuel: 1. Properties and grindability of biochars produced from the pyrolysis of mallee wood under slow-heating conditions. *Energy & Fuels* 2009, 23, (8), 4174-4181.
10. Titirici, M.-M.; Thomas, A.; Antonietti, M., Back in the black: hydrothermal carbonization of plant material as an efficient chemical process to treat the CO<sub>2</sub> problem. *New J. Chem.* 2007, 31, 787-789.
11. Hu, B.; Yu, S.-H.; Wang, K.; Liu, L.; Xu, X.-W., Functional carboneaceous materials from hydrothermal carbonization of biomass: an effective chemical process. *Dalton Transactions* 2008.
12. Phillip, E., Organic chemical reactions in supercritical water. *Chemical Reviews* 1999, 99, 603-621.
13. Masaru, W.; Takafumi, S.; Hiroshi, I., Chemical reactions of C1 compounds in near-critical and supercritical water. *Chemical Reviews* 2004, 104, 5803-5821.
14. Savovaa, D.; Apakb, E.; Ekinci, E.; Yardimb, F.; Petrov, N.; Budinovaa, T.; Razvigorovaa, M.; Minkovaa, V., Biomass conversion to carbon adsorbents and gas. *Biomass and Bioenergy* 2001, 21, (2), 133-142.
15. Bergius, F.; Specht, H., Die Anwendung hoher Drucke bei chemischen Vorgängen und eine Nachbildung des Entstehungsprozesses der Steinkohle.Verlag Wilhelm Knapp. *Halle an der Saale* 1913, 58.
16. Marta, S.; Antonio, B. F., The production of carbon materials by hydrothermal carbonization of cellulose. *Carbon* 2009, 47, 2281-2289.

17. Titirici, M.-M.; Antonietti, M.; Baccile, N., Hydrothermal carbon from biomass: a comparision of the local structure from poly- to monosaccharides and pentoses/hexoses. *Green Chem.* 2008, 10, 1204-1212.
18. Varhegyi, G.; Szabo, P.; Till, F.; Zelei, B.; Antal, M. J. J.; Dai, X., TG, TG-MS, and FTIR Characterization of high-yield biomass charcoals. *Energy & Fuels* 1998, 12, 969-974.
19. Cheng, L.; Ye, X. P.; He, R.; Liu, S., Investigation of rapid conversion of switchgrass in subcritical water. *Fuel Processing Technology* 2009, 90, 301-311.
20. Rezaei, K.; Temelli, F.; Jenab, E., Effects of pressure and temperature on enzymatic reactions in supercritical fluids. *Biotechnology Advances* 2007, 25, 272-280.
21. Peterson, A. A.; Vogel, F.; Lachance, R. P.; Froling, M.; Michael Jerry Antal, J.; Tester, J. W., Thermochemical biofuel production in hydrothermal media:A review of sub- and supercritical water technologies. *Energy and Environmental Science* 2008, 1, 32-65.
22. Patrick, H. R.; Griffith, K.; Liotta, C. L.; Eckert, C. A., Near critical water: A benign medium for catalytic reactions. *Ind. Eng. Chem. Res.* 2001, 40, 6063-6067.
23. Sakanishi, K.; Ikeyama, N.; Sakaki, T., Comparison of the hydrothermal decomposition reactivities of chitin and cellulose. *Ind. Eng. Chem. Res.* 1999, 38, 2177-2181.
24. Kong, L. Z.; Li, G. M.; He, W., Reutilization disposal of sawdust and maize straw by hydrothermal reaction. *Energy Sources, Part A* 2009, 31, 876-887.

25. Biagini, E.; Barontini, F.; Tognotti, L., Devolatilization of biomass fuels and biomass components studied by TG/FTIR technique. *Ind. Eng. Chem. Res.* 2006, 45, 4486-4493.
26. Qian, Y. J.; Zuo, C. J.; Tan, J., Structural analysis of bio-oils from sub-and supercritical water liquefaction of woody biomass. *Energy & Fuels* 2007, 32, (3), 196-202.
27. Kobayashi, N.; Okada, N.; Hirakawa, A.; Sato, T.; J.Kobayashi; Hatano, S.; Itaya, Y.; Mori, S., Characteristics of solid residues obtained from hot-compressed-water treatment of woody biomass. *Industrial and Engineering Chemistry Research* 2009, 48, 373-379.
28. Segal, L.; Creely, J. J.; Martin, A. E.; Conrad, C. M., An empirical method for estimating the degree of crystallinity of native cellulose using the X-ray diffractometer. *Textile Res. J.* 1959, 29, 786-794.

## 7. Application of Biochar for the Removal of Heavy Metal Contaminants from Ground Water

### 7.1 Introduction

Besides the use of biochar as solid fuels, this carbonaceous material can be potentially used for the removal of heavy metals contamination from ground water.<sup>1-3</sup>

Nano-porous structure of biochar with available oxygen functional groups on the surface provides an excellent opportunity to adsorb heavy metal ions from the aqueous solution.<sup>4</sup>

<sup>6</sup> The cost of the adsorbent is the most important criteria in its large scale application. Abundantly available lignocellulosic biomass is a promising raw material for the production of activated carbons considering their low cost. But the main disadvantage of activated carbon is its relatively high production cost due to the high expense of energy used during its production.<sup>7</sup> As a traditional method for biochar production, pyrolysis processes typically use dry biomass sources and temperature range from 500 to 800°C. So the higher energy consumption is needed in the pyrolysis process for biochar production. Considering the cost factor, biochar produced by subcritical water carbonization technology, which is relatively less energy intensive process is viewed as the potentially low-cost process for obtaining organic adsorbents. The pyrogenic organic matters (eg. biochar, charcoal, soot and activated carbon) have been studied extensively for their high affinity and capacity of absorbing organic compounds.<sup>8</sup>

Raw biomass such as peat, poplar sawdust, coconut shells have been reported to show affinity towards heavy metal ions even at low ion concentration.<sup>9, 10</sup> However use of raw biomass as adsorbent is associated with the risk of leaching of the organic pollutants.<sup>3</sup> Raw biomass is also biodegradable. On the other hand, biochar as sorbent is useful in avoiding such risks. The earlier studies have been reported on the use of biochar for removing the metal contaminants such as lead, mercury, and arsenics from aqueous solutions.<sup>11-13</sup> Among the several metal contaminants of concern, uranium is considered as top priority metal contaminant by the U.S. Department of Energy. Ground water contamination caused by the radionuclides, in particular uranium is a serious environmental problem worldwide.<sup>14</sup> Uranium, a radiotoxic also possesses the risk related to chemical toxicity. Among the various oxidation states of uranium, +4 and +6 oxidation states are the most important states in geological environments. The chemical toxicity of uranium is predominantly caused by the highly reactive hexavalent uranyl ions.

In the early 1940's the naturally occurring radioactive element, uranium (U), was heavily used in the nuclear weapons program and energy production. Ever since, the wide use of uranium has left a legacy of contaminants in the subsurface environment especially at most of the U.S. Department of Energy sites. Considering some of the U contaminated sites adjoin river boundaries, the subsurface mobility of uranium poses a huge concern to both humans and the environment. The common remediation strategies used to address U(VI) contamination are precipitation of uranium to its least soluble minerals, abiotic/biotic reduction of U(VI) to its less soluble form U(IV), sorption of U(VI) to strongly adsorbing agents (zero valent iron, fish bone etc.).

In this study, we focus on the adsorption of uranium on to biochar prepared from switch grass in subcritical water. Although the scientific literature is replete with studies focusing on the adsorption of contaminants on to biochar obtained from agricultural products, the application of biochar to U(VI) adsorption is not studied. Moreover, the effective use of wastes from biorefinery processes for contaminant remediation would enhance the goal of the green process. The batch adsorption experiments were conducted where uranium [U(VI)] was loaded as a solute at both the natural pH of biochar (~4.0) and at a higher pH (~5.7).

## 7.2 Experimental Section

*Biochar Preparation:* Auburn grown switchgrtass (chopped to 5-10 mm long size) was used for producing biochar. De-ionized (D.I.) water was used for conducting the experiments. Conversion of switchgrass to biochar was conducted in a high pressure batch type reactor. The set up consists of a 500 ml high temperature, high pressure metal reactor equipped with a state of art control system comprising Proportional-Integral-Differential (PID) controllers. Switchgrass (50 g) and 350 ml of water were charged into the reaction vessel and the reactor temperature was raised to 300°C with a heating rate of 7°C/min. After maintaining the temperature at 300°C for 30 min reactor under autogeneous pressure condition, reactor was rapidly cooled to ambient condition using water through cooling coil. The product biochar is separated from the liquid after reaction and further washed with D.I. water. The biochar was air dried and used for the further characterization.

*Batch adsorption kinetic experiments:* Batch kinetic experiments were performed at two different solid to solution ratio (SSR: 4 and 5 g L<sup>-1</sup>) and initial U(VI) concentration (ca.

30 and 10 mg L<sup>-1</sup>) to estimate the equilibrium time for the adsorption reaction. The experiments were performed at the natural pH of biochar (ca. pH 3.9 ± 0.2) with 0.1 M NaNO<sub>3</sub> as the background solution. The experiments were carried out for 72 hours and samples were taken at regular intervals by sacrificing the tubes. U(VI) was measured using kinetic phosphorescence analyzer (KPA, Chemchek Instruments, Inc.) after filtration of the samples through 0.45 µm PTFE filter units and acidifying the samples to pH 1.0. The difference between the initial U(VI) concentration and aqueous U(VI) concentration was attributed to the adsorption of U(VI) onto biochar. Both the experiments had duplicate test tubes for each sampling interval, blank [no U(VI)], and controls (no biochar).

*Batch adsorption equilibrium experiment:* Batch isotherm experiment was performed at a solid loading of 5g L<sup>-1</sup> and at a pH of about 3.9 ± 0.2. The initial concentration of U(VI) was varied between 5 to 30 mg L<sup>-1</sup> and the experiment was conducted in a 0.1 M NaNO<sub>3</sub> background solution. Moreover, to study the effect of solid to solution ratio on adsorption, duplicate tubes were set up at 1 g of biochar L<sup>-1</sup> containing an initial U(VI) concentration 10 mg L<sup>-1</sup>. The test tubes were prepared in duplicates and tumbled for about 34 hours at 25 °C. At the end of the equilibrium time, aqueous samples were filtered and acidified and analyzed. Similar to the kinetic experiments, the difference between the initial U(VI) concentration and aqueous U(VI) concentration was attributed to the adsorption of U(VI) onto biochar.

### 7.3 Results and Discussion

Table 7.1 compares the elemental composition and ash content in raw switchgrass and the biochar. It was observed that elemental carbon in biochar increased to 70.46% as

a result of subcritical water carbonization. The oxygen content in raw switchgrass is typically 40-43%.<sup>15</sup> As a result of carbonization process in subcritical water more than 70% of deoxygenation could be achieved.

Table 7.1 Composition of switchgrass and biochar.

**Table 1: Composition of switchgrass and biochar**

Elements	C (wt%)	Ash (wt%)	Ca	K	Mg	P (ppm)	Fe	Mn	Na	Pb
Switchgrass	44.61	4.5	2105	4082	4514	941	115	48	701	1
Biochar	70.46	3.7	2029	665	2215	481	258	53	395	<0.1

The biochar yield and higher heating value (HHV) of biochar produced from switchgrass was 48.2 wt% and 27.5 MJ/kg on oven dry basis, respectively. The effects of temperature, pressure and residence time on the yield and HHV of biochar have been studied separately (Chapter 6). The biochar had specific surface area of 18 m<sup>2</sup>/g, as determined by nitrogen physisorption using five point Brunauer-Emmett-Teller (BET) methods at 77 K using Autosorb-1 instrument (Quantachrome).

Figures 7.1(a,b) show the results of thermogravimetric (TG) and derivative thermogravimetric (DTG) analyses conducted under helium gas flow to understand the thermal stability of materials upto 700°C. TG was conducted using a TGAQ 5000 instrument under high purity (99.99%) helium gas flow. Samples were placed in a sample pan and heated from room temperature to 700°C with a heating rate of 10°C/min. The TGA curves were obtained directly from the apparatus while the derivative thermogravimetric (DTA) curves were obtained by the software Universal V4.3A.

Weight loss in switchgrass was observed over a wide range of temperature upto 700°C, but majority of weight loss (70%) happened in the range of 200 to 400°C (Figure 7.1a). The rapid weight loss below 400°C is mainly due to the decomposition of holocellulose fractions of the switchgrass.<sup>16</sup> On contrary, the weight loss in biochar is relatively gradual upto 700°C. In fact, nearly 45% of biochar remains even at 700°C which confirmed the thermal stability of biochar relative to the switchgrass.

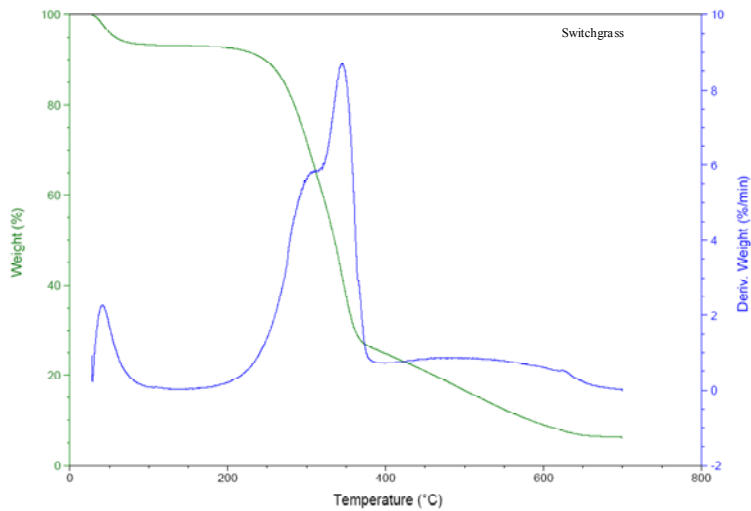


Figure 7.1a TG and DTG pattern of switchgrass under inert (helium) atmosphere.

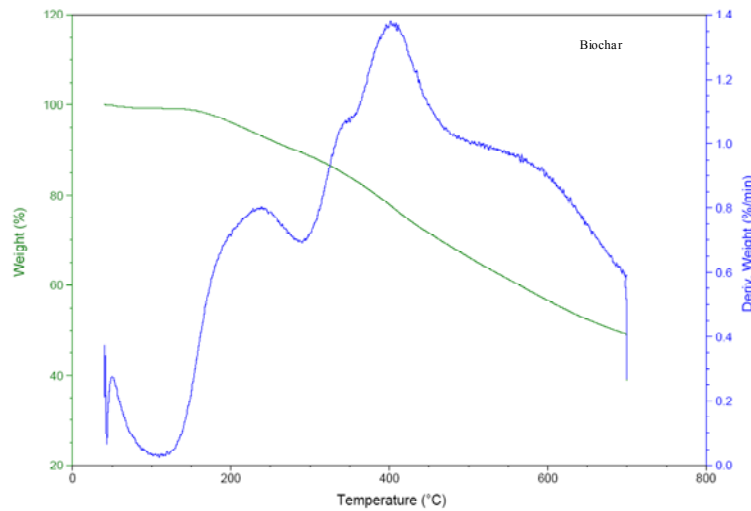


Figure 7.1b TG and DTG pattern of biochar under inert (helium) atmosphere.

The kinetic experiments indicate about 90% of initial U(VI) adsorption resulting within 8 hours, at both the SSR (Figure 7.2). Based on the reaction kinetics, about 34 hours of equilibrium time was chosen for the batch isotherm experiments.

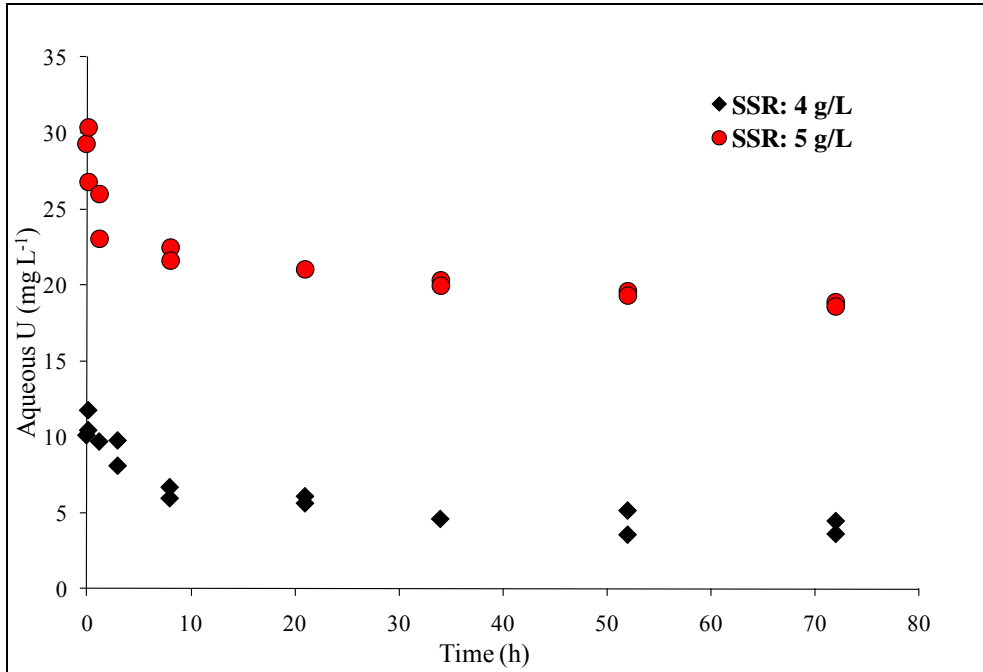


Figure 7.2 Kinetics of U(VI) adsorption on to biochar at different solid loadings and initial U(VI) concentrations. Circles represent a SSR of 5 g L<sup>-1</sup> and an initial U(VI).

The batch adsorption isotherm is shown in Figure 7.3. The adsorption of U(VI) onto biochar followed a H-type isotherm.

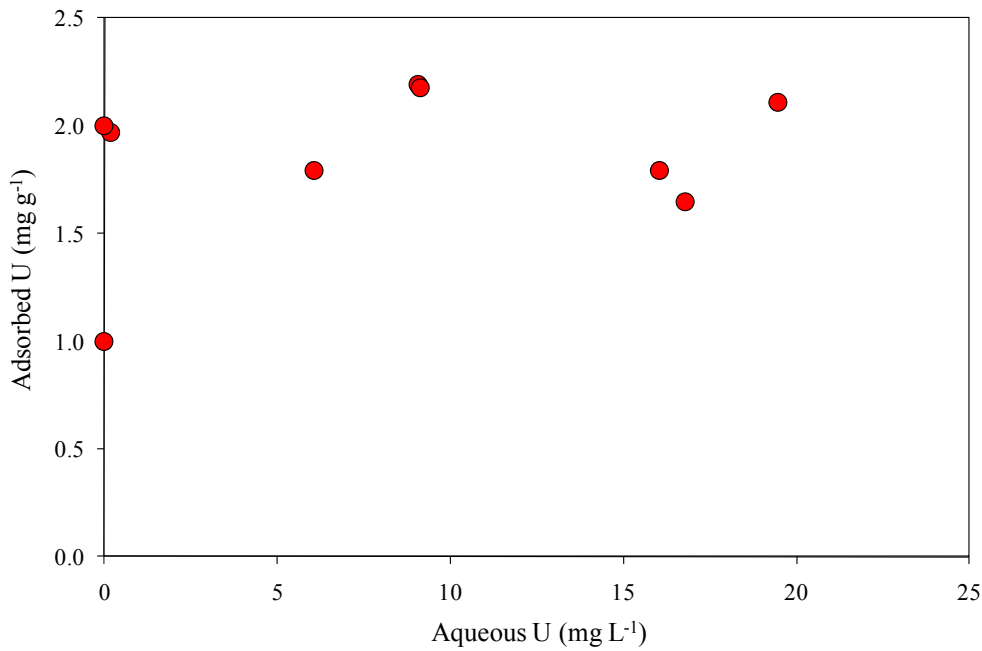


Figure 7.3 Adsorption isotherm of U(VI) on to biochar. SSR: 5 g L<sup>-1</sup> pH: 3.9 ± 0.2; ionic strength: 0.1 M NaNO<sub>3</sub>.

This could have been due to the filling of biochar pores by the uranyl cations. Once the pore volume gets completely filled, the biochar ceases to trap more uranium resulting in a plateau at about 2 mg g<sup>-1</sup>. Furthermore, the isotherm indicates an adsorption capacity of ca. 0.2% (w/w). Figure 7.4 indicates the variation in adsorption with respect to solid loading. The distribution coefficient is about three times higher at a SSR of 1 g L<sup>-1</sup> when compared with 5 g L<sup>-1</sup>.

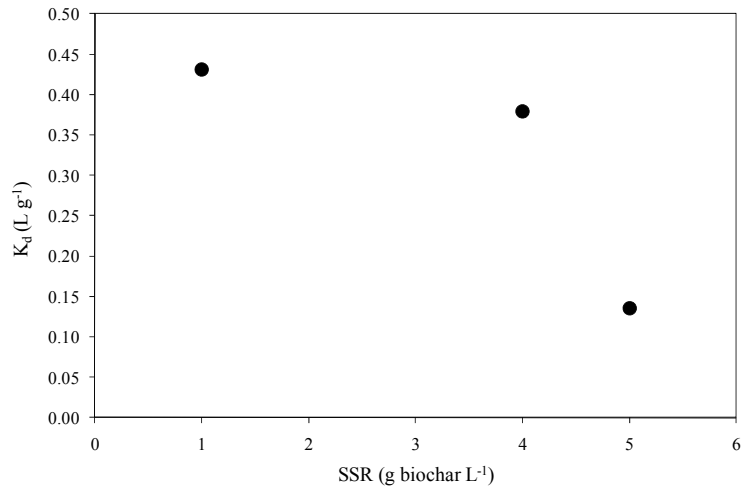


Figure 7.4 Adsorption of U(VI) on to biochar at different SSR. pH:  $3.9 \pm 0.2$ ; ionic strength: 0.1 M NaNO<sub>3</sub>.

#### 7.4 Conclusion

The study clearly shows that the adsorption of uranium on to biochar could be considered as one of the possible alternatives to treat U(VI) contaminated water. Kinetically, the sorption process is fast and the extent of adsorption is fixed. Compared to other remediation strategies, feasibility of biochar as U adsorbent is supported by its environmental benign nature. Thus the study illustrates the proof of concept that biochar could serve as an effective adsorbent of uranium containing groundwater without causing environmental damages. But the practical application of biochar in the field needs further studies including desorption and flow through column experiments.

## 7.5 References

1. Bailey, S. E.; Olin, T. J.; Bricka, R. M.; Adrian, D. D., A review of potentially low-cost sorbents for heavy metals. *Water Res.* **1999**, 33, 2469–2479.
2. Dias, J. M.; Alvim-Ferraz, M. C. M.; Almeida, M. F.; Rivera-Utrilla, J.; Sanchez-Polo, M., Wastematerials for activated carbon preparation and its use in aqueous-phase treatment: a review. *J. Environ. Manage.* **2007**, 85, 833-846.
3. Liua, Z.; Zhang, F.-S., Removal of lead from water using biochars prepared from hydrothermal liquefaction of biomass *Journal of Hazardous Materials* **2009**, 167, (1-3), 933-939.
4. Tan, W. T.; Ooi, S. T.; Lee, C. K., Removal of Cr(VI) from solution by coconut husk, palm pressed fibers. *Environ. Technol.* **1993**, 14, 277–282.
5. Sevilla, M.; Fuertes, A. B., The production of carbon materials by hydrothermal carbonization of cellulose. *Carbon* **2009**, 47, 2281-2289.
6. Hu, B.; Yu, S.-H.; Wang, K.; Liu, L.; Xu, X.-W., Functional carboneaceous materials from hydrothermal carbonization of biomass: an effective chemical process. *Dalton Transactions* **2008**.
7. Savovaa, D.; Apakb, E.; Ekinci, E.; Yardimb, F.; Petrov, N.; Budinovaa, T.; Razvigorovaa, M.; Minkovaa, V., Biomass conversion to carbon adsorbents and gas. *Biomass and Bioenergy* **2001**, 21, (2), 133-142.
8. Smernik, R. J., Biochar and sorption of organic compounds. In *Biochar for Environmental Management: Science and Technology*, Lehmann, J.; Joseph, A., Eds. Earthscan: London, 2009; pp 289-300.

9. McKay, J. F. P. G., Equilibrium parameters for the sorption of copper, cadmium and zinc ions onto peat. *J. Chem. Technol. Biotechnol.* **1997**, 69, 309-320.
10. Sciban, M.; Radetic, B.; Kevresan, Z.; Klasnja, M., Adsorption of heavy metals from electroplating wastewater by wood sawdust. *Bioresour. Technol.* **2007**, 98, 402-409.
11. Budinova, T.; Ekinci, E.; Yardim, F.; Grimm, A.; Bjornbom, E.; Minkova, V.; M. Goranova, Characterization and application of activated carbon produced by H<sub>3</sub>PO<sub>4</sub> and water vapor activation. *Fuel Process. Technol.* **2006**, 87, 899–905.
12. Kalderis, D.; Koutoulakis, D.; Paraskeva, P.; Diamadopoulos, E.; Otal, E.; J.O. Valle d.; Fernandez-Pereira, C., Adsorption of polluting substances on activated carbons prepared from rice husk and sugarcane bagasse. *Chem. Eng. J.* **2008**, 144, (42-50).
13. Amuda, O. S.; Giwa, A. A.; I.A. Bello, Removal of heavy metal from industrial wastewater using modified activated coconut shell carbon. *Biochem. Eng. J.* **2007**, 36, 174-181.
14. Srivastava, S.; Bhainsa, K. C.; D'Souza, S. F., Investigation of uranium accumulation potential and biochemical responses of an aquatic weed *Hydrilla verticillata* (L.f.) Royle. *Bioresour. Technol.* **2010**, 101, 2573-2579.
15. Berg, D. V. D.; Visser, P. D. *Final Report FAIR 5-CT97-3701 “Switchgrass”*. BTG (Biomass Technology Group), Enschede, The Netherlands: pp 50-52.
16. Chen, B.; Chen, Z., Sorption of naphthalene and 1-naphthol by biochars of orange peels with different pyrolytic temperatures. *Chemosphere* **2009**, 76, 127-133.

## **8. Summary and Future Works**

The dissertation has successfully demonstrated that hydrothermal technology can play an important role in developing future biorefineries. The inherently high moisture content (considered as a major drawback) of biomass can be used advantageously to produce commercially viable biofuels without prior drying or using toxic/expensive chemicals. The dissertation encompasses and concludes the important finding in the area of pretreatment for bioethanol, liquefaction of biomass for biocrude and hydrothermal carbonization process for biochar production.

Lignocellulosic biomass can be efficiently pretreated in subcritical water in a short residence time. The process is not dependent on the type of biomass. Further, the research work has also established an alternative pathway for the utilization of liquid hydrolyzate generated during the pretreatment process. In other studies, cellulose and switchgrass were liquefied in subcritical water to water-soluble products. In fact, nearly 70 wt% yield of sugar compounds from cellulose liquefaction in subcritical water was achieved. Similarly, switchgrass was converted to biocrude and high energy density biochar in subcritical water. Fundamental study on the conversion of cellulose in sub- and super-critical water was completed. The use of potassium carbonate helped in catalyzing the depolymerization/liquefaction process. Further, switchgrass was converted a high heating value (coal-like) biochar for solid fuels applications.

The nano-porous structure of biochar available with oxygen functional groups on the surface provided an excellent opportunity to develop this material as an adsorbent for heavy metal contaminants in ground water. The present research has opened up several avenues for continuing the fundamental and development research works on biofuels. Following research area may be further explored to support the future biorefineries.

i. *Pretreatment of Biomass by Transient Heating in Hydrothermal Medium:*

Pretreatment is an important and first step in the bioconversion process of biomass to ethanol. Typically it accounts for up to 40% of the total processing cost. Conventional pretreatment methods employ variety of chemicals for fractionating lignin and/or hemicelluloses to improve the enzymatic reactivity of biomass. Majority of these processes limit the exposure of biomass to below 220°C, which may not be sufficient to cause substantial structural changes in cellulose. In the present study on pure cellulose, it was observed that cellulose depolymerizes rapidly above 300°C and also undergoes changes in hydrogen bonding arrangements. Therefore, rapid heating and quenching (i.e. transient heating) of switchgrass in subcritical water above 300°C is expected to cause some structural changes because of re-orientation / changes in hydrogen bonding patterns. The very short time (order of few seconds) exposure of switchgrass in hydrothermal medium will also help in minimizing the generation of inhibitory compound. The physical alteration in cellulose structure caused by exposure to high temperature is expected to increase its enzymatic reactivity by manifolds.

ii. *Upgradation of biocrude:* Rapid depolymerization of biomass components in subcritical water results in the formation of oxygenated hydrocarbons (biocrude). The

liquid mixture, which consists of cyclic molecules (e.g., glucose, furans, and oligosaccharides) and aromatic cyclic molecules (e.g, phenols) can be upgraded to liquid fuel by aqueous phase or supercritical water reforming. The presently available aqueous phase reforming technology is mostly applicable to model compound such as glucose, HMF, furfural, etc. and employs costly noble metals catalysts. The development of an economical catalyst which can be used to upgrade the mixture of biomass derived liquid products will immensely help in supporting the commercial development of petroleum like fuels from biomass.

iii. *Biochar related research:* Hydrothermally produced biochar is a high energy density (coal-like) powder which has a potential to be compatible with coal infrastructure. The oxygen content in biochar was typically 22-23 wt% which is much lower compared to original biomass (> 40 wt%). Therefore, pyrolysis products from such biochar are expected to have a higher heating value compared to the conventional pyrolysis oil. Due to the high moisture content and the low surface area of untreated biomass, conventional pyrolysis or gasification processes require drying and size reduction of biomass prior to processing. On the other hand, hydrothermally produced biochar can be potentially developed as a feedstock for pyrolysis/gasification process due to almost uniform C, H, and O composition, fine particle size and reduced moisture retention capacity (i.e. hydrophobicity). The process may substantially eliminate the current costs associated with biomass drying and size reduction.

In view of biochar's sorption properties, it is recommended to continue research for employing it as an economical alternative for removing subsurface contaminants.

## Appendix A: Structure and Composition of Lignocellulosic Biomass

### A.1 Introduction

Lignocelluloses are derived from wood, grass, agricultural residues, forestry waste and municipal solid wastes. The major components of lignocellulosic material are cellulose, lignin, hemicelluloses and others (extractives and ash). Small percentage of extractives and ash are also present in lignocellulosic biomass. Cellulose and hemicelluloses are polymers based on different sugars, whereas lignin is an aromatic polymer mainly built of phenylpropanoid precursors. Composition of these polymers within single plant varies with age, and stage of growth.<sup>1</sup>

### A.2 Composition and Structure

**Cellulose:** Discovered 150 years ago, cellulose is most abundant organic matter on the earth. It is the main structural constituent of plants and algal cell walls. Cellulose in wood is mixed with many polymers such as hemicelluloses and lignin. Fluffy fiber of cotton ball is the purest naturally occurring form of cellulose. It is an unbranched chain and homopolymer of  $\beta$ -D-glucopyranose units linked together by (1 $\rightarrow$ 4)-glycosidic bonds with a repeating unit of  $C_6H_{10}O_5$  strung together by  $\beta$ -glycosidic linkages. The  $\beta$ -linkages in cellulose form long linear chains (called elemental fibril) that are highly stable and resistant to chemical attack because of the high degree of hydrogen bonding that can

occur between chains of cellulose.

Hemicellulose and lignin cover microfibrils (which are formed by elemental fibrils). Hydrogen bonding between cellulose chains makes the polymers more rigid, inhibiting the flexing of the molecules that must occur in the hydrolytic breaking of glycosidic linkages. Hydrolysis can reduce cellulose to a cellobiose repeating unit,  $C_{12}H_{22}O_{11}$ , and ultimately to glucose.<sup>2-4</sup>

There are six known polymorphs of cellulose (I, II, III<sub>I</sub>, III<sub>II</sub>, IV<sub>I</sub>, and IV<sub>II</sub>) which can also interconvert. The interconversion of cellulose is shown in Figure A.1. Cellulose I, also termed as native cellulose, has parallel arrangement of chains and is the only polymorph that occurs naturally. Cellulose II is converted through mercerization or solubilization-regeneration of native or other celluloses. Cellulose II is thermodynamically more stable structure with a low energy crystalline arrangement having an antiparallel arrangement of the strands (two cellulose chains lie antiparallel to one another) and some inter-sheet hydrogen bonding. Cellulose III<sub>I</sub> and III<sub>II</sub> can be obtained from Cellulose I and II, respectively, by treatment with liquid ammonia or some amines, whereas polymorphs IV<sub>I</sub> and IV<sub>II</sub> can be obtained from heating cellulose III<sub>I</sub> and III<sub>II</sub>, respectively, to 206°C in glycerol.<sup>2-5</sup> Two decades ago, it was reported that native cellulose (cellulose I) exists as a mixture of two crystalline forms I <sub>$\alpha$</sub>  and I <sub>$\beta$</sub> , having triclinic and monoclinic unit cells, respectively.<sup>6</sup> Cellulose I <sub>$\alpha$</sub>  is thermodynamically less stable, as shown by its conversion to cellulose I <sub>$\beta$</sub>  by annealing at 260°C. In both crystalline forms, cellobiose is the repeating unit with a strong intra-chain H-bond from 3-OH to the preceding ring O5, whereas the inter-chain H-bonding and packing of the crystal are slightly different in the two forms.<sup>7</sup>

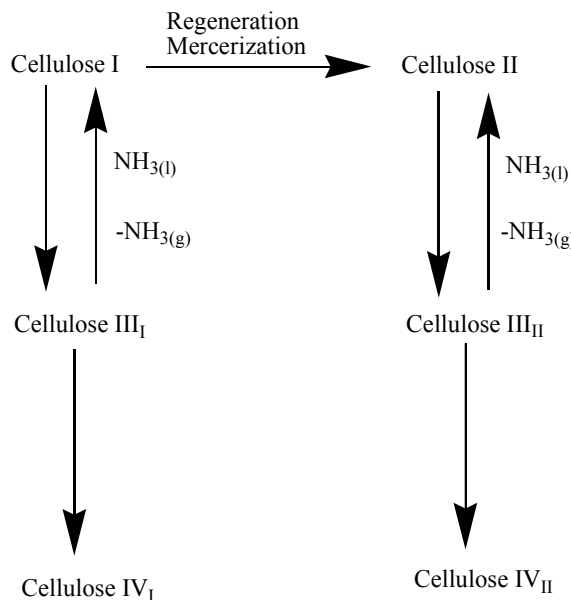


Figure A.1 Inter-conversion of polymorphs of cellulose (redrawn from O'Sullivan).<sup>3</sup>

The comparatively lower stability of  $I_a$  may provide the site of initial reaction in the microfibril. Cellulose molecules have reducing end group, as chemical linkage between C<sub>1</sub> carbon and the ring oxygen. It is a hemiacetal and allows ring to open to form an aldehyde. The other end-group is a secondary alcohol and commonly referred as non reducing end group. The structural unit of cellulose has three hydroxyl groups, one primary and two secondary. These groups undergo chemical modifications (e.g. esterifications and etherifications) during the reactions. But the accessibility of the reactants is limited because of the high degree of crystallinity of the native cellulose.<sup>8</sup>

Cellulases enzyme hydrolyze the  $\beta$ -1,4-glycosidic linkages of cellulose. They are divided in two classes and referred as endoglucanases (endo-1,4- $\beta$ -glucanases, EGs) and cellobiohydrolases (exo-1,4- $\beta$ -glucanases, CBHs). EGs hydrolyze preferably the amorphous region of cellulose and releases new terminal ends. Whereas CBHs act on

existing or EGs generated chain ends. Both enzymes can degrade amorphous cellulose, but only CBHs enzyme act efficiently on crystalline cellulose. Thus CBHs and EGs work synergistically in cellulose hydrolysis and releases cellobiose molecules.  $\beta$ -glucosidases are required to further break down the cellobiose to two glucose molecule.<sup>1</sup>

**Hemicelluloses:** Hemicelluloses are important carbohydrate fraction in plants made of mixed polysaccharides and stick to cellulose via hydrogen bonds, to create polysaccharide microfibrils. Together these give a strong rigidity to plant cell walls but the added lignin improves this strength greatly. The molecules are much smaller than the cellulose (degree of polymerization  $\approx 10^2$ ) and are dominated by hydrogen bond from the 3-OH of one sugar to the ring oxygen of preceding sugar. Hemicelluloses are a class of polymers of sugars including the six carbon sugars mannose, galactose, glucose and 4-*O*-methyl-D-glucuronic acid and five carbon sugars xylose and arabinose. Unlike cellulose, hemicelluloses possess side chains. The side groups include acetic acid, pentoses ( $\beta$ -D-glucose,  $\beta$ -D-mannose,  $\alpha$ -D-galactose), hexuronic acids ( $\beta$ -D-glucoronic acid,  $\alpha$ -D-4-*O*-methylglucoronic acid,  $\alpha$ -D-galacturonic acid) and deoxyhexoses ( $\alpha$ -L-rhamnose  $\alpha$ -L-fructose) and are responsible for the solubility of hemicelluloses in water and / or alkali. These side groups stop hemicelluloses molecules to aggregate and make them more susceptible to chemical degradation than cellulose. Within the plant, hemicelluloses are bound to cellulose and lignin component by covalent & non-covalent bonds in the cell wall and are thus fixed in the fiber structure.<sup>9, 10</sup>

Xylans, mannans (glucomannans) and galactans are the major categories of hemicelluloses. The xylans have backbone of  $\beta$ -(1 $\rightarrow$ 4)-glycosidic linked xylose units and some of the xylose molecules have  $\alpha$ -(1 $\rightarrow$ 2)-bonded 4-*O*-methylglucoronic acids. The

xyloses also contain acetyl groups. In softwoods, xylose molecules are connected to arabinose by  $\alpha$ -(1→3)-glycosidic bonds. Corncobs are highly concentrated in xylans. Hardwoods have mannose and glucose units linked by  $\beta$ -(1→4)-glycosidic bonds. Acetyl and galactose groups are connected to glucose-mannose backbone structure in softwoods. A summary of hemicelluloses composition in hardwoods (deciduous trees) and in softwoods (coniferous trees) are given in Table A.1.

Table A.1 Composition and degree of polymerization (DP) of hemicelluloses.<sup>9</sup>

Hemi-celluloses	Hardwoods (deciduous trees)			Softwoods (coniferous trees)		
	Percentage	DP	Compounds	Percentage	DP	Compounds
Xylans	20-30	100-200	Xylose (Xyl), 4-O-methyl-glucoronic acid (Mga), Acetyl gr. (Ac)	5-10	70-130	Xylose (Xyl), 4-O-methyl-glucoronic acid (Mga), Acetyl gr. (Ac.)
Mannans	3-5	60-70	Mannose (Man), Glucose (Glu)	20-25	-	Mannose (Man), Glucose (Glu) Galactose (Gal), Acetyl group (Ac)
Galactans	0.5-2	-	Galactose (Gal), Arabinose (Ara), Rhamnose (Rha)	0.5-3	200-300	Galactose (Gal), Arabinose (Ara)

Acetyl groups present in hardwood xylans and softwood galatoglucomannans are hydrolysable by acid at elevated temperatures. The acetic acid released provides the acidity to the reaction media. The presence of uronic acid groups reduces the hydrolysis rate of glycosidic linkages appreciably.<sup>9</sup>

Hemicelluloses are biodegraded to monomeric sugars and acetic acid. Xylan is the main carbohydrate found in hemicelluloses and degradation requires the cooperative action of a variety of hydrolytic enzymes. Endo-1,4- $\beta$ -xylanase generates oligosaccharides from the cleavage of xylan and 1,4- $\beta$ -xylosidase produces xylose from the xylan

oligosachharides. Hemicelluloses biodegradation requires accessory enzymes such as xylan esterases, ferulic and p-coumeric esterases,  $\alpha$ -l-arabinofuranosidases, and  $\alpha$ -4-O-methyl glucuronosidases to work synergistically on wood xylans and mannans.<sup>1, 11</sup>

**Lignin:** Lignin is a complex aromatic polymer. It is synthesized by the generation of free radicals released during peroxidise-mediated dehydrogenation of three phenylpropionic alcohols: trans-*p*-coumaryl (*p*-hydroxyphenyl propanol), coniferyl alcohol (guaiacyl propanol), and sinapyl alcohol (syringyl propanol). The structure of lignin monomers are shown in Figure A.2. The polymerization results in a heterogeneous structure whose basic units are linked by C-C and aryl-ether linkages, with aryl-glycerol  $\beta$ -aryl ether being the predominant structure. Lignin is an amorphous heteropolymer, non-water soluble and optically inactive.<sup>1</sup>

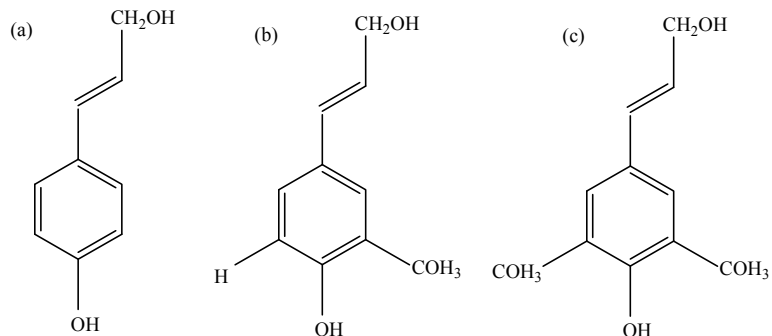


Figure A.2 Lignin monomers (a) trans-*p*-coumaryl alcohol, (b) coniferyl alcohol, and (c) sinapyl alcohol (redrawn from Bobleter).<sup>9</sup>

The structural complexity of the lignin and its high molecular weight is the main reason why it is so hard to degrade by enzymes. Lignin content in wood or lignocellulosic varies based on the species type, growing conditions, part of the plant tested and numerous other factors. Lignin mainly acts as adhesive or binder in wood that

provides strength and structure to the cellular composites of the plant and protects against microorganism or chemical attack. It controls the fluid flow, acts as antioxidant by absorbing UV lights and stores energy. When lignin binds, it crosslinks with the regular structure of the microfibrils made of cellulose and hemicelluloses.<sup>12, 13</sup> Isolated lignin shows maximum solubility in the solvents including dioxane, acetone, methyl cellosolve (ethylene glycol monomethyl ether), tetrahydrofuran, dimethyl formaldehyde (DMF) and dimethyl sulfoxide (DMSO).

Carbon-carbon linkages are very resistant to chemical attack, and degradation of lignin is largely limited to the cleavages of ether units at  $\alpha$ - and  $\beta$ -positions. Functional groups of lignin follows<sup>14</sup>:

- *Hydrolyzable ether linkages:*  $\beta$ -aryl,  $\alpha$ -aryl, and  $\alpha$ -alkyl ether linkages are the main hydrolysable ether units in lignin. Lignin may also contain some  $\alpha$ -ether linked 1 to carbohydrate, which are hydrolyzed at relatively lower rates.
- *Phenolic hydroxyl groups:* It plays an important role in promoting alkali-catalyzed cleavages of interunitary ether linkages, oxidative degradation of lignin, and in lignin modification reactions.
- *Aliphatic hydroxyl groups:* Two major aliphatic hydroxyl groups in lignin are located at the  $\gamma$ - and  $\alpha$ - positions of the side chains. Aliphatic hydroxyl group at  $\alpha$ -position is a benzyl alcohol, which is very reactive and plays a dominant role in lignin reactions.
- *Uncondensed Units:* Units at position C2, C3, C5, and C6 are free or substituted by methyl groups are defined as uncondensed units. Hardwood lignin which contains high syringical units, have high content of uncondensed units.

- *Unsaturated groups*: Lignin contains some unsaturated groups, mainly as coniferyl alcohol and coniferaldehyde end groups.
- *Ester group*: Grass lignins contain significant amount of *p*-coumeric acid and ferulic acid moieties, which are mainly esterified. These functional groups are liable to mild alkali treatment and mainly present at the  $\alpha$ -position.
- *Methoxyl groups*: These groups are relatively resistant to both acidic and alkaline hydrolysis.
- *Accessibility*: Lignin have very high tendency to form hydrogen bonding like hemicelluloses and cellulose.

Lignin empirical formulae are based on ratios of methoxy groups to phenylpropanoid groups ( $\text{MeO:C}_9$ ). The general empirical formula for lignin monomers is  $\text{C}_9\text{H}_{10}\text{O}_2(\text{OCH}_3)_n$ , where n is the ratio of MeO to C9 groups. Where no experimental ratios have been found, they are estimated as follows: 0.94 for softwoods; 1.18 for grasses; 1.4 for hardwoods. These are averages of the lignin ratios found in the literature. Paper products, which are produced primarily from softwoods, are estimated to have an  $\text{MeO:C}_9$  ratio of 0.94 (source: NREL).

*Extractives*: Extractives are low to moderately high molecular weight compounds, which are soluble in water or organic solvents. They impart color, odor, and taste to the biomass. The composition of extractives varies widely based on the species and class of wood. Some of the important classes of extractives are Terpenes, triglycerides, fatty acids, and phenolic compounds.<sup>15</sup>

*Ash*: Ash contains metallic ions of sodium, potassium, calcium, and the corresponding ions of carbonate, phosphate, silicate, sulfate, chloride etc.

### A.3 References

1. Pérez, J.; Muñoz-Dorado, J.; Rubia, J. T. D. I.; Martínez, J., Biodegradation and biological treatments of cellulose, hemicellulose and lignin: an overview *Int Microbiol* **2002**, 5, 53-63.
2. Sarko, A., Cellulose - how much do we know about its structure? *Wood and Cellulosics: Industrial utilization, biotechnology, structure and properties* **1987**, (J.F.Kennedy ed.), 55-70.
3. O'Sullivan, A. C., Cellulose: the structure slowly unravels. *Cellulose* **1997**, 4, (3), 173-207.
4. Marchessault, R. H.; Sarko, A., X-Ray Structure of Polysaccharides. *Advances in Carbohydrate Chemistry* **1967**, 22, 421-482.
5. Sarko, A., What is the crystalline structure of cellulose ? *Tappi* **1978**, 61, 59-61.
6. Atalla, R. H.; Vanderhart, D. L., Native Cellulose: A Composite of Two Distinct Crystalline Forms. *Science* **1984**, 223, (4633), 283 - 285.
7. Sinnott, M. L., *Chapter 4: Primary structure and conformation of oligosaccharides and polysaccharides*. RSC publishing: 2007.
8. Dumitriu, S., *Preparation and properties of cellulose bicomponent fibers*. CRC Press: 2004.
9. Bobleter, O., Hydrothermal degradation of polymers derived from plants. *Prog. Polym. Sci.* **1994**, 19, 797–841.
10. Saha, B. C., Hemicellulose Bioconversion. *J Ind Microbiol Biotechnol* **2003**, 30, 279-291.

11. Sukumaran, R. K., Bioethanol from lignocellulosic biomass: part II production of cellulases and hemicellulases. In *Hand book of plant based biofuels*, 2009; pp 141-157.
12. Meister, J. J., Chemical modification of lignin. In *Chemical modification of lignocellulosic materials*, Hon, D. N.-S., Ed. Marcel Dekker Inc.: 1996; pp 129-157.
13. Sjostrom, E., *Wood chemistry: Fundamentals and applications*. Academic press, New York: 1981.
14. Hon, D. N.-S.; Shiraishi, N., *Wood and cellulosic chemistry*. second ed.; 2000; p 275-384.
15. Biermann, C. J., *Handbook of pulping and paper making*. Academic press: 1996.

## Appendix B: Summary of Pretreatment Methods

Table B.1 Summary of the important pretreatment methods.

Methods	Treatment time	Temperature	Pressure	Remarks
<b><i>Acid Catalyzed</i></b>				
Dilute Acid ( $\text{H}_2\text{SO}_4$ )	5-30 min	140-190°C	0.4-1.3 MPa	0.5 - 1.5%
Concentrated Acid ( $\text{H}_3\text{PO}_4$ )	30-60 min	50°C	0.1 MPa	85%
Peracetic Acid ( $\text{C}_2\text{H}_4\text{O}_3$ )	1-180 h	25-75°C	0.1 MPa	2-10% $\text{C}_2\text{H}_4\text{O}_3$
<b><i>Base Catalyzed</i></b>				
Sodium Hydroxide ( $\text{NaOH}$ )	24-96 h	25°C	0.1 MPa	1% $\text{NaOH}$ , 0.1 g $\text{NaOH}/\text{g biomass}$
Lime ( $\text{Ca(OH)}_2$ )				
Low Lignin (12-18%)	24-96 h	100-120°C	0.1-0.2 MPa	0.10 g $\text{Ca(OH)}_2/\text{g biomass}$
Medium Lignin (18-24%)	≈30 days	≈55°C	0.1 MPa	0.10-0.15 g $\text{Ca(OH)}_2/\text{g biomass}$
High Lignin (> 24%)	2 h	≈ 150°C	1.5 MPa	0.15-0.20 g $\text{Ca(OH)}_2/\text{g biomass}$
Ammonia Recycle Percolation (ARP)	≈15 min	180°C	≈2.0 MPa	15% $\text{NH}_3$
Ammonia Fiber Explosion (AFEX)	≈ 5 min	60-100°C	≈2.0 MPa	1 g $\text{NH}_3/\text{g biomass}$

<b>Oxidative Alkali (NaOH + H<sub>2</sub>O<sub>2</sub> or O<sub>3</sub>)</b>	<b>6-25 h</b>	<b>20-60°C</b>	<b>0.1 MPa</b>	<b>1-15% H<sub>2</sub>O<sub>2</sub> or O<sub>3</sub>, pH =11.5</b>
<b>Ionic Liquid</b>	<b>5-12 h</b>	<b>50-150°C</b>	<b>-</b>	<b>Ionic liquids</b>
<b>Organosolv</b>	<b>60 min</b>	<b>180°C</b>	<b>3.5-7.0 MPa</b>	<b>1.25% H<sub>2</sub>SO<sub>4</sub>, 60% ethanol</b>
<b>Steam Explosion</b>	<b>0.3-50 min</b>	<b>190-250°C</b>	<b>1.2-4.0 MPa</b>	<b>Steam</b>
<b>Hydrothermal</b>	<b>1-15 min</b>	<b>160-220°C</b>	<b>0.6-3.5 MPa</b>	<b>Subcritical water</b>
<b>Supercritical CO<sub>2</sub></b>	<b>1 h</b>	<b>35-80°C</b>	<b>7-27 MPa</b>	<b>CO<sub>2</sub></b>

## Appendix C: Reaction Pathways of Cellulose, Hemicelluloses, and Lignin in Hydrothermal Medium

Lignocellulosic biomass is a mixture of cellulose (38-50 wt%), hemicelluloses (23-32 wt%), and lignin (15-25 wt%) which are held together by covalent bonding, various intermolecular bridges, and van der Waals forces forming a complex structure. Several studies have been conducted using model compounds such as cellulose, hemicelluloses, and lignin in sub-and supercritical water to establish the reaction pathways of these compounds in hydrothermal medium. The chemistry behind the reactions of the individual components of biomass under hydrothermal conditions is well understood. The generalized individual reaction pathways of the major components of biomass (cellulose, hemicelluloses, and lignin) are discussed in following section:

### C.1 Cellulose Reaction Pathways

Hydrothermal degradation of cellulose is a heterogeneous and pseudo-first-order reaction for which detailed chemistry and mechanism have been proposed earlier.<sup>1-4</sup> Cellulose reaction in hydrothermal and catalyst free medium mainly proceeds via hydrolysis of glycosidic linkages. The long chain of cellulose starts breaking down in such condition to smaller molecular weight water soluble compounds (oligomers) and further to glucose (monomer). Glucose is water soluble and undergoes rapid degradation in hydrothermal medium at elevated temperature.

The key products from the glucose decomposition are shown in Figure C.1. These products are formed mainly via dehydration, isomerization, reverse aldol condensation, and fragmentation reactions.

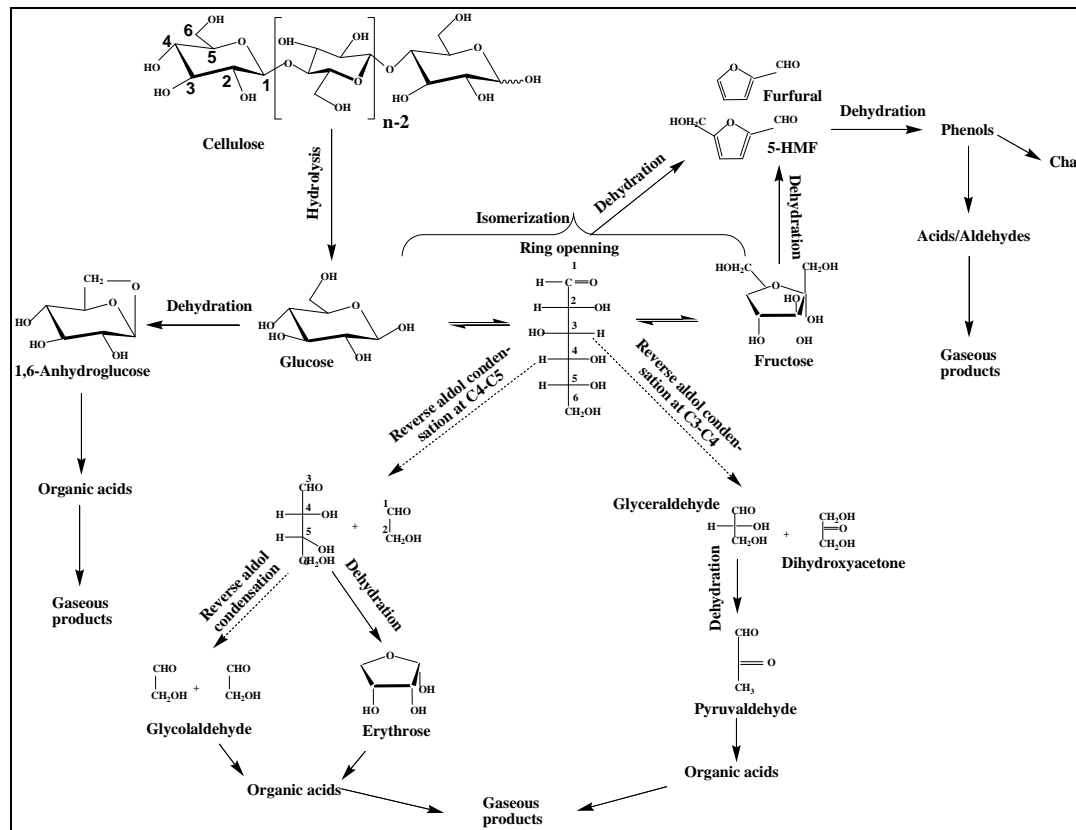


Figure C.1 Key reaction products from cellulose hydrolysis in catalyst free hydrothermal medium.<sup>5-8</sup>

## C.2 Hemicelluloses Reaction Pathways

Hemicelluloses are polysaccharides of five carbon sugar such as xylose or six carbon sugars other than glucose. They are usually branched and have much lower degree of polymerization. Figure C.2 shows a hardwood xylan with branch chain.

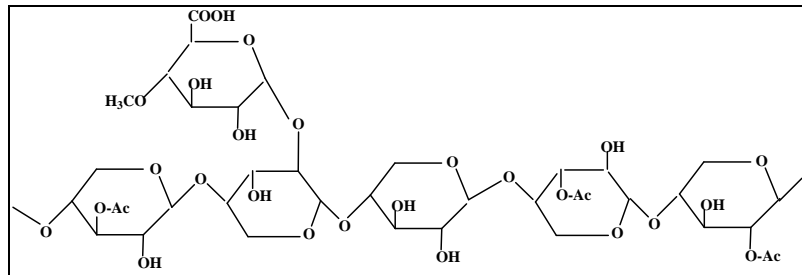


Figure C.2 A segment of hardwood xylan, *O*-acetyl-4-*O*-methylglucuronoxylan (redrawn from bobleter et. al.).<sup>1</sup>

Branches in the chains do not allow the formation of tightly packed fibrils. Hemicelluloses are not crystalline and easily hydrolysable to their respective monomers. In fact, about 95% of hemicelluloses were extracted as monomeric sugars using water at 34.5 MPa and 200-230°C in a span of just few minutes.<sup>2</sup> In hydrothermal medium, Hemicelluloses are hydrolyzed to sugars, which subsequently degrade into furfural and other degradation compounds. Furfural (2-furaldehyde) is commercially produced from hemicelluloses-derived xylose.<sup>5</sup>

### C.3 Lignin Reaction Pathways

Lignin is a complex and high molecular weight polymer of phenylpropane derivatives (p-coumaryl alcohol, coniferyl alcohol, and sinapyl alcohol). The density of hydrothermal medium is found to be a key parameter in lignin decomposition. In hydrothermal reaction medium, most of the hemicelluloses and part of the lignin are solubilized below 200°C. Lignin fragments have high chemical reactivity. Part of these fragments again cross links and re-condenses to form high molecular weight water insoluble products.<sup>1</sup> Recently, Fang *et al.* have proposed the reaction pathway for lignin in supercritical water. The reaction steps consist of four phases: oil phase, aqueous phase,

gas phase, and a solid residue phase.<sup>9, 10</sup> Their study concluded that lignin can be completely dissolved and undergoes homogeneous hydrolysis and pyrolysis preventing further re-polymerization. The proposed (Fang *et al.*) reaction pathway of lignin in supercritical water is shown in Figure C.3.

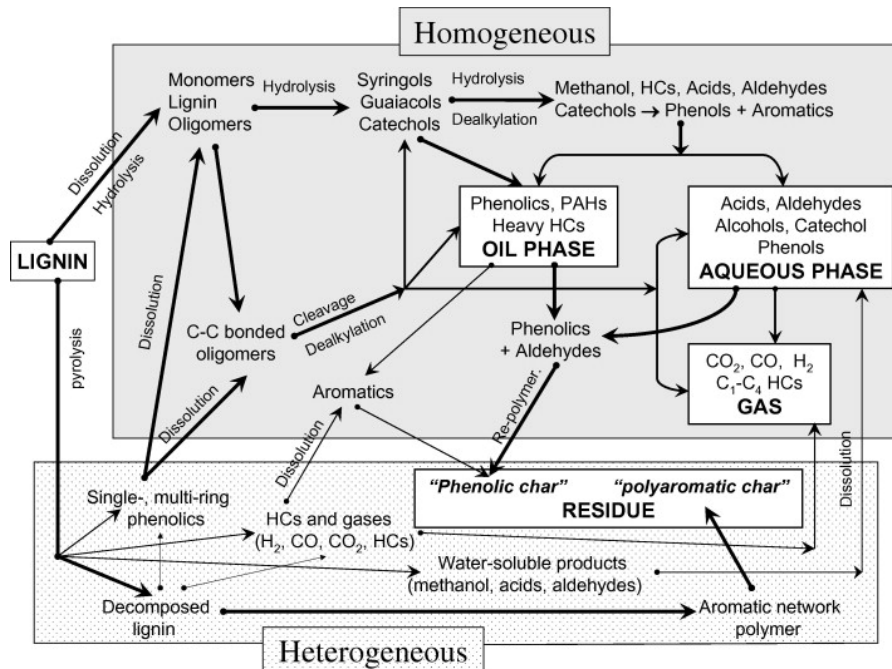


Figure C.3 Reaction pathway of lignin in supercritical water (taken from Fang *et al.*).<sup>10</sup>

#### C.4 References

1. Bobbleter, O., Hydrothermal degradation of polymers derived from plants. *Prog. Polym. Sci.* **1994**, 19, 797–841.
2. Mok, W. S.; Antal, M. J., Uncatalyzed solvolysis of whole biomass hemicellulose by hot compressed liquid water. *Ind. Eng. Chem. Res.* **1992**, 31, 1157-1161.
3. Mok, W. S. L.; M.J., A. J.; Varhegyi, G., Productive and parasitic pathways in dilute-acid-catalyzed hydrolysis of cellulose. *Ind. Eng. Chem. Res.* **1992**, 31, 94-100.

4. Schwald, W.; Bobleter, O., Hydrothermolysis of cellulose under static and dynamic conditions at high temperatures. . *J. Carbohydr. Chem.* **1989**, 8, (4), 565-578.
5. Peterson, A. A.; Vogel, F.; Lachance, R. P.; Froling, M.; Michael Jerry Antal, J.; Tester, J. W., Thermochemical biofuel production in hydrothermal media:A review of sub- and supercritical water technologies. *Energy and Environmental Science* **2008**, 1, 32-65.
6. Sasaki, M.; Goto, K.; Tajima, K.; Adschariri, T.; Arai, K., Rapid and selective retro-aldol condensation of glucose to glycolaldehyde in supercritical water. *Green Chem.* **2002**, 4, 285-287.
7. Kabyemela, B. M.; Adschariri, R.; Malaluan, R. M.; Arai, K.; Ohzeki, H., Rapid and selctive conversion of glucose to erythrose in supercritical water. *Ind. Eng. Chem. Res.* **1997**, 36, 5063-5067.
8. Watanabe, M.; Aizawa, Y.; Iida, T.; Levy, C.; Aida, T. M.; Inomata, H., Glucose reactions within the heating period and the effect of heating rate on the reactions in hot compressed water. *Carbohydrate Research* **2005**, 340, 1931-1939.
9. Behrendt, F.; Neubauer, Y.; Oevermann, M.; Wilmes, B.; Zobel, N., Direct liquefaction of biomass. *Chem. Eng. Technol* **2008**, 31, (5), 667-677.
10. Fang, Z.; Sato, T.; Jr., R. L. S.; Inomata, H.; Arai, K.; Kozinski, J. A., Reaction chemistry and phase behaviour of lignin in high-temperature and super critical water. *Bioresource Technology* **2008**, 99, 3424-3430.

## Appendix D: Salt Solubility in Hydrothermal Medium

### D.1 Salt-water Binary System

Ambient water is an excellent solvent (typically several 100 g/l) for most of the salts. On the other hand, solubility of these salts goes down drastically (1-100 ppm) in the low density supercritical water. The reduced solubility in supercritical region causes salts to precipitate as fine-crystalline solids, which may lead to plugging of the reactor even at high flow velocities.<sup>1</sup> Salt's solubility in supercritical water is reduced to such an extent that electrolytes can be effectively recovered through the precipitation and solid separation.<sup>2</sup>

The solubility behavior of water-salt systems differ considerably in sub- and supercritical water conditions. In the temperature range of 100-200°C and at varying pressure, the diversity of solubility criteria is mainly due to the abundance of crystalline hydrates. The crystalline hydrate ceases to exist at higher temperature and precipitate as solid phase with immiscible fluid phase.<sup>3</sup> The phase behavior of salt-water systems at high temperature depends on the nature of the salt as well as its initial concentration. Salts are classified as Type 1 or Type 2 based on their liquid phase solubility changes with temperature in binary salt-water system saturated with the salt. Type 1 binary systems are characterized by increasing salt solubility in the liquid phase with temperature (positive temperature coefficient of solubility) at vapor and higher pressure

upto the melting point of salt. Type 1 systems exhibit high salt solubility in the vicinity of critical point of water.<sup>2-4</sup>

In case of Type 2 binary systems, the salt solubility in liquid solution decreases with temperature (negative temperature coefficient of solubility) under subcritical conditions. Type 2 system exhibits very low salt solubility of the order of parts per million near the critical point. Generally, Type 1 salts have melting points below 800-1000°C (can be lower or higher than the critical temperature of water), while Type 2 salts have melting points above 700-800°C (always higher than the critical temperature). Table D.1 shows the classification of binary mixtures of salt-water systems.

Table D.1 Classification of salt-water binary system (taken from Valyashko).<sup>5</sup>

Type 1 salts	Type 2 salt
KF, RbF, CsF	LiF, NaF
LiCl, LiBr, LiI	Li <sub>2</sub> CO <sub>3</sub> , Na <sub>2</sub> CO <sub>3</sub>
NaCl, NaBr, NaI	Li <sub>2</sub> SO <sub>4</sub> , Na <sub>2</sub> SO <sub>4</sub> , K <sub>2</sub> SO <sub>4</sub>
K <sub>2</sub> CO <sub>3</sub> , Rb <sub>2</sub> CO <sub>3</sub>	Li <sub>2</sub> SiO <sub>3</sub> , Na <sub>2</sub> SiO <sub>3</sub>
Rb <sub>2</sub> SO <sub>4</sub> ,	Li <sub>3</sub> PO <sub>4</sub> , Na <sub>3</sub> PO <sub>4</sub>
Na <sub>2</sub> SeO <sub>4</sub>	CaF <sub>2</sub>
K <sub>2</sub> SiO <sub>3</sub>	SaF <sub>2</sub>
K <sub>3</sub> PO <sub>4</sub>	BaF <sub>2</sub>
CaCl <sub>2</sub> , CaBr <sub>2</sub> , CaI <sub>2</sub>	
SrCl <sub>2</sub> , SrBr <sub>2</sub>	
BaCl <sub>2</sub> , BaBr <sub>2</sub>	

In brief, Type 1 salts have increasing solubility in water with temperature, where as Type 2 salts shows opposite trend. For example, Type 2 salt, sodium carbonate (Na<sub>2</sub>CO<sub>3</sub>) has about 30 wt% solubility in ambient water and its solubility near the critical temperature of water approaches zero.<sup>6</sup> On the other hand, sodium chloride (NaCl), an

example of Type 1 salt has 37 wt% solubility in subcritical water at 300°C and about 120 ppm at 550°C.<sup>7</sup>

## D.2 References

1. Kritzer, P.; Dinjus, E., An assessment of supercritical water oxidation (SCWO): Existing problems, possible solutions and new reactor concepts. *Chemical Engineering Journal* **2001**, 83, 207-214.
2. Wofford, W. T.; Dell'Orco, P. C.; Gloyna, E. F., Solubility of potassium hydroxide and potassium phosphate in supercritical water. *J. Chem. Eng. Data* **1995**, 40, 968-973.
3. Valyashko, V.; Urusova, M., Solubility behaviour in ternary water-salt systems under sub= and supercritical conditions. *Monatshefte fur Chemie* **2003**, 134, 679-692.
4. Hodes, M.; Marrone, P. A.; Hong, G. T.; Smith, K. A.; Tester, J. W., Salt precipitation and scale control in supercritical water oxidation-Part A: fundamentals and research. *J. of Supercritical Fluids* **2004**, 29, 265-288.
5. Valyashko, V. M., Phase equilibria in water-salt systems: some problems of solubility at elevated temperature and pressure. *High temperature and high pressure electrochemistry in aqueous solutions, Natl. Assoc. Corrosion Eng.* **1976**, 4, 153.
6. Keevil, N. B., Vapor pressures of aqueous solutions at high temperature. *J. Am. Chem. Soc.* **1942**, 64, 841-850.
7. Sourirajan, S.; Kennedy, G. C., The System of H<sub>2</sub>O-NaCl at elevated temperatures and pressures. *Am. J. Sci.* **1962**, 260, 115-141.

## Appendix E: Journal Publications and Conference Presentations

### PATENT APPLICATION

1. Biomass to biochar conversion in subcritical water (provisional patent # 6124591, USPTO, September 2009).

### JOURNAL PUBLICATIONS

1. **Kumar, S.**; Gupta, R. B.; Lee, Y. Y.; Gupta, R. B., Cellulose Pretreatment in Subcritical Water: Effect of temperature on molecular structure and enzymatic reactivity. *Bioresour. Technol.*, **2010**, 101 (4) 1337-1347.
2. **Kumar, S.**; Gupta, R. B., Biocrude Production from Switchgrass using Subcritical Water. *Energy & Fuels*, **2009**, 23 (10) 5151-5159.
3. **Kumar, S.**; Gupta, R. B., Hydrolysis of Cellulose in Sub- and Supercritical Water in a Continuous Flow Reactor. *Ind. Eng. Chem. Res.*; **2008**, 47, 9321-29.
4. **Kumar, S.**; Kothari, U.; Lee, Y. Y.; Gupta, R. B., Hydrothermal Pretreatment of Switchgrass and Corn Stover for Production of Ethanol and Carbon Microspheres *Biomass & Bioenergy*, Feb. **2010** (submitted).
5. **Kumar, S.**; Kong, L.; Gupta, R. B., Production of Biochar from Switchgrass by Hydrothermal Carbonization. *Energy & Fuels*, Feb. **2010** (submitted).
6. **Kumar, S.**; Loganathan, V. A.; Barnett, M. O.; Gupta R. B.; Heavy Metal Adsorption on Biochar prepared from Switchgrass (to be submitted).

## CONFERENCE PRESENTATIONS

1. **Kumar, S.**; Kothari, U.; Lee, Y.Y.; Gupta, R.B., Hydrothermal Pretreatment of Switchgrass for Ethanol Production. AIChE annual conference, Nov. 2009.
2. **Kumar, S.**; Kong, L.; Gupta, R.B., Hydrothermal Carbonization of Switchgrass for Biochar Production. AIChE annual conference, Nov. 2009.
3. **Kumar, S.**; Byrd, A.; Gupta R.B., Sub- and Super-critical Water Technology for Biofuels: Swtichgrass to Ethanol, Biocrude, and Hydrogen, at 31st Symposium on Biotechnology for Fuels and Chemicals, San Francisco, May 2009.
4. **Kumar, S.**; Kothari, U; Lee, Y.Y.; Gupta, R.B., Hydrothermal pretreatment of switchgrass: Effect of temperature and potassium carbonate on enzymatic reactivity, (**poster**) 31st Symposium on Biotechnology for Fuels and Chemicals, San Francisco, May 2009.
5. **Kumar, S.**; Byrd, A.; Kong, L.; Cullinan, H.; Gupta, R.B.' Hydrothermal (sub- and super-critical water) technology for biofuel production from switchgrass, (**poster**) tcbiomass 2009, The International Conference on Thermochemical Conversion Science, Chicago, Sept. 16-18, 2009.
6. **Kumar, S.**; Gupta, R; Lee, Y. Y.; Gupta R. B., Enhancement of Enzymatic Digestibility of Microcrystalline Cellulose by Treatment in Subcritical Water, AIChE conference, Nov. 2008.
7. **Kumar, S.**; Demirbas A. Gupta, R. B., Hydrolysis of Microcrystalline Cellulose in Subcritical and Supercritical Water in a Continuous Flow Reactor, AIChE annual conference, Nov. 2008.

- 8.** Kumar, S.; Gupta, R. B., Biocrude Production from Switchgrass using Subcritical Water, AIChE annual conference, Nov. 2008.
- 9.** Byrd, A.; Kumar, S.; Gupta, R. B., Cellulose Liquefaction and Hydrogen Production in Supercritical Water, AIChE annual conference, Nov. 2008.
- 10.** Kothari, U; Kumar, S.; Gupta, R.B.; Lee, Y.Y., Improvement of Enzymatic Hydrolysis for Hydrothermally-Treated Switchgrass Using Mixed-Enzymes, submitted for 32<sup>nd</sup> Symposium on Biotechnology for Fuels and Chemicals, May 2010.